Analysis and Optimal Planning of Nuclear-Renewable Hybrid Energy Systems for Ships

by

Md Ibrahim Adham

A thesis submitted to the
School of Graduate and Postdoctoral Studies in partial
fulfillment of the requirements for the degree of

Master of Applied Science in Nuclear Engineering

Faculty of Energy Systems and Nuclear Science

University of Ontario Institute of Technology (Ontario Tech University)

Oshawa, Ontario, Canada

June 2021

THESIS EXAMINATION INFORMATION

Submitted by: **Md Ibrahim Adham**

Master of Applied Science in **Nuclear Engineering**

Thesis title:
Analysis and Optimal Planning of Nuclear-Renewable Hybrid Energy Systems for Ships

An oral defense of this thesis took place on June 24, 2021 in front of the following examining committee:

Examining Committee:

Chair of Examining Committee	Dr. Jennifer McKellar
Research Supervisor	Dr. Hossam Gaber
Examining Committee Member	Dr. Filippo Genco
Thesis Examiner	Dr. Marc Rosen

The above committee determined that the thesis is acceptable in form and content and that a satisfactory knowledge of the field covered by the thesis was demonstrated by the candidate during an oral examination. A signed copy of the Certificate of Approval is available from the School of Graduate and Postdoctoral Studies.

ABSTRACT

Ocean-going ships are one of the sources of global GHG emissions. Several actions are being taken to reduce the GHG emissions from maritime vessels, and integration of Renewable Energy Sources (RESs) is one of them. Due to some limitations, RESs are not suitable for large ships and often mix with fossil fuel-based generators. Fossil fuel-based generators need to be replaced by emissions-free energy sources to make marine ships free from emissions. Nuclear energy is emissions-free, and small-scale nuclear reactors like Microreactors (MRs) have the potential to replace fossil fuel-based generators. In this study, the technical, economic, and environmental competitiveness of Nuclear-Renewable Hybrid Energy Systems (N-R HES) in marine ships are assessed. The results determine that N-R HES has the lowest NPC compared to the other conventional energy systems. A sensitivity analysis is carried out to see the impact of different system parameters on this study's findings.

Keywords: Nuclear Power; Renewable Energy; Life Cycle Cost; Optimal Planning; Sensitivity Assessment.

AUTHOR'S DECLARATION

I hereby declare that this thesis consists of original work of which I have authored. This is a true copy of the thesis, including any required final revisions, as accepted by my examiners.

I authorize Ontario Tech University (UOIT) to lend this thesis to other institutions or individuals for the purpose of scholarly research. I further authorize Ontario Tech University (UOIT) to reproduce this thesis by photocopying or by other means, in total or in part, at the request of other institutions or individuals for the purpose of scholarly research. I understand that my thesis will be made electronically available to the public.

Md Ibrahim Adham

STATEMENT OF CONTRIBUTIONS

Part of the work described in this thesis has been published as:

- **Conference Paper**
  - ✓ **C-01**: M. R. Abdussami, Md. I. Adham, and H. A. Gabbar, "Modeling and performance analysis of nuclear-renewable micro hybrid energy system based on different coupling methods", in TMREES Conference Series: Technologies and Materials for Renewable Energy, Environment and Sustainability - 2020, June 25-27, Athens, Greece, Energy Report (Elsevier), In-Press. (**Best Paper Award**)
- **Journal Paper**
  - ✓ **J-01:**H. A. Gabbar, M. I. Adham, and M. R. Abdussami, "Analysis of Nuclear-Renewable Hybrid Energy System for Marine Ships", Energy Reports, vol. 07, p. 2398 – 2417, Apr. 2021, doi: https://doi.org/10.1016/j.egyr.2021.04.030
  - ✓ **J-02:**H. A. Gabbar, M. I. Adham, and M. R. Abdussami, "Optimal Planning of Integrated Nuclear-Renewable Energy System for Marine Ships Using Artificial Intelligence Algorithm", *Energies vol. 14, Issue. 11, ISSN. 1996-1073, doi: 10.3390/en14113188*
  - ✓ **J-03**: H. A. Gabbar, M. R. Abdussami, and M. I. Adham, "Techno-Economic Evaluation of Interconnected Nuclear-Renewable Micro Hybrid Energy Systems with Combined Heat and Power," *Energies*, vol. 13, no. 7, p. 1642, Apr. 2020, doi: 10.3390/en13071642.

ACKNOWLEDGEMENTS

I would like to thank and offer my sincerest gratitude to my thesis supervisor, Dr. Hossam Gaber, for his encouragement, supervision, and support. I cannot imagine having any better advisor for my thesis regarding his knowledge, perceptiveness, and motivation.

Besides, I would like to thank Dr. Filippo Genco for his timely guidance. I would also like to thank all of my lab members for their time and support.

I am indebted forever to my parents, my wife (Tanzeen Sultana), and other family members for their patience, understanding, and endless encouragement during this study.

Md Ibrahim Adham
Oshawa, Ontario, Canada
June 2021

Table of Contents

List of Tables

List of Figures

Nomenclature

$BAT_{in}(t)$	Amount of energy (kWh) that can be given to the battery at time step t
$BAT_{out}(t)$	Amount of energy (kWh) that is needed from the battery at time step t
$BAT_{take}(t)$	Amount of energy (kWh) that can be taken by the battery at time step t
$BAT_{give}(t)$	Amount of energy (kWh) that can be given by the battery at time step t
$BAT_{chrg}(t)$	Capacity of battery (kWh) after charging at time step t
$BAT_{dischrg}(t)$	Capacity of battery (kWh) after discharging at time step t
$BAT_{SOC,max}$	Maximum SOC (%) of the battery bank
$BAT_{SOC,min}$	Minimum SOC (%) of the battery bank
C_{TBHS}	Total hull resistance coefficient of ship
C_{Fs}	Coefficient of frictional resistance
C_{Rs}	Coefficient of residual resistance
$\boldsymbol{P_{ship\,(x,y)}}$	Effective power (kW) of the ship in a certain position (x,y)
$P_{MR}(t)$	Total power (kW) from MR at time step t.
$P_w(t)$	Total power (kW) from the wind turbine at time step t.
$P_{gen}(t)$	Total power (kW) generation at time step t.
$P_{pv}(t)$	Total power (kW) from solar PV at time step t.
R_{TBHS}	Total bare hull resistance (kW) of the ship
$V_{whub}(t)$	Wind speed (m/s) at the hub height (m/s) at time step t
$V_{s(x,y)}$	Speed (m/s) of the ship in a certain position (x,y).

Acronym Library

ACE	Annual CO_2 emissions (tonne)
ACO	Ant Colony Optimizer
BAU	Business As Usual
CCE	Cost associated with CO_2 emissions penalty
COE	Cost of Energy
CS	Cuckoo Search
CSP	Concentrated Solar Power
DGR	Deep Geological Repository
DLA	Data License Agreement
EEDI	Energy Efficiency Design Index
ERPO	Extended Reduced Power Operation
FFG	Fossil Fuel-based Generator
GA	Genetic Algorithm
GRF	Generation Reliability Factor
HAS-TS	Hybrid Simulated Annealing-Tabu Search
HBB-BC	Hybrid Big Bang-Big Crunch
HFPA-SA	Hybrid Flower Pollination Algorithm and Simulated Annealing
HGA-ES	Hybrid GA and an Exhaustive-Search
HNS	Hazardous and Noxious Substance
IDC	Interest During Construction
IMarEST	Institute of Marine Engineering, Science and Technology
IMO	International Maritime Organization
IRR	Internal Rate of Return
ISAPSO	Improved Simulated Annealing Particle Swarm Optimization
ITTC	International Towing Tank Conference
KPI	Key Performance Indicators
LCOE	Levelized Cost of Energy
LP	Linear Programming
LPSP	Loss of Power Supply Probability
LR	Learning Rate
MarKov-GA	MarKov-based GA
MEG	Micro Energy Grid
MEPC	Marine Environment Protection Committee
MESCA	Modified Electric System Cascade Analysis
MILP	Mixed Integer Linear Programming
NPP	Nuclear Power Plant
NSGA	Non-dominant Sorting Genetic Algorithm
PSO	Particle Swarm Optimization
PWR	Power to Weight Ratio
R	Rate of Cost Reduction
RAVEN	Risk Analysis Virtual Environment
RINA	Royal Institution of Naval Architects
UOIT	Ontario Tech University

Chapter 1: Introduction

This chapter covers the background of the research, motivation of this study, identification of the problems, objectives, and outline of this thesis.

1.1. Background

Reducing GHG emissions is the main objective to avoid the negative impact of climate change. The average target of the Kyoto protocol was to reduce GHG emissions by around 5% relative to the 1990 levels by 2012. International shipping was not included in Paris Agreement but it is responsible for global GHG emissions to a large extent. If global shipping were a country, it would be considered as the sixth-largest producer of CO_2 after the United States, China, Russia, India, and Japan. Ocean-going shipping is responsible for more than 3% of global CO_2 emissions [1]. Although international shipping is not a part of the Paris Agreement, the International Maritime Organization (IMO) is focusing on a strategy to reduce the GHG emissions from ships. They have set a phase-wise target and emphasized technical, operational, and innovative solutions to lessen GHG emissions.

Ships are accounted for around 1 billion tonnes of GHG emissions each year from 2007 to 2012. Table 1-1 represents the trend of global CO_2 emissions from 2008 to 2015 along with the CO_2 emissions from different types of marine vessels. It can be seen from the table that international shipping is accounted for more than 80% of CO_2 emissions among all the CO_2 emissions from marine vessels and it is increasing [2].

Table 1-1 Global CO_2 Emissions (2008-2015)

	Thrid IMO GHG Study (million tonnes)					ICCT (million tonnes)		
Year	**2008**	**2009**	**2010**	**2011**	**2012**	**2013**	**2014**	**2015**
Global CO2 Emissions	32,133	31,822	33,661	34,726	34,968	35,672	36,084	36,062
CO2 Emissions from Internation Shipping	916	858	773	853	805	801	813	812
CO2 Emissions from Domestic Shipping	139	75	83	110	87	73	78	78
CO2 Emissions from Fishing	80	44	58	58	51	36	39	42
Total CO2 Emissions from Shipping	1,135	977	914	1,021	943	910	930	932
Total CO2 Emissions from Shipping (%)	4	3	3	3	3	3	3	3
Percentage of International Shipping to Total Shipping Emissions	81	88	85	84	85	88	87	87

Around 15% of global NO_x and 13% of global SO_x are emitted from the shipping industry. It has been projected that maritime CO_2 emissions will be increased by 50% to 250% in four BAU scenarios [3] within 2050.

It is the responsibility of the IMO to regulate the world shipping sector. To date, there is only one regulation to improve the ship's energy efficiency related to new ship design: the Energy Efficiency Design Index (EEDI). The target of this regulation is to improve ship efficiency by 10%, 20%, and 30% within 2019, 2024, and 2025 or after, respectively. As the regulation is related to the new ship only, clearly it cannot reduce the GHG emissions effectively. However, IMO is developing strategies to reduce GHG emissions from maritime vessels. The initial strategy has been delivered in 2018, and the comprehensive strategy will be available within 2023. IMO strategy will include short, mid, and long-term actions to reduce the GHG emissions from marine transportation. In the short-term measure, it includes limiting the ship's speed as the power requirement of the main engine is proportional to the cube of the speed. It has been found that reducing ship speed is a cost-effective option to lower GHG emissions [4]. In the mid and long-term initiatives, the main focus is on new marine technologies and low and zero-carbon fuels. The Institute of Marine Engineering, Science and Technology (IMarEST) and the Royal Institution of Naval Architects (RINA) suggested that with the help of existing technology, the GHG emissions can be reduced 7.5% to 19.4%. However, for a large amount of GHG emissions reduction, zero or low-carbon fuels are needed.

Natural gas is a potential candidate that can be used in marine vessels. Natural gas has some limitations like limited availability due to higher land-based demand and lower density of volumetric energy. Also, natural gas requires a higher area for storage compared to fossil fuel. The fuel cell is another potential candidate to solve the emissions problem from marine ships. However, due to lower availability and lower volumetric energy density, the fuel cell is not a feasible option. Also, the fuel cells employ natural gas or traditional fossil fuel which will make the system more complex and will not solve the emissions problem. Battery electric propulsion could be used to reduce GHG emissions from maritime vessels. Although battery is promising in the marine industry, mass using of the battery will have some environmental impact as it requires metals, non-metals, and rare earth material which generates environmental pollutants. The negative impact of large-scale battery usage will significantly change the implementation of batteries in the marine sector [5]

Renewable energy sources could be possible solutions to reduce GHG emissions. Possible renewable energy sources for marine ships are wind energy, solar energy, biofuels, wave energy. Wind energy can be used as soft sails, rotors, fixed wings, kites, and conventional wind turbines. Marine ships may need to be retrofitted to integrate the renewable energy or design accordingly during shipbuilding. The contribution of renewable energy in marine

ships will be limited even in optimistic scenarios because the availability of renewable energy resources depends on the weather, large amount of energy cannot be stored economically with existing technology, and constraints to implementing renewable energy in marine ships. Hence, renewable energy can offer to reduce fuel consumption by integrating with the marine diesel engine. As the contribution of renewable energy is limited, most of the energy will be served by the diesel engine. Hence, the integration of renewable energy with fossil-fuel-based energy systems is not a feasible option to reduce GHG emissions to the desired level. To make the marine vessels free from emissions, fossil fuel-based energy systems need to be replaced by emissions-free energy systems. Nuclear energy is free from emissions during operation although there are some pollutants emit during the mining, milling, transportation, plant construction, and decommissioning stage. As per IMarEST reports, nuclear power the only option which is emission-free and can replace fossil fuels [6]. Hence, small-scale nuclear reactor: Microreactor (MR) could be a suitable candidate to replace the fossil fuel-based energy systems from marine transportation.

In this study, Nuclear-Renewable Hybrid Energy Systems (N-R HES) is introduced in marine vessels. The energy requirement of the marine ship is estimated based on real data. The proposed system is analyzed and compared with conventional energy systems based on technical, environmental, and economic KPIs. The technical and economic model has been developed in HOMER and MATLAB Software. The optimal configuration of the systems is determined by using the Differential Evolution (DE) algorithm. A sensitivity analysis is carried out to reinforce the findings of the study.

1.2. **Motivation**

Emissions from ocean-going ships are almost twice the emissions from total registered cars in the US. 15 largest ships emit as much SOx as the world's total 760 million cars [7]. While lots of actions are being taken to reduce the GHG emissions from road transportation, marine ships are often unnoticed. The Marine Environment Protection Committee (MEPC) of the International Maritime Organization (IMO) has set a target in April 2018 to reduce GHG emissions by at least 50% by 2050 compared to 2008 [8]. For reducing GHG emission, increasing energy efficiency & innovation are two prime requirements. IMO has set a target to increase energy efficiency by 30% within 2025 compared to 2014. Several studies have been carried out to improve the energy efficiency of marine ships; like: Identification of optimal trim configurations [9], up to 10% reduction of fuel consumption by optimizing ship operation [10]. Besides, several innovative approaches have been taken. The introduction of renewable energy in the marine ship is one of the innovative approaches to reduce GHG emissions. Integration of RESs in ocean-going marine ships could be an option to make marine transportation free from emissions. Ocean-going marine ships require a large amount of reliable energy to support the propulsive load demand.

RESs are intermittent, and a large amount of energy cannot be stored economically by the available energy storage techniques. Additionally, the penetration of RESs in a marine ship is limited by the available area and total weight carrying capacity of that marine ship. Because of these limitations of RESs in marine ships, there is a requirement of integrating other types of energy sources with RESs to support the baseload energy demand and to avoid the variableness of RESs. Conventional fossil fuel-based generators, like diesel generators, can be incorporated with RESs to overcome these shortcomings of RESs. However, as the penetration of RESs is limited to marine ships, most of the energy is supplied by fossil fuel-based generators. Therefore, the integration of RESs with fossil fuel-based generators merely reduces GHG emissions and is not a feasible option to make marine ships free from emissions. Fossil fuel-based generators need to be replaced by emissions-free and reliable energy sources to make the marine ships free from emissions. Small scale nuclear reactors, such as Small Modular Reactors (SMRs) and Microreactors (MRs), are free from GHG emissions and are competitive candidates to replace fossil fuel-based generators.

To the best of the authors' knowledge, Nuclear-renewable Hybrid Energy System (N-RHES) on marine ships has not been studied. Although N-R HES is a potential solution to make marine transportation free from emissions, its competitiveness over traditional and other hybrid energy systems needs to be evaluated.

1.3. Problem Definition

The integration of nuclear-renewable energy in marine ships could be a possible option to reduce the GHG emission of marine ships. There is a dearth of understanding on how to integrate nuclear and renewable energy in marine ships that covers design, optimization, and techno-economic analysis of this hybrid energy system. A systematic approach is required to study the whole system, not the individual parts. To the authors' best knowledge, no study has been carried out on the integration of nuclear-renewable energy in marine ships. Although lots of studies are being carried out for land-based N-RHES, the marine sector is completely different from the land-based system in terms of energy demand and environmental attributes (solar irradiance, wind speed). Unlike, land-based system, the energy demand of marine ships is not readily available. Hence, estimation of the energy demand of marine ships on a given route is required to solve real-world problem. To evaluate the competitiveness of this hybrid energy system, a comparison among other energy systems in terms of technical and economical KPIs is required.

Optimization of this hybrid system needs to be studied to reduce the operational cost, GHG emissions, and increase the revenue which will help the ship operators to take decision on the investment. The optimization of this interconnected system needs to address all the lifecycle costs of the major system components to make the analysis more realistic. Also, there are some constraints to implement the N-R HES in marine ships in terms of available area and load-carrying capacity of the marine ships. The energy management and reliability

of the proposed energy system need to be verified. An intelligent optimization technique can address these constraints and evaluate the energy management and reliability of the system.

The validation of the result is an important criterion of any scientific research. The validation can be made by comparing with previous works or using another approach and check the trend of change by varying any system parameter. A sensitivity analysis is required to see the behavior of the findings. Sensitivity analysis helps the user to determine whether or not the proposed system is sensitive to certain parameters. Sensitivity analysis is carried out by changing certain parameters like project lifetime, availability of renewable energy resources, discount rate, inflation rate, project lifetime, electrical power demand. By using the sensitivity analysis, research findings are reinforced by carrying out the sensitivity analysis

1.4. **Objectives**

The main objective of this thesis is to design a simple hybrid nuclear-renewable energy system in the marine ship, techno-economic evaluation of Nuclear-Renewable Hybrid Energy Systems for marine ship, and optimize the systems to propose the optimal sizing of nuclear and renewable energy sources to minimize the Net Present Cost (NPC), Levelized Cost of Energy (LCOE), and CO_2 emissions while addressing the related constraints. The objectives of the thesis are as follows:

1. Estimate energy demand of marine ship based on real data using ITTC-57 method and Gertler Series Data chart for a given route.
    - Take a marine ship and identifying its' route for a given period
    - Collect Automatic Identification System (AIS) data of that marine ship containing time-wise GPS position, speed, and heading. This AIS data is collected from FleetMon, a German-based company that collects real-time ship information. With the Data License Agreement (DLA) between Ontario Tech University and FleetMon, they supported solely this thesis by providing all necessary AIS data.
    - Estimate marine ship propulsive energy demand based on speed, breadth, draught, frictional resistance, residual resistance and using ITTC-57 method and Gertler Series Data chart.
2. Propose a simplified design of hybrid energy system of the marine ship to replace conventional fossil fuel-based energy system with Nuclear-Renewable Hybrid Energy Systems.
    - Estimate the electrical energy demand of marine ship
    - Calculate the solar irradiance to estimate the energy from solar PV module in every position of the marine ship route
    - Calculate the wind speed to estimate the output power of the wind turbine

3. Techno-economic evaluation of nuclear-renewable hybrid energy system in marine ships and make comparison with three other energy systems in terms of Net Present Cost (NPC), Cost of Energy (COE), and GHG emission in HOMER software.
    - Model four energy systems namely 'Conventional Fossil Fuel-based energy system', 'Standalone Nuclear Energy System', 'Renewable and fossil fuel-based hybrid energy system', and 'Nuclear-Renewable Hybrid Energy System'.
    - Define key performance indicators to make a techno-economic evaluation of these four energy systems
    - Identify the limitations of HOMER software in this study
4. Optimize the nuclear-renewable hybrid energy system in MATLAB Software to address the shortcomings of HOMER software.
    - Define objective function
    - Define constraints of energy systems in marine ships
    - Optimize the system by using the Differential Evolution (DE) algorithm
    - Analyze the different costs of the energy systems and determine how different cost contributing to different energy systems
    - Compare the optimized energy systems and identify the most feasible energy system for maritime transportation based on technical, economic, and environmental KPIs
    - Compare the findings of the DE algorithm with PSO to validate and measure the performance of the DE optimization technique. Evaluate the impact of the control parameters of the DE algorithm by employing the Adaptive Differential Evolution (ADE) algorithm.

5. Conduct a sensitivity analysis and make a comparison among different optimization techniques
    - Identify the parameters for the sensitivity analysis
    - Vary the parameters and determine the impact on the performance of different energy systems
    - Identify the performance of different optimization techniques of N-R HES in marine ships and compare them to determine the best performer.

.

1.5. Thesis Outline

There are seven chapters in this thesis. The current chapter is about the "Introduction" of the thesis. This chapter covers the background, motivation, problem description, and objectives of the thesis.

The 2nd chapter is about the literature review on the impact of marine transportation on the environment, future ship powering options, nuclear power in ship, integration of renewable and fossil fuel in marine vessels, nuclear-renewable energy integration on land-based

systems, a brief discussion on Micro Modular Reactor (MMR), different optimization technique of Hybrid Energy System (HES), and key performance indicators (KPIs).

Chapter-03 focuses on the methodology of this thesis. This chapter covers the research framework of the thesis, methods of data collection and calculation, analysis on methodological choice, and assumptions that are considered in this study.

The system modeling of each component of energy systems is discussed in Chapter-04. The modeling of MR, Solar PV, Wind Turbine and Energy Storage systems, and Diesel generators is covered in this chapter. The associated parameters of the system components are tabulated in this chapter.

Chapter-05 is about the modeling of the simulation in MATLAB software and HOMER. This chapter discusses the objective function, constraints, decision variables that are needed for the optimization in MATLAB software. The steps of DE, ADE, PSO, and HOMER optimization are addressed here.

The result of this study is captured in Chapter-06. In the first part, the findings from HOMER software are discussed. The findings from DE optimization technique are discussed in the second part of this chapter. The performance of DE, ADE, and PSO is evaluated in this chapter. Finally, a sensitivity analysis is carried out by varying different system parameters.

Finally, Chapter-07 concludes with a summary and future scope of work of this study. The main contribution of this research is also discussed in this chapter.

Chapter 2: Literature Review

To the best of the authors' knowledge, nuclear-renewable hybrid energy system for ocean-going ships has not been discussed and analyzed extensively. However, several studies have been carried out on the stand-alone nuclear energy system and fossil fuel-renewable hybrid energy system in marine ships. Some studies focused on the land-based energy system. The literature reviewed for this research is presented in seven main sections. Section 2.1 provides an overview of the impact on the environment due to maritime transportation, and ship powering options. Section 2.2 offers a discussion on nuclear energy in marine ships and previous studies on it. The integration of renewable and fossil fuel is discussed in Section 2.3. Nuclear-Renewable Hybrid Energy Systems (N-R HESs) in land-based applications is reviewed in Section 2.4. As MR is a new concept, a brief idea of MR and a short discussion on the lifecycle of nuclear fuel and MR are carried out in Section 2.5. Section 2.6 is about the review of different optimization techniques for hybrid energy systems. The Key Performance Indicators (KPIs) that are considered in this research are covered in section 2.7.

2.1. Marine Transportation, Environment and Future Ship Powering Options

More than 90% (by weight) of global trade is carried out by marine transportation. The volume of seaborne trade was more than 10 billion tons in 2015. The trend of international seaborne trade is presented in Figure 2-1. The international trade by marine transportation has been increased in the shown years except 2009. In 2009, the total amount of trade was 7,858 million tons that was reached 10,048 million tons (+21.79%) in 2015.

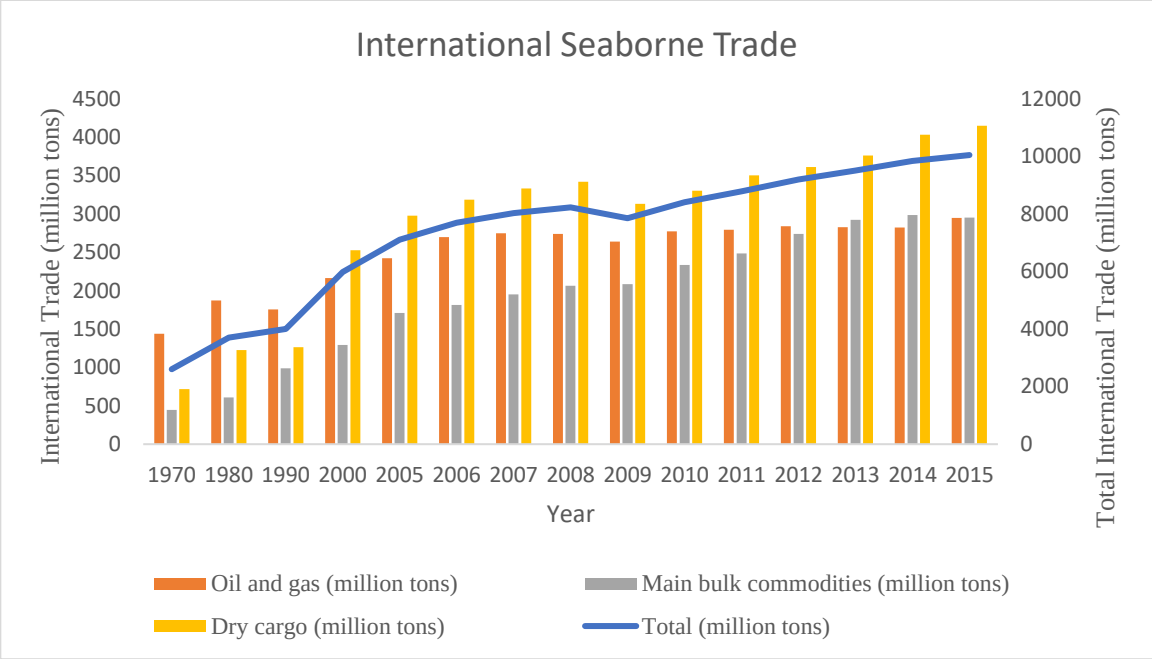

Figure 2-1: International Seaborne Trade

Merchant ships can be categorized as general cargo ships, bulk cargo ships, container ships, tankers, dry bulk carriers, passenger ships & tugs. The total number of merchant ships was 53,629 as of 1st January 2019 [11]. Figure 2-2 shows the number of merchant ships of different ship classes. The General Cargo Ships & Bulk Cargo Ships comprise more than 50% of merchant ships.

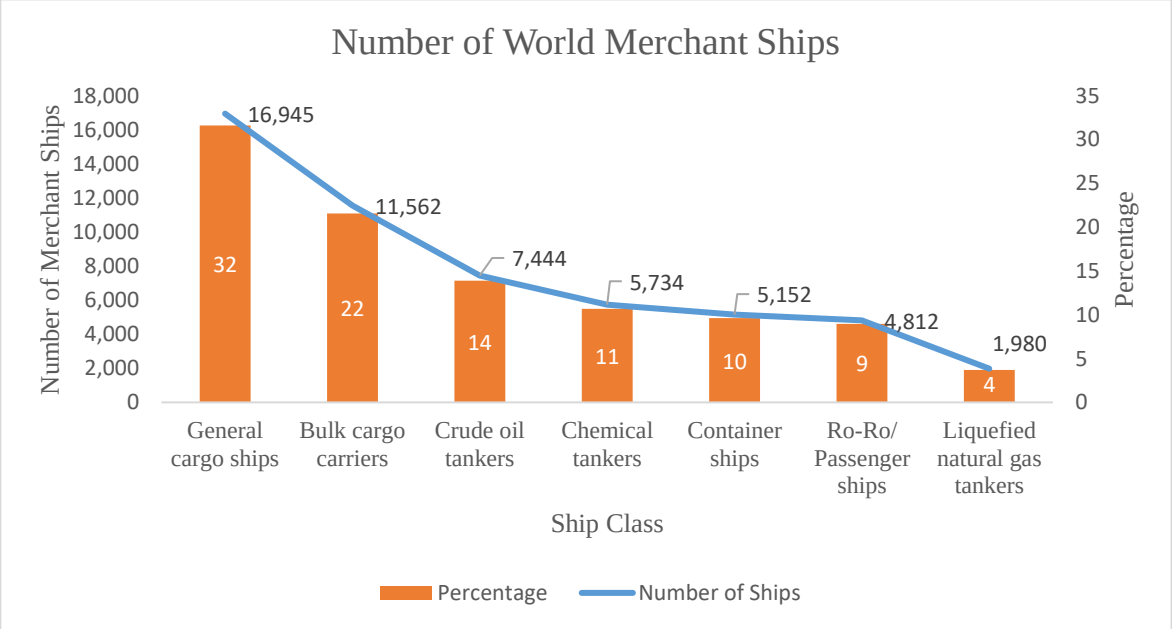

Figure 2-2: Distribution of World Merchant Ships

Although international shipping is helping in the global trade, it has negative impact on the environment like air pollution, underwater noise, negative effects associated with oil spills, Hazardous and Noxious Substance (HNS) spills, and end-of-life ship disposal. Marine transportation is responsible for 33% of the global trade-related emissions, and accounted for 3.3% of global CO_2 emissions [12]. Marine transportation is responsible for 10% to 15% of global anthropogenic NO_x and SO_x emissions. In 2007, around 25 million tons of NO_x, 15 million tons of SO_x , and 1.8 million tons of PM were emitted from maritime shipping. The CO_2 emissions from the shipping industry were 910 million tons in 2013, and in 2015 it was 932 million tons (+2.4%). International shipping is accounted for 87% of total CO_2 emissions while domestic shipping and fishing are responsible for the rest 13% of CO_2 emissions. With respect to ship class, container ships, bulk carriers, and oil tankers emit 55% of the total CO_2. They emit 23%, 19%, and 13% of CO_2 respectively. These three ship classes are also accounted for 84% of total shipping transport. Similarly, out of 223 flag states, six flag states are responsible for 53% of CO_2 emissions, and these six flag states are accounted for 66% of the world shipping fleet's deadweight tonnage [2]. Figure 2-3 presents the CO_2 emissions from different ship classes and Figure 2-4 shows the CO_2 emissions from different flag states.

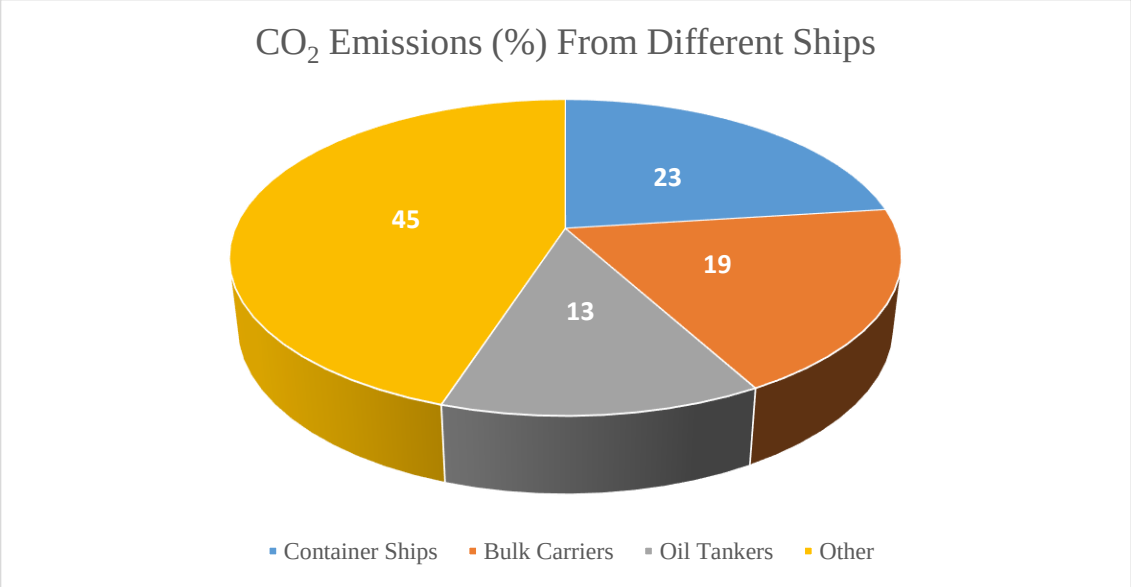

Figure 2-3: Percentage of CO_2 Emissions from Different Types of Ships

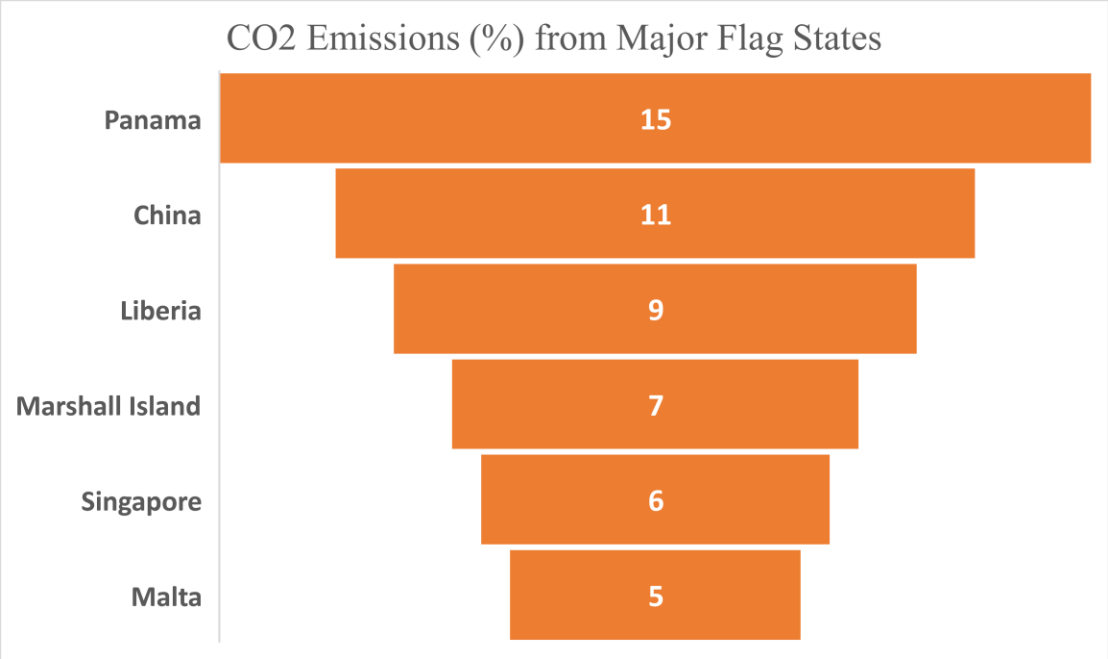

Figure 2-4: Percentage of CO_2 Emissions from the Major Flag States

Several studies have been carried out to analyze the impact of maritime transportation on the environment. Gara et al.[13] estimated the emissions in the port of Barcelona. They considered GHG emissions per ton of cargo handled or per passenger as the indicators of GHG emissions from the port. They found out a total of 331,390 tons of GHG emissions (CO_2 eq) in the port in 2008. They also revealed that ship movement was account for half of the emissions while the other half was attributed to port-related operations. The ship movement-related emissions were due to the ship's arriving, departing, hotelling, and maneuvering. The consumption of electricity in the port, fuel heating, fuel transportation, and waste management were responsible for port-related emissions in this study. They also identified the car carrier ships as the highest GHG emitter with 6 kg GHG emissions per ton of cargo handling.

The investigation of GHG emissions in four ports namely, Port of Long Beach, Port of Gothenburg, Port of Osaka, and Sydney Ports was carried out in [14]. To quantify the amount of GHG emissions they used the model developed by the IVL Swedish Environmental Research Institute. The authors considered five operational modes of ships that were "in the fairway channel", "at anchor", "in the port basin", "maneuvering", and "at berth". The calculated GHG emissions for Sydney, Osaka, Long Beach, and Gothenburg were 95,000, 97,000, 240,000, and 150,000 tons respectively. They concluded that to reduce the GHG emissions from maritime transportation, alternative fuel, and ship design need to be under more strict policy and regulation. Also, the authors suggested some processes to the port authority to facilitate the reduction of GHG emissions.

Chang et al. [15] investigated the relation among GHG emissions, energy consumption, and GDP. They used co-integration and Granger causality test in the study. Eight countries

of Kyoto Protocol's Annex 1 were evaluated in their investigation. The authors found that GDP and marine energy consumption were the main contributors to increased GHG emissions. They concluded that emissions from marine transportation were strongly tied with energy consumption rather than the GDP. They suggested the policymakers to focus on the energy efficiency of marine vessels by exploring the innovative design of the ship hull and engine.

The Royal Academy studied the conventional and future ship powering options in [16] that are shown in Figure 2-5. The authors divided the ship powering options into two major categories; conventional ship powering options and non-conventional (future) ship powering options. The conventional ship powering option is categorized into Diesel engine, Biofuels, LNG, and Gas Turbine. The diesel engine is the most common ship power option. They outlined that although there are some advantages of diesel engine technology, it causes significant damage to the environment. Biofuels can be an alternative to conventional fuels. However, to satisfy the current demand for marine transportation, a significant amount of land areas are needed. A heat source is required to evaporate LNG from the gas which is one of the shortcomings of LNG. Gas turbines have a high power density but the efficiency of gas turbines decreases with the increase of ambient temperature. Also, the thermal efficiency of the gas turbine is less than the diesel engines.

Under the non-conventional ship powering option, nuclear propulsion is a promising solution to reduce GHG emissions. The authors outlined that nuclear propulsion will give flexibility in the ship design and will make the ship free from future price fluctuation like fossil fuel. However, international regulation, perception of general people towards nuclear-powered merchant ships, training, refueling, and storage of spent fuel are some of the areas where the related stakeholders should focus. The battery-powered ship could be an option to reduce GHG emissions. This study concluded that battery is suitable for small to medium-sized ships for short sea voyages. Further development is required for fully battery-powered marine ships. The fuel cell is an innovative solution for marine propulsion but this is suitable for hybrid and low power propulsion and use for auxiliary machinery in marine ships. Also, the fuel cell has a lower power density than the diesel engine and produce DC electrical current, which are some of the shortcomings of fuel cell in marine ship. Renewable energy like wind energy and solar energy can be used to reduce GHG emissions from marine ships. Nevertheless, due to the intermittency of renewable energy sources, it is not suitable for standalone marine propulsion, and more preferable for auxiliary propulsion. Hydrogen is another option for future marine propulsion but there are some safety issues with hydrogen and it has a lower power density than other potential ship powering options. Anhydrous ammonia is a poisonous and dangerous gas that can be burned in both diesel engines and gas turbines. However, handling this poisonous gas requires new procedures to adopt. In the hybrid propulsion option, two or more powering options are employed to optimize the performance of the energy systems in terms of technical, economic, and operational points of view.

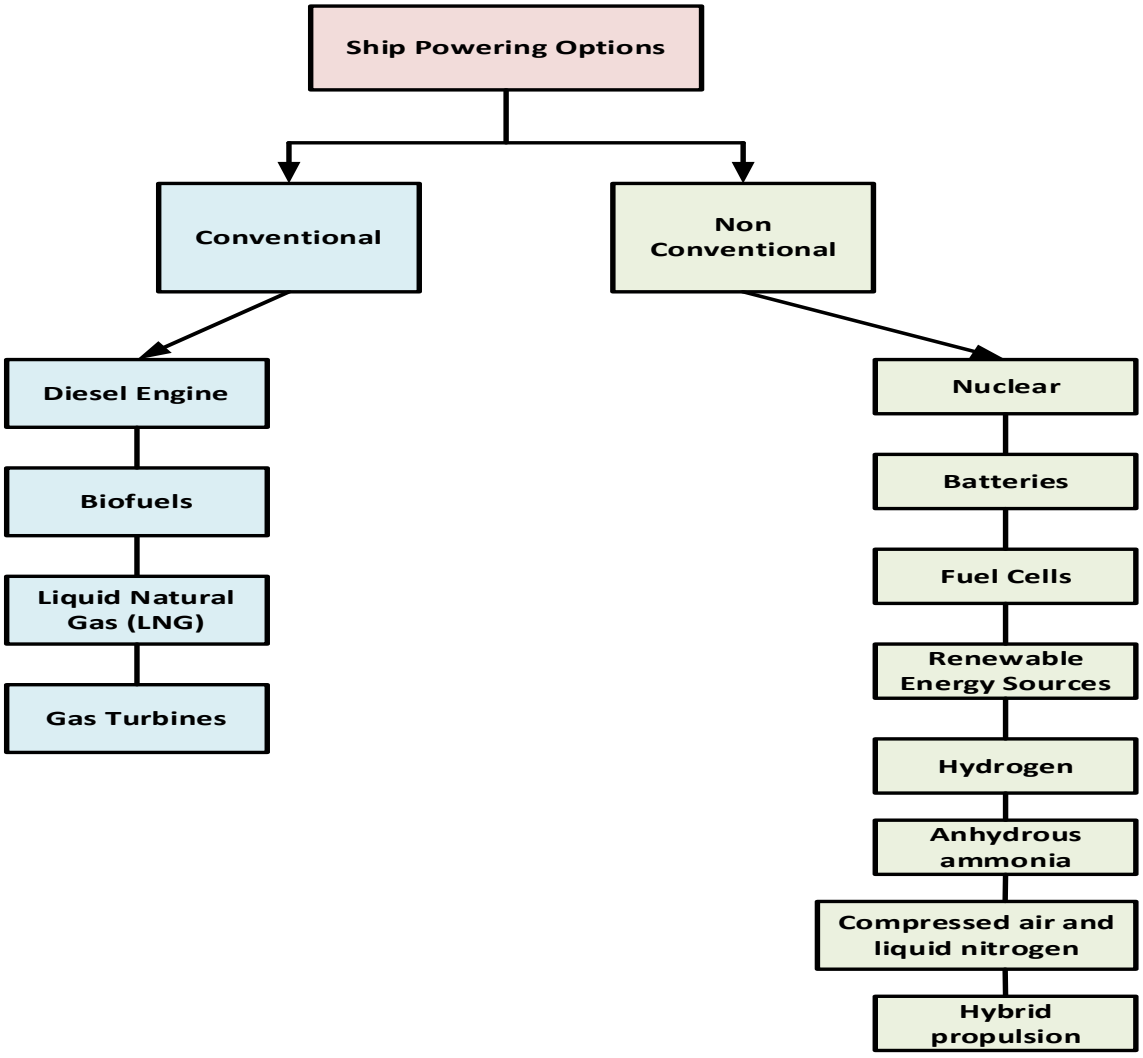

Figure 2-5: Ship Powering Options

2.2. **Nuclear Power in Ships**

Nuclear power in marine vessels is not a new idea. There were about 700 naval nuclear reactors and 200 of them are still in operation for military use [17]. In the past, there were also nuclear-powered merchant ships. In 1962, a nuclear-powered cargo/passenger ship 'NS Savannah' was built. The cargo and passenger carrying capacity of this ship was 10,000 tons and 60 passengers respectively. Around 90 million dollars was spent to build this ship and 12 million was earned in the 5 years operation. This ship used low enriched uranium, and the civil work was completed by the Westinghouse. The ship was abandoned in 1971 due to economic competitiveness, lack of component reliability, and wage dispute between nuclear engineers and deck workers. The nuclear-powered German ship 'NS Otto Hann' was ordered in 1962 to the shipyard 'Kieler Howaldtswerke AG'. It was in operation

for 10 years and was dismantled in 1979. This ship was traveled around 650,000 nautical miles. This ship faced regulatory issues, like refusal from many port authorities to enter into the ports. Due to the restriction from port authorities and high operating costs, the ship was taken off earlier than expected. This ship used compact PWR specially made for that ship. Japan built the 'NS MUTSU' which has reactor power rating as 36 MW. This ship was completed in 1972 and just after the first test announcement, local people including fishermen protested against it. However, the government managed to test in the deep sea with low power in 1974. During the test, when the reactor reached 1.4% of its' total power, neutron radiation was detected outside the nuclear shielding. The ship was undergone major repair and was completed again in 1991. Due to negative public perception and multi companies involvement, this ship was decommissioned in 1992. Table 2-1 represents a list of nuclear-powered ships (non-military), country of origin, reactor type, power output, building year, current status, and decommissioning year. Figure 2-6 shows the distribution of nuclear-powered ships presented in the below table.

Table 2-1 Nuclear Powered Ship (Non-Military)

Ship Name	Country	Ship Type	Reactor Type	Power Output (MW)	Built	Status	Decommissioning Year
Savannah	USA	Container	PWR	80	1962	Not In Service	1977
Otto Hahn	Germany	Ore Carrier	FDR	38	1968	Not In Service	1982
Mutsu	Japan	Cargo	PWR	36	1972	Not In Service	1996
Vaygach	Russia	Icebreaker	KLT-40M	171	1989	In Service	
Artika	Russia	Icebreaker	PWR	342	1975	Not In Service	2008
Sevmorput	Russia	Icebreaker	KLT-40M	135	1988	In Service	
Taimyr	Russia	Icebreaker	KLT-40M	171	1989	In Service	
Sovetski Souz	Russia	Icebreaker	OK-900A	342	1989	In Service	
Let Pobedy	Russia	Icebreaker	OK-900A	342	2007	In Service	
Lenin	Russia	Icebreaker	PWR	318	1989	Not In Service	2008

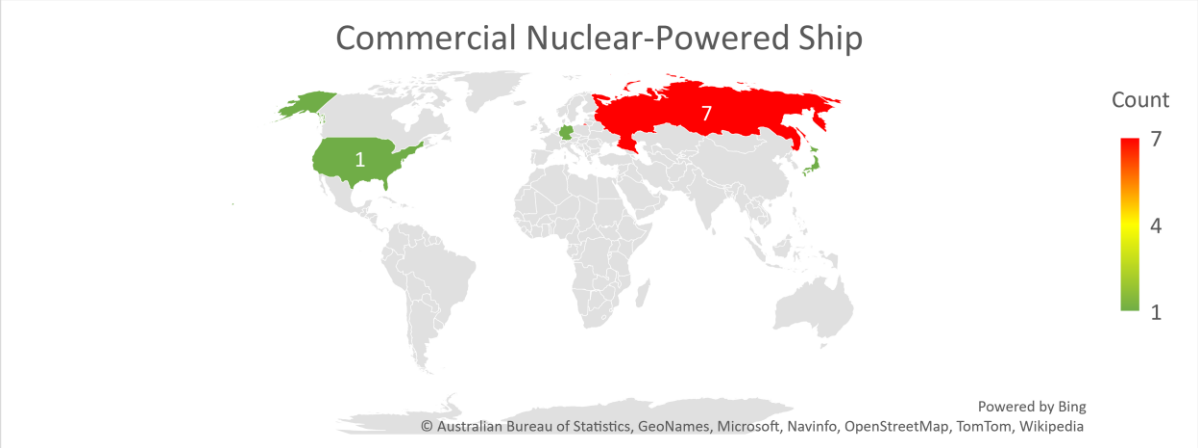

Figure 2-6: Distribution of Nuclear Powered Ships

Several researchers studied the nuclear-powered ship, and discussed the past work, design, associated risk, position of the nuclear plant in the ship, and safety of the ship.

A survey on the past nuclear-powered merchant ships is done in [17]. In this paper, the authors summarized the past nuclear-powered merchant ships in terms of the timeline of the ships, types of reactors, engineering designs, and underlying reasons for the success and failures. They pointed out social issues like the different public perceptions about the nuclear safety of nuclear-powered merchant ships and military ships. They also explained how nuclear accidents affect the public acceptance of nuclear ships. The authors concluded that nuclear propulsion is economically feasible and people engagement is important for the success of nuclear propulsion which can be achieved by informing the gain of using nuclear power and minimizing the misinformation about it.

A review of the past work and recent development in the area of nuclear-powered ocean-going ships was studied in [18]. The authors proposed a concept design of a cargo ship, powered by a 25 MWe. SMR. They also studied the associated risk with different power train systems and SMR locations. The authors suggested that SMR location would be preferred at the aft of the cargo tank.

Carlton et al. [19] summarized the nuclear physics and discussed nuclear plants for marine ships considering reactor control, reliability, location of the plant in the ship, protection of reactor, irradiation effect on structural steel of the ship, refueling, and radiation hazard area. They also studied the application of nuclear plant on different marine ships. They considered tankers, container ships, and cruise ships. For each type of ship, they took two sizes, one is a larger size and another is a conventional size. This study concludes that there is no technological ground that can prevent the use of nuclear energy in merchant ships. However, they emphasized altering the general arrangement of ships to provide the best possible operating environment to the reactor. They also considered the importance to design the structure of the ship to distribute and absorb the energy of impact and make the ship safe against vibration and collision risks.

Gravina et al. [6] addressed two important flaws of nuclear-powered containership, which are route restrictions to enter some national territorial waters, and the risk of accident with severe consequences. They proposed a conceptual design of a nuclear-powered containership that can operate freely without any objection from the port states and can withstand any accident without any cataclysmic consequences. They suggested a modular containership where there would be two modules, one is a propulsion module and the other is a cargo module. The propulsion module contains the nuclear plant whereas the cargo module carries the payload. These two modules will be disjointed before entering into national territorial waters. The propulsion module will remain in international waters and the cargo module will enter into national territorial water with the help of any secondary propulsion system. They analyzed five different modular nuclear containership concepts and concluded that the tug/barge system would be the best concept based on subjective analysis. For avoiding any catastrophic incident resulted from an accident, they suggested strengthening the reactor compartment by cutting decks technology or providing 'Y' shaped frames consisting of sandwich material.

The feasibility of nuclear propulsion in 'FastShip' is studied in [20]. The 'FastShip' is a conceptual cargo ship which speed is greater than the conventional ship. The speed of the 'FastShip' is 35 knots, whereas the average speed of the general cargo ship is 18 to 21 knots. The 'FastShip' can provide service within five to seven days across the Atlantic Ocean, and for the conventional ship, it takes around 14 to 35 days. In this study, the authors considered two types of energy systems for the ship. The first energy system is only nuclear power-based, and the second energy system is a hybrid energy system (Gas Turbine Modular Helium Reactor). This study concludes that although the standalone nuclear power-based energy system is an economically feasible option for the 'FastShip', the hybrid energy system is preferred due to the difference between maximum speed and cruising speed, better cost balance in operation, and redundancy in the power source.

After getting inquiries from Murmansk Shipping Company, HBR (Haven Bedrijf Rotterdam; Harbor Company Rotterdam) researched the cost of getting a permit to enter into the port for 'Sevmorput'- a nuclear-powered ship. It investigated the route between Rotterdam and the Far East. This study concluded that it would cost at least €522,000 for a single permit without considering political disinclination and other policies [21].

The potential of nuclear-powered marine vessels is enormous. The total power capacity of the world's merchant shipping is around 410 GWt which is one-third of the total nuclear power in the world. In 2009, Chinese shipping company 'Cosco' started a collaboration with China's nuclear authority to develop marine vessels powered by nuclear energy. However, the accident in Fukushima in 2011 made them aborting the project. The Babcock International's marine division studied the feasibility of the nuclear-powered LNG. They concluded that for some specific routes, nuclear energy is more attractive than conventional energy. Although the fuel cell has a prospect for becoming the alternative fuel in the future in marine transportation, it will be limited to short-range ships due to the high storage cost [22]

Some companies started working on the nuclear propulsion system. TerraPower, a nuclear innovation company, founded by Bill Gates has recently started a collaboration with 'Core-Power', a London-based company working in the area of marine nuclear reactor design. This project aims to produce synthetic zero-carbon fuels for the smaller ships, and design a reactor that will be capable to drive the large ocean-going ships. They divided the project into two phases. In the first phase from 2024 to 2028, they will focus on the production of synthetic zero-carbon fuels, and in the second phase from 2028 onwards, they will focus on the design of nuclear reactors for large ships [23]

Another company 'HolosGen' is working on developing a modular nuclear reactor that can deliver power from 3 MWe to 81 MWe. This reactor could fit into an ISO standard shipping container (40 ft). It uses 8% to 15% enriched TRISO fuel and the refueling interval is 12 to 20 years. One of the applications of this reactor is using it in a large ship. They considered a typical Neo Panamax (NPX) cargo ship that is capable to carry 12,000 TEU for one of the potential ships of this reactor. They showed that their reactor will cost only 219 million USD whereas the conventional fuel will cost 1.6 billion USD in 20 years of project life [24].

2.3. **Renewable and Fossil Fuel in Ship**

Shuli et al. [25] studied the economic advantages of introducing renewable energy in the marine ship. They considered a hybrid energy system, comprising solar PV, wind power generation, ESS, and diesel generator. They analyzed three different cases of energy systems of an oil tanker namely, 'Only Diesel Generator', 'Diesel Generator and Renewable Energy', and 'Diesel Generator, Renewable Energy and ESS'. This study shows that with optimization, 'Diesel Generator, Renewable Energy and ESS' is economically more feasible than the other two energy systems and has the lowest CO_2 emissions among the three cases. However, the amount of CO_2 emissions from the optimized energy system is still significant due to the presence of fossil fuel-based generator.

Techno-economic analysis of integrated PV systems with diesel generator into marine ships has been done by Qiu et al [26]. In this case study, they considered six different navigation routes namely 'Asia-Buka-Australia', 'Asia-Bering-Europe', 'Asia-Malacca-Gibraltar-Europe', 'Asia-Panama-Europe', 'Europe-America', and 'Europe-Cape Town-Australia'. They compared the navigation routes in terms of Net Present Value (NPV), Internal Rate of Return (IRR), and Levelized Cost of Energy (LCOE). This study showed that the hybrid PV-Diesel power system for the marine ship was financially feasible. Also, they marked the 'Asia-Malacca-Gibraltar-Europe' navigation route as the most feasible route among all the six routes for the hybrid energy system.

Diab et al. [27] compared hybrid energy systems between marine ship and land-based system. They took a route from Dalian in China to Aden in Yemen of an oil tanker. In the

hybrid renewable energy systems, the authors considered two diesel generators and solar PV. They considered the same electrical load demand for both ship and land-based system. The authors calculated the average solar radiation of six stops in the ship navigation route, and the same solar radiation was considered for the land-based system. For the land-based system, the authors did not consider any limitation for solar PV system capacity but for the ship, they limited the solar PV system to 300 kW considering the usable area of that ship. They analyzed four combinations namely 'Only Diesel Generator', 'Diesel Generator and Battery', 'Diesel Generator and Solar PV System', and 'Diesel Generator, Solar PV System, and Battery'. For 'Only Diesel Generator' and 'Diesel Generator and Battery', there is no difference between the ship and the land-based system in terms of COE, NPC, and GHG emissions. This study suggests that for both ship and land-based systems, 'Diesel Generator, Solar PV system, and Battery' is the optimal solution although GHG emissions are around 9 times higher in ship compare to the land-based system because of the low penetration of PV system in the ship.

Optimal sizing of solar PV, diesel generator, and battery ESS in an oil tanker was studied in [28]. The authors considered four different cases for economic analysis namely 'cost analysis for diesel generator only', 'cost analysis for diesel generator and solar PV', 'cost analysis for diesel generator, solar PV, and EES', and 'cost analysis considering multi-objective optimization for diesel generator, solar PV, ESS, and CO_2 emissions'. They suggested that with optimization, Net Present Cost (NPC) and CO_2 emissions of a hybrid energy system would be the lowest.

Feasibility analysis on a pure battery-electric propulsion system for large ocean-going ships was carried out in [29]. This paper analyzed three different sizes of container ships, four different sizes of bulk carriers, and one large ro-ro ship. This study suggests that a battery-powered energy system is feasible only for a short distance of a ro-ro ship. They also concluded that pure battery-electric propulsion was not feasible for long-distance voyage due to battery weight and volume.

The feasibility of integrated solar PV, fuel cell, and diesel generator in a cruise ship is studied in [30]. The cruise ship operates in the baltic sea between Mariehamn (the Aland Islands) and Stockholm (Sweden). The authors used an optimization technique to determine the optimal configuration of the system components. In the latter part, this hybrid system is compared with the conventional diesel-electric system in terms of COE, renewable energy penetration, and CO_2 emissions. They concluded the hybrid energy system had higher renewable energy penetration, and lower CO_2 emissions. However, the COE is higher in the Hybrid energy system due to the high upfront cost of renewable energy systems, and the lower availability of solar irradiance in the considered sea route. They proposed that this hybrid system could be cost-effective if it was considered in an area where the solar irradiance is high like Sharjah, UAE.

2.4. **Nuclear-Renewable Integration**

Diab et al. [27] showed the difference between the land-based HRES and ship-based HRES. They indicated that the solar irradiance on land is fixed but for the ship, it changes according to the position (latitude and longitude) of the ship and the angle of the sun rays incidence. Also, the wind speed changes as the ship change its' position but on land, it is fixed. The total allowable area of the ship to install the hybrid energy system is limited but there is no such kind of limitation in land-based energy systems. Moreover, the total cargo carrying capacity of a ship is fixed and is directly related to the revenue of the ship. The shipping authority will not be interested to carry the additional load for installing the hybrid energy system compared to conventional energy systems as it will decrease their revenue. This study addresses all the differences between the land-based energy system and ship-based energy system while planning the N-R HES on Ship.

To the best of the authors' knowledge, no study has been carried regarding N-R HES for maritime vessels. However, several studies have been done on land-based N-R HES systems. A combination of renewable energy generation, nuclear reactors, and industrial processes have been explored in [31]. Six features of interconnection have been identified in this study—electrical, thermal, chemical, hydrogen, mechanical, and information. This study concluded that the integration of nuclear and renewable energy could be a potential solution for long-term projects. This document also pointed out that the nuclear-renewable hybrid system could supply load-following power, and excess energy could be used for the production of secondary energy-intensive products. Nevertheless, system analysis, technical advancement, and optimization are required to implement this hybrid system in practice.

A comparison of three scenarios, namely a nuclear power plant, a combination of a nuclear plant and a wind facility, and a mixture of nuclear and wind energy sources with a hydrogen generation facility, was done in [32]. This study reported that with optimization, the nuclear-wind system with a hydrogen production facility could be an economically viable option in the future. Sensitivity analysis has also been carried out to realize the impact of the energy market, depreciation rate, discount rate, and time horizon in terms of internal rate of return (IRR), Levelized cost of energy (LCOE), net present value (NPV), and payback period.

In [33], the author highlighted the critical challenges of nuclear-renewable integration, such as integration values, regulatory, financial, technological, plant testing, and plant operation. The author suggested that the information linkage-based nuclear-renewable coupling would be able to overcome the complexities of the integration process.

Three scenarios of N-R HES to supply thermal energy from the system were examined in [34]. The first arrangement includes a nuclear reactor, thermal power cycle, wind power plant, and electric boiler; the second scenario comprises a nuclear reactor, thermal power cycle, wind power plant, and electric thermal storage; the third configuration is a combination of a nuclear reactor, thermal power cycle, wind power plant, electric boiler,

and thermal storage. The electric thermal storage stores thermal energy that is generated by electricity. The financial performance analysis tells us that the third arrangement has the lowest NPV and IRR. The result is evident since the authors assumed that the cost of heat generated from the nuclear reactor is less than the price of heat generated from gas (electric boiler).

The financial analysis of nuclear-renewable energy integration was carried out in [32]. The authors considered three cases, namely nuclear/hydrogen/wind hybrid energy system, nuclear/wind energy system, and only nuclear energy system. They compared the three scenarios based on the payback period, Cost of Energy (COE), Internal Rate of Return (IRR), and Net Present Value (NPV). They concluded that for energy generation in the future, nuclear/hydrogen/wind hybrid energy system could be a feasible project.

Baker et al. explored a nuclear hybrid energy system comprising of a 300 MWe Small Modular Reactor (SMR), Wind Turbine (WT), battery storage, and a reverse osmosis desalination plant in [35]. They took the SMR as the primary source of energy and considered a fixed rating of SMR. The authors employed dispatch rule built within Risk Analysis Virtual Environment (RAVEN) to model the system. This study concludes that the investment of batteries is only feasible when the penetration of renewable energy is high.

A conceptual hybrid nuclear power plant was studied in [36]. This hybrid energy system consisted of a nuclear power plant, solar PV, and a thermal energy storage system. The authors considered the electricity from the solar PV to superheat the nuclear steam. They compared thermal energy storage with compressed air storage and pumped hydro storage. They concluded that thermal energy storage was economical than pumped hydro and compressed air storage. They also showed that the initial cost of a standalone nuclear power plant was higher than the hybrid nuclear power plant.

Five different energy systems, such as Nuclear-Renewable Micro-Hybrid Energy Systems (N-R MHES), conventional standalone fossil fuel-based energy systems, standalone nuclear energy systems, standalone RES-based energy systems, and RES/fossil fuel-based energy systems are compared in [37]. They compared the five energy systems based on Net Present Cost (NPC), Cost of Energy (COE), and GHG emissions. They concluded that N-R MHES was the most economical energy system. The authors also conducted a sensitivity analysis to reinforce the findings of their study.

An alternative of a diesel generator in a MEG was examined in [38]. The authors considered Microreactor (MR) as a possible candidate to replace the diesel generator within a MEG of Ontario Tech University (UOIT). They considered both the electric and thermal demand of UOIT. They used Particle swarm optimization to minimize the Net Present Cost of the Hybrid energy systems and find out the optimal configuration of it. The hybrid energy system contained wind turbine, solar PV, hydropower, biogas generator, and diesel generator. To check the feasibility of the MR as an alternative to DG, the DG was replaced by MR in the hybrid energy systems. They employed a CHP unit to utilize the waste heat

from the DG and BG. To store the electrical energy, they used electrochemical energy storage (EES) and hydrogen storage. The technical and economic KPIs such as Loss of Power Supply Probability (LPSP), Surplus Energy Fraction (SEF), Level of Autonomy (LA), NPC, and LCOE were studied in this paper. They concluded that MR could be an outstanding replacement for the diesel generator considering the technical and economic KPIs for land-based MEG.

Two configurations of N-R HESs in Texas and Arizona were optimized in [39] to learn the system opportunities, difficulties, and complexities. They considered a heat generation plant that was consisted of an SMR, electric grid, wind energy, solar PV, and additional energy conversion units that generate chemical products, like Liquefied Petroleum Gas (LPG), gasoline, and freshwater. The study demonstrated that economic gain could be achieved by the proposed optimizer. They concluded that the higher gain would be achieved if the system decreased its' engagement to produce electricity and increased its' participation to produce secondary commodities like LPG, freshwater, and gasoline. The authors suggested developing online optimization to work with the real-time energy market and commodity prices.

Three types of nuclear-renewable hybridization were presented in [40]. The authors discussed "Direct Coupling", "Single Resource and Multiple products-based coupling", and "Multiple Resources and Multiple products-based coupling". The mathematical model of N-R MHES's economy was done in MATLAB software. To achieve the optimal system configuration and to minimize the Net Present Cost (NPC), Particle Swarm Optimization (PSO) was used in this study. The authors showed that "Multiple Resources and Multiple products-based Coupling" had the lowest NPC, and it was 1.8 times and 1.3 times lower NPC than "Direct Coupling" and "Single Resource and Multiple product-based coupling" respectively. A sensitivity analysis was carried out by varying the peak demand, seasonal demand, average energy demand, system equipment cost, project lifetime, inflation rate, discount rate, and capacity factor to strengthen the findings.

2.5. Micro Modular Reactor (MMR)

The initial cost of conventional NPP is very high, and it needs a large area to be installed. Therefore, conventional NPP is not appropriate where the power requirement is low [41]. SMR and Micro Reactors (MRs) are innovative solutions to reduce the high initial cost of NPP and to eliminate the requirement of a large installation area. SMR is a fourth-generation nuclear reactor having power equivalent to 300 MWe or less. Modular fabrication, passive safety systems, and enhanced protection against man-made or natural hazards are some advanced features of SMR. A subcategory of SMR is vSMR which power rating is less than 15 MWe[42]. Another subcategory of SMR is Microreactor (MR), which typically ranges from 1 MWe to 50 MWe [43].

The SMR and MRs are getting attention from researchers and manufacturers for the smaller size, passive safety, high reliability, and affordability. Design of more than 50 SMR is in

progress for different applications. SMR is categorized into 'Water cooled SMR (Land Based)', 'Water cooled SMR (Marine Based)', 'High temperature gas cooled SMR', 'Fast neutron spectrum SMR', 'Molten salt SMR', and 'Other SMR' based on the types of coolants[44]. Among these 50 SMRs, the industrial demonstration of three SMR is in the advanced stage of construction in Russian Federation (KLT40s), in China (HTR-PM), and in Argentina (CAREM). These SMRs are expected to be in operation within 2022. Also, Russia has already manufactured six RTM-200 reactors and four of them are installed in Sibir and Arktika icebreakers. Several countries are working on the development of SMR. Figure 2-7 shows the number of SMR development in different countries.

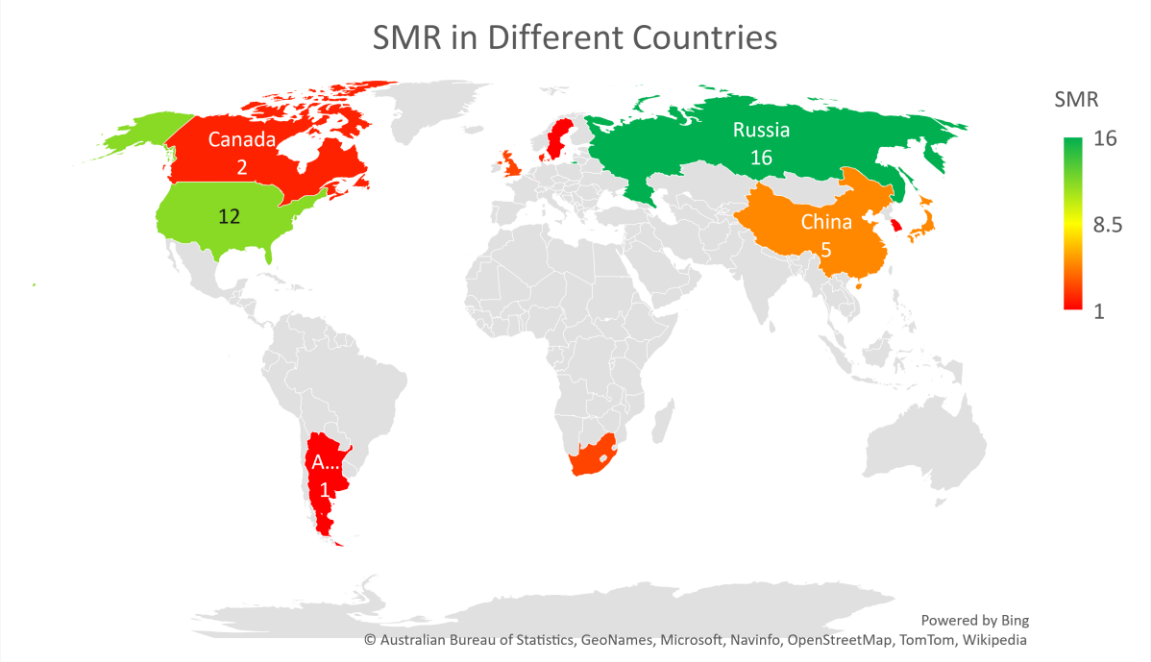

Figure 2-7: SMR Development in Different Countries

Russia and the USA are leading in the development of SMR. China, Japan, South Africa, and the United Kingdom are also progressing well. The SMR development in different countries is in different stages which is represented in Figure 2-8

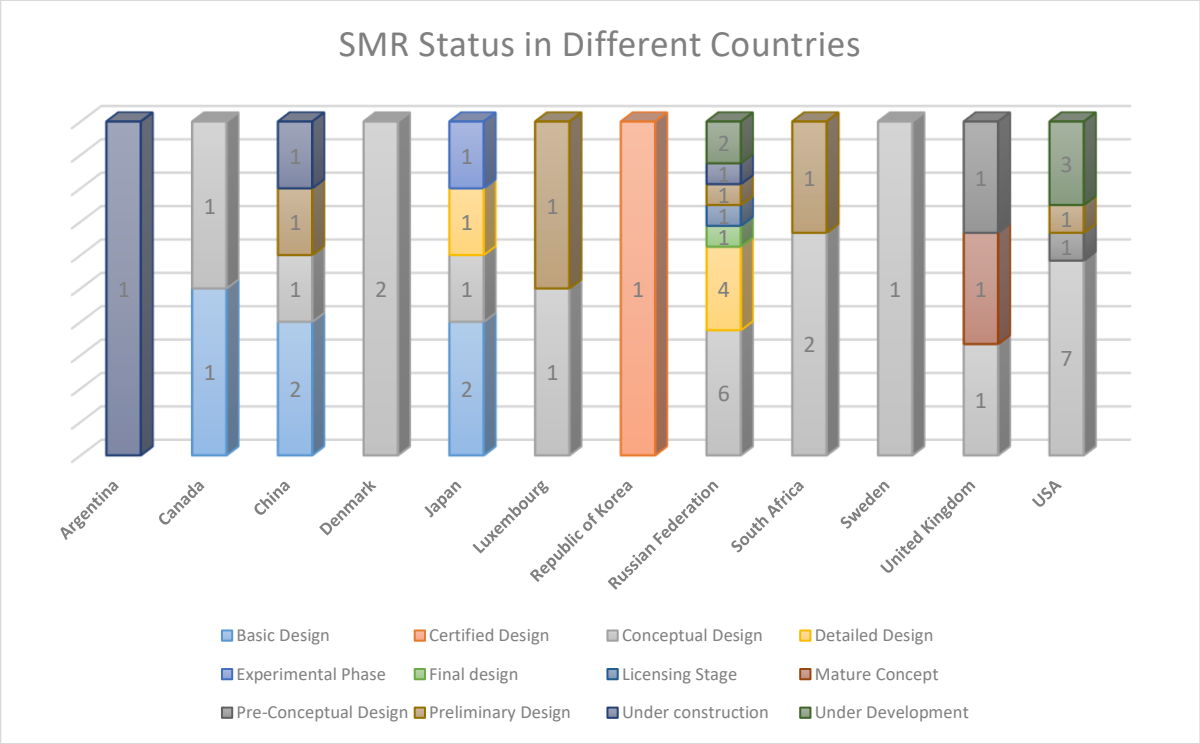

Figure 2-8: SMR Status in Different Countries

Table 2-2 presents the list of MR under development with reactor type, power rating, company, and country of origin. It is expected that within a few years MR will be in operation.

Table 2-2 Summary of MRs under development [45]

Company	Reactor type	Rating (MWe)	Country of origin
NuScale Power	Integral pressurized water	50	U.S.
Westinghouse Electric Co	eVinci micro reactor	<25	U.S.
StarCore Nuclear	High-temperature gas prismatic block	10	Canada/U.S.
LeadCold	Molten lead pool fast spectrum	3-10	Sweden / Canada
Ultra Safe Nuclear/Global First Power	High-temperature gas prismatic block	5	U.S.
U-Battery	High-temperature gas prismatic block	4	UK

The MMR facility can be divided into two major components, Nuclear Plant and Adjacent Plant [46]. The Nuclear Plant includes Citadel Building, Nuclear Building, Nuclear Plant Molten Salt System, and Waste Handling and Storage Area. The Adjacent plant includes the Adjacent Plant Molten Salt System, the Power Generation System, the Steam Turbine Generator System, and the Air Cooled Condenser System. The Adjacent plant includes all the equipment that is required to produce electricity by using the heat generated in the Nuclear Plant. The Adjacent Plant has also an office, visitor, and training center.

The Citadel Building contains the MMR reactor and the Nuclear Heat Supply System. The Nuclear Heat Supply System is used to remove the reactor-generated heat via Intermediate Heat Exchanger. MMR plants use helium to extract heat from the reactor core. The cold helium is circulated through the reactor core via Helium Circulator, and removes the heat from the reactor core. The hot helium is then passed through the Intermediate Heat Exchanger (IHEx). In the IHEx, the hot helium transfer the heat to the Nuclear Plant Molten Salt System. After transferring the heat, the hot helium gets cold, and it is recirculated to the reactor core by the Helium Circulator.

The Nuclear building of the Nuclear Plant includes the main control room, security room, air conditioning, heating, ventilation, and electrical equipment room. The Nuclear Plant Molten Salt System is connected with the Adjacent Plant Molten Salt System and is used to transfer the heat from the Nuclear Plant to the Adjacent Plant. The Nuclear Plant Molten Salt System contains valves, pipes, and a drainage system. The Waste Handling and Storage Area of the Nuclear Plant is utilized to package, process, and store the intermediate and low-level waste. This waste is periodically transported to the designated facility. The transportation is managed under associated regulation for transporting dangerous goods. A simplified process diagram is shown in Figure 2-9.

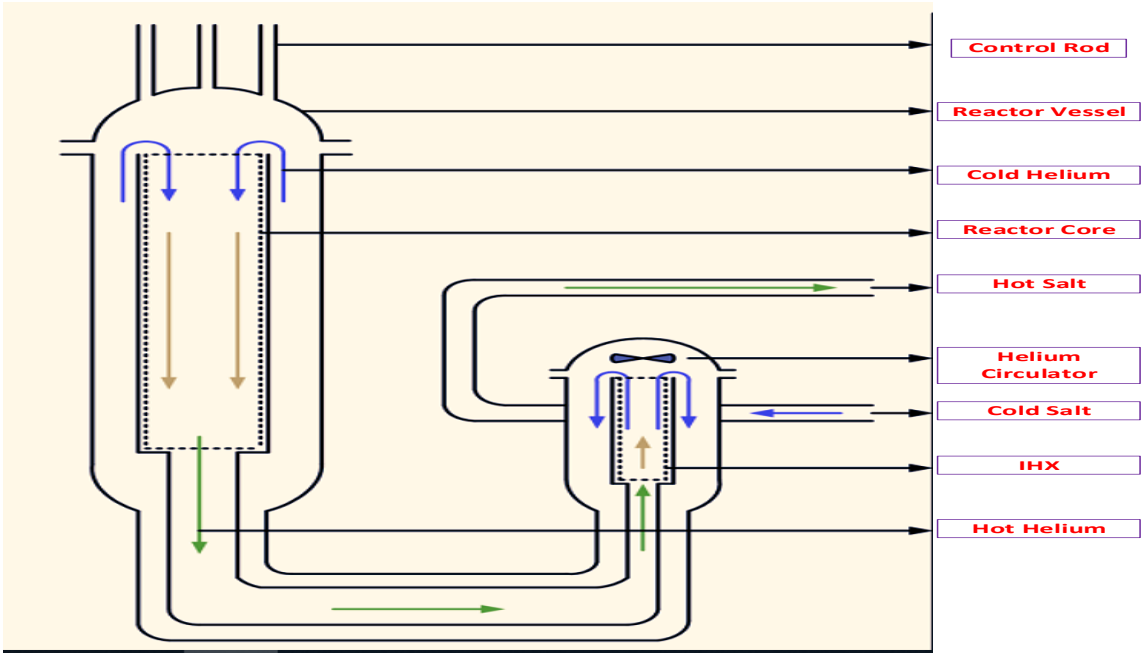

Figure 2-9: Simplified Process Diagram of MR (Nuclear Plant)

Figure 2-10 shows the process diagram of the Adjacent Plat [46]. The Adjacent Plant Molten Salt System consists of pipes, pumps, gas furnaces, hot and cold molten salt storage tanks. This system is acted as a mediator to transfer the heat from the Nuclear Plant to the Adjacent Plant via a heat exchanger. The hot molten salt is pumped from the hot molten salt storage tank by hot salt pump, and transfer heat to the water of the turbine of the electricity generator. The storage tanks are used as an energy storage system and can regulate the flow of molten salt. The hot molten salt is kept in cold storage before it is sent to the Nuclear Plant by the cold salt pump. For maintaining the temperature of the molten salt during shutdown or maintenance scenarios, a gas-fired burner is used.

The Power Generation System and Steam Turbine Generator of the Adjacent Plant are responsible for generating electricity by using the heat supplied by the molten salt. The produced electricity is delivered to the electrical grid via a transformer and other controller infrastructure.

The Air Cooled Condenser System is used to dissipate the excess heat that is produced during the steam condensation. The water is heated during the operation of the steam turbine by using the heat received from the molten salt. This steam then condenses before using it again.

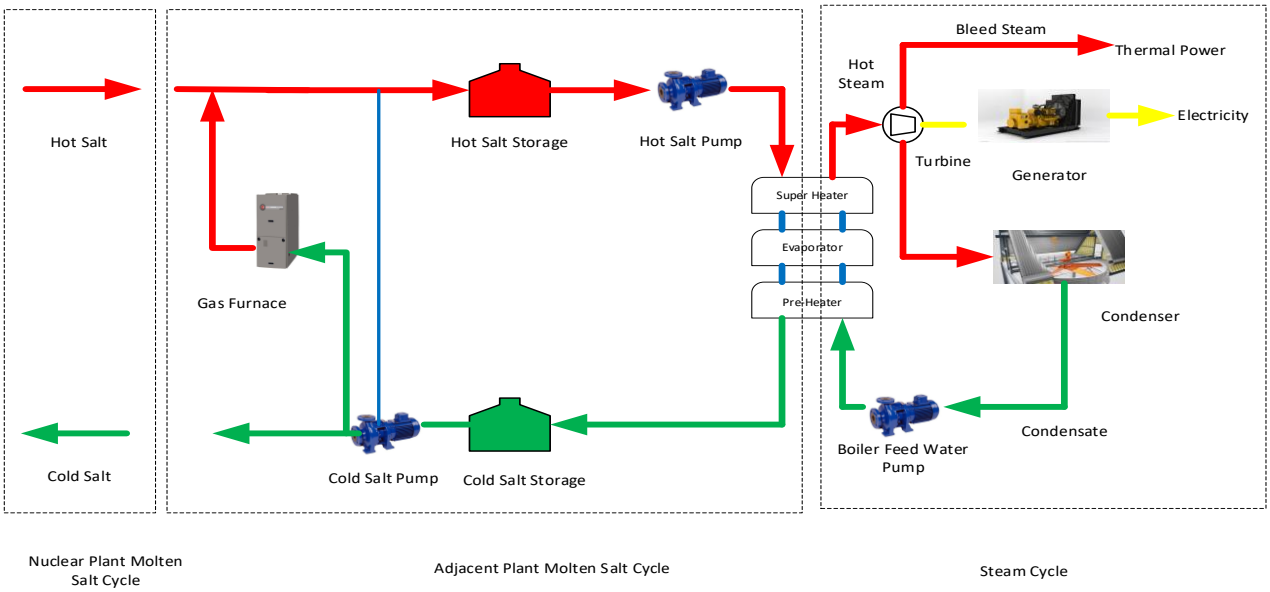

Figure 2-10: Simplified Process Diagram of MR (Adjacent Plant)

In this study, the technical and economical feasibility of the N-R HES in the ocean-going ship is assessed. Hence, it is needed to include all the costs of SMR lifecycle including nuclear fuel. In this part, the lifecycle of MR and nuclear fuel will be discussed.

Figure 2-11 represents the lifecycle phases of SMR (red boundary) and nuclear fuel (blue boundary). Lifecycle phases of nuclear fuel include mining and milling, conversion, enrichment, fuel fabrication, operation, and Used Nuclear Fuel (UNF) dispositioning. The lifecycle stages of SMR include site preparation and construction, plant operation, decommissioning, and abandonment.

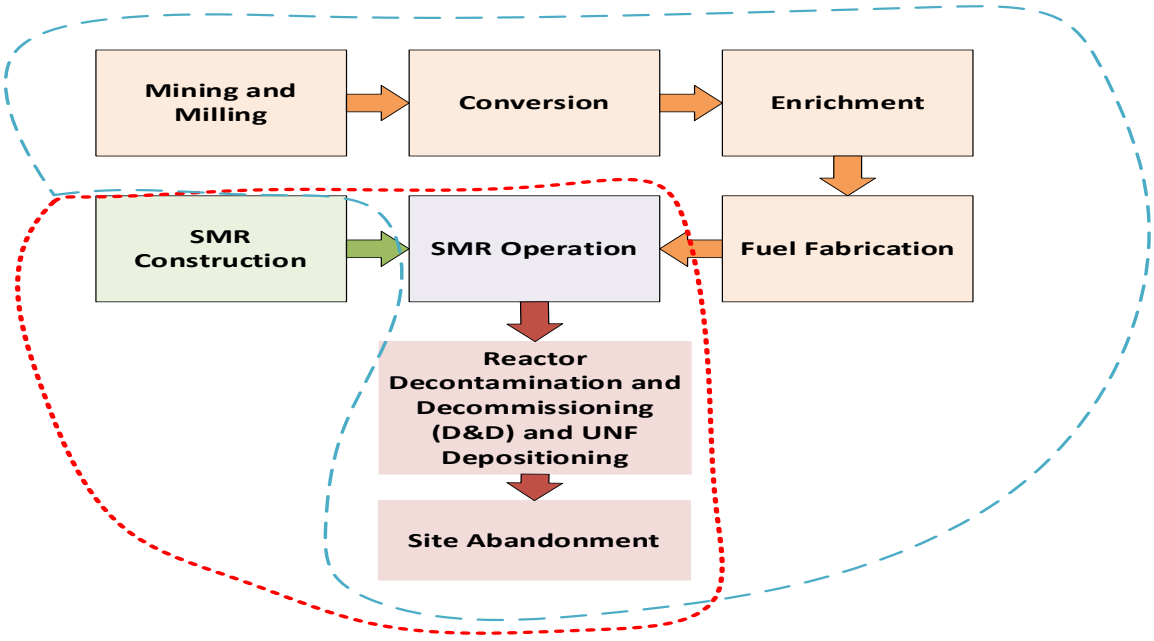

Figure 2-11: Lifecycle of Nuclear Fuel (Blue Border) and SMR (Red Border)

In the mining milling stage of the lifecycle of nuclear fuel, nuclear ore is mined by underground mining, open-pit methods, or in situ leach mining. The extracted uranium ore is then milled to purify the uranium ore and remove the other materials. The final product after the milling stage is called the 'yellowcake (U_3O_8)' The 'yellowcake' that is produced in the mining and milling stage is around 70% to 90% purified. The 'yellowcake' is then converted to UF_6 by simultaneous purification and conversion. The most commonly used methods for this transformation are dry hydrodfluor and wet solvent extraction processes. There are many methods of enriching uranium, and gas centrifugation is one of the ways that is being used in the U.S. In this phase, heavy $^{238}UF_6$ and light $^{235}UF_6$ are separated. This enriched UF_6 is then reheated to a gas and UO_2 powder is produced. This UO_2 is pressed into a pellet and then sintered. These pellets are loaded to fuel rods. After the operation of nuclear fuel, it is disposed of after cooling it in wet pool storage. The current plan of Canada is to dispose of the UNF in a Deep Geological Repository (DGR) [47], [48].

The site preparation phase of SMR includes excavation and clearing the site area. In this phase, service utilities like firewater, domestic water, sewage, electrical, and communication are installed. The construction of the support building, parking area, and access road are also included in the site preparation phase. In the construction stage, concrete structures, fencing, construction of main buildings, and assembly of pre-constructed modules are carried out. The total time for the site preparation and construction phase is expected to be completed within two to three years. NuScale estimated the

completion time of SMR as 28.5 months from the concrete pouring to the final physical construction. It is anticipated that most of the components will be mass-producible and shipped to the target location for assembly. The operation stage of SMR contains the commissioning, inspection, verification, maintenance, and testing during plant operation. The decommissioning phase includes the dismantling of all the equipment, interim storage of used nuclear fuel (UNF), final disposal of the nuclear fuel, and demolition of all the buildings and facilities. The decommissioning phase is expected to be finished within two to three years. The final stage of the SMR is the abandonment of the site. In this phase, the licensee release from all the regulatory controls. The licensee will ensure the site is usable in the future for other purposes like greenfield or industrial purposes.

2.6. **Optimization of Hybrid Energy System**

The optimal design of any hybrid energy system is important to ensure the lowest investment while maintaining reliability, performance, and satisfying the related constraints. Different researchers use different optimization techniques to determine the optimal configuration. The optimization techniques for hybrid energy systems can be classified broadly into three categories: Classical, Meta-Heuristic, and Computer Software. Classical optimization can be divided into Linear Programming (LP) and Mixed Integer Linear Programming (MILP). Meta-Heuristic optimization can be categorized into Single algorithms and Hybrid algorithms. Figure 2-12 shows the classification of optimization techniques.

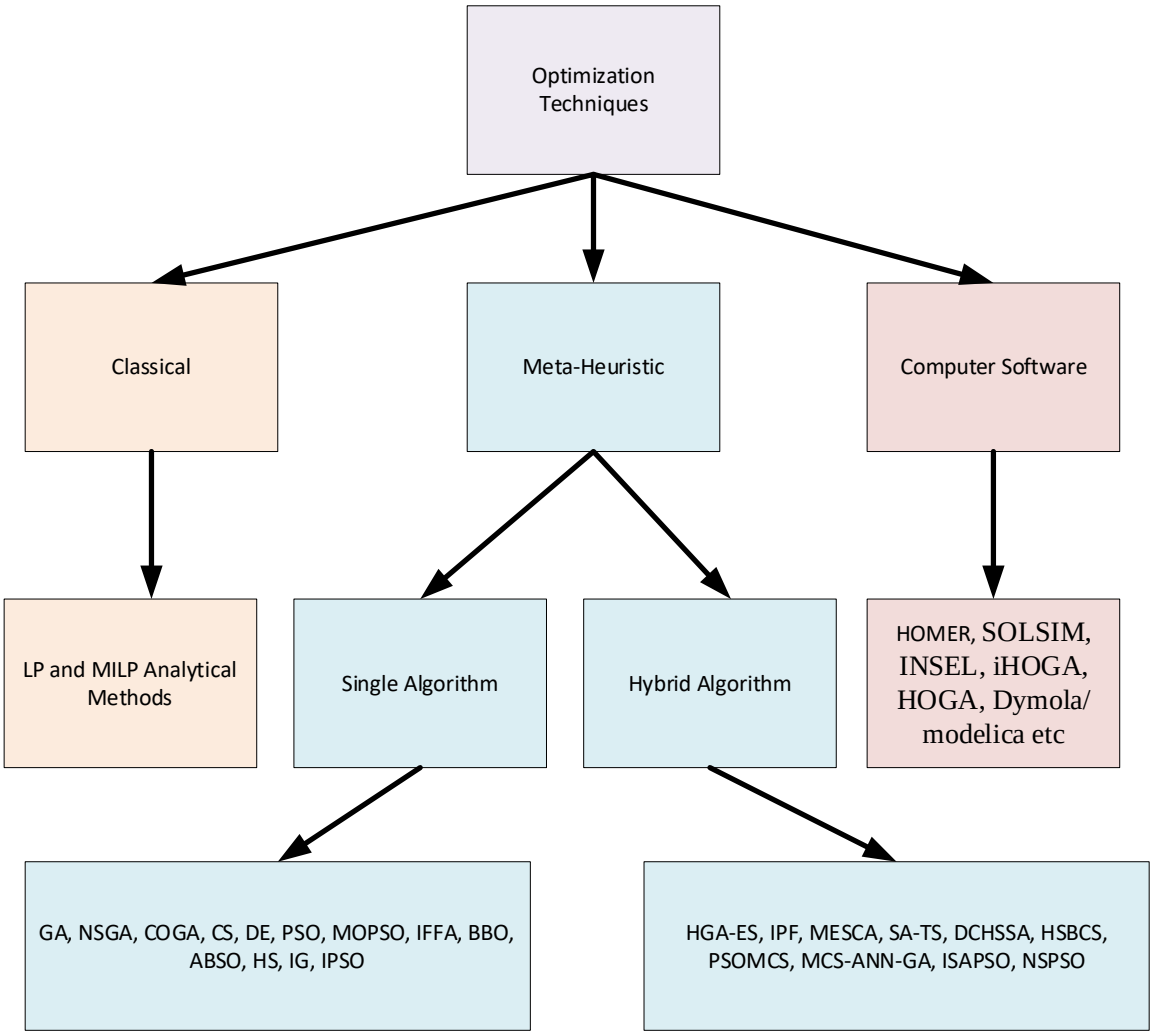

Figure 2-12: Classification of Optimization Techniques

The base of the classical optimization techniques is numerical analysis, iterative methods, and graphical construction. Classical optimization can be divided into Linear Programming (LP) and Mixed Integer Linear Programming (MILP). The LP and MILP are employed when the objective functions and constraints of the systems have a linear expression, and the decision variables are continuous. Nagabhushana et al. [49] used LP to identify the size of the components of Hybrid Renewable Energy Systems (HRES) comprising of wind turbine and solar PV. They considered three different locations in Karnataka (India) that are Mangalore, where wind speed is dominant, Hubli, where solar radiation is leading, and Belgaum, where both wind speed and solar radiation share the same percentage but in less amount. The MILP was used in [50] to design optimal management and operation of a grid-connected system. The system includes fuel cell, solar PV, and batteries. The authors conducted the environmental and economical assessment, They concluded that from the economic perspective, supplying load from the fuel cell and grid, and sell the electricity from solar PV to the grid is the most viable option. From the environmental point of view, supplying all the load from solar PV is the optimal solution.

Considering the complexity of hybrid energy systems in terms of constraints, system component performance, and availability of resources, classical optimization is not a good option to optimize the hybrid system [51]. Hence, meta-heuristics optimization techniques have been widely used to optimize the hybrid energy system because of its' efficiency and accuracy. Meta-heuristics optimization is grouped into single algorithm and hybrid algorithm. Particle Swarm Optimization (PSO), Differential Evolution (DE), Genetic Algorithm (GA), Ant Colony Optimizer (ACO), Cuckoo Search (CS), Non-dominant Sorting Genetic Algorithm (NSGA) are some of the single algorithms optimization techniques. The hybrid algorithms use two or more single algorithms of classical optimization or meta-heuristic optimization techniques. The examples of the hybrid algorithm are Hybrid GA and an Exhaustive-Search (HGA-ES), Modified Electric System Cascade Analysis (MESCA), MarKov-based GA (MarKov-GA), Improved Simulated Annealing Particle Swarm Optimization (ISAPSO), Teaching-Learning-based Optimization (HT-LBO), Hybrid Big Bang-Big Crunch (HBB-BC), Hybrid Flower Pollination Algorithm and Simulated Annealing (HFPA-SA), and Hybrid Simulated Annealing-Tabu Search (HAS-TS).

A Non-dominant Sorting Genetic Algorithm was used by Zhao et al. [52]. They considered a hybrid energy system consists of solar PV, wind turbine, diesel generator, and lead-acid battery. The objective of this optimization is to minimize the power generation cost and battery life cost. They considered the system load as 510 kW. NSGA gives the user a set of solutions that are not dominated by others, called the Pareto-Optimal set or Pareto-Optimal front. All the solutions of the Pareto-optimal set are possible solutions for the problem and users can determine the solutions as per their preference.

Sanchez et al. [53] optimized a hybrid system of solar PV, wind turbine, and fuel cell to minimize the cost while fulfilling the demand. They primarily used the Particle Swarm Optimization (PSO) technique to optimize the system, and in the latter section, they compared the performance of the PSO with another meta-heuristic optimization technique, Differential Optimization (DE). They showed that PSO outperformed DE, and gave the lowest total cost although the difference between these two optimization techniques is minimal. The performance of PSO and DE was carried out in [54]. In this study, the authors used some benchmark functions that were optimized by both PSO and DE. They compared both optimization techniques in terms of robustness and the number of iteration that are required to bring the solution to a feasible region. They concluded that DE outperformed PSO and the favored value of scaling factor of crossover probability of DE parameters are 0.5 and 0.9 respectively.

A number of researchers used computer software for hybrid energy system analysis. Among all the computer software, Hybrid Optimization of Multiple Energy Resources (HOMER) has been widely used [55]. HOMER is a powerful and efficient tool to optimize any hybrid energy system for planning and design purposes. The techno-economic analysis can be carried out using the HOMER software. HOMER uses two types of optimization

which are original grid search optimization and proprietary derivative-free optimization. In the original grid search optimization, suitable system configuration needs to be defined in the search space and HOMER searches the least-cost combination of equipment with meeting the electric load. In derivative-free optimization, users need not give any input in the search space, HOMER finds the optimized rating of the system components. Understanding the electric load and cost information of the system component are needed in derivative-free optimization [56]. The conventional energy sources along with other energy sources like wind turbine, solar PV, fuel cell, flywheel, battery energy storage, converters, hydropower, hydrogen tank, biomass can be modeled in HOMER. The techno-economic analysis of a hybrid energy system in the rural area of Jordan was carried out in [57]. The hybrid energy system includes solar PV, diesel generator, and battery. The author used HOMER software to optimize and design the system. The optimal hybrid system consists of 2 kW PV array, 4 kW diesel generator, and 2 kW storage system. Shaagid et al. [58]studied the economic analysis of hybrid energy systems in different provinces of Saudi Arabia by using HOMER software. In the hybrid energy system, they considered Solar PV, diesel generator, and battery energy storage system. The optimal hybrid energy system includes 4 kW solar PV, 10 kW diesel generator, and battery storage of 3 hours autonomy. The penetration of solar PV in different provinces is between 20% to 22%. This study also exhibited that by increasing the PV penetration, carbon emissions can be decreased but the COE will increase.

HOMER optimizer considers a fixed rating of all the system parameters for the project lifetime which is one of the shortcomings of it. HOMER optimizer can not optimize a system if any of the system parameters change over time. In reality, some of the system parameters change over time to a varying degree. The main drawback of HOMER software is that it considers several simplifications during the optimization process which affects the accuracy of the result [59]. Also, in HOMER there are some fixed areas where user can put constraints but in real-world problem, there are many different types of constraints which HOMER can not handle. Some other computer softwares are used by researcher to optimize hybrid energy systems. Some of the computer software are Hybrid designer, SOLSIM, HYBRIDS, ARES, iGRHYSO, INSEL, iHOGA, HOGA, Dymola/modelica, HYSYS, SOMES, RAPSIM, Hysim, RETScreen, TRNSYS, Hybsim, HYBRID2 [60].

Table 2-3 shows the list of works that used meta-heuristic optimization technique and HOMER software to analyze the hybrid energy systems

Table 2-3 Summary of Optimizations of HESs by Meta-Heuristic Technique and HOMER Software

Objective Function	Optimization Technique	Result/ Conclusion	Reference
COE, LPSP	MOPSO	A hybrid microgrid consists of solar PV, wind turbine, diesel generator, and battery storage was optimized by using Multi-Objective Particle Swarm Optimization (MOPSO). The authors used linear scalarization to convert the multi-objective into single-objective problem.	[61]
Life Cycle Cost (LCC), Reliability	PSO	A stand-alone hybrid energy system is optimized in this study. The hybrid energy system includes solar PV, wind turbine, and battery. The authors considered three variables namely, the total area covered by solar PV, total swept area by wind turbines' blades, and the number of batteries. The authors concluded that the adaptive inertia weight-based PSO algorithm provides better result compared to other variants of PSO	[62]
NPC, Availability of electricity	MOGA	A grid-connected hybrid energy system consisting of solar PV and wind turbine was assessed to ensure the availability of electricity and to minimize the total cost of the system.	[63]
Total Annualized Cost (TAC), LPSP, fuel cost	HT-LBO	Optimization of hybrid energy system consists of wind turbine, diesel generator, solar PV, and battery storage was carried out while ensuring the reliability of the system	[64]
Loss of Load Probability (LPP), System Cost	Iterative-GA	The authors optimized a hybrid system that comprises solar PV and wind turbine to find out the minimum system cost while keeping the LPP within a limit. The iterative method was first used to find out possible solutions and GA was used later on to determine the optimum solution.	[65]
NPC, Initial Capital Cost, COE	HOMER	Electrification in three off-grid villages was studied. A stand-alone hybrid power system with wind turbine, solar PV, and diesel generator was optimized with HOMER software to determine the most cost-effective and efficient energy system	[66]
System Cost, Environmental Impact	HOMER	The authors studied five different combinations of energy sources, namely standalone diesel, PV+Diesel, Wind+Diesel, PV+Wind, and PV+Wind+Diesel. These five energy sources were compared to identify the most feasible energy source in terms of cost and environmental impact. The authors found that PV+Wind+Diesel is the most economical while PV+Wind energy system has zero emissions.	[67]

2.7. **Key Performance Indicators (KPIs)**

KPIs evaluate the benefits and the drawbacks of a system. KPI works as an important decision-making factor for designers. Since an N-R MHES is a complex integrated system, it is necessary to identify and evaluate KPIs for system deployment. From the literature review, KPIs of a hybrid energy system are categorized in mainly four sections: Technical, Economical, Environmental, and Socio-Economical. This study primarily focuses on technical, economic, and environmental KPIs. The discussion of socio-cultural indicators is beyond this study. Some critical KPIs considered in this study are discussed as follows.

2.7.1. Generation Reliability Factor (GRF)

GRF is one of the reliability factors that indicates the amount of demand of a system is accomplished by the energy system [40]. The mathematical formula of GRF for the demand of the system can be expressed by the following equation [68].

$$GRF_e = \frac{\sum_{t=1}^{t_{total}} P_{gen}(t) \times \Delta t}{\sum_{t=1}^{t_{total}} P_L(t) \times \Delta t} \times 100\% \qquad \forall\, t \in t_{total} \quad \textit{Eq. 2-1}$$

Where, GRF_e is the generation reliability factor. $P_{gen}(t)$ and $P_L(t)$represents the power generation and electric load demand at time step t. Δt shows the time step considered in the calculation. The higher value of GRF implies the system is more reliable.

2.7.2. Loss of Power Supply Probability (LPSP)

The LPSP is another reliability factor that determines the amount of unserved energy of a system when the system demand is higher than the generation. To ensure the reliability of the system, it is important to maintain the LPSP within a boundary. Therefore, this KPI is considered as one of the constraints in the optimization of the system. The LPSP is determined for each time step and for the total time step to assure the utmost reliability of the system. Below equations are used to determine the LPSP [69],[70]

$$LPSP_e = \frac{\sum_{t=1}^{t_{total}} (P_L(t) - P_{gen}(t))}{\sum_{t=1}^{t_{total}} P_L(t)} \times 100\% \qquad P_L(t) > P_{gen}(t) \quad \textit{Eq. 2-2}$$

$$LPSP_e(\mathrm{t}) = \frac{P_L(t) - P_{gen}(t)}{P_L(t)} \times 100\% \qquad P_L(t) > P_{gen}(t) \quad \textit{Eq. 2-3}$$

Where, $LPSP_e$ represents the loss of power supply probability for the total time step, $LPSP_e(\mathrm{t})$ shows the loss of power supply probability at each time step. The maximum and minimum value of LPSP is 1 and 0 respectively. The lower LPSP infers the higher reliability of the system.

2.7.3. CO_2 Gas Emissions

It is an environmental KPI. Several pollutants are emitted from the energy generators namely Carbon Monoxide, Particulate matter, Nitrogen Oxides, Carbon Dioxide, Sulfur Dioxide, and Unburned Hydrocarbons (UHC) in the lifecycle of the generators. In this study, only CO_2 gas emission is considered. The amount of CO_2 emissions from any generators is calculated by the below equation [71]

$$CO2\ emissions = Emission\ Factor\ \left(\frac{kg}{MWh}\right) \times TAEG\ (MWh) \qquad \textit{Eq. 2-4}$$

Where, $TAEG$ is the total annual electricity generation from the generators. The emissions factor for diesel generators and SMR is 700kg/MWh and 4.55 kg/MWh respectively [47], [48]. The penalty for CO_2 emissions is considered during the calculation of NPC. The annual penalty for CO_2 emissions can be calculated by using the following equation

$$CCE = ACE \times CEP \times \frac{i(1+r)^n}{(1+r)^n - 1} \qquad \textit{Eq. 2-5}$$

Where, CCE is the cost associated with CO_2 emissions penalty ($), ACE is the annual CO_2 emissions (tonne), and CEP is the CO_2 emissions penalty ($/tonne). The CO_2 emissions penalty differs from country to country. Till 2015, around 40 national governments and 20 sub-national governments introduced carbon pricing. Among these national and sub-national governments, 15 have explicit carbon taxes. Figure 2-13 shows the tax rate on CO_2 emissions [72]

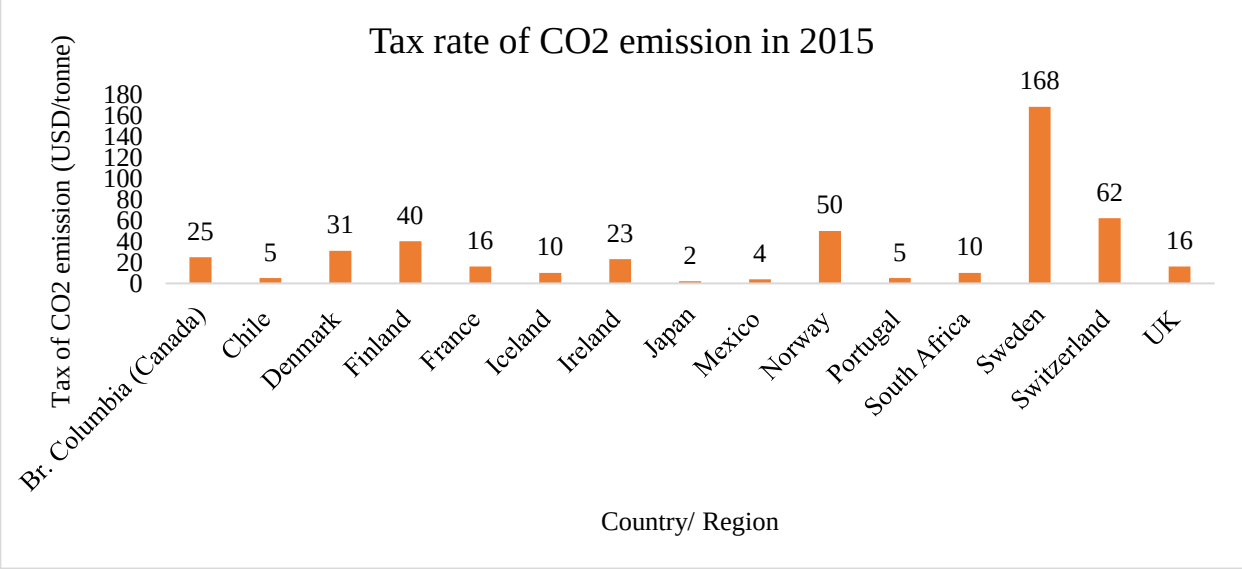

Figure 2-13: Tax Rate of CO_2 Emissions in Different Countries/ Regions

Although nation-wise carbon tax varies a lot, IMF calculated large CO_2 emitter countries should be charged between 50 USD/ton to 100 USD/ton by 2030 to fulfill their

commitments to lessen the carbon emissions [73]. For the shipping industry, IMF proposed 30 USD/ton CO_2 emissions as a penalty [74]. In this study 30 USD/ ton CO_2 emissions is considered as CO_2 emissions penalty to show the impact on NPC and LCOE.

2.7.4. Power to Weight Ratio (PWR)

The PWR is an important criterion to choose the energy system for the marine ship. The PWR measures the performance of any power source or system. The heavyweight of the power system of marine ships results in higher displacement and lower speed.

The higher PWR allows the marine ship to carry more load while maintaining the high speed [75]. The PWR of a power system can be calculated by using the following equation [76]

$$PWR = \frac{Power\ rating\ of\ the\ system\ (kW)}{Weight\ of\ the\ system\ (kg)} \qquad \textit{Eq. 2-6}$$

As the proposed N-R HES will replace the conventional energy system of marine system, the PWR of the current marine ship engine is considered as one of the constraints in optimization problem to maintain the minimum PWR for the marine ship

Table 2-4 shows the PWR of the different components of the system.

Table 2-4: PWR of the different components of the system

Component Name	Power (kW)	Weight (kg)	PWR (kW/kg)	Reference
MR/vSMR	50,000	7,00,000	0.07	[77]
Diesel Generator	28,700	9,90,000	0.02	[78]
Solar Panel	375	21.591	0.05	[79]
Wind Turbine	1500	1,49,000	0. 01	[80]
Battery	1,600	48,000	0.03	[29]

The weight of the wind turbine includes the weight of the nacelle, blade, and tower. The weight of the battery comprises the weight of the racks, cooling systems but does not cover the weight of the associated transformer and converters.

2.7.5. Levelized Cost of Energy (LCOE)

LCOE is a fundamental economic matrix to compare different generation sources and energy systems. It accounts for capital cost, replacement cost, Operations and Maintenance

(O&M) cost, and other financial indices throughout the project lifetime. Lower LCOE resembles a higher profit for investors.

LCOE ($/kWh) is the average cost per unit of electricity or energy (kWh). The following equation is used to calculate LCOE [69].

$$LCOE = \frac{NPC_{total}}{\sum_{t=1}^{8760}(P_{EL}(t) + P_{TL}(t)) \times \Delta t} \times \frac{i(1+i)^n}{(1+i)^n - 1} \quad \textit{Eq. 2-7}$$

Where, NPC_{total} is the system total NPC ($), i is the real interest rate (%), and n is the project lifetime (years).

The Net Present Cost (NPC) and Net Present Value (NPV) are similar concepts and they only differ in sign. The NPV is the present value of all future cash flows (positive and negative) of an investment with a discount rate [81]. The lower NPC implies a higher profit to the investors. The following equation can be used to calculate the NPC. As NPV and NPC differ only in sign, NPC and NPV are related as follows.

$$\text{Net Present Cost (NPC)} = -\text{Net Present Value (NPV)} \quad \textit{Eq. 2-8}$$

$$\text{NPV} = \frac{\text{Cash flow}}{(1+\text{rld})^{\text{t}}} - \text{Initial Investment} \quad \textit{Eq. 2-9}$$

$$rld = \frac{\text{i} - f}{1+f} \quad \textit{Eq. 2-10}$$

Where, $rld, f,$ i and t denote the real discount rate (%), nominal discount rate (8%), inflation rate (2%), and time periods number, respectively. In the nominal discount rate/ interest rate, the inflation rate is covered. To factor out the impact of the inflation rate, the real discount rate is considered in this study. The equation for calculating the real interest rate is also known as Fisher equation [82].

For calculating the NPC for a longer project lifetime with multiple cash flows, the formula can be modified as per the below equation.

$$\text{NPV} = \sum_{\text{t=0}}^{\text{n}} \frac{\text{R}_{\text{t}}}{(1+rld)^{\text{t}}} \quad \textit{Eq. 2-11}$$

Where R_{t} and n refer to net cash inflow-outflow in a unit time period, and project lifetime, respectively.

Chapter 3: Methodology

In this chapter, the steps of the research are presented in section 3.1. The system configuration and control algorithm are discussed in section 3.2. Section 3.3 covers the method of data collection and calculation. Analysis of methodological choice is discussed in section 3.4. The assumptions that are considered in this study are summarized in section 3.5.

3.1. Research Framework

The research framework is illustrated in Figure 3-1. The literature review is carried out to understand the problem and the gap of previously suggested solutions. The N-R HES analysis in marine transportation requires lots data like ship speed to estimate the energy demand, solar irradiance to calculate the solar PV output, and wind speed to determine the wind power of wind turbine. These data are collected from FleetMon and NASA Surface meteorology and Solar Energy database. After getting these data, the energy requirement of the ship, solar power, and wind power are calculated. The planning of the energy systems is completed by designing the system components, identifying the system KPIs, and implementing the control algorithm. All the energy systems are then optimized to determine the lowest NPC. Initially, the HOMER software is used to get the primary idea on the feasibility of N-R HES in marine ships compared to other energy systems. For further tuning and addressing shortcomings of HOMER software, the mathematical cost model of the energy systems in MATLAB Software is carried out. The objective functions, constraints, and decision variables are formulated to optimize the models by DE, ADE, and PSO optimization techniques. Primarily, the DE algorithm is used to identify the optimal energy systems and sensitivity analysis. The ADE is employed to understand the impact of control parameters on the DE algorithm. The PSO is used to measure the performance and validate the findings of the DE algorithm. As the N-R HES in marine transportation employs several variables like economic parameters, and meteorological resource availability, a sensitivity analysis is conducted in this study to reinforce the findings.

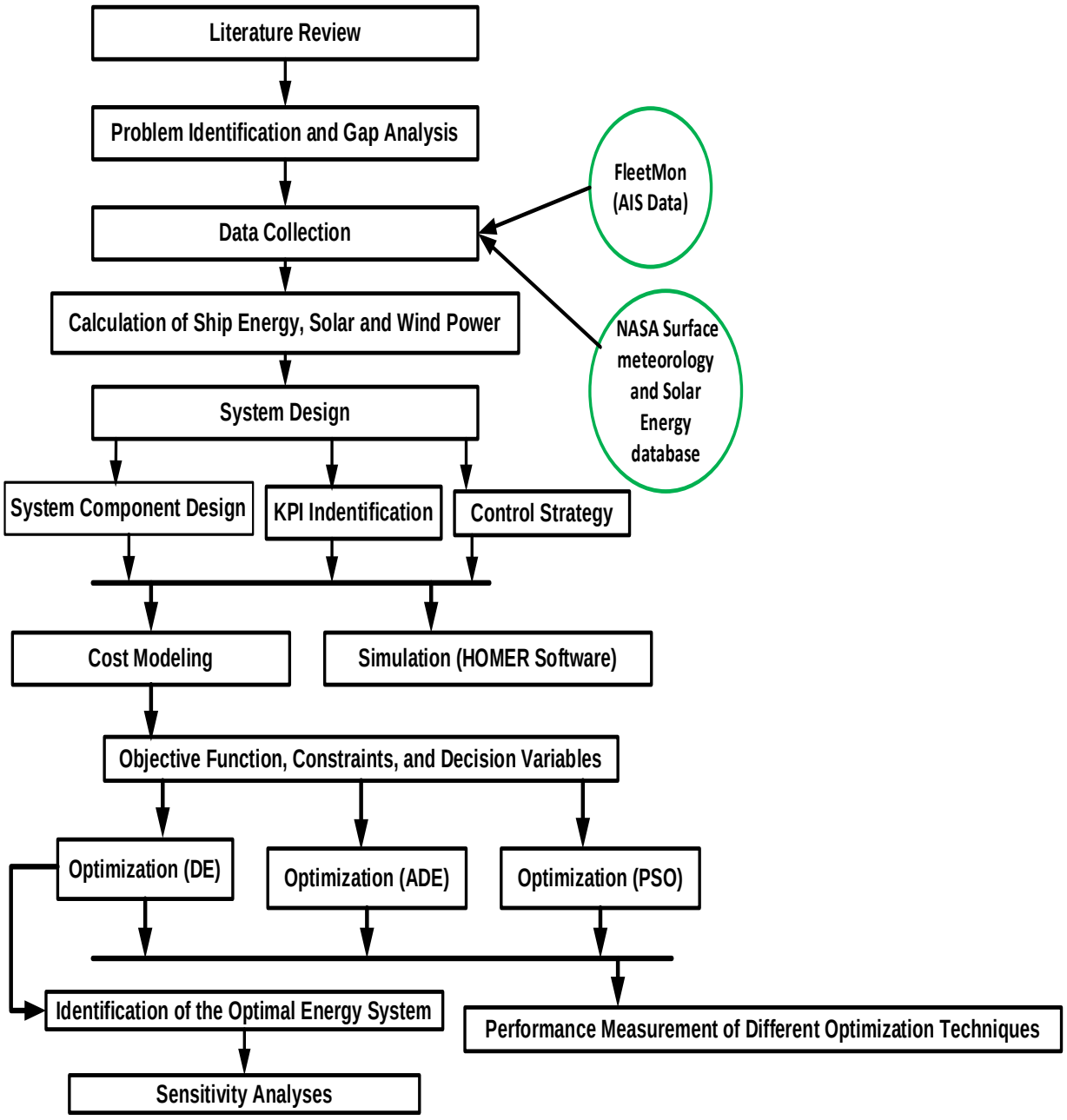

Figure 3-1: Research Framework

3.2. System Configuration and Control Algorithm

A simplified system configuration is presented in Figure 3-2. The proposed N-R HES for a marine ship consisting of MRs, solar PV panels, wind turbines, energy storage systems, controllers, AC/DC converters, and DC/AC converters. Oil tanker 'Baltic Sunrise' is considered in this case study. A vessel data collection company 'FleetMon' provided the AIS data of the ship [83] under the Data License Agreement (DLA) between FleetMon and Ontario Tech University solely for this study. The energy demand of the ship is estimated based on speed, breadth, draught, frictional resistance, residual resistance, and using the ITTC-57 method and Gertler Series Data chart. Some specific KPIs- Net Present Cost (NPC), Cost of Energy (COE), Greenhouse Gas (GHG) emissions, Generation Reliability Factor (GRF), Loss of Power Supply Probability (LPSP), and Power to Weight Ratio (PWR) are assessed in this study. The project lifetime of the system is assumed as 40 years. Discount rate and Inflation rate are considered as 8% and 2% respectively. Initially, HOMER Pro software is used for simulations, system modeling, and KPI analysis to build the base case and for primary understanding. The rating of system components is obtained from the HOMER optimizer. HOMER uses two types of optimization, which are original grid search optimization and proprietary derivative-free optimization. In the original grid search optimization, suitable system configuration needs to be defined in the search space and HOMER searches the least-cost combination of equipment with meeting the electric load. In derivative-free optimization, users need not to give any input in the search space, while HOMER finds the optimized rating of the system components. Understanding the electric load and cost information of the system component is needed in derivative-free optimization [56]. In this study, the rating of the system components is obtained by the combination of both optimization techniques in HOMER.

Addressing the shortcomings of HOMER software, MATLAB mathematical model is used to optimize the system. The Differential Evolution (DE) algorithm is used for optimization. To validate and reinforce the findings of the DE algorithm is compared with Adaptive Differential Evolution (ADE) and Particle Swarm Optimization (PSO).

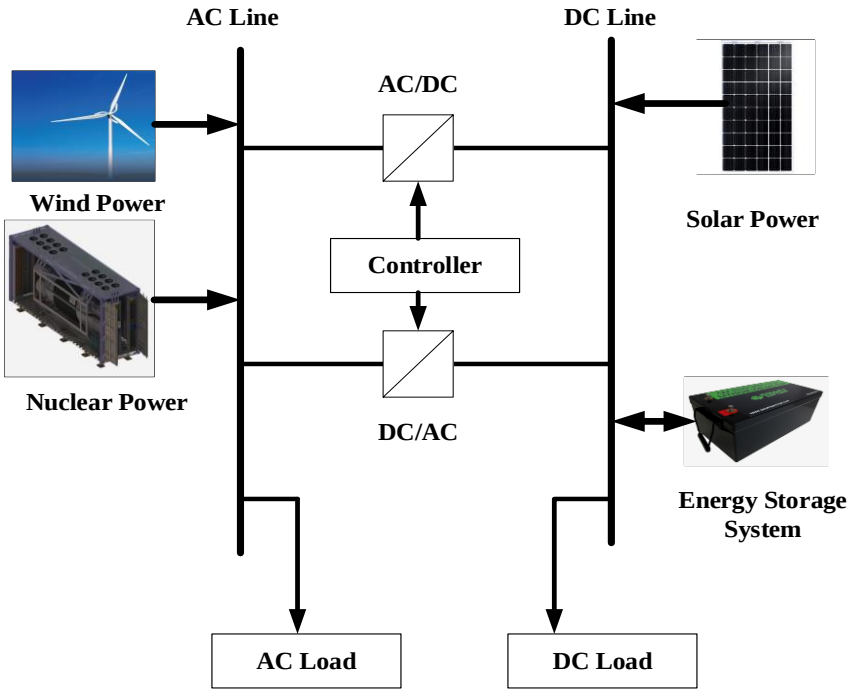

Figure 3-2: Simplified Configuration of N-R HES

The control strategy is shown in Figure 3-3. Firstly, available resources are assessed, and then load assessment is taken place. The control algorithm is divided into two parts. The control algorithm inside the green border refers to the algorithm of the supervisory controller and the algorithm inside the blue border refers to the algorithm of the low-level controller. This Hierarchical control strategy was used by Garcia et al [84] for Nuclear Hybrid Energy Systems (NHES) Configuration. The supervisory controller dynamically identifies the electrical load and the required electrical energy delivery to the load with the help of the operation optimizer and renewable energy generation profile. Based on the information of the supervisory controller, the low-level controllers change the parameters accordingly.

The load demand $P_L(t)$ updates in each time step based on the load profile and the energy resources can be calculated by the following equation

$$P_{gen}(t) = P_{pv}(t) + P_w(t) + P_{MR}(t) \quad \textit{Eq. 3-1}$$

Where, $P_{gen}(t)$, $P_{pv}(t)$, $P_w(t)$, and $P_{MR}(t)$ refer to the total energy generation, total energy from solar PV, total energy from the wind turbine, and total energy from MR at time step t, respectively. \

The amount of energy that can be given to the battery and the amount of energy that is needed from the battery bank at any time step can be calculated by the following equations

$$BAT_{in}(t) = \left(P_{gen}(t) - P_L(t)\right) \times \eta_{bat}; \qquad P_{gen}(t) > P_L(t) \qquad \textit{Eq. 3-2}$$

$$BAT_{out}(t) = \frac{P_L(t) - P_{gen}(t)}{\eta_{bat}}; \qquad P_{gen}(t) < P_L(t) \qquad \textit{Eq. 3-3}$$

Where, $BAT_{in}(t)$ is the amount of energy that can be given to the battery at time step t, $BAT_{out}(t)$ is the amount of energy that is needed from the battery at time step t, and η_{bat} is the battery efficiency. However, the amount of energy that the battery can give to the system and the amount of energy that can be taken by the battery at any time step depend on the energy status of the previous time step which can be formulated by the below equations

$$BAT_{take}(t) = BAT_{SOC,max} - BATe(t-1) \qquad \textit{Eq. 3-4}$$

$$BAT_{give}(t) = BATe(t-1) - BAT_{SOC,min} \qquad \textit{Eq. 3-5}$$

Where, $BAT_{take}(t)$ is the amount of energy that can be taken by the battery at time step t, $BAT_{give}(t)$ is the amount of energy that can be given by the battery at time step t, and $BATe(t-1)$ is the amount of battery energy at the time step $(t-1)$.
The charging and discharging of the battery can be formulated by the following equations

$$BAT_{chrg}(t) = BAT_{SOC,max}\,; \qquad P_{gen}(t) > P_L(t) \;\&\; BAT_{in}(t) \geq BAT_{take}(t) \qquad \textit{Eq. 3-6}$$

$$BAT_{chrg}(t) = BATe(t-1) + BAT_{in}(t)\,; \qquad P_{gen}(t) > P_L(t) \;\&\; BAT_{in}(t) < BAT_{take}(t) \qquad \textit{Eq. 3-7}$$

$$BAT_{dischrg}(t) = BAT_{SOC,min}\,; \qquad P_{gen}(t) < P_L(t) \;\&\; BAT_{out}(t) \geq BAT_{give}(t) \qquad \textit{Eq. 3-8}$$

$$BAT_{dischrg}(t) = BATe(t-1) - BAT_{out}(t)\,; \qquad P_{gen}(t) < P_L(t) \;\&\; BAT_{out}(t) < BAT_{give}(t) \qquad \textit{Eq. 3-9}$$

$$BAT_e(t) = BATe(t-1)\,; \qquad P_{gen}(t) = P_L(t) \qquad \textit{Eq. 3-10}$$

Where, $BAT_{chrg}(t)$ is the capacity of battery after charging, $BAT_{dischrg}(t)$ is the capacity of battery after discharging and $BAT_e(t)$ is the capacity of the battery when generation and demand are exactly the same, at step t.
In the control algorithm, if the generation is higher than demand, it first charges the battery and after that, excess energy is dumped. Also, when the generation is lower than the demand, it takes energy from the battery and any further energy is taken from the standby generator. The authors were motivated to use this control algorithm by [85], [38].

The LPSP in each time step is regarded as 8% for the electric load. The value of 8% signifies that each timestep the maximum unmet load will be 8%. Also, the total LPSP is 8% which signifies that the total unmet load won't exceed 8% of the total load in the whole simulation time (t=8670). Also, the constraint of the total area for the solar PV installation and power to weight ratio is considered which will be discussed later. These assumptions and constraints confirm the utmost reliability of the optimized system.

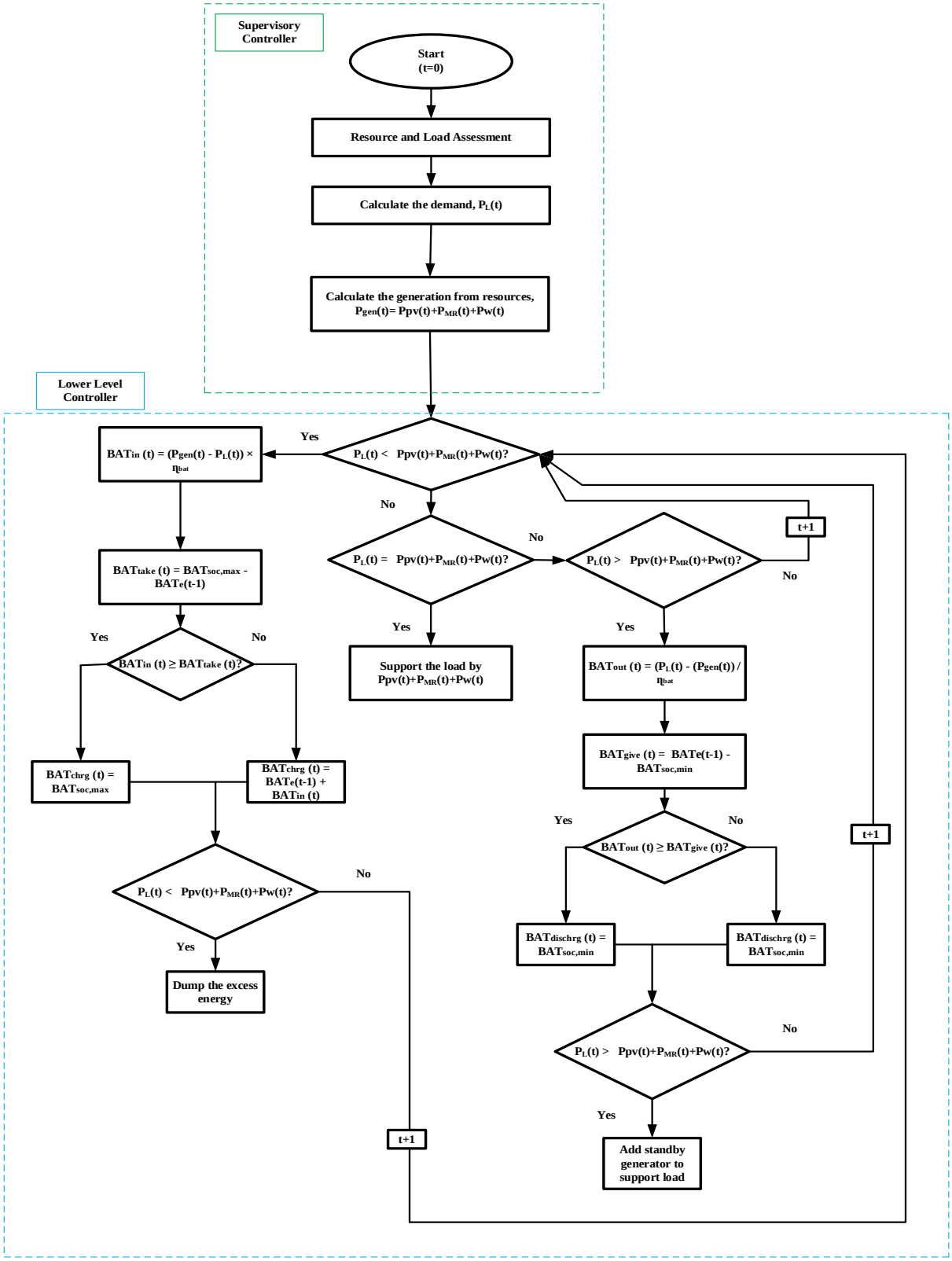

Figure 3-3: Control Algorithm

3.3. Methods of Data Collection and Calculation

To analyze the N-R HES in marine transportation, different kinds of data are required, like electrical energy demand of ship, solar irradiance, wind speed, and temperature. Unlike, land-based systems (residential and industrial), the electrical energy requirement is not readily available. However, the electrical energy requirement of ships can be estimated based on the speed of the ship. In this study, an oil tanker, named 'Baltic Sunrise' is chosen. Several companies provide the position, speed, port calls, master data, voyage history, historical AIS data, real-time AIS data of marine vessels. Marine-Traffic [86], FleetMon [87], Shipfinder [88], Vesselfinder [89], Vessletracker [90], VT Explorer [91], Myshiptracking [92], and Cruise mapper [93] are some of the companies that provide the AIS data of marine ships. This researcher made several communications to the vessel tracking companies to get the required ship data (e.g. speed, latitude, longitude, and direction), and FleetMon agreed to provide the data with standard Data License Agreement (DLA). The data relating to MR was collected by extensive literature review and investigating different websites, manufacturers, and organization's reports. The solar irradiance, wind speed, and temperature data were collected from NASA Surface meteorology and Solar Energy database by using the HOMER Pro software library resources. The data of capital cost, replacement cost, O&M cost, decommissioning cost, carbon emissions penalty, and refuelling cost of different components were obtained from different high impact journal papers, different manufacturers and industry partners website and paper. These data were cross-checked with other sources to get the most realistic data.

In this study, 'Baltic Sunrise' is taken as a reference marine vessel. The IMO number of this ship is 9307633. Detailed parameters of this ship are shown in Table 3-1.

Table 3-1: Description of Baltic Sunrise [94]

SL. NO	SHIP DESCRIPTION	
1	Ship's name (IMO number)	Baltic Sunrise (9307633)
2	Date delivered / Builder (where built)	Nov 08, 2005 / Hyundai Heavy Industries Co. Ltd., Ulsan Shipyard, Korea
3	Flag / Port of Registry	Marshall Islands / Majuro
4	Call sign	V7NP2 / 538006485
5	Type of ship	Oil Tanker
6	Length overall (LOA)	333.12 m
7	Length between perpendiculars (LBP)	324.00 m
8	Extreme breadth (Beam)	60.04 m
9	Deadweight	309373 MT
10	Displacement	352410 MT

This ship started its voyage on 1st May'19 from Iraq and ended in Singapore on 31st July'19 via Egypt and Netherland. Figure 3-4 shows the route of this oil tanker for 3 months of 2019.

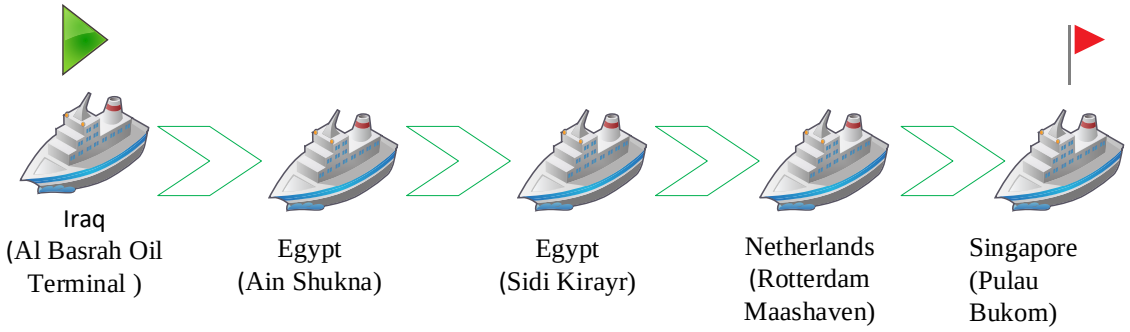

Figure 3-4: Shipping Route of 'Baltic Sunrise'

The speed of this ship was different in different positions. The route along with the speed of the 'Baltic Sunrise' is shown in Figure 3-5. It is created from the data that is provided by FleetMon and plotted in map. The maximum speed of this ship was 17.8 kn with average speed of 11.94 kn. The maximum draught and minimum draught of the ship were 21.6 m and 10.7 m respectively.

Figure 3-5: Route and speed (kn) of 'Baltic Sunrise'

The effective propulsive power of the ship in each position can be estimated by using the speed of the ship in that position, draught, breadth, residual resistance, and frictional resistance. ITTC-57 method and Gertler series data chart are used in this calculation. Figure 3-6 shows the steps of calculating the effective ship power.

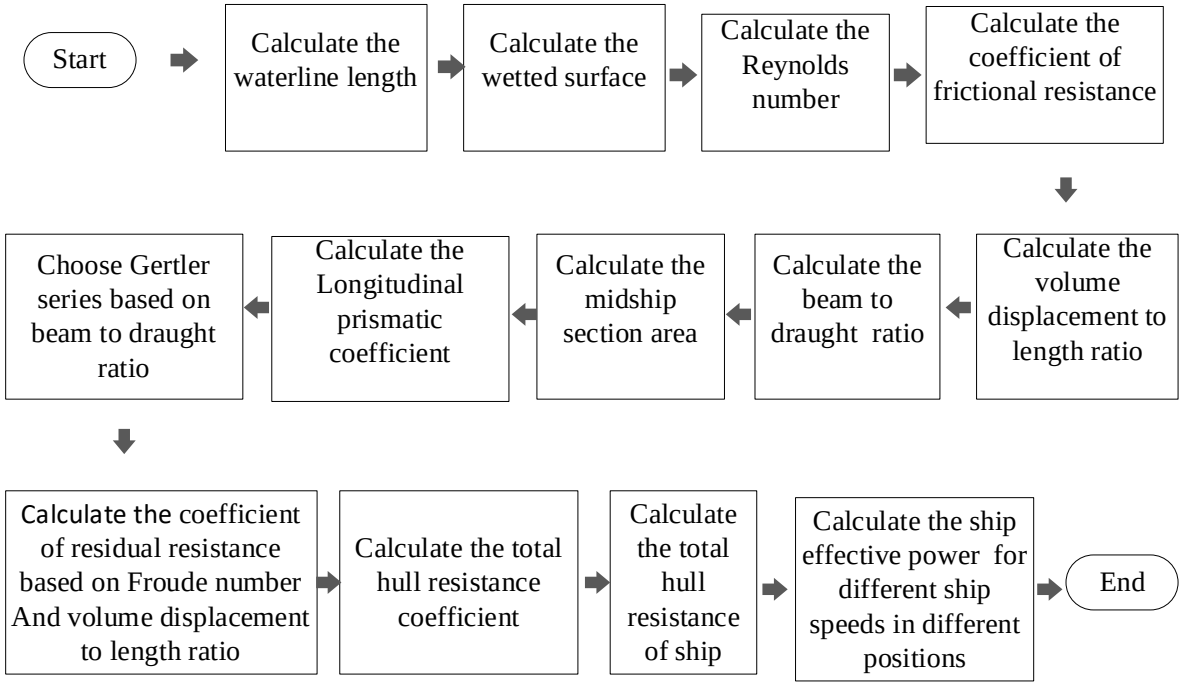

Figure 3-6: Steps of Calculating the Effective Ship Power

The Parameters and assumptions that have been considered in this calculation are summarized in Table 3-2.

Table 3-2: Parameters/ Assumption of 'Baltic Sunrise'

SL. No	Parameter/ Assumption	Category	Notation	Value	Reference
1	Beam of the ship	Parameter	B	60 m	[94]
2	Volume displacement of the ship	Parameter	v	344649.08 m^3	[94]
3	Draught of the ship	Parameter	D	21.60 m	[95]
4	Extreme breadth (Beam)	Parameter	Bex	60.04 m	[94]
5	Average draught of the ship	Parameter	D_avg	16.15 m	[95]
6	Length between perpendiculars	Parameter	LBP	324 m	[94]
7	Gravitational acceleration	Parameter	g	9.81 m/s^2	
8	Seawater density at 30^0C temperature	Parameter	ρ_w	1021.7 kg/m^3	[96]
9	Seawater viscosity at 30^0C temperature	Parameter	γ_w	0.84×10^{-6} m^3s^{-1}	[96]
10	Average speed of the ship	Parameter	Vs_avg	11.94 kn or 6.14 ms^{-1}	[95]
11	Incremental resistance coefficient due to surface roughness of ship	Assumption	C_A	0.0004	[96]
12	Maximum speed of the ship	Parameter	Vs_max	17.9 kn or 9.22 ms^{-1}	[95]

To estimate the effective ship power, the total hull resistance of that ship needs to be calculated. The following formula is used to calculate the total hull resistance [96].

$$R_{THR} = C_{THR} \cdot \frac{1}{2}\rho_w \cdot s_s \cdot {V_{s\_avg}}^2 \qquad \textit{Eq. 3-11}$$

Where, R_{THR} is the total hull resistance, C_{THR} is the coefficient of the total hull resistance, ρ_w is the density of the water, s_s represents the ship wetted surface, and V_{s_avg} is the average speed of the ship.
The coefficient of the total hull resistance and ship wetted surface can be calculated by the following equations

$$C_{THR} = C_{Fs} + C_{Rs} + C_A \quad \textit{Eq. 3-12}$$

$$S_s = 1 \cdot 7L_{wl} \cdot B + \frac{v}{D} = 55410.60 \text{ m}^2 \quad \textit{Eq. 3-13}$$

Where, $C_{Fs}, C_{Rs}, C_A, L_{wl}, B,\ v$, and D denote the coefficient of the frictional resistance, residual resistance coefficient, incremental resistance coefficient due to surface roughness of ship, waterline length, beam of the ship, volume displacement of the tanker, and draught of the ship respectively. The coefficient of the frictional resistance can be obtained by the following equations [97]

$$C_{Fs} = \frac{0.075}{(\log R_{ns} - 2)^2} = 1.37 \times 10^{-3} \quad \textit{Eq. 3-14}$$

$$R_{ns} = \frac{Vs\_avg \times L_{wl}}{\gamma_w} = 2.42 \times 10^{9} \quad \textit{Eq. 3-15}$$

$$L_{wl} = \frac{LBP}{0 \cdot 97} = 334.02\ m \quad \textit{Eq. 3-16}$$

Where, R_{ns} refers to Reynolds number, and LBP represents the lengths between perpendiculars. To obtain the value of residual resistance, the Gertler series need to be chosen for which Beam to Draught ratio and Longitudinal prismatic coefficient (Cp) is calculated as follows

$$\frac{B}{D} \cong 3.00 \quad \textit{Eq. 3-17}$$

$$C_p = \frac{v}{A_m L_{w_l}} \cong 0.6 \quad \textit{Eq. 3-18}$$

$$A_m = B_{ex} \times D = 1296.86 \text{ m}^2 \quad \textit{Eq. 3-19}$$

Where, A_m is the midship section of the ship, and B_{ex} is the extreme breadth. C_{Rs} value is selected from Gertler series by volume displacement to length ratio and Froude number of 'Baltic Sunrise' which are calculated as below

$$\frac{v}{L_{w_l}^3} = 9.2 \times 10^{-3} \quad \textit{Eq. 3-20}$$

$$F_{ns} = \frac{Vs\_max}{\sqrt{g \times L_{w_l}}} = 0.16 \quad \textit{Eq. 3-21}$$

Where, F_{ns} is the Froude number of the ship. By using this information, the C_{Rs} is calculated as 0.75×10^{-3} [98]. Now by *Eq. 3-1* and *Eq. 3-2*, R_{THR} can be obtained. After

getting the value of R_{THR}, ship effective power can be calculated for different positions at different speeds by using the following equation [96]

$$P_{ship\ (x,y)} = R_{THR} \cdot V_{s(x,y)} \qquad \textit{Eq. 3-22}$$

Where, $P_{ship\ (x,y)}$is the ship effective power at a position (x,y), R_{THR} is the total bare hull resistance of the ship, and $V_{s(x,y)}$ is the speed of the ship at a position (x,y).

The three months effective ship power is replicated into yearly (8,760 data set) effective power. Figure 3-7 shows the yearly power demand of the ship. Here, the 1st three months' data suggests the power demand from Iraq to Singapore. The 2nd three months' data shows the power requirement from Singapore to Iraq. The 3rd three months' data indicates the power requirement from Iraq to Singapore, and the 4th three months' data implies the power demand from Singapore to Iraq. For the simplicity of the calculation, the author considered that the ship started from Iraq in January'19 and reached Singapore in March'19.

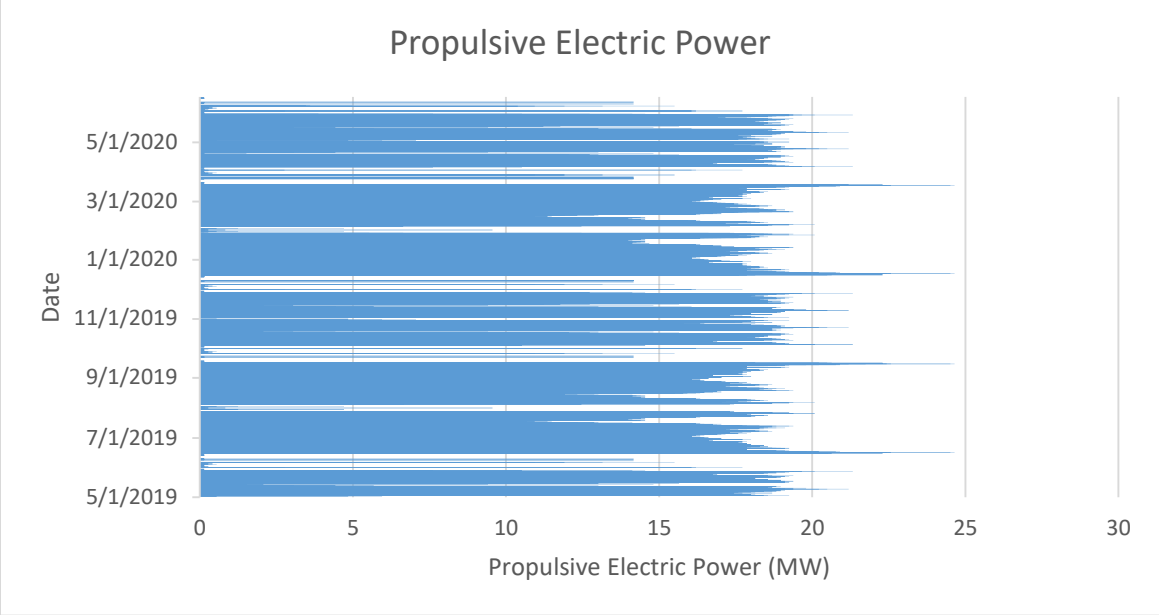

Figure 3-7: Ship Propulsive Power Requirement (Yearly)

From the above calculation, the maximum rating of propulsive electric power of this ship is 24.64 MW. Another type of electric power, namely 'Auxiliary Load', is considered along with propulsive power. Auxiliary load emulates the electrical load demand for lights, cooling systems, feed systems, pumps, and air compressors. Grzegorz et al. [99] assessed the auxiliary load to propulsive load ratio for different types of maritime vessels by collecting the data from ships register, logbook record and interviewing the captains of ships, chief engineers, and stations pilot.
Table 3-3 shows the auxiliary load to propulsive load ratio of different marine vessels.

Table 3-3: Auxiliary Load to Propulsive Load Ratio

Ship Type	Tanker	Reefer	RORO	General Cargo	Passenger Ship	Container Ship	Bulk Carrier
Auxiliary to Propulsion Ratio	0.21	0.41	0.26	0.19	0.28	0.22	0.22

Figure 3-8 shows the total electric load demand of the ship considering the auxiliary to propulsion ratio as 0.211. From this calculation the auxiliary load is around 5 MW which is considered for all the time including when the ship is in port for loading and unloading the cargo.

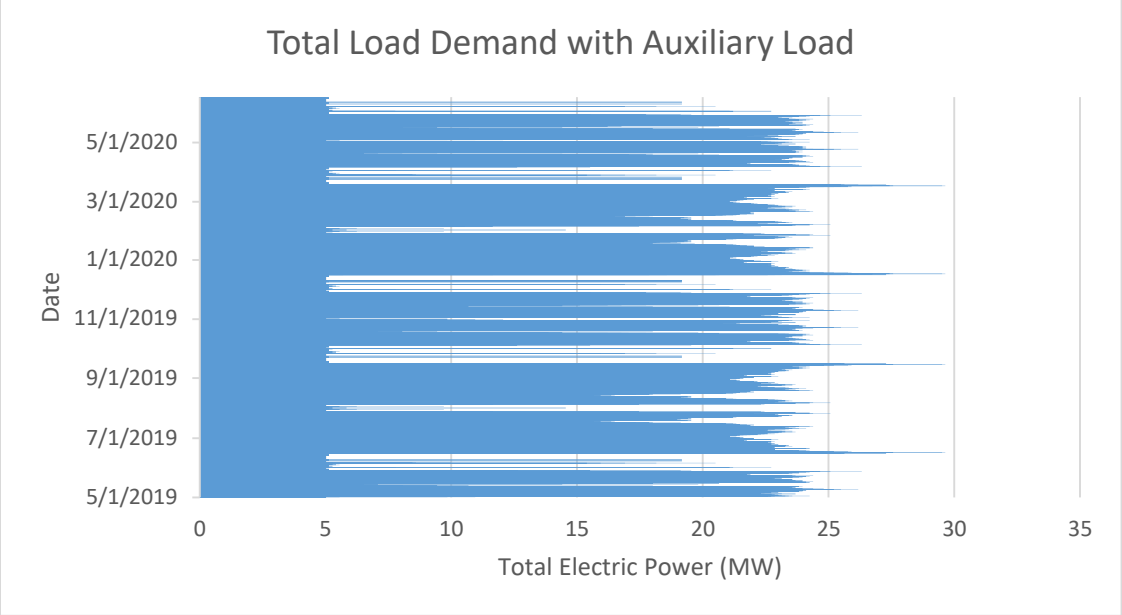

Figure 3-8: Ship Power Requirement (Yearly)

The above calculation shows that the maximum power demand for this ship is 29.64 MW and in practice, the ship power is 29.35 MW [94]. So, the estimation of ship power is very close to the real data.

To calculate the output power from solar PV and Wind turbine, hourly solar irradiance, temperature, and wind speed is required. The hourly data for one year holds a total of 8,760 data points. The solar radiation and wind speed differ in the shipping route with longitude and latitude, time, and date. To keep the calculation simple, the data of solar irradiance, wind speed, and temperature are obtained based on the monthly position of the ship in the adjacent port. The 8,760 data points of ship electrical energy demand, solar irradiance, wind speed, and temperature are used to determine the optimal configuration of N-R HES for marine transportation. Figure 3-9, Figure 3-10, and Figure 3-11 show hourly solar radiation, wind speed, and temperature data for one year respectively.

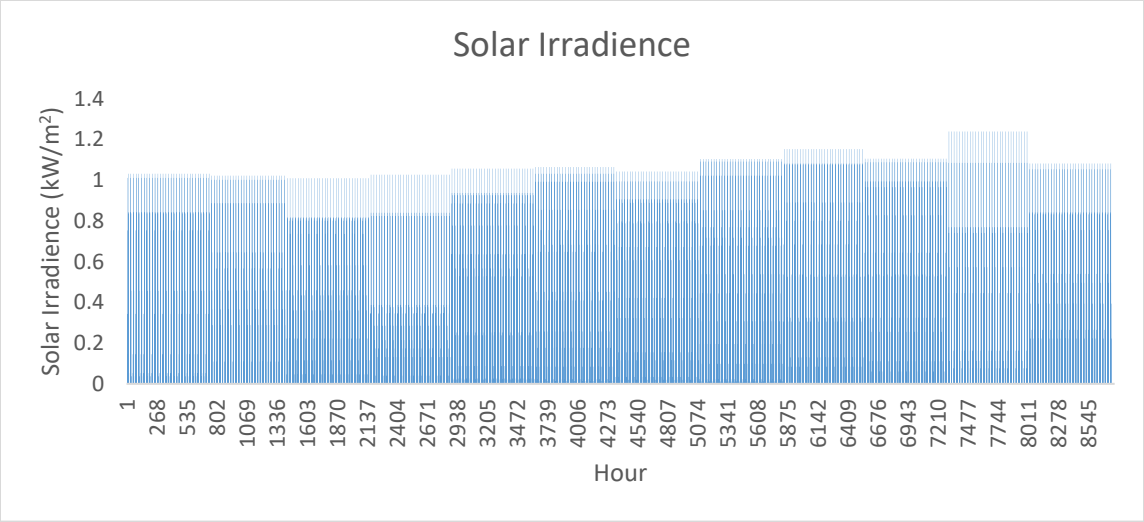

Figure 3-9: Hourly Solar Irradiance

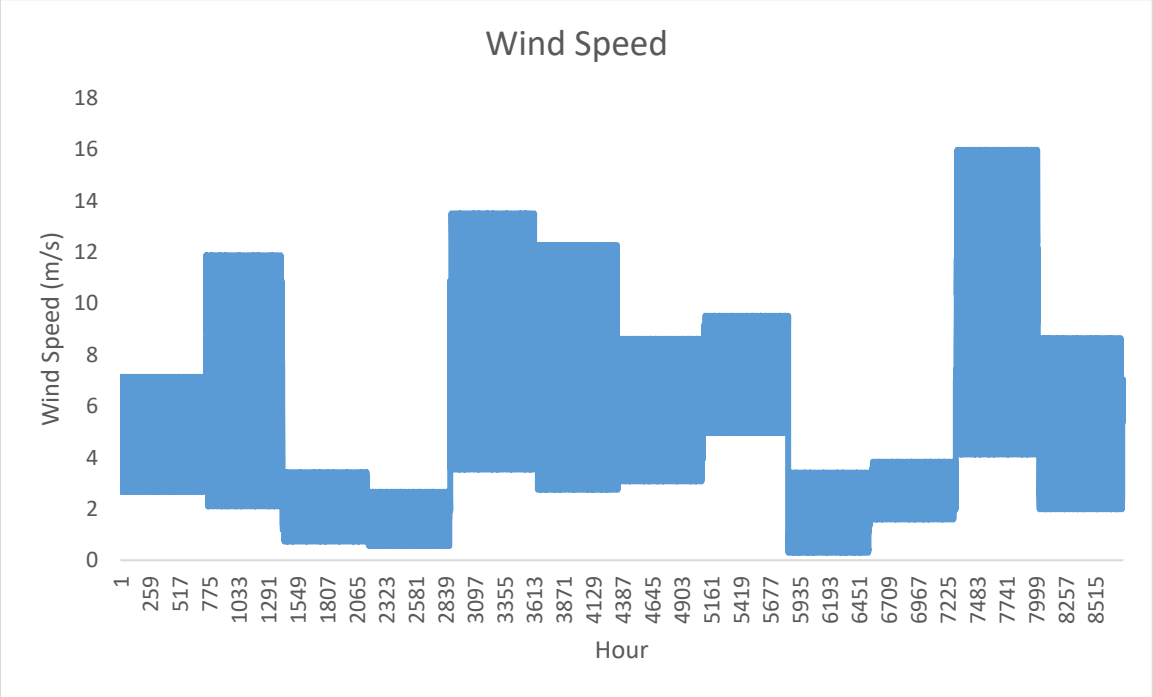

Figure 3-10: Hourly Wind Speed

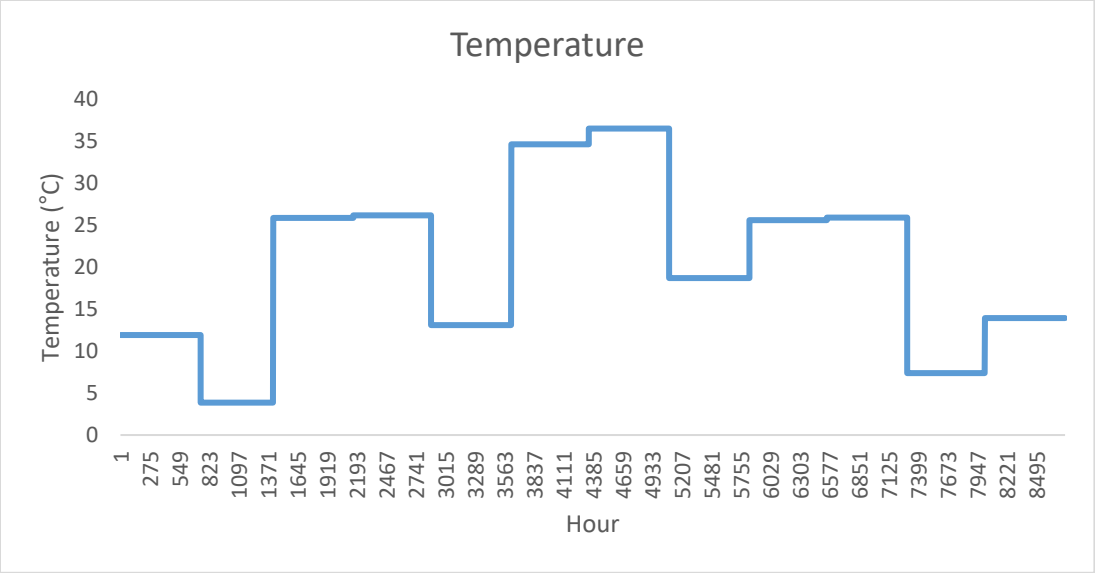

Figure 3-11: Hourly Temperature

3.4. **Analysis of Methodological Choice**

As discussed in section 2.6, the optimization techniques for hybrid energy systems can be divided into three major categories, Classical, Meta-Heuristic, and Computer Software. Considering the complexity of hybrid energy systems in terms of constraints, system component performance, and availability of resources, classical optimization is not a good option to optimize the hybrid system [51]. Computer software like HOMER is used by many researchers for the planning and optimization of Hybrid Energy Systems. In this study, the HOMER software is used to get an initial idea about the feasibility of N-R HES in marine ships. However, there are some limitations of HOMER software to optimize any hybrid systems.

Firstly, in HOMER, only predefined constraints can be given but in a real-world scenario, there are different constraints and those are very important to be addressed to find out the reliable and practical optimal configuration of the system. For example, there is a constraint of integrating solar panels in marine ships based on the available area. Also, the weight of the total energy system components should be within a certain limit which will ensure that the cargo-carrying capacity of the marine ship will not be impacted due to the weight of the system components. This reliability needs to be checked every time step and yearly. So, there are several constraints that HOMER cannot address

Secondly, while optimizing the system in HOMER, the upper bound and lower bound of all the system components can not be defined. For the generator (MR and Diesel Generator), the user needs to define the search space in HOMER based on the understanding of the system. All the possible solution candidates can not be defined in the search space as there could be thousands of possible solutions.

Thirdly, HOMER does not disclose its' optimization algorithm. It only refers that it uses a proprietary derivative-free algorithm for the optimization. There are lots of derivate free optimization algorithms like Bayesian optimization, Cuckoo Search, Genetic Algorithms, and Pattern search. So, HOMER optimization is a black box from the outside and users are unable to know how the optimization is working and validate the result. The main drawback of HOMER software is that it considers several simplifications during the optimization process which affects the accuracy of the result [59]

In this study, all the energy systems are evaluated and compared by using HOMER software. This study gives a preliminary idea of the technical, economical, and environmental performance of different energy systems. However, considering the shortcomings of Classical Optimization techniques and HOMER software, Meta-Heuristic optimization (Differential Evolution) is also studied in this research. The DE algorithm is a global optimization technique. It is reliable, easy to implement, and simple to understand. The basis of DE is the genetic algorithm that is first introduced by Storn and Price in 1997. The principle idea of the DE algorithm is to produce temporary individual best based on the individual differences within the population and then rebuild the population evolutionary. Because of its robustness, the suitability of different numerical optimization, and better global convergence, it has been used extensively in many problems like image classification, linear array, neural network, and monopoles antenna [100]. The number of publications by using the DE algorithm in different years is shown in Figure 3-12. It can be seen that since 2009 the usage of DE has been increased a lot. Figure 3-13 represents the different areas where DE optimization was used in 2019. Computer science, Engineering, and Mathematics were the major areas where DE was used in 2019.

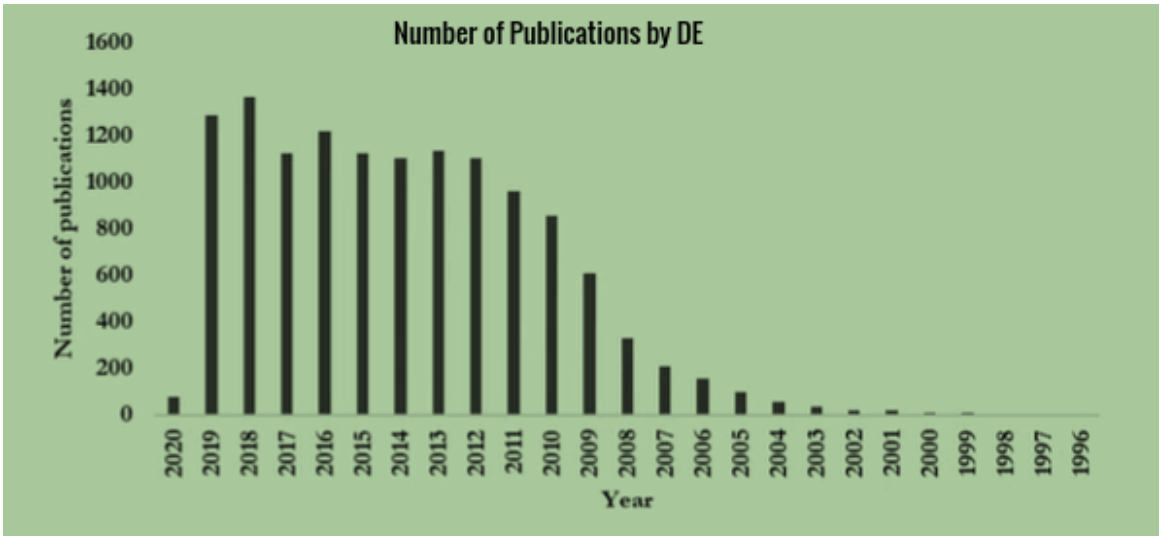

Figure 3-12: Number of Publication by DE Optimization Algorithm

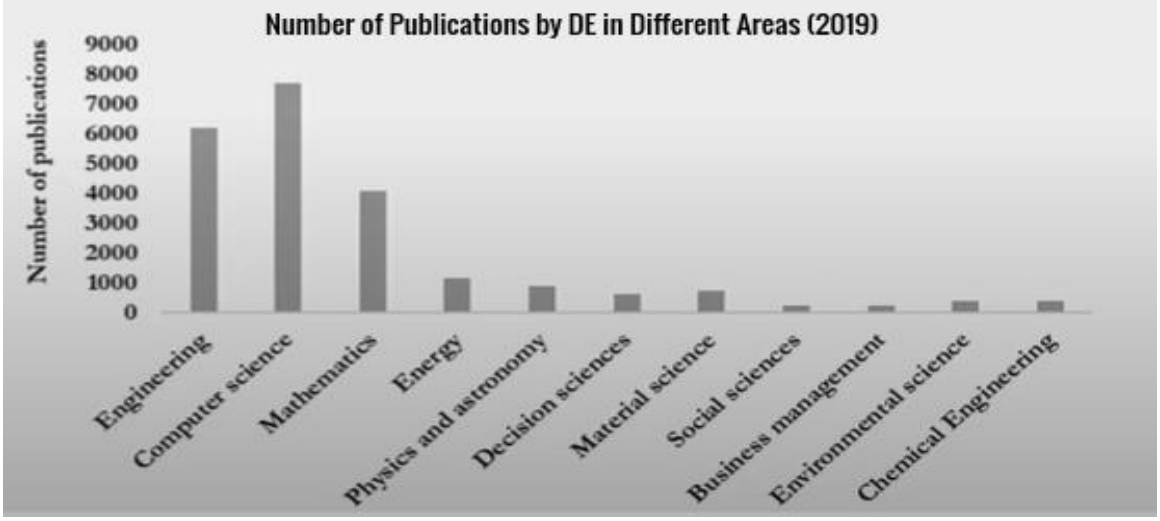

Figure 3-13: Number of publications by DE Optimization in Different Areas (2019)

Along with DE, PSO is widely used for optimization purposes. TLBO is another emerging optimization technique which is being used by many researchers recently. The comparison among DE, PSO, and TLBO is presented in Figure 3-14 [101].

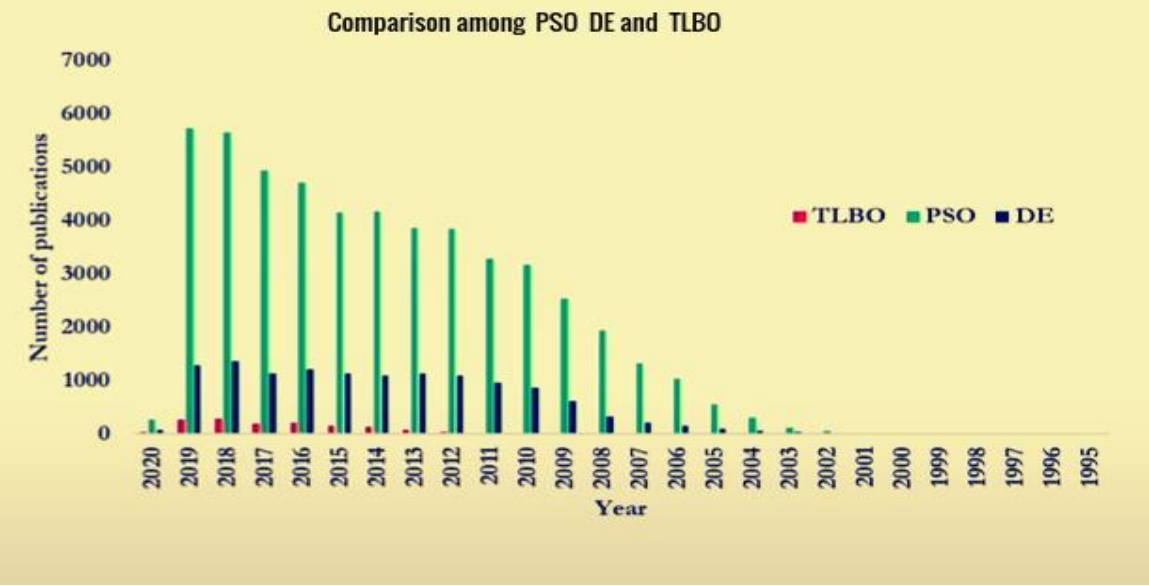

Figure 3-14: Comparison Among PSO, DE, and TLBO

The performance of PSO and DE was carried out in [54]. In this study, the authors used some benchmark functions that were optimized by both PSO and DE. They compared both optimization techniques in terms of robustness and the number of iteration that are required to bring the solution to a feasible region. They concluded that DE outperformed PSO and

the favored value of scaling factor of crossover probability of DE parameters are 0.5 and 0.9 respectively.

This author acknowledges that the performance of the DE algorithm depends on the evolutionary parameters, and different optimization techniques may result in different values of the objective function. To address this issue, the optimized system obtained by the DE algorithm is compared with the PSO algorithm. Also, an adaptive parameter adjustment method is used with the DE algorithm to check the effect of the control parameters on the DE algorithm performance.

3.5. Assumptions

This study considered several assumptions. The topic-specific assumptions have been addressed in that specific topic. Some key assumptions are summarized below

- This study considers the three months energy requirement of the 'Baltic Sunrise' and assumes that this data can be used for yearly energy requirements.
- The solar irradiance and wind speed of the ship are the same as the adjacent port.
- Seawater temperature is considered as 30°C while calculating the energy requirement of the ship. This assumption is made based on the route of the ship and the seawater temperature along the route. The global seawater temperature can be found in [102].
- This study assumes that the refueling of the nuclear reactor will be done when the ship will be in the port for loading and unloading the cargo or oil. In another word, the impact of refueling on energy management has not been considered in this study.
- The study considers that the manufacturers can provide MR/vSMR, solar PV, and wind turbine as per the required rating from the customer (ship operators/ shipbuilders)
- This study only considers the electrical requirement of the ship. Other applications like CHP or the production of secondary commodities (e.g. seawater desalination, and hydrogen production) are out of the scope of this study.

Chapter 4: System Modeling

This chapter covers the system modeling of different components of the energy systems including Microreactor, Solar PV, Wind Turbine, Diesel Generator, and Energy Storage Systems (ESS)

4.1. Nuclear Power Plant (Microreactor)

This study evaluates the lifecycle cost of vSMR and focuses on the economic model of it. SMR is a fourth-generation nuclear reactor having power equivalent to 300 MWe or less. Modular fabrication, passive safety systems, and enhanced protection against man-made or natural hazards are some advanced features of SMR. A subcategory of SMR is vSMR which power rating is less than 15 MWe[42]. Another subcategory of SMR is Microreactor (MR), which typically ranges from 1 MWe to 50 MWe [43].

Based on the lifecycle phases of SMR and nuclear fuel, the cost of vSMR can be divided into three major categories which are capital costs, annual operating costs, and backend costs[47]. Figure 4-1 represents the cost breakdown of vSMR. Capital costs of vSMR include overnight costs, costs of initial fuel, and Interest During Construction (IDC). The overnight costs can be further broken down into three subcategories, direct costs, indirect costs, and owners' costs. The direct costs, indirect costs, and owners' costs cover 70%, 10% to 15%, and 15% to 20% cost of overnight costs, respectively. The initial fuel costs cover the cost associated with the lifecycle phases (uranium ore, conversion, enrichment, and fabrication) of nuclear fuel. Annual operating costs include fuel costs (refueling) and non-fuel costs. The backend costs refer to costs related to D&D and UNF. The costs of UNF can be broken down to wet storage costs, dry storage costs, waste conditioning costs, transportation costs, and DGR costs. The design and licensing costs are included in the capital costs of the vSMR

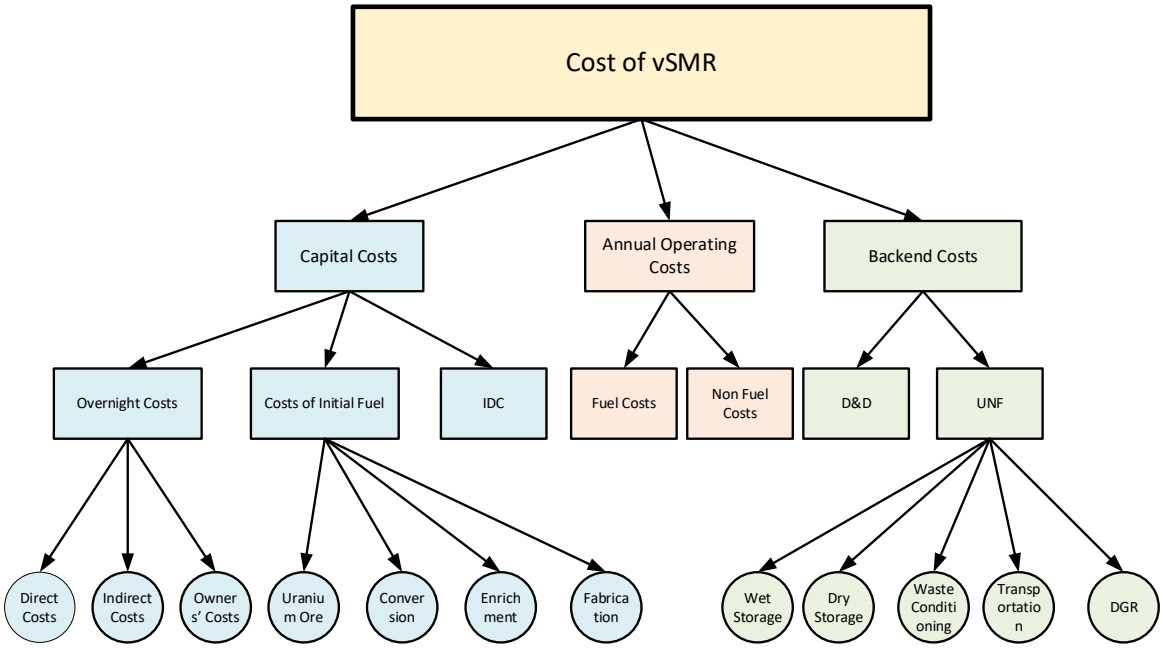

Figure 4-1: Cost Breakdown of vSMR

The first deployment cost of any technology is higher compared to the subsequent deployment. The rate of cost reduction of the next deployment depends on the lesson learned from the prior deployment. The cost reduction depends on the learning rate of the factories. The learning rate refers to the cost reduction of a factory which can be achieved by the experience and learning on how to execute a process and use different tools to deliver a product. It has been observed that with optimal conditions learning rate can be 20% or above.

Different industries are experiencing different learning rates and it varies based on the characteristics, production rates, and standard of the industry. Figure 4-2 shows the learning rates of different industries [103].

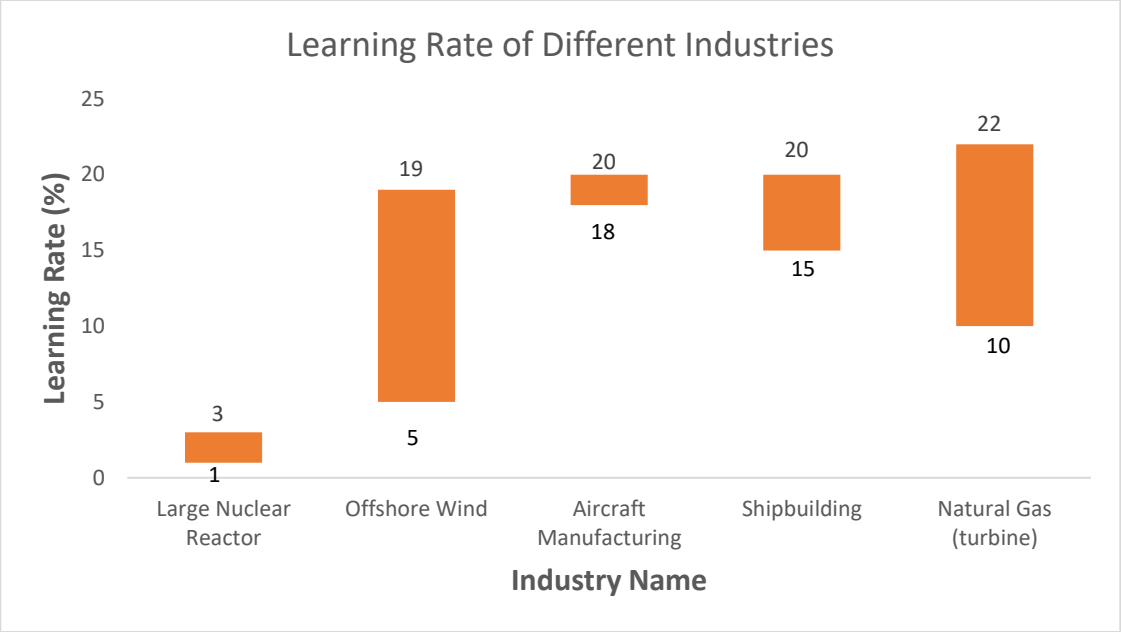

Figure 4-2: Learning Rate of Different Industries

The learning rate of SMR industry depends on five key factors that are Modularisation and factory build, Production rates, Supply Chain, Design standardization, and Regulatory stability. The learning rate of SMR could be 8% to 10% by enhancing the five key factors. The relation between learning rate and cost reduction can be expressed by the following equation [104]

$$R = \log2(1 - \mathrm{LR}) \qquad \textit{Eq. 4-1}$$

Where, R is the rate of cost reduction and LR is the learning rate. In this study, the learning rate is considered as 10% [105]. The reduction in fuel cost is also expected as nuclear fuel will be produced in bulk amount in the future to cater to the SMR demand. The operation and maintenance costs will be reduced also from the maintenance and operating experience. However, the cost reduction is considered only for the overnight cost in this study. The relation between the vSMR capital cost and the rate of cost reduction can be expressed by the following equation

$$vSMRC_u = vSMRC_{1st} \times {N_{th}}^R \qquad \textit{Eq. 4-2}$$

Where, $vSMRC_u$ is the unit cost of N_{th} vSMR ($), $vSMRC_{1st}$ is the 1st vSMR cost ($), and R is the rate of cost reduction.

vSMR is capable to perform both baseload operation and load-following operation. In the load following operation mode, vSMR is will supply energy by matching with the energy demand. The load-following feature is desired to add flexibility to the power system. The load following characteristic can be achieved in vSMR by bypassing the steam turbine,

controlling the reactor rods, and taking some modules offline. In the baseload operation, vSMR always supplies constant power. As the initial investment of nuclear power is high, continuous or baseload operation of vSMR is expected to recover the high initial cost. The SMR vendor outlines that load following feature of SMR affects the main steam supply and coolant system components and frequent replacement might be required. The service life of the heat exchanger is also impacted by the load following characteristics. However, the load following operation of SMR is viable if flexible power contracts are offered to SMR operators which will give them additional value [103]. As per the European Utility Requirements, the new reactors should be able to follow the load to 50% and 100% power with a ramp rate of around 5% per minute. During the Extended Reduced Power Operation (ERPO), reactors can operate as low as 30% of its' rated power for several days to several months. In this study, the baseload operation of vSMR is considered for all the time except the time of loading and unloading the cargo/liquid (oil) in the port when ERPO (30% of the rated power) is considered in MATLAB software. However, the HOMER software considers the load following feature. The parameters of MR are summarized in Table 4-1 [47] [106]

Table 4-1: Parameters of MR

Parameters	Value
Reactor size (kWe)	1000
Plant lifetime (Years)	40
Overnight capital cost ($/kWe)	15000
Fixed O&M cost ($/kWe)	350
Fuel cost ($/MWh)	10
Refueling cost of fuel module ($)	20 million
Core lifetime (Years)	10
Decommissioning cost ($/MWh)	5
Capacity factor (%)	95
Plant efficiency (%)	40
CO_2 emission (kg/MWh)	4.55

Although there are no CO_2 emissions during the operation of SMR, CO_2 emits in the lifecycle of SMR, mainly in the construction stage due to concrete production and in the

fuel processing stage due to the high demand for electricity and fossil fuel. The refueling cost does not include the fuel cost; it refers to the transportation cost from the factory to the site with associated labor cost. The refueling cycle is considered 10 years in this study. Some SMR can be designed to have a refueling cycle of more than ten years. A long refueling cycle offers some advantages like higher fuel security and lower logistical costs [107]. Literature review, technical paper, reports from IAEA and CNL, and email communication are the basis of cost collection of MR.

4.2. **Solar Energy**

There are two ways to utilize solar energy, one is Concentrated Solar Power (CSP), and another is Solar Photovoltaic (Solar PV). In the CSP, mirror technology is used to concentrate the sun's energy onto a receiver and then convert the energy into heat. This heat is used to generate steam and this steam is used to drive a turbine to generate electricity. There are four types of CSP technologies: Parabolic Trough Systems, Power Tower Systems, Linear Fresnel Systems, and Parabolic Dish Systems [108].

In the Solar PV systems, PV cell absorbs sunlight. This absorbed sunlight dislodge the electrons of the PV cell from their atoms. The flow of the loose electrons creat current which is transferred by wires. There are mainly two types of solar cells: monocrystalline and polycrystalline. There are other types of Solar PV like thin-film cells, organic cells, or perovskites. However, monocrystalline and polycrystalline are used for commercial and residential purposes [109]. There are two common configurations for solar panels, which are 60-cell and 72-cell. 60-cell solar panels range from 285 W to 315 W, and 72-cell solar panels range from 335 W to 375 W. For a 6.5 kW system, 18 panels of the 72-cell solar panel are required [110]. The length and width of each 72-cell solar panel are 77 inches and 36 inches respectively. So, around 5 m^2 area is required for a unit (1 kW) solar panel.

The generation of solar power from solar PV depends on the ambient temperature, solar irradiance, and solar PV area. The output power from solar PV can be calculated by using the following equation [111].

$$P_{SPV}(t) = Num_{SPV} \times \eta_{SPV}\,(\mathrm{t}) \times PV_A \times R_t(t) \qquad \forall\, t \in t_{total} \qquad \textit{Eq. 4-3}$$

Where, $P_{SPV}(t)$ is the output power from the solar PV (W), Num_{SPV} is the number of solar PV, η_{SPV} (t) is the instantaneous efficiency of the solar PV, PV_A is the area occupied by the solar PV, and $R_t(t)$ is the solar irradiance (W/m^2).

The instantaneous efficiency of the solar PV can be obtained by the below equation

$$\eta_{SPV}(t) = \eta_{pv-ref} \times \eta_{MPPT} \times \left[1 + \beta(T_c(t) - T_{c-ref})\right] \qquad \forall\, t \in t_{total} \qquad \textit{Eq. 4-4}$$

Where, $\eta_{SPV}(t)$ is the instantaneous efficiency of the solar PV (%), η_{pv-ref} is the reference efficiency of the solar PV (%), η_{MPPT} is the efficiency of the Maximum Power Point Tracking (MPPT) unit which is 1 in this study, $T_c(t)$ is the temperature of the PV cell (℃) at time step t , T_{c-ref} is the reference temperature of the PV cell (℃), and β is the temperature coefficient of efficiency ($℃^{-1}$).

The PV cell temperature can be obtained by the proposed PV model by Markvar [112]. The below equation

$$T_c(t) = T_a(t) + \left(\frac{NOCT - 20}{800}\right) \times R_t(t) \qquad \forall\, t \in t_{total} \qquad \textit{Eq. 4-5}$$

Where, $T_a(t)$ is the ambient temperature at time step t, and $NOCT$ is the normal operating temperature. All the parameters that are considered in this study are listed in the below table

Table 4-2: Parameters of the Solar PV Panel

Parameter	Value	Reference
Area Occupied by unit PV panel (m^2)	5	[40]
Capital Cost ($/kW)	640	[37]
Replacement Cost ($/kW)	640	[37]
O&M Cost ($/kW/Year)	12	[113]
Lifetime (Years)	25	[114]
Reference Efficiency of PV Panel (%)	24	[115]
Efficiency of the MPPT unit (%)	100	[28]
Temperature Coefficient ($℃^{-1}$)	-0.0041	[116]
PV panel reference temperature (°C)	25	[116]
Nominal Operating Cell Temperature (°C)	45	[116]

4.3. **Wind Energy**

The wind is a great source of energy and has the potential to generate electricity without any fuel. Several models can be used to estimate the output power of the wind turbine, like the model based on Weibull parameters [117], [118], the linear model [119],[120], and the quadric model. In this study, the quadric model is used. To calculate the output power of the wind turbine, the wind speed at hub height needs to be obtained by the following equation [121]

$$V_{whub}(t) = V_{wref}(t) \times \left(\frac{H_{whub}}{H_{wref}}\right)^{\mu} \qquad \forall\, t \in t_{total} \qquad \textit{Eq. 4-6}$$

Where, $V_{whub}(t)$ is the wind speed at the hub height (m/s) at time step t, $V_{wref}(t)$ is the wind speed at the anemometer height (m/s) at time step t, H_{wref} is the anemometer height (m), H_{whub} is the hub height (m), and μ is the power-law coefficient of the wind speed.

After measuring the wind speed at the hub height, it is used to calculate the wind turbine power by using the following equations [122].

$$P_W(t) = \begin{cases} 0, & V_{whub}(t) < V_{cin}, V_{whub}(t) > V_{cout} \\ \frac{P_r}{V_r^3 - V_{cin}^3} \times V^3{}_{whub}(t) - \frac{V_{cin}^3}{V_r^3 - V_{cin}^3} \times P_r, & V_{min} \le V(t) \le V_r \\ P_r, & V_r \le V(t) \le V_{max} \end{cases} \quad \text{Eq. 4-7}$$

Where, $P_W(t)$ is the output power of the wind turbine (kW) at time step t, P_r is the rated power of the wind turbine (kW), V_r is the rated wind speed of the wind turbine (m/s), V_{cin} is the cut-in speed of the wind turbine (m/s), V_{cout} is the cut-out wind speed (m/s), and V_{whub} is the measured wind speed at the hub height (m/s). A typical power curve of a wind turbine is shown in Figure 4-3 The parameters that have been considered in this study are listed in Table 4-3.

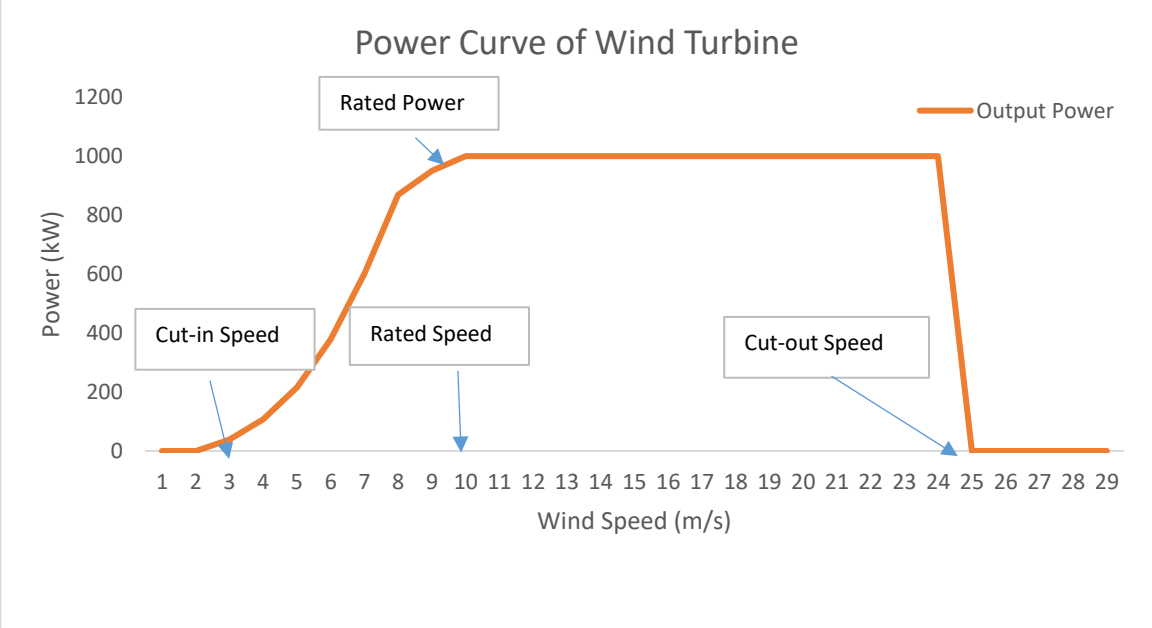

Figure 4-3: Typical Power Curve of a Wind Turbine

Table 4-3: Parameters of the Wind Turbine

Parameter	Value	Reference
Nominal Capacity (kW)	50	[123]
Capital Cost ($/kW)	1130	[124]
Replacement Cost ($/kW)	1130	[124]
O&M Cost ($/kW/Year)	48	[125]
Lifetime (Years)	25	[126]
Hub Height (m)	45	[123]
Anemometer Height (m)	50	[127]
Minimum wind speed (m/s)	3	[128]
Maximum wind speed (m/s)	25	[123]
Rated wind speed (m/s)	10	[128]
Power Law Exponent	1/7	[121]

4.4. **Energy Storage System**

The EES is considered in this study to store the excess energy in the form of chemicals and supply when requires. The rating of the EES depends on the rating of the load, autonomy hour, depth of discharge of the battery, the efficiency of the battery, and the inverter. The rating (kWh) of the battery can be expressed by the following equation [61].

$$BAT_{rating} = \frac{P_{load} \times AH \times N_{bat}}{DOD_{bat} \times \eta_{inv} \times \eta_{bat}} \quad \textit{Eq. 4-8}$$

Where, P_{load} is the rating (kW) of the load, AH is the autonomy hours, N_{bat} is the number of battery, DOD_{bat} is the depth of discharge of the battery, η_{inv} is the efficiency of the inverter, and η_{bat} is the efficiency of the battery. In this study, the load is considered as 70 kW [129]which refers to the total load demand of navigation light, all types of radio installations, all types of communication equipment, navigational equipment, fire detection and alarm system, and one of the main fire pumps. These facilities need to be served in the time of emergency [129]. The autonomy hour refers to the required amount of time to serve the load continuously in an emergency situation. The autonomy hour is between 12 hours to 18 hours [130]. In this paper, autonomy hour is taken as 18 hours. The DOD_{bat}, η_{inv}, and η_{bat} is 80% [105], 95% [131], and 85% [132] respectively.

The state of charge (SOC) of the battery bank depends on the DOD and rating of the battery. The maximum and minimum SOC of the battery can be calculated by the following equations

$$BAT_{SOC,max} = BAT_{rating} \times DOD_{bat} \quad \textit{Eq. 4-9}$$

$$BAT_{SOC,min} = BAT_{rating} \times (1 - DOD_{bat}) \quad \textit{Eq. 4-10}$$

Where, $BAT_{SOC,max}$ is the maximum SOC of the battery bank and $BAT_{SOC,min}$ is the minimum SOC of the battery bank. The charging and discharging of the battery bank at any time step depend on the available energy that can be given to the battery bank, the amount of energy that is needed from the battery bank, and the SOC of the battery bank in the previous time step. $BAT_{SOC,min}$ is considered the initial SOC of the battery in this paper.

The amount of energy that can be given to the battery and the amount of energy that is needed from the battery bank at any time step can be calculated by the following equations

$$BAT_{in}(t) = \left(P_{gen}(t) - P_L(t)\right) \times \eta_{bat}\,; \qquad P_{gen}(t) > P_L(t) \qquad \textit{Eq. 4-11}$$

$$BAT_{out}(t) = \frac{P_L(t) - P_{gen}(t)}{\eta_{bat}}\,; \qquad P_{gen}(t) < P_L(t) \qquad \textit{Eq. 4-12}$$

$$P_{gen}(t) = P_{pv}(t) + P_w(t) + P_{MR}(t) \qquad \forall\, t \in t_{total} \qquad \textit{Eq. 4-13}$$

$$P_{gen}(t) = P_{pv}(t) + P_w(t) + P_{GNRT}(t) \qquad \forall\, t \in t_{total} \qquad \textit{Eq. 4-14}$$

Where, $BAT_{in}(t)$, $BAT_{out}(t)$, $P_{gen}(t)$, $P_L(t)$, $P_{pv}(t)$, $P_w(t)$, $P_{MR}(t)$, $P_{GNRT}(t)$ is the amount of energy that can be given to the battery bank, the amount of energy that is needed from the battery bank, the total electric energy generation, the total electric load, the total electric energy from the solar panel, the total electric energy from the wind turbine, the total electric energy from MR, and the total electric energy from diesel generator at the time step (t), respectively.

The amount of energy that the battery bank can take and give at any time step can be formulated by the below equations

$$BAT_{SOC,min} \le BATe(t-1) \le BAT_{SOC,max}$$

$$BAT_{take}(t) = BAT_{SOC,max} - BATe(t-1)\,; \quad \forall\, t \in t_{total} \qquad \textit{Eq. 4-15}$$

$$BAT_{give}(t) = BATe(t-1) - BAT_{SOC,min}\,; \qquad \forall\, t \in t_{total} \qquad \textit{Eq. 4-16}$$

Where, $BATe(t-1)$ is the battery energy at time step $(t-1)$, $BAT_{take}(t)$ is the amount of energy that can be taken by the battery bank at the time step (t), and $BAT_{give}(t)$ is the amount of energy that can be given by the battery bank at the time step (t).

The charging and discharging of the battery bank can be calculated by the following equations

$$BAT_{chrg}(t) = BAT_{SOC,max}\,; \qquad P_{gen}(t) > P_L(t)\ \&\ BAT_{in}(t) \ge BAT_{take}(t) \qquad \forall\, t \in t_{total} \qquad \textit{Eq. 4-17}$$

$$BAT_{chrg}(t) = BATe(t-1) + BAT_{in}(t)\,; \qquad P_{gen}(t) > P_L(t)\ \&\ BAT_{in}(t) < BAT_{take}(t) \qquad \forall\, t \in t_{total} \qquad \textit{Eq. 4-18}$$

$$BAT_{dischrg}(t) = BAT_{SOC,min}\ ; \quad P_{gen}(t) < P_L(t)\ \&\ BAT_{out}(t) \geq BAT_{give}(t) \quad \forall\ t \in t_{total} \qquad \text{Eq. 4-19}$$

$$BAT_{dischrg}(t) = BATe(t-1) - BAT_{out}(t)\ ; \quad P_{gen}(t) < P_L(t)\ \&\ BAT_{out}(t) < BAT_{give}(t) \quad \forall\ t \in t_{total} \qquad \text{Eq. 4-20}$$

$$BAT_e(t) = BATe(t-1)\ ; \quad P_{gen}(t) = P_L(t) \quad \forall\ t \in t_{total} \qquad \text{Eq. 4-21}$$

Where, $BAT_{chrg}(t)$, $BAT_{dischrg}(t)$, and $BAT_e(t)$ refers to the battery capacity after charging, battery capacity after discharging, and battery capacity when energy generation and demand are exactly the same, respectively at time step (t). If there is any excess energy that will be dumped. The parameters of EES are tabulated in Table 4-4

Table 4-4: Parameters of the EES

Parameter	Value	Reference
Capital Cost ($/kWh)	398	[133]
Replacement Cost ($/kWh)	398	[133]
O&M Cost ($/kWh/Year)	10	[134]
Lifetime (Years)	5	[133]
Efficiency (%)	85	[135]
Days of Autonomy (Days)	3	[61]
Depth of Discharge (%)	80	N/A
Inverter Efficiency (%)	95	[136]

4.5. **Diesel Generator**

For comparing the proposed N-R HES with the conventional energy systems for ocean-going marine ships, Fossil Fuel-based Generator (FFG) is considered in this study. A marine vessel's traditional energy system consists of a main engine, auxiliary engine, heat recovery steam generator, and shaft generator [137]. Figure 4-4 shows the lifecycle cost of a diesel generator. The cost of a diesel generator can be categorized broadly into three major categories, 'Capital Cost,' 'Operating Cost,' and 'Decommissioning Cost.' Since the decommissioning cost of a diesel generator is minimal, it can be ignored. The capital cost includes overnight cost and Interest during Construction (IDC). The overnight cost of a diesel generator refers to the expense if the diesel generator is built right away. Overnight cost does not include the interest rate during the construction of the diesel generator [47]. Typically, overnight cost includes construction costs, supply and installation costs, electrical controls costs, and project costs, including labor costs, and scaffolding costs.

Operating costs of diesel generators consist of fuel costs and non-fuel costs. Non-fuel cost includes lubricant costs, wages to operator personal, supplies and service costs, travel and accommodation costs. Fuel and lubricant expenses comprise 44.6% of total Operating and Maintenance (O&M) costs [138]. The input parameters of the diesel generator considered in this study are presented in Figure 4-4

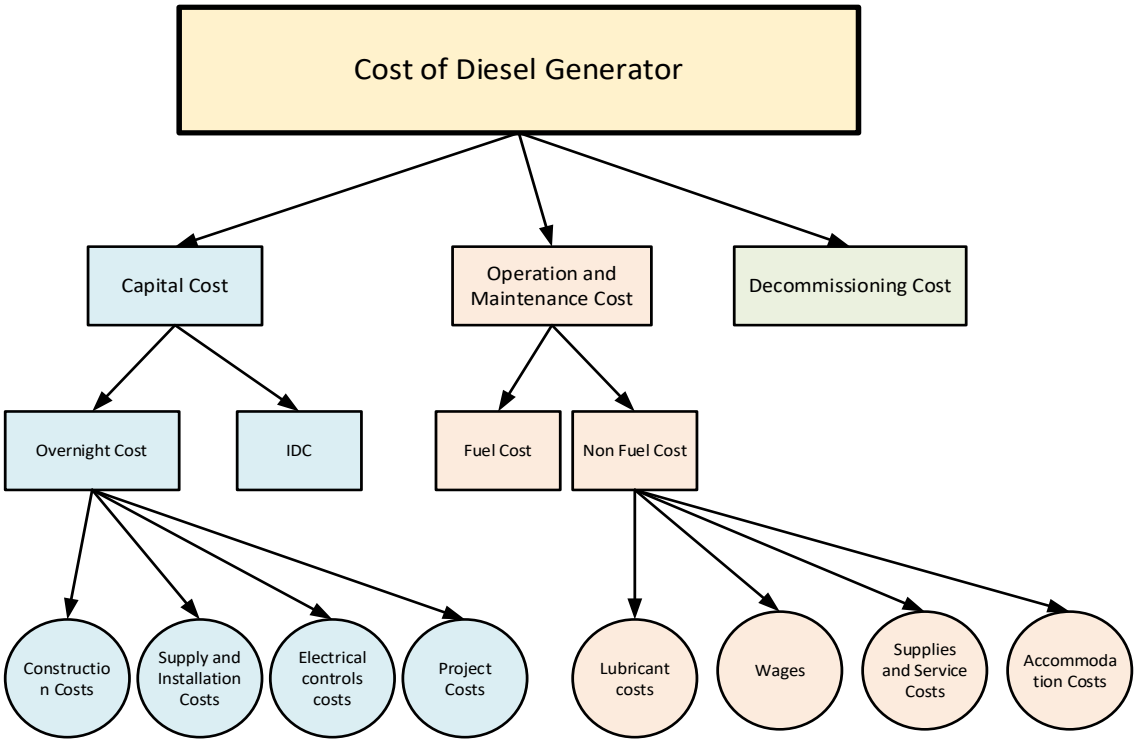

Figure 4-4: Cost Breakdown of Diesel Generator

Table 4-5: Specification of diesel generator

Parameters	Value	Reference
Generator Size (kW)	1000	[137]
Capital Cost (USD/kW)	800	
Replacement Cost (USD/kW)	800	
Fixed O & M cost (USD/kW/Year)	35	
Lifetime (Years)	2.5	
Fuel cost (USD/MWh)	202	[47]
CO_2 emission (kg/MWh)	700	

Chapter 5: System Optimization

This section formulates the optimization model to find out the optimal configuration of different HESs. The chapter also discusses the decision variables, the optimization constraints, the optimization problem's boundary conditions, and steps of implementing DE, ADE, and PSO algorithm. The mathematical modeling is used to optimize the energy systems in MATLAB environment. The computer software-based tool (HOMER) is also used to optimize the system. However, to optimize the energy systems in HOMER, authors do not need to model objective function, constraints, and decision variables. There are some built-in and pre-defined constraints, objective function, and decision variables are available in HOMER software.

5.1. Objective Function

The objective of the optimization problem is to identify the optimal configuration of the HES components to achieve the lowest NPC. Along with the N-R HES, other three energy systems, namely 'Standalone Fossil Fuel Based Energy Sytems', 'Renewable and Fossil Fuel Based Hybrid Energy System', and 'Standalone Nuclear Energy System' are optimized also to compare with the proposed N-R HES. The objective function represents the economic KPI and the constraints of the optimization problem cover the technical and other KPIs like LPSP, PWR. The fitness function of the optimization problem is the total NPC of all the system components. The fitness function of the optimization problem can be formulated as below

$$\min f_{NPC} = \sum_{j \in K} NPC_j \qquad \textit{Eq. 5-1}$$

Where, K is the system component set and NPC_j refers to the NPC of the j^{th} component. The system components comprise solar PV, wind turbine, MR, battery, and diesel generator. The NPC of any component represents the present value of the total cost of the component including capital cost, O&M cost, cost of replacement, cost of fuel, and salvage value. For MR, decommissioning cost and refueling cost is added additionally. The NPC of any system component can be expressed as follows

$$NPC_j = C_{capc,j} + C_{repc,j} + C_{O\&Mc,j} + C_{fuelc,j} - C_{salvc,j} \qquad \forall i \in G \qquad \textit{Eq. 5-2}$$

Where, $C_{capc,j}$, $C_{repc,j}$, $C_{O\&Mc,j}$, $C_{fuelc,j}$, and $C_{salvc,j}$ represent the present value of capital cost, replacement cost, O&M cost, fuel cost, and the salvage value of the j^{th} component respectively. The salvage value of a component refers to the remaining value of a component at the end of the project lifetime [139]

The capital cost of any component is calculated at the beginning of the project. The total capital cost involves the capital cost of each component and the number of components. As the capital cost is calculated at the starting of the project lifetime, the discount rate and the inflation rate are not considered during the calculation of the capital cost. The capital cost can be calculated by using the following formula

$$C_{capc,j} = N_{com,j} \times C_{capc,unit(j)} \qquad \forall i \in G \qquad \textit{Eq. 5-3}$$

Where, $C_{capc,j}$, $N_{com,j}$, and $C_{capc,unit(j)}$ refers to the capital cost, the number of components, and the unit cost of the j^{th} component.

The capital cost of MR is calculated in a different formula as the cost reduction is included in the capital cost. The rate of cost reduction of MR is related to the learning rate which is discussed in section 4.1. The capital cost of MR can be calculated by using the formula as follows [140].

$$C_{capc,MR} = \sum_{k=1}^{N_{MR}} C_{capc,MR(1st)} \times (N_{MR})^{R} \qquad \textit{Eq. 5-4}$$

Where, $C_{capc,MR}$, $C_{capc,MR(1st)}$, $N_{MR}, and\ R$ imply the total capital cost of MR, the unit price of the 1st MR, the number of MR, and the rate of cost reduction respectively.

The O&M cost of a component occurs each year and continues till the end of the project lifetime. The O&M cost of a component is considered the same each year and is calculated by the following equation [141].

$$C_{O\&Mc,j} = N_{com,j} \times C_{O\&M,yearly(j)} \times \frac{\{(1+rld)^{n}\} - 1}{rld(1+rld)^{n}} \qquad \forall i \in G \qquad \textit{Eq. 5-5}$$

Where, $C_{O\&Mc,j}$, $N_{com,j}$, n, rld and $C_{O\&M,yearly(j)}$ indicates the present worth of the total O&M cost, number of components, project lifetime, real discount rate, and yearly O&M cost of the j^{th} component.

The replacement of any component happens at the end of its' lifetime. The number of replacements depends on both the component lifetime and the lifetime of the project. The present value of the replacement cost of the component is calculated as follows [142]

$$NR = ceil\left[\frac{n}{CLT_j}\right] - 1 \qquad \textit{Eq. 5-6}$$

$$F_{rep} = \sum_{k=1}^{NR} \left(k \times CLT_j\right) \qquad \textit{Eq. 5-7}$$

$$C_{repc,j} = N_{com,j} \times \sum_{k=1}^{NR} C_{rep,unit(j)} \times \frac{1}{(1+rld)^{F_{rep}}} \qquad \forall i \in G \qquad \textit{Eq. 5-8}$$

Where, $C_{repc,j}$ is the present value of the replacement cost of the j^{th} component, NR is the number of required replacement, CLT_j is the lifetime of the j^{th} component, and $C_{rep,unit(j)}$ is the per-unit replacement cost of the j^{th} component. $ceil\ (X)$ is a function that rounds X to the nearest integer equal or greater than X.

The fuel cost is considered for MR and fossil fuel-based generators. There is no fuel cost associated with renewable energy sources like solar PV, wind turbines. Also, for energy storage devices like battery, there is no fuel cost either. The fuel cost is calculated yearly and the present value of the fuel cost is formulated by using the below equation [141]

$$C_{fuelc,j} = E_{yearly,j} \times CU_{fuel,j} \times \frac{\{(1+rld)^n\} - 1}{rld(1+rld)^n} \qquad \forall j \in G \qquad \textit{Eq. 5-9}$$

$$E_{yearly,j} = N_{com,j} \times RAT_j \times 365 \times 24 \qquad \forall j \in G \qquad \textit{Eq. 5-10}$$

Where, $C_{fuelc,j}$ is the present worth of the fuel cost ($) of the j^{th} component, $E_{yearly,j}$ is the yearly energy generation (MWh) from the j^{th} component, $CU_{fuel,j}$ fuel price per unit energy generation of the j^{th} component, RAT_j is the rating of the j^{th} component.

The salvage value of a component is the remaining useful value of a component at the end of the project lifetime. The linear depreciation is considered in the calculation of the salvage value. The linear depreciation means the salvage value of the component is directly proportional to the remaining life of the component. The replacement cost is considered during the salvage value calculation instead of capital cost. However, if the lifetime of the component is greater than the project lifetime, the capital cost needs to be considered. Also, if the project lifetime is the multiples of the component, then there will be no salvage value for that component. The present worth of the salvage value is calculated as follows [139].

$$C_{salv,j} = N_{com,j} \times C_{rep,unit(j)} \times \frac{CLT_{rem,j}}{CLT_j} \times \frac{1}{(1+rld)^n} \qquad \forall i \in G \qquad \textit{Eq. 5-11}$$

$$CLT_{rem,j} = CLT_j - (n - LT_{rep,j}) \qquad \textit{Eq. 5-12}$$

$$LT_{rep,j} = CLT_j \times \text{floor}\left[\frac{\text{n}}{CLT_j}\right] \qquad \textit{Eq. 5-13}$$

Where, $C_{salv,j}$ is the present worth of the salvage value of the j^{th} component, $CLT_{rem,j}$ is the remaining year of the j^{th} component at the end of the project lifetime. $floor\ (X)$ is a function that rounds X to the nearest integer equal or less than X.

The decommissioning cost and refueling cost is considered only for MR. Although The decommissioning cost of MR occurs at the end of the project, the annual distribution of decommissioning cost is considered in this study [143]

$$C_{decom,MR} = E_{yearly,MR} \times CU_{decom,MR} \times \frac{\{(1+rld)^n\} - 1}{rld(1+rld)^n} \quad \textit{Eq. 5-14}$$

Where, $C_{decom,MR}$ is the present value of the total decommissioning cost ($) of MR, $E_{yearly,MR}$ is the yearly energy generation (MWh) from the MR, $CU_{decom,MR}$ is the decommissioning cost per unit ($/MWh).

The lifetime of the fuel bundle is considered 10 years in this study so the refueling of the MR occurs every ten years. The refueling cost of the MR does not include the cost of fuel. The refueling cost includes the cost associated with transportation of the fuel, and labor cost. The present value of the refueling cost is calculated by the following equations [141].

$$C_{refueling,MR} = N_{MMR} \times \sum_{k=1}^{MR_{refuel}} C_{refueling,MR(unit)} \times \frac{1}{(1+rld)^{F_{refuel}}} \quad \textit{Eq. 5-15}$$

$$MR_{refuel} = ceil\left[\frac{n}{LT_{fb(MR)}}\right] - 1 \quad \textit{Eq. 5-16}$$

$$F_{refuel} = \sum_{k=1}^{MR_{refuel}} \left(n \times LT_{fb(MR)}\right) \quad \textit{Eq. 5-17}$$

Where, $C_{refueling,MR}$ is the present value of the refueling cost of the MR, $C_{refueling,MR(unit)}$ is the refueling cost in every 10 years, $LT_{fb(MR)}$ is the lifetime of the fuel bundle, and MR_{refuel} is the number of the required refueling in the project lifetime.

5.2. **Constraints**

Constraints are used in the optimization problem to ensure the reliability, resiliency, and performance of the proposed energy systems. Some constraints are used to address some real-world limitations to implement the energy systems in the marine ship.

The energy generation from any energy source must be equal or less than the maximum capability of that energy source. This can be represented as below

$$P_{gen}^{j}(\mathrm{t}) \leq P_{gen,max}^{j} \qquad \forall\, j, \forall\, t \qquad \textit{Eq. 5-18}$$

Where, $P_{gen}^{j}(\mathrm{t})$ is the electric generation of the j^{th} component at time step t and $P_{gen,max}^{j}$ is the maximum electric generation capacity of the j^{th} component at time step t

To ensure the reliability and resiliency of the system, the total generation of the system must be greater or equal to the total requirement of the system. The below equations are used to represent the constraints of the energy management of the system.

$$\sum P_{gen}^{z}(\mathrm{t}) \geq \sum_{\mathrm{t}=1}^{t_{total}} P_{EL}^{z}(t) \qquad \forall\, t \in t_{total}, \forall\, z \qquad \textit{Eq. 5-19}$$

$$\sum P_{gen}^{z}(t) = \sum_{t=1}^{t_{total}} Num_{PV} P_{pv}(t) + \sum_{t=1}^{t_{total}} Num_{WT} P_{w}(t) + \sum_{t=1}^{t_{total}} Num_{MR} P_{MR}(t) \qquad \forall\, t \in t_{total}, \forall\, z \qquad \textit{Eq. 5-20}$$

Where, $P_{gen}^{z}(\mathrm{t})$ is the generation of electric power (kW) at time t of the year z. $P_{EL}^{z}(t)$ refers to the power demand at time step t of the year z. Num_{PV}, Num_{WT}, and Num_{MR} indicate the number of solar PV, the number of wind turbine, and the number of MR respectively. $P_{pv}(t)$, $P_{w}(t)$, and $P_{MR}(t)$ refer to the power generation from solar PV, wind turbine, and MR at the time t sequentially.

The power generation for Renewable and Fossil Fuel-based Hybrid Energy System (F-R HES), Standalone Nuclear Energy System, and Standalone Fossil Fuel-Based Energy System can be formulated by the Eq. 5-21, Eq. 5-22, and Eq. 5-23 respectively.

$$\sum P_{gen}^{z}(t) = \sum_{t=1}^{t_{total}} Num_{PV} P_{pv}(t) + \sum_{t=1}^{t_{total}} Num_{WT} P_{w}(t) + \sum_{t=1}^{t_{total}} Num_{DG} P_{DG}(t) \qquad \forall\, t \in t_{total}, \forall\, z \qquad \textit{Eq. 5-21}$$

$$\sum P_{gen}^{z}(t) = \sum_{t=1}^{t_{total}} Num_{MR} P_{MR}(t) \qquad \forall\, t \in t_{total}, \forall\, z \qquad \textit{Eq. 5-24}$$

$$\sum P_{gen}^{z}(t) = \sum_{t=1}^{t_{total}} Num_{DG} P_{DG}(t) \qquad \forall\, t \in t_{total}, \forall\, z \qquad \textit{Eq. 5-23}$$

The energy storage device is used to store excess energy. The following constraints are considered in this study to ensure the proper energy management of the system and maintain the desired SOC of the storage device

$$SOC_{EES,min} \leq SOC_{EES}^{z}(t) \leq SOC_{EES,max} \qquad \forall\, t \in t_{total}, \forall\, z \qquad \textit{Eq. 5-22}$$

Where, $SOC_{EES}^{z}(t)$ is the SOC (%) of the energy storage device at the time step t in the year z. $SOC_{EES,min}$ and $SOC_{EES,max}$ refer to the minimum and maximum SOC of the energy storage component.

To ensure the reliability, resiliency, and performance of the energy system, the reliability parameters LPSP is considered as the constraint of the optimization problem. The LPSP is considered for each time step and also for the total time step to ensure the utmost reliability of the system. The lower value of the LPSP refers to the higher reliability of the system. The reliability constraints can be formulated as below

$$LPSP_e \leq LPSP_{e,max} \qquad \textit{Eq. 5-23}$$

$$LPSP_{e(t)} \leq LPSP_{e(t),max} \qquad \textit{Eq. 5-24}$$

Where, $LPSP_{e,max}$ is the maximum limit of the LPSP for the total time step and $LPSP_{e(t),max}$ represents the maximum limit of the LPSP in each time step. The maximum limit of $LPSP_e$ and $LPSP_{e(t)}$ is considered as 8% in this study which is within the acceptable margin [61]

To ensure the cargo-carrying capacity of the marine ship, PWR is inserted as one of the constraints in the optimization problem. This constraint can be formulated by the following equation

$$SYS_{wr} \leq SYS_{wr,max} \qquad \textit{Eq. 5-25}$$

Where, SYS_{wr} is the ratio between the total weight of the energy system and the total cargo-carrying capacity of the ship, and $SYS_{wr,max}$ is the maximum limit of the ratio. In this study the $SYS_{wr,max}$ is taken as 0.005 considering the weight of the current energy system that is being used in the ship to ensure that the proposed system will not reduce the cargo-carrying capacity of the marine vessel. The total weight of the components of the N-R HES, F-R HES, Standalone Nuclear Energy System, and Standalone Fossil Fuel-Based Energy System can be calculated by using the .Eq. 5-26, Eq. 5-27, Eq. 5-28, and Eq. 5-29 respectively.

$$SYS_{w,NR} = TW_{MR} + TW_{PV} + TW_{Wind} + TW_{BAT} \quad \text{Eq. 5-26}$$

$$SYS_{w,FR} = TW_{DG} + TW_{PV} + TW_{Wind} + TW_{BAT} \quad \text{Eq. 5-27}$$

$$SYS_{w,N} = TW_{MR} \quad \text{Eq. 5-28}$$

$$SYS_{w,F} = TW_{DG} \quad \text{Eq. 5-29}$$

Where, TW_{MR}, TW_{PV}, TW_{Wind}, and TW_{BAT} represent the total weight of the MR, solar PV, wind turbine, and battery. The weight of the MR, solar PV, wind turbine, and battery can be formulated by the Eq. 5-30, Eq. 5-31, Eq. 5-32, Eq. 5-33, and Eq. 5-34 respectively

$$TW_{MR} = Num_{MR} \times PWR_{MR} \times Rat_{MR} \quad \text{Eq. 5-30}$$

$$TW_{DG} = Num_{DG} \times PWR_{DG} \times Rat_{DG} \quad \text{Eq. 5-31}$$

$$TW_{PV} = Num_{PV} \times PWR_{PV} \times Rat_{PV} \quad \text{Eq. 5-32}$$

$$TW_{Wind} = Num_{Wind} \times PWR_{Wind} \times Rat_{Wind} \quad \text{Eq. 5-33}$$

$$TW_{BAT} = Num_{BAT} \times PWR_{BAT} \times Rat_{BAT} \quad \text{Eq. 5-34}$$

Where, PWR_{MR}, PWR_{DG}, PWR_{PV}, PWR_{Wind}, and PWR_{BAT} refer to the power to weight ratio of MR, fossil fuel based generator, solar PV, wind turbine, and battery respectively. The Rat_{MR}, Rat_{DG}, Rat_{PV}, Rat_{Wind}, and Rat_{BAT} refer to the rating of the MR, fossil fuel-based generator, solar PV, wind turbine, and battery, sequentially.

Unlike land-based system, marine ship has a limited area to accommodate the energy system components. To ensure that the system components can be accommodated with the available useable area of the ship, another constraint is addressed in the optimization problem. Solar PV is installed on the upper surface of the ship and requires a considerable amount of area compared to other energy sources [144]. So, this constraint is used in the optimization problem to confirm that the solar PV can be implemented within the area of the ship. This constraint can be formulated as below

$$Solar_{ratio} \leq Solar_{ratio,max} \quad \text{Eq. 5-35}$$

Where, $Solar_{ratio}$ is the ratio between solar PV area and ship area, and $Solar_{ratio,max}$ is the maximum limit of the ratio between solar PV and ship area. The area of the solar PV can be calculated as follows

$$Area_{PV} = Num_{PV} \times UA_{PV} \times Rat_{PV} \quad \text{Eq. 5-36}$$

Where, $Area_{PV}$ is the area of the solar PV (m^2), and UA_{PV} is the area requirement of solar PV for per unit power (m^2/kW). The UA_{PV} is considered as 4.952 (m^2/kW) in this study [110]. Considering the area requirement for wind turbine installation and all the area of the marine ship is not practically available for solar PV, the $Solar_{ratio,max}$ is considered as 0.4 which is within the reasonable margin [28]

5.3. Decision Variables

The target of this optimization problem is to identify the optimized configuration of the energy system to minimize the NPC of the systems. Four different energy systems are optimized in this research and compared with each other to find out the most feasible energy system for the marine ship. The decision variables of this optimization problem are the number of the required MR, fossil fuel-based generator, solar PV, wind turbine, and battery. These decision variables are used to identify the size of the MR, fossil fuel-based generator, solar PV, wind turbine, and battery. The decision variables can be expressed as follows

$$0 \leq Num_{MR} \leq Num_{MR,max} \qquad N_{PV} \in \mathbb{Z} \quad \text{Eq. 5-37}$$

$$0 \leq Num_{DG} \leq Num_{DG,max} \qquad N_{WT} \in \mathbb{Z} \quad \text{Eq. 5-38}$$

$$0 \leq Num_{PV} \leq Num_{PV,max} \qquad N_{MMR} \in \mathbb{Z} \quad \text{Eq. 5-39}$$

$$0 \leq Num_{WT} \leq Num_{WT,max} \qquad N_{Htank} \in \mathbb{Z} \quad \text{Eq. 5-40}$$

$$0 \leq Num_{BAT} \leq Num_{BAT,max} \qquad N_{Htank} \in \mathbb{Z} \quad \text{Eq. 5-41}$$

Where, $Num_{MR,max}$, $Num_{DG,max}$, $Num_{PV,max}$, $Num_{WT,max}$, and $Num_{BAT,max}$ refer to the maximum number of MR, fossil fuel-based generator (Diesel Generator), solar PV, wind turbine, and battery.

5.4. Implementation of Optimization Algorithm (Differential Evolution)

The differential evolution algorithm was 1st proposed by Kenneth Price and Rainer Store [145]. It is a popular optimization technique which uses a population of individual solutions to solve multidimensional real-valued function.

The differential evolution has four major stages which are initialization, mutation, recombination/crossover, and selection.

In the initialization stage, random solutions are generated within a boundary. Then each solution undergoes mutation and recombination phases, and lastly, the best solution is selected. This process takes place till it meets any stopping criteria.

The program needs to generate the initial solutions randomly within the minimum and maximum value of each variable. The number of solutions will be equal to the number of the population size (N_p). Any random solution which is generated in the initialization phase can be formulated as follows [145]

$$S_{(N,d)} = S_{(min,d)} + rand \times [S_{(max,d)} - S_{(min,d)}] \quad \textit{Eq. 5-42}$$

Where, N refers to the N^{th} solution to be optimized and d represents the parameter variables to be optimized. $S_{(min,d)}$ and $S_{(max,d)}$ represent the minimum and maximum range of the d parameter variables. The $rand$ is a random number between 0 and 1.

In the mutation stage, the random solutions (target solutions) which are generated in the initialization stage are optimized by mutating the solution. This solution is called the donor solution. The new solution after the mutation phase can be formulated as follows

$$Z_{(N,d)} = S_{(r1,d)} + F \times \left[S_{(r2,d)} - S_{(r3,d)}\right] \quad \textit{Eq. 5-43}$$

Where, $r1$, $r2$, and $r3$ are random solutions selected from 1 to N_p and these solutions are mutually exclusive. F represents the scaling factor which is between 0 and 2. The target solution does not participate in the mutation phase. Hence, in the differential evolution, the minimum population size is four.

After the mutation phase, the solution undergoes a crossover/recombination phase to add diversity to the solution. The solution after the crossover phase is called the trial solution. In this phase, the trial solution can be obtained either from the target solution or the donor solution based on the below condition

$$T_{(N,d)} = \begin{cases} Z_{(N,d)} & \varphi \le C_p \quad or \quad d = \lambda \\ S_{(N,d)} & \varphi > C_p \quad and \quad d \neq \lambda \end{cases} \qquad \lambda \in d \quad \textit{Eq. 5-44}$$

Where, C_p is the crossover probability, and φ is the random number between 0 and 1. λ is a randomly selected variable location from d. The $d = \lambda$ condition ensures that at least one solution in the crossover phase is taken from the donor solution. After getting the trial solution, its' boundary needs to be checked. If the trial solution is greater than the maximum limit then the solution is bounded back to the maximum value and if the trial solution is less than the minimum value then it is bounded back to the minimum value.

In the selection stage, the objective function values are computed for all the solutions. The better solution between the target solution and the trial solution is selected for the next iteration which is called the greedy selection method. After completing all the iteration, the best objective function value is obtained, and the associated solution is the global optimal solution.

Differential Evolution implementation steps are discussed in detail as follows.

Step 1:	Read the following input data of the energy systems planning problem: A. Load the electrical demand data (hourly propulsive electric and auxiliary load data for one year) B. Load the climatological data (hourly wind speed, solar irradiance, and ambient temperature) to calculate the renewable energy. C. Load the system component's features (energy generation from MR, fossil fuel-based generator, solar PV, wind turbine, and charging and discharging from energy storage device) D. Load economic and other parameters of the system and system components, such as project lifetime, inflation rate, discount rate, capital cost, O&M cost, replacement cost, fuel cost, refueling cost, decommissioning cost, and the salvage value
Step 2:	Initialize the parameters of DE and required system components: A. Set the population size, N_p=50, and the maximum number of iterations as 200 B. Set the scaling factor, F = 0.5 C. Set the crossover probability, C_p = 0.7

	D. Set the constraints of the optimization problem as follows $LPSP_e \leq 0.08$ $LPSP_{e(t)} \leq 0.08$ $SYS_{wr} \leq 0.005$ $Solar_{ratio} \leq 0.4$ A fixed value ((1×10^{20})) will be added to the objective function if there is any violation in the constraints. E. Set the lower and upper limit of the decision variables ▪ The lower and upper bound of the number of MR/DG [0, 100] ▪ The lower and upper bound of the number of solar PV [0, 100] ▪ The lower and upper bound of the number of wind turbine [0, 100] ▪ The lower and upper bound of the number of battery [0, 100]
Step 3:	Generate the initial solutions randomly within the boundary of the decision variables. The number of the randomly generated solution is equal to the population size. These solutions are called target solutions.
Step 4:	Generate the donor solutions by mutating the target solutions
Step 5:	Generate the trail solutions by recombing the donor the solutions (crossover)
Step 6:	Bound the trial solutions within the boundary of the decision variables
Step 7:	Evaluate the objective function for the target solutions and trial solutions. The solution that gives the lower value (minimization problem) of the objective function is selected as the target solution for the next iteration. Store the best cost value (lowest value) in every iteration
Step 08:	When the number of iteration reaches the maximum limit of the iteration, then stop. Otherwise, continue from ***Step 3*** to ***Step 7.*** After completing all the iteration, the best objective function value is obtained, and the associated solution is the global optimal solution.

5.5. Adaptive Differential Evolution (ADE)

Currently, the adjustment of control parameters (scaling factor and crossover probability) of DE is considered as a global behavior. However, these parameters affect the convergence speed and may cause a premature phenomenon. An adaptive adjustment method of the control parameters was discussed in [100]. The authors used sine and cosine functions with a value of (-1,0), and (0,1) respectively. The scaling factor (F) and the crossover probability (C_p) can be written as below formula

$$F_{(t)} = \begin{cases} \Upsilon + (1-\Upsilon) \times \sin(\frac{\pi t}{maxit} - \frac{\pi}{2}) & t \leq \frac{maxit}{2} \\ \Upsilon - (1-\Upsilon) \times \cos(\frac{\pi}{2} - \frac{\pi t}{maxit}) & otherwise \end{cases} \quad \textit{Eq. 5-45}$$

$$C_{p_{(t)}} = \begin{cases} \beta + (1-\beta) \times sin(\frac{\pi t}{maxit} - \frac{\pi}{2}) & t \leq \frac{maxit}{2} \\ \beta - (1-\beta) \times cos(\frac{\pi}{2} - \frac{\pi t}{maxit}) & otherwise \end{cases} \quad \textit{Eq. 5-46}$$

Where, $F_{(t)}$ is the scaling factor, $C_{p_{(t)}}$ is the crossover probability, t is the iteration number, and $maxit$ is the maximum number of iterations. Υ and β are constant and the value of Υ and β is 0.8 and 0.75 respectively in this study. This study will evaluate the performance of standard DE and ADE, and will compare the performance between these two techniques.

5.6. Particle Swarm Optimization (PSO)

The PSO is another metaheuristic optimization algorithm, proposed by Kennedy and Eberhart in 1995. The main idea of the PSO algorithm is communication among the population called the swarm and, evolutionary computation. In this technique, two values are compared in each position of a particle. The first value is the best value obtained by that particle so far, called the personal best and the 2nd value is the best value among all the particles, called the global best. The optimizer compares these two values for each particle and stores the best value till it reaches a stopping criteria (number of iterations or pre-defined value of the fitness function). Each particle moves towards the personal best and global best based on its current position and velocity. The position of a particle can be expressed as per the below equation

$$Z^i_{\mathrm{T}+1} = Z^i_T + V^i_{\mathrm{T}+1} \quad \textit{Eq. 5-47}$$

Where, Z is the position of the particle, i is the number of the particle, V is the velocity of the particle, and T is the number of iterations. The velocity of the particle can be obtained by the following equation [146]

$$V_{T+1}^{i} = W[V_T^i + c_1 r_1 (p_T^i - Z_T^i) + c_2 r_2 (p_T^g - Z_T^i)] \quad \textit{Eq. 5-48}$$

Where, W is the constriction coefficient, p^i is the personal best position, p^g is the global best position, c_1 is the acceleration coefficient (individual), c_2 is the acceleration coefficient (social), and r_1 and r_2 are random numbers between 0 and 1. The constriction coefficient can be calculated as the following equation

$$W = \frac{2k}{\left|2 - \varphi - \sqrt{\varphi^2 - 4\varphi}\right|} \quad \textit{Eq. 5-49}$$

$$\varphi = c_1 + c_2 > 4 \quad \textit{Eq. 5-50}$$

The typical value of k, c_1, and c_2 is 1, 2.05, and 2.05 respectively. The implementation steps of PSO is discussed below

Step 1:	Read the following input data of the energy systems planning problem: E. Load the electrical demand data (hourly propulsive electric and auxiliary load data for one year) F. Load the climatological data (hourly wind speed, solar irradiance, and ambient temperature) to calculate the renewable energy. G. Load the system component's features (energy generation from MR, fossil fuel-based generator, solar PV, wind turbine, and charging and discharging from an energy storage device) H. Load economic and other parameters of the system and system components, such as project lifetime, inflation rate, discount rate, capital cost, O&M cost, replacement cost, fuel cost, refueling cost, decommissioning cost, and the salvage value
Step 2:	Initialize the parameters of PSO and required system components: F. Set the population size, N_p=50, and the maximum number of iterations as 200

	G. Set the acceleration coefficient, c_1=c_2 = 2.05 H. Calculate the value of the constriction coefficient, W I. Set the constraints of the optimization problem as follows $LPSP_e \leq 0.8$ $LPSP_{e(t)} \leq 0.8$ $SYS_{wr} \leq 0.005$ $Solar_{ratio} \leq 0.4$ A fixed value ((1×10^{20}) will be added to the objective function if there is any violation in the constraints. J. Set the lower and upper limit of the decision variables ▪ The lower and upper bound of the number of MR [0, 100] ▪ The lower and upper bound of the number of solar PV [0, 100] ▪ The lower and upper bound of the number of wind turbine [0, 100] ▪ The lower and upper bound of the number of battery [0, 100]
Step 3:	Generate the initial solutions randomly within the boundary of the decision variables.
Step 4:	Use the individual particle position to determine the objective function value
Step 5:	Update the best position of the individual particle by comparing it with all other populations.
Step 6:	Compare the personal best with the global best and update the global best with the individual particle's personal best that has the minimum value of the objective function
Step 7:	Update the velocity of the individual particle
Step 8:	Update the position of the individual particle.
Step 9:	Repeat step 3 to step 8 till all particles are evaluated in each iteration. Store the best cost value
Step 10:	Stop the simulation if it reaches the maximum number of iterations.

5.7. Hybrid Optimization of Multiple Energy Resources (HOMER)

In this section, the use of HOMER to optimize the four energy systems is discussed. HOMER is a simple and strong tool to evaluate the feasibility of different energy systems. The electrical demand, solar irradiance, wind speed, and temperature are imported to HOMER software. The annual peak load is considered as 15% in the constraint HOMER simulation to give some reliability. This 15% means that the system will be able to cater to the demand if the peak is 15% more than the current peak demand. From 1kg uranium 24 GWh energy is produced [147], [148] that is used to model the MR in HOMER. Load following feature of the energy sources is considered in HOMER. Figure 5-1, Figure 5-2, Figure 5-3, Figure 5-4, and Figure 5-5 show the monthly average of electrical demand, wind speed, solar irradiance, temperature, and sample model of N-R HES, respectively. The system parameters of each component are added while doing the simulation in HOMER. It should be noted that only some pre-defined constraints can be addressed in HOMER which is one of the major differences between the simulation between HOMER and MATLAB. Another drawback of HOMER is that the search space of generators (MR/DG) needs to be defined in HOMER by the user. Hence, the result of HOMER can not be compared with the result of MATLAB. HOMER software is used to get a preliminary idea and build a base model. The author 1st validated the idea by using HOMER. To make the analysis more realistic and address some real-world constraints like the availability of area for renewable energy sources, cargo-carrying capacity, the mathematical model is built in MATLAB and then optimized by Differential Evolution (DE) algorithm.

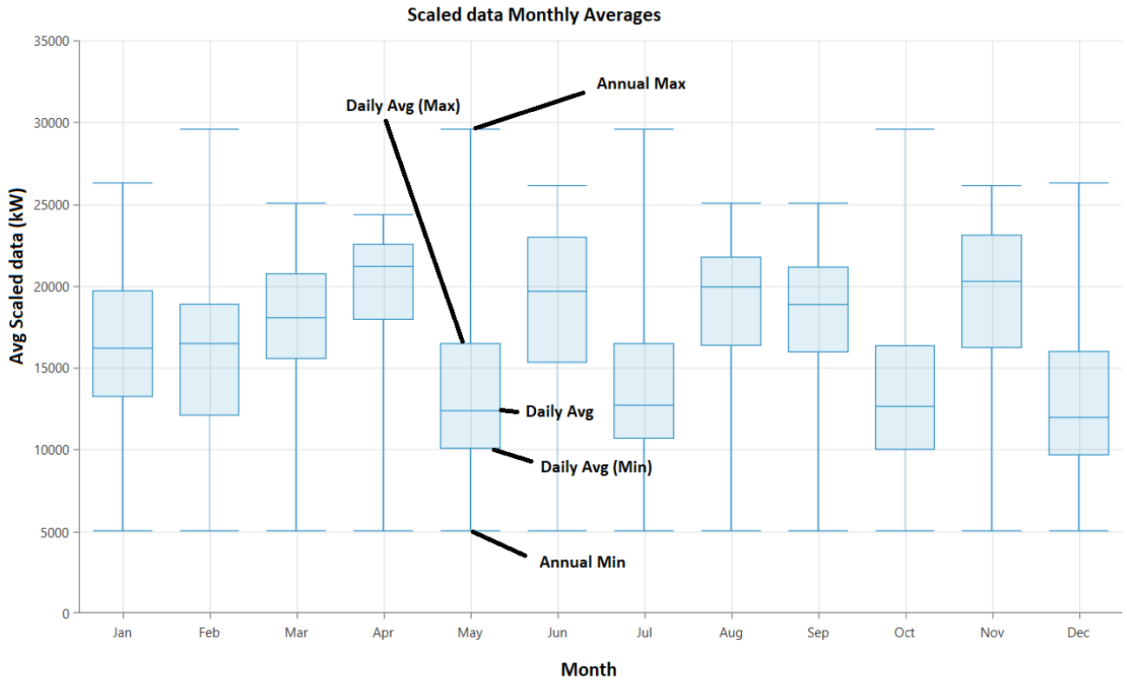

Figure 5-1: Monthly Average of Electrical Demand

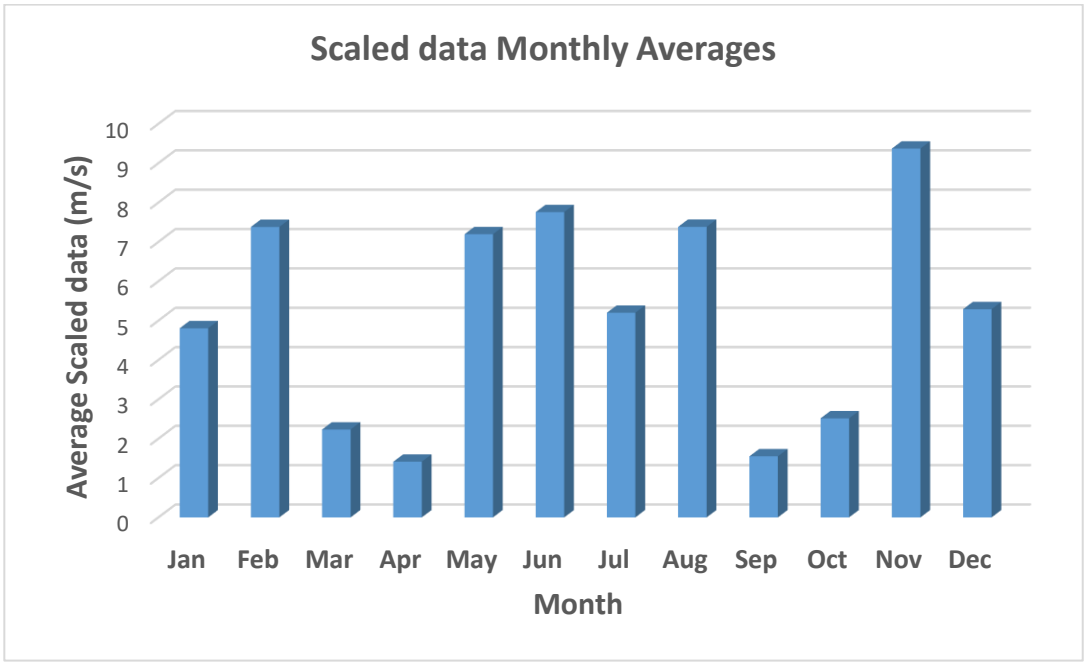

Figure 5-2: Monthly Average Wind Speed

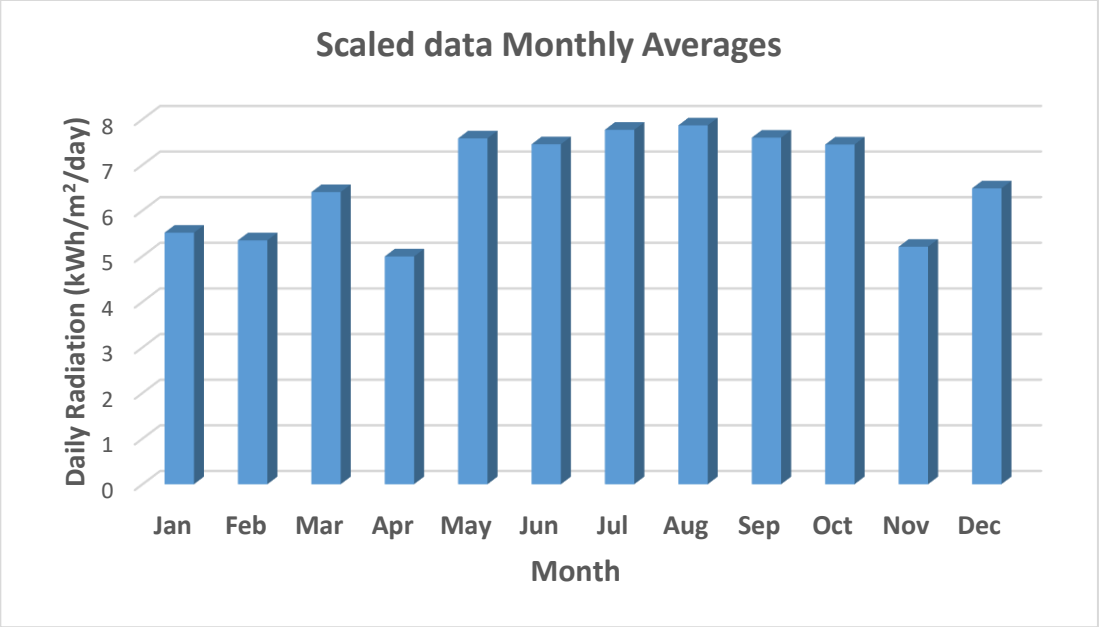

Figure 5-3: Monthly Average Solar Irradiance

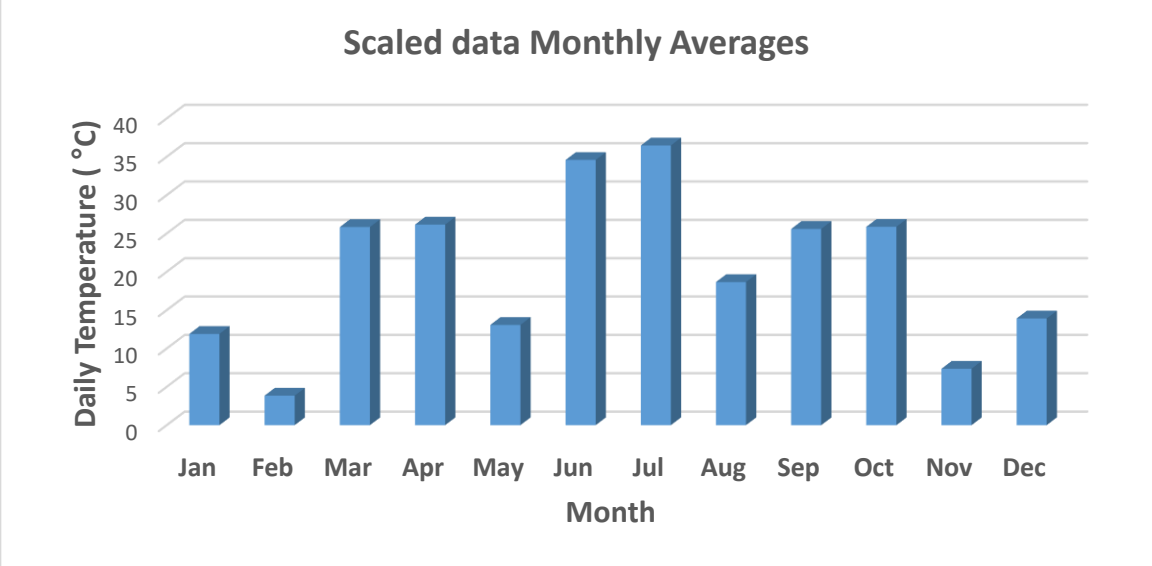

Figure 5-4: Monthly Average Temperature

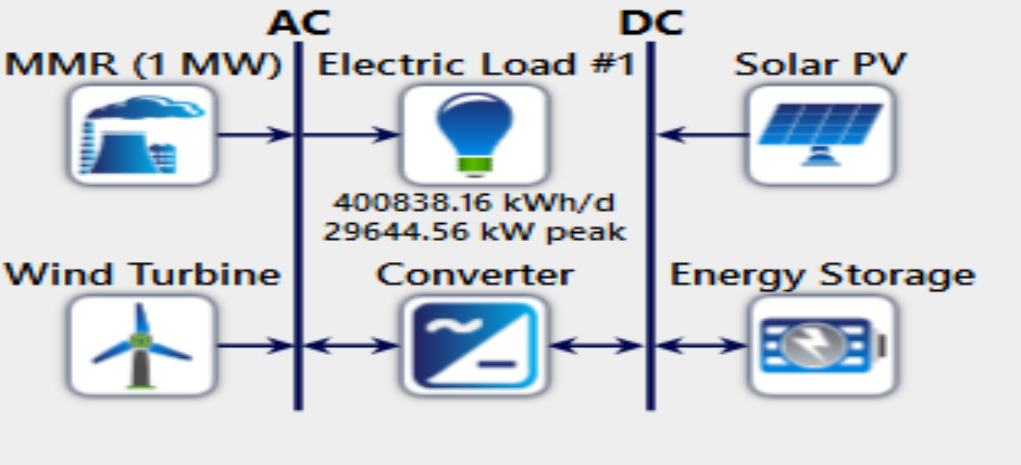

Figure 5-5: N-R HESs in HOMER

Chapter 6: Results and Discussions

This chapter covers the results from HOMER software and MATLAB (DE algorithm). Section 6.1 covers the comparison among different energy systems (HOMER Software). The comparison among different energy systems (DE algorithm) is carried out in section 6.2. Section 6.3 is all about the comparison among different optimization techniques and validation of results. Section 6.4 focuses on the sensitivity analysis to evaluate the energy systems performance by changing the system's parameters to a varying degree.

6.1. Comparison among the Proposed Hybrid Energy Systems (HOMER)

Four different types of energy systems are discussed and simulated in this section. HOMER software is used to simulate different types of energy systems. Various components are included in the simulation such as solar power, electric load, wind power, energy storage system, FFG, MR, and power electronics devices.

***Case-01**: Stand-alone Fossil Fuel-based Energy System*

Conventional fossil fuel-based energy source (diesel generator) along with energy storage system is considered in this case - a common for ocean-going marine ships. There are no renewable energy sources in this case, and this energy system is considered to compare with the proposed N-R HES of marine ships. Figure 6-1 represents the system configuration of this case.

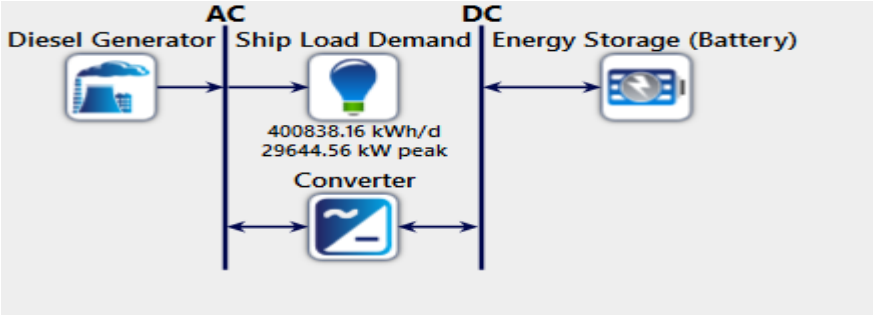

Figure 6-1: Stand-alone Fossil Fuel-based Energy System

As there are no other energy sources other than diesel generator, all electricity is produced by diesel generator. The rating of the diesel generator and battery for this case is 28 MWe

and 2.2 MW, respectively. Figure 6-2 represents the total energy production by different energy sources and the total load that is served by the energy sources.

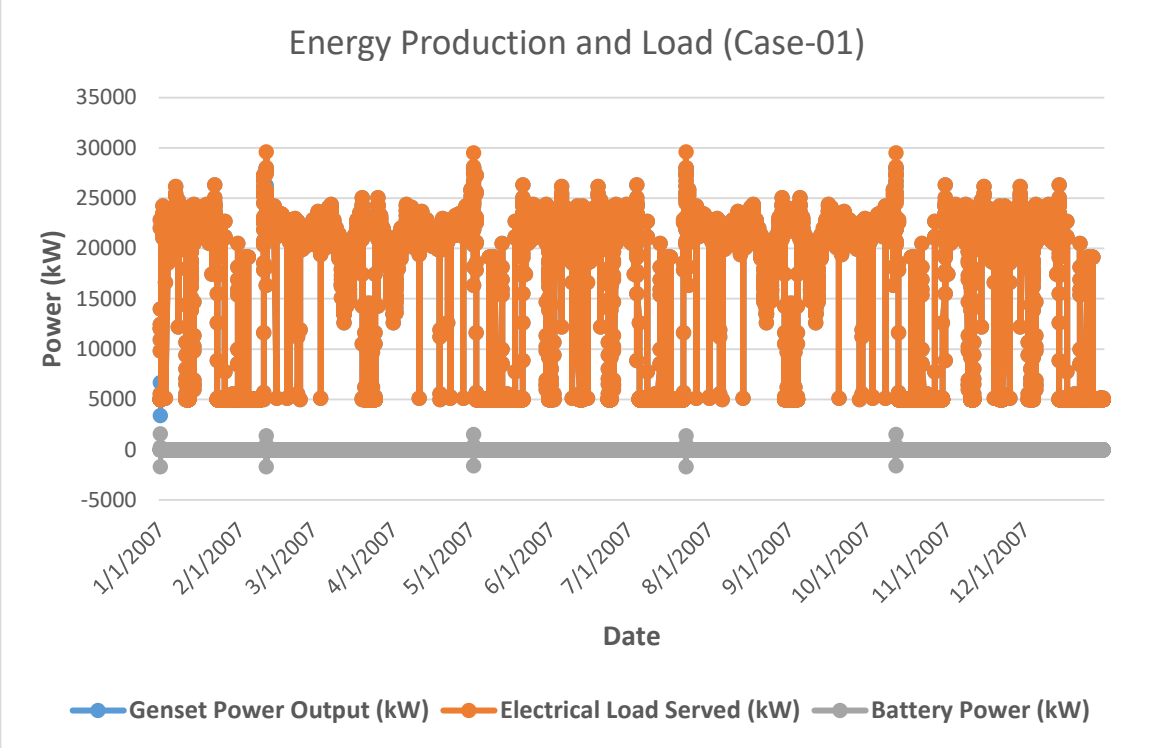

Figure 6-2: Total Energy Production and Total Load Served (Case-01)

***Case-02**: Renewable Energy and Fossil Fuel-based Hybrid Energy System*

In this case, renewable energy sources are integrated with a diesel generator. Parameters of solar and wind energy sources are summarized previously. Figure 6-3 represents the system configuration.

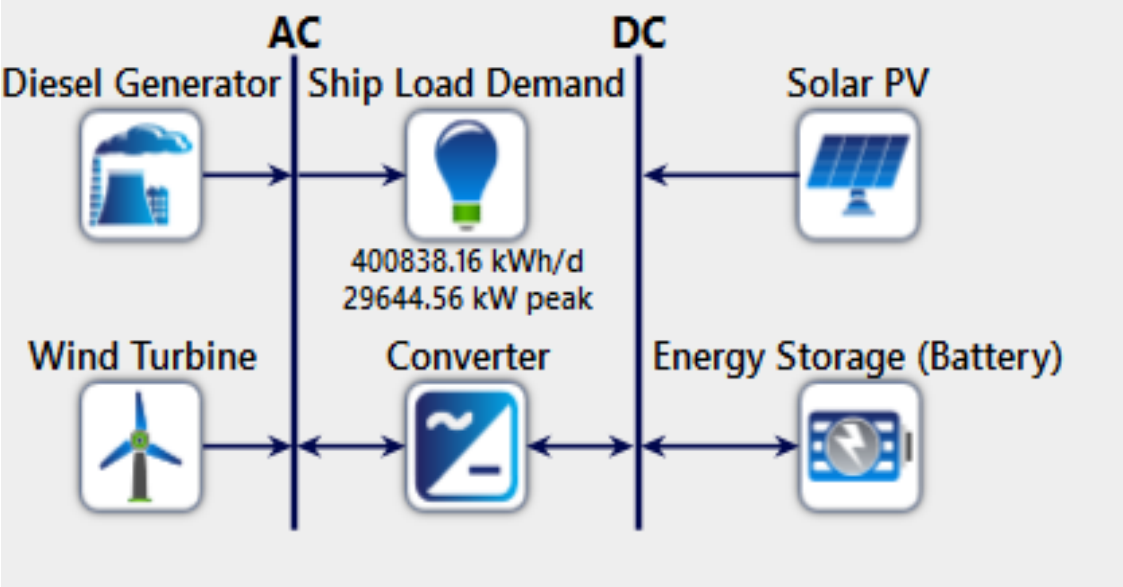

Figure 6-3: Renewable Energy and Fossil Fuel-based Hybrid Energy System

In this case, renewable energy penetration is around 10.1%. Most of the electricity is produced by the diesel generator, which is around 89.9%. The rating of diesel generator, solar PV, wind turbine, and battery for this case is 27 MWe, 1.5 MW, 5 MW, and 2.2 MW, respectively. Figure 6-4 shows the energy production from different energy sources and the total load served.

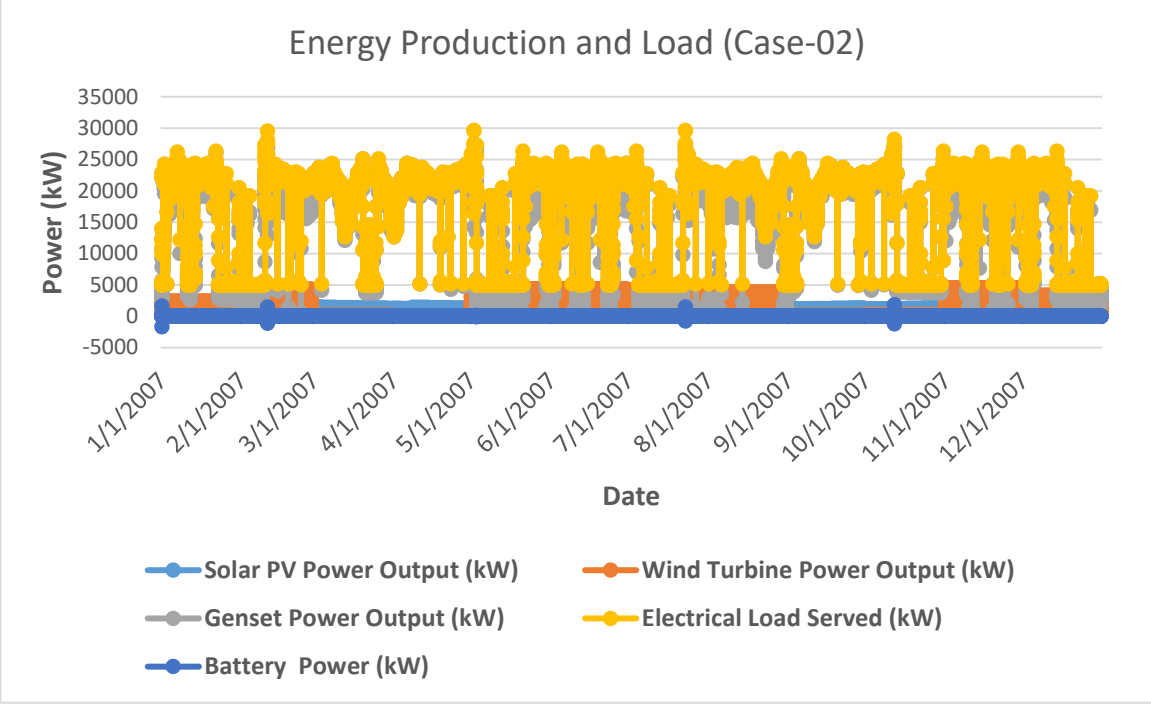

Figure 6-4: Total Energy Production and Total Load Served (Case-02)

Case-03: Stand-alone Nuclear Energy System

This case is similar to Case-1 except the diesel generator is replaced by the MR. Figure 6-5 depicts the system configuration for Case-03.

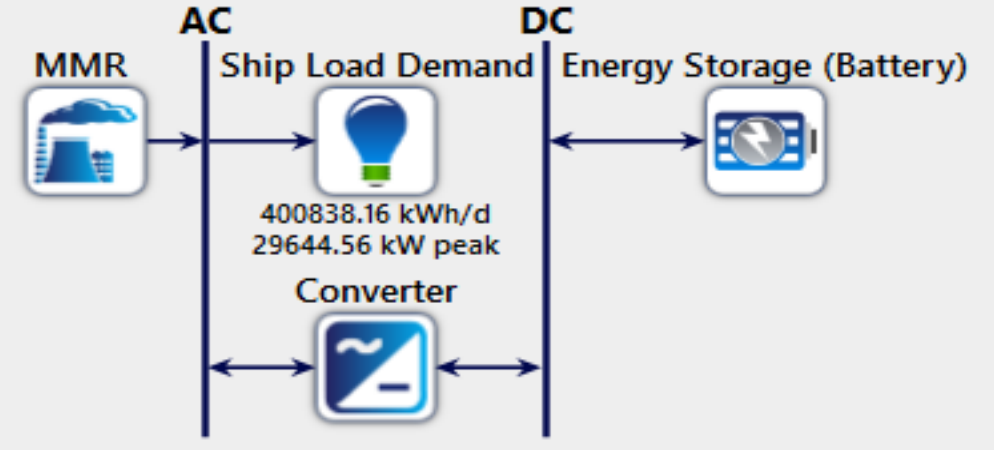

Figure 6-5: Stand-alone Nuclear Energy System

In this case, MR offers a continuous supply of electricity and total electricity is produced by it. The rating of MR is 28 MWe and the battery rating is 5.8 MW. Figure 6-6 shows the energy output from MR, battery, and the total load served.

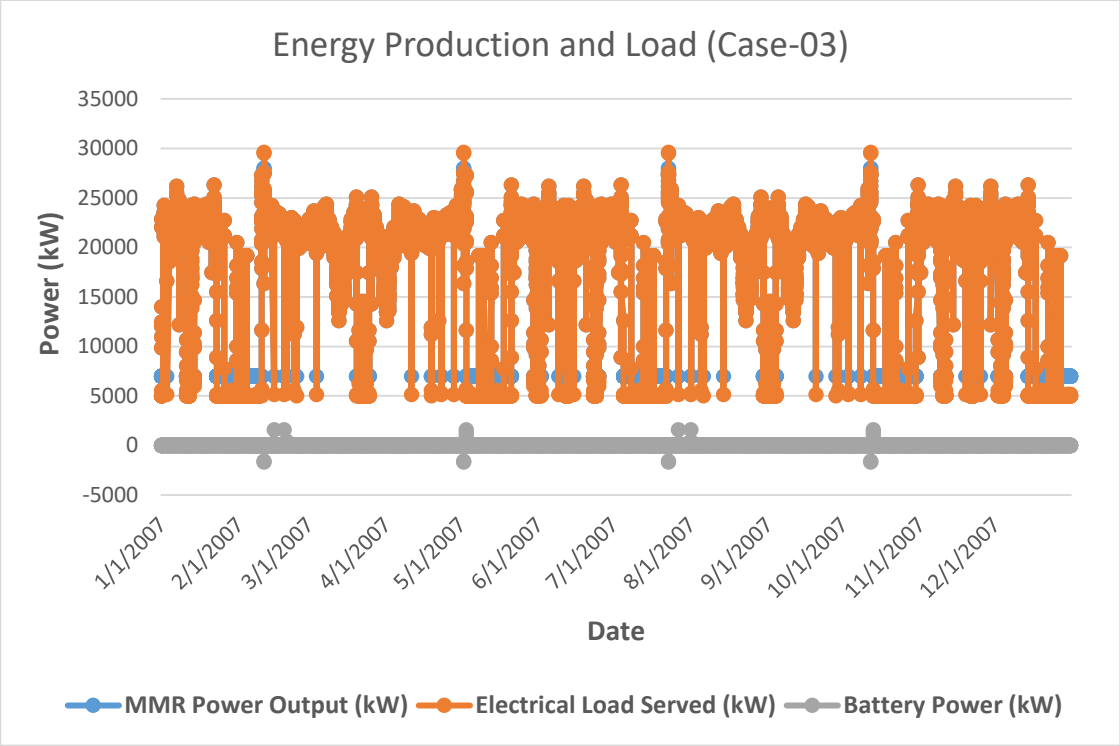

Figure 6-6: Total Energy Production and Total Load Served (Case-03)

Case-04: Nuclear-Renewable Hybrid Energy System (N-R HES)

The integration of nuclear and renewable energy is represented in this case. This case similar to Case-02, where renewable energy is integrated with a diesel generator. The diesel generator of Case-02 is replaced by MR in Case-04. Figure 6-7 represents the system configuration.

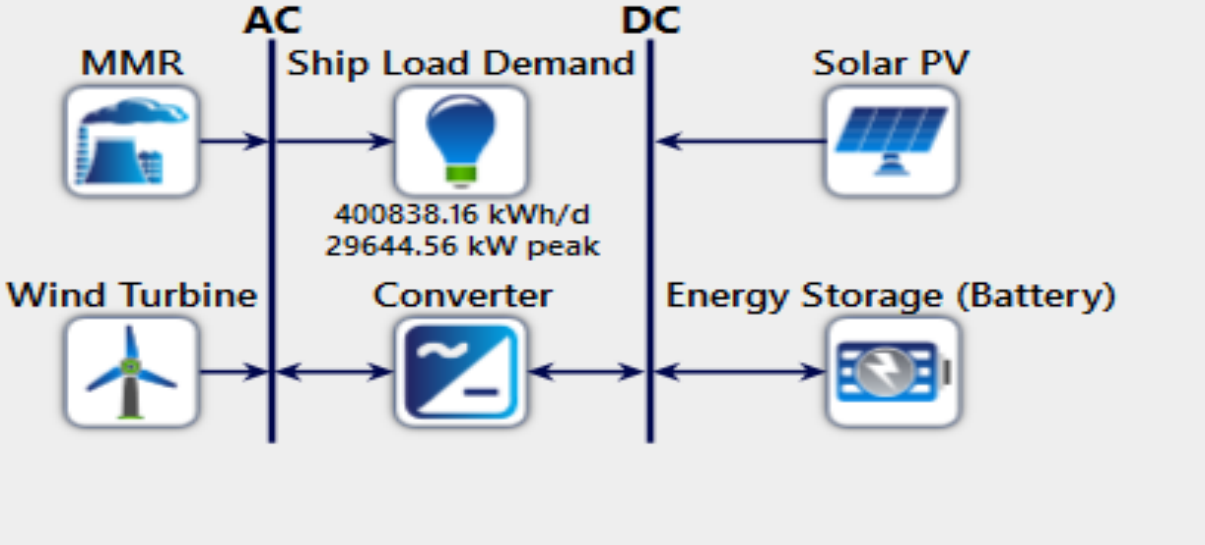

Figure 6-7: Nuclear-Renewable Hybrid Energy System (N-R HES)

Most of the electricity is produced by MR which is around 88.6%. The rest of the electricity is produced by renewable energy sources. The penetration of renewable energy is 11.4%, where solar energy is 1.2% and wind energy is 10.2%. Ratings of MR, solar PV, wind turbine, and the battery are 27 MWe, 0.97 MW, 1.5 MW, and 1.6 MW, respectively. Figure 6-8 shows the energy output from MMR, solar PV, wind turbine, battery, and the total load served.

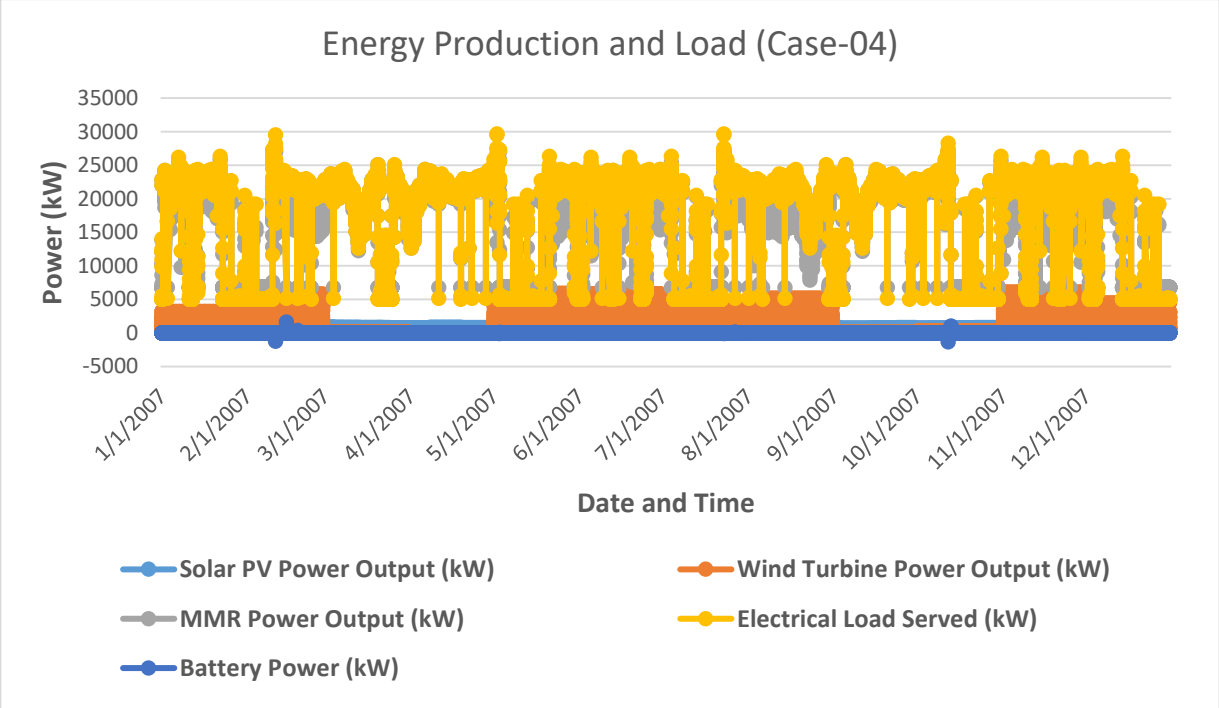

Figure 6-8: Total Energy Production and Total Load Served (Case-04)

NPC and LCOE of all four cases are shown in Figure 6-9. In terms of NPC and LCOE, Case-01 exhibits the highest value. For Case-01, NPC is 738.82 million USD, and LCOE is 0.33 USD/kWh. In Case-01, 100% of electricity is produced by the diesel generator, and there is no penetration of renewable energy. Total electricity production in the first year of project life is 146 GWh. Total fuel consumption is 58 ML in the first year of project life with daily and hourly average fuel consumption are 160 kL and 6,680 L, respectively.
After integrating renewable energy sources with diesel generator both NPC and LCOE are reduced to 687.98 million USD and 0.31 USD/kWh, respectively in Case-02. Around 10.1% of electricity is produced from renewable energy. Total electricity production from the diesel generator in the first year of project life for Case-02 is 131 GWh. In this case, total fuel consumption is 52 ML with daily and hourly average fuel consumption is 144 kL and 6,013 L, respectively.

Compared to Case-01 and Case-02, the NPC and LCOE are reduced to a great extent for Case-03 after introducing nuclear energy. In this case, NPC is 492.77 million USD, and LCOE is 0.22 USD/kWh. In this case, 100% of electricity is produced by MR, and the total electricity production in the first year of project life is 151 GWh. Total fuel consumption is 6.3 kg in this case with daily and hourly average fuel consumption are 0.02 kg and 0.000719 kg, respectively.

Case-04 shows the lowest NPC and LCOE among all the cases. NPC and LCOE in Case-04 are 486.18 million USD and 0.22 USD/kWh, respectively. The total electricity produced by MR is 137 GWh whereas solar PV and wind turbine produce 17 GWh combined in the first year of the project lifetime. Due to the integration of renewable energy in Case-04, both NPC and COE are reduced compared to Case-03. Total fuel consumption in the first year for this case is 5.74kg. Daily and hourly average fuel consumption are 0.02 kg and 0.000656 kg, respectively.

Figure 6-10 shows the cost distribution of different energy systems. For Case-01 and Case-02 the largest contributors are fuel cost and replacement cost while for Case-03 and Case-04, capital cost and O&M cost are the greatest contributors.

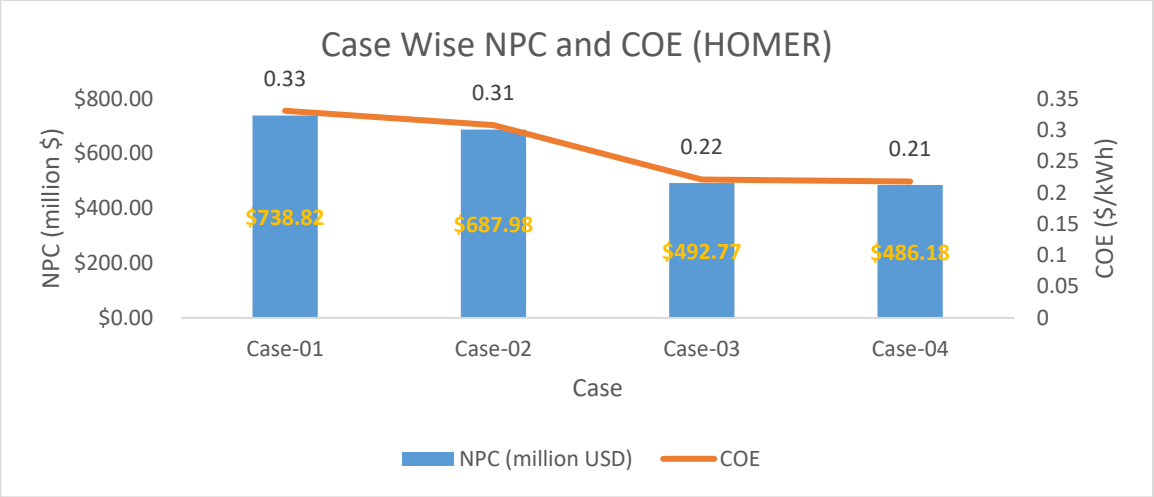

Figure 6-9: Case Wise NPC and COE (HOMER)

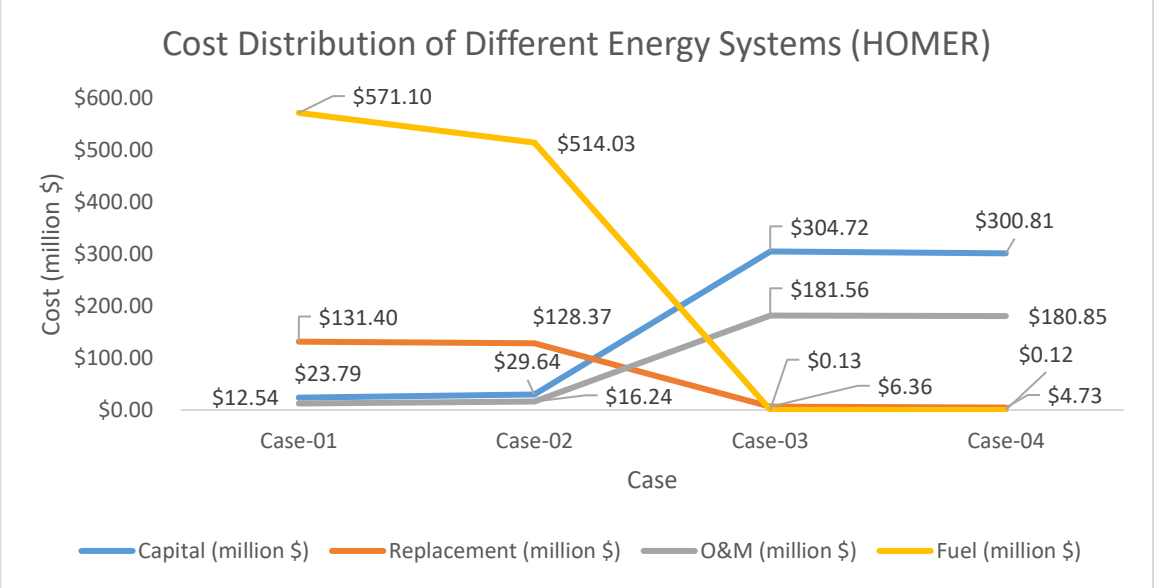

Figure 6-10: Cost Distribution of Different Energy Systems (HOMER)

6.2. **Comparison among the Proposed Hybrid Energy Systems (DE Algorithm)**

The Differential Evolution (DE) algorithm is used to determine the lowest Net Present Cost of the four energy systems proposed for marine transportation. The four energy systems are defined as

Case-01: Standalone Fossil fuel-based Energy Systems

Case-2: Renewable and Fossil fuel-based Hybrid Energy Systems

Case-3: Standalone Nuclear Energy Systems

Case-04: Nuclear Renewable Hybrid Energy Systems (N-R HES)

Case-04 shows the lowest NPC ($ 532.11 million) among all the energy systems, while Case-01 has the highest NPC ($ 877.61 million). After introducing renewable energy with fossil fuel in Case-02, the NPC ($ 875.90 million) reduces around 1.7 million USD compared with Case-01. Case-03 exhibits lower NPC ($ 538.05 million) than Case-01 and Case-02 but a little bit higher than Case-04. The LCOE of all four cases follows a similar trend of NPC. The NPC and LCOE of all four cases are shown in Figure 6-11and Figure 6-12, respectively.

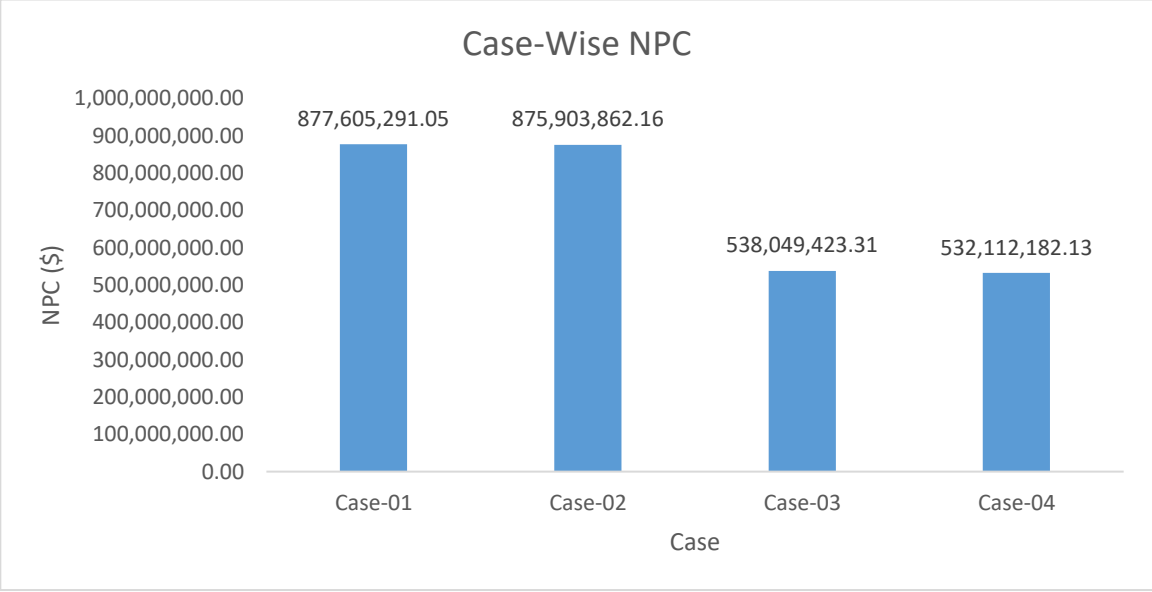

Figure 6-11: Comparison of NPC of Different Energy Systems

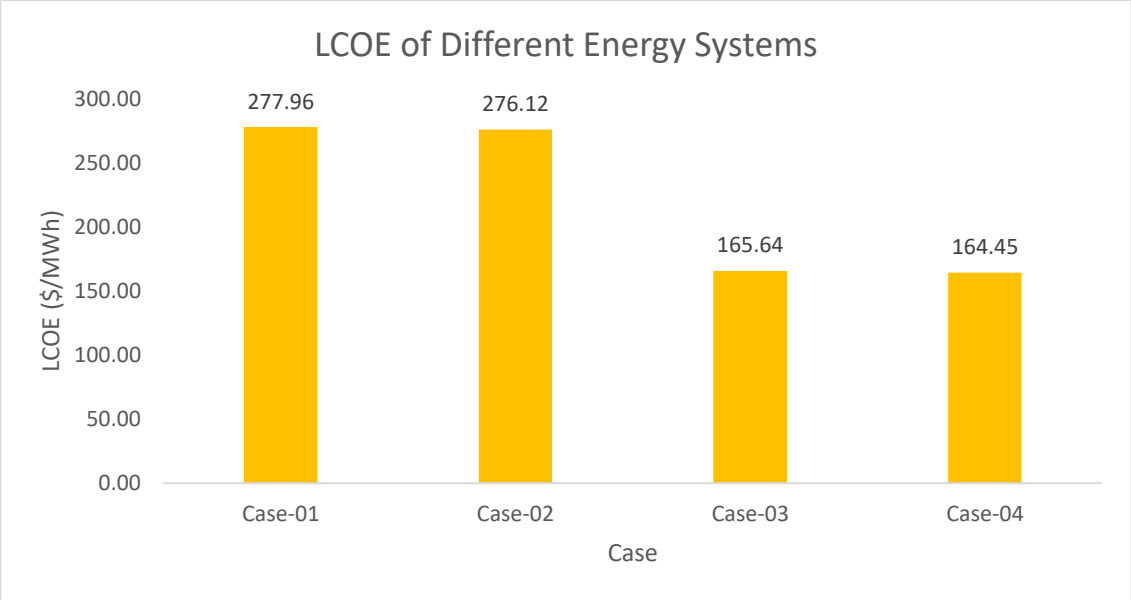

Figure 6-12: Comparison of LCOE of Different Energy Systems

Table 6-1 shows the optimal configuration of all four energy systems. For all the energy systems, most of the energy is delivered by the diesel generator or MR based on the type of the energy system. The renewable energy penetration is higher in Case-04 compared to Case-02. The renewable energy penetration in Case-04 is about 1.61% where the renewable energy penetration in Case-02 is around 1.39%. Case-02 shows the highest dependency on the energy storage device, whereas Case-03 exhibits the lowest dependency on the energy storage device for the optimal energy configuration. The ratings of the energy storage device for Case-01, Case-02, Case-03, and Case-04 are 2,341.38 kWh, 3,907.92 kWh, 637.17 kWh, and 1,351.92 kWh, respectively. The Loss of Power Probability (LPSP) of all energy systems is within the defined range (less or equal to 8%) that ensures the utmost reliability while optimizing the systems. The GRF is another reliability factor that ensures the system's reliability in terms of energy generation. For a reliable energy system, usually, the GRF should be at least 100%. Among the four cases, Case-03 has the highest value of GRF (145.38%), and Case-01 has the lowest GRF (141.31%). The GRF of Case-04 is 144.82%, which is very close to Case-03. Therefore, Case-04 performs better than the other three energy systems in the ship in terms of economic (NPC, LCOE) and reliability (LPSP, GRF) KPIs.

Table 6-1: Optimal configuration of energy systems

Parameter	Case-01	Case-02	Case-03	Case-04
NPC ($)	877,605,291.05	875,903,862.16	538,049,423.31	532,112,182.13
LCOE ($/MWh)	277.96	276.12	165.64	164.45
Generator/ MMR (MW)	28.15	28.14	28.96	28.00
Solar PV (kW)	0.00	396.79	0.00	0.09
Wind (kW)	0.00	0.00	0.00	3,050.30
Battery (kWh)	2,341.38	3,907.92	637.17	1,351.92
Solar ratio	N/A	0.10	N/A	0.01
Energy System Weight (kg)	1,546,864.99	1,545,210.58	445,816.43	779,799.66
LPSP	0.080	0.079	0.080	0.08
CO2 Emissions (ton/year)	144,714.33	144,655.35	967.73	935.57
Wratio	0.005	0.005	0.001	0.0025
Excess Energy Ratio	29.24	29.57	31.21	30.95
GRF	141.31	141.98	145.38	144.82
Capital Cost ($)	26,083,959.77	25,882,395.10	313,231,568.67	308,562,984.45
Replacement Cost ($)	131,028,335.96	129,934,105.16	651,048.07	3,710,762.34
Operation and Maintenance Cost ($)	16,414,843.54	16,310,161.71	154,912,891.56	152,358,576.04
Fuel Cost ($)	637,771,484.30	637,511,569.11	32,482,148.04	31,402,690.09
Decommissioning Cost ($)	N/A	N/A	16,241,074.02	15,701,345.05
Refuel Cost ($)	N/A	N/A	20,087,311.63	20,087,311.63
Carbon Penalty ($)	66,302,976.09	66,275,955.20	443,381.32	428,646.72
Salvage Value ($)	0.00	10,324.12	0.00	140,134.20

The CO_2 emissions is an environmental KPI that determines the impact of energy systems on the environment. Figure 6-13 and Figure 6-14 show the CO_2 emissions and penalty for it of all the four energy systems sequentially. In terms of environmental impact, Case-04 shows the least impact on the environment. Only 935.57 ton of CO_2 is emitted from N-R HES whereas, from Case-01, 144,714.33 ton of CO_2 emits each year. Hence, the proposed N-R HES will reduce around 99% of CO_2 emissions compared to fossil fuel-based energy systems (Case-01). The penalty for emitting CO_2 is the highest for Case-01 and lowest for Case-04.

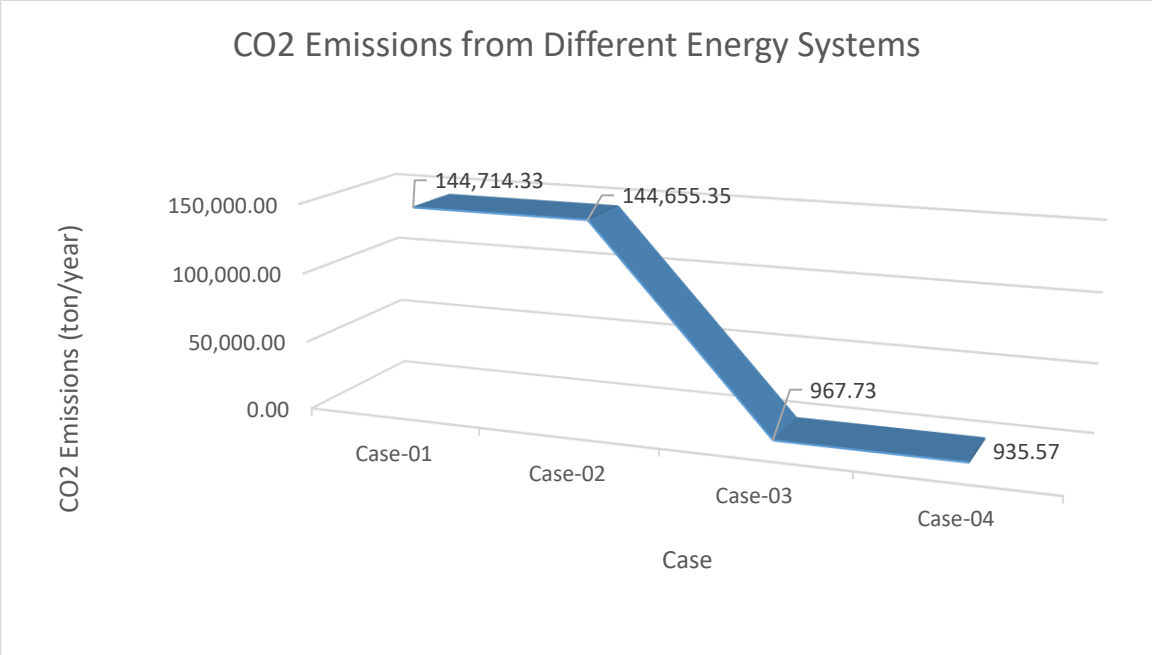

Figure 6-13: CO_2 Emissions of Different Energy Systems

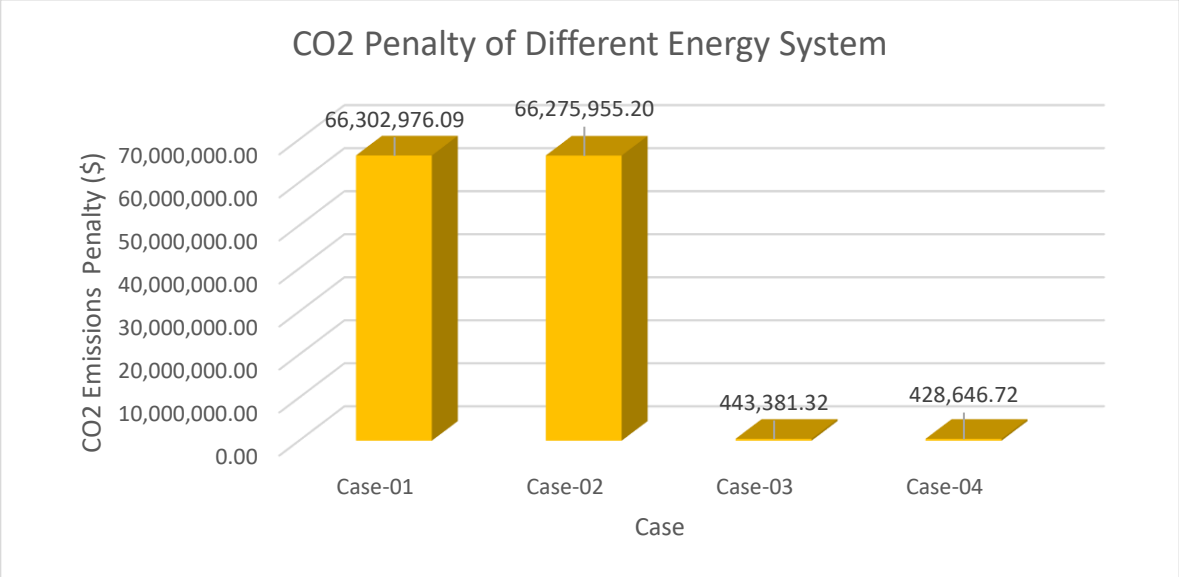

Figure 6-14: CO_2 Emissions Penalty of Different Energy Systems

The weight of the energy systems and W_{ratio} (the ratio between the total weight of the energy system and the total cargo-carrying capacity of the ship) are two important factors that determine the cargo-carrying performance of the ship. The energy system weight for Case-03 and Case-04 are lower compared to Case-01 and Case-02. The energy system weight of Case-01, Case-02, Case-03, and Case-04 is 1,546,864.99 kg, 1,545,210.58 kg,

445,816.43 kg , and 779,799.66 kg respectively. Compared to Case-01, the energy system weight of Case-03 and Case-04 is around 3 and 2 times lower respectively. By using the proposed N-R HES in the ship, the ship operator will be able to carry 767 ton more cargo which will increase the revenue of the ship. Considering the revenue per Ton-Mile as $0.01 [149], and the distance between Iraq and Singapore as 4462 miles [150], the 'Baltic Sunrise' would earn an additional $34,223 (767 × 0.01 × 4462) from each voyage from Iraq to Singapore. The lower value of W_{ratio} is expected to carry more cargo by the ship. The energy system weight and W_{ratio} of four energy systems are presented in Figure 6-15.

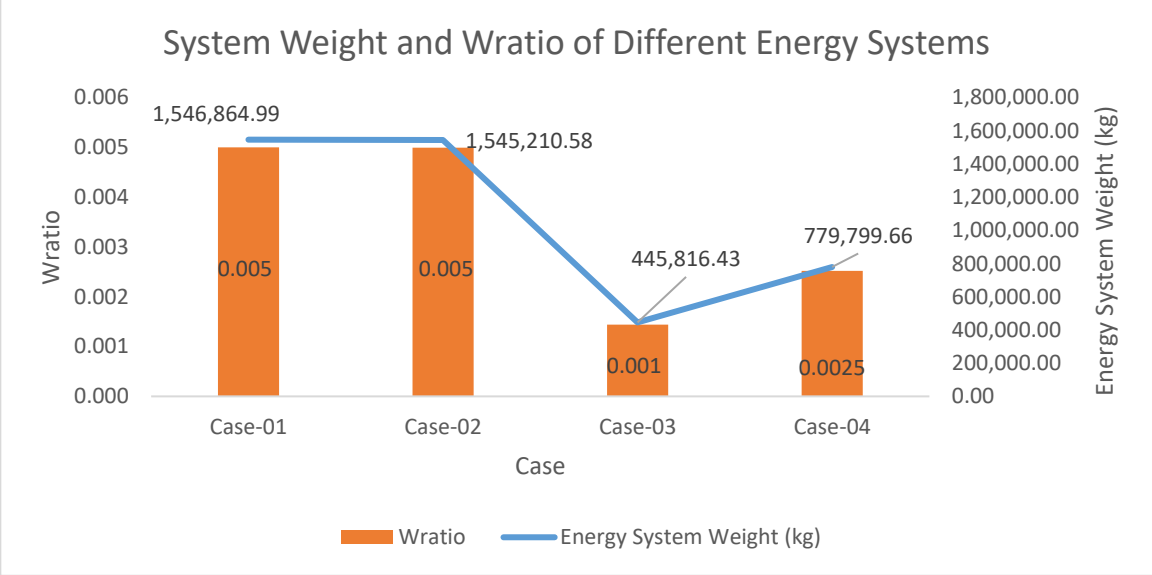

Figure 6-15: System Weight and W_{ratio} of Different Energy Systems

The cost distribution of different energy systems is shown in Figure 6-16. The capital cost of Case-01 and Case-02 is very low compared to Cae-03 and Case-04. Case-03 has the highest capital cost ($313.23 million), and Case-02 has the lowest capital cost ($25.88 million). After introducing renewable energy, the capital cost is reduced compared to standalone system. For example, the capital cost of Case-01 is $26.08 million, and after renewable energy integration, the capital cost is reduced to $25.88 million in Case-02. Also, for Case-03 the capital cost is $313.23 million that is reduced to $308.56 million after renewable energy addition in Case-04. The operation and maintenance cost follows the same trend as the capital cost. Case-02 has the lowest O&M cost ($16.31 million) whereas Case-03 has the highest O&M cost ($154.91 million). The fuel cost shows that Case-01 and Case-02 have a higher cost associated with fuel compared to Case-03 and Case-04. Case-01 has the highest fuel cost ($ 637.77 million) as the price of diesel fuel (per MWh) is much higher than nuclear fuel. After incorporating renewable energy in Case-02, the fuel cost ($637.31 million) is reduced a little bit. With nuclear energy, the fuel cost is reduced to a great extent. The fuel cost of Case-03 is $32.48 million, and by introducing renewable energy with nuclear energy, the fuel cost is reached the lowest value in Case-04 ($31.40 million). The replacement cost of Case-01 is the maximum ($131.03 million) among all

the energy systems. The replacement cost reduced a bit in Case-02 ($129.93 million). Unlike other costs, Case-04 has a higher replacement cost ($3.71 million) compared to Case-03 ($0.65 million). In Case-03, only battery replacement cost contributes to the total replacement cost, but in Case-04 replacement cost of renewable energy along with the battery replacement cost added to the total replacement cost. This cost distribution will give a clear idea about the cash flow in different stages of the project lifetime to the manufacturers, investors, and operators of maritime transportation.

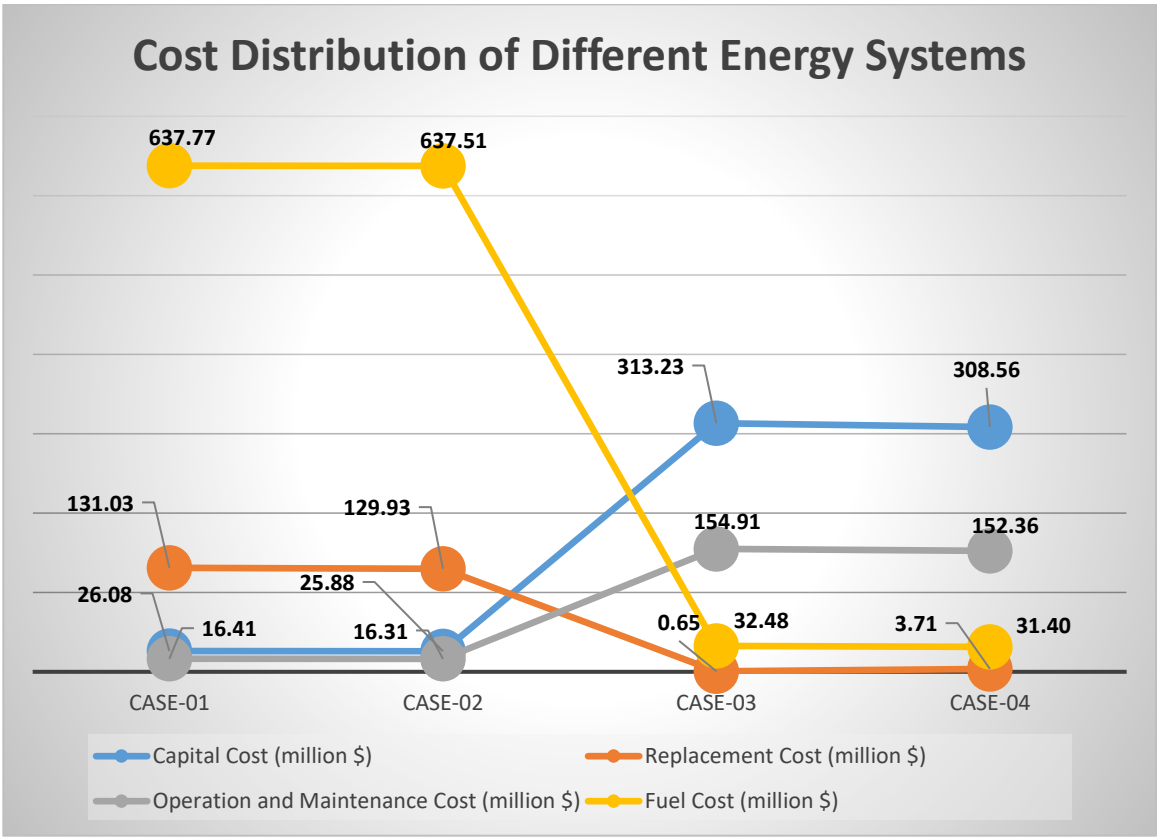

Figure 6-16: Cost Distribution of Different Energy Systems

Figure 6-17 shows the percentage of excess energy ratio from different optimized energy systems. Excess energy ratio is the ratio between the unused energy to the total energy generation. The percentage of the excess energy of Case-03 is maximum (31.21%) and in Case-01, it is minimum (29.24%). The amount of excess energy produced by any hybrid energy system largely depends on the types of energy sources, size of the energy system components, profile, and availability of the meteorological resources (solar irradiance, wind), and load profile of the demand [85]. For example, the excess energy ratio of an optimal energy system in Turkey consisting of a wind turbine was reported as 64.2% [151]. Some researchers proposed to dump the excess energy while some suggested utilizing the excess energy by other means like selling back the excess energy to the grid, producing hydrogen in an electrolyzer, pumping water uphill, using for cooling purpose, storing in

thermal energy storage, seawater desalination, and space heating. In this study, the excess energy is dumped, although seawater desalination could be an option to use the excess energy. However, as the usage of excess energy employs additional cost, the impact of using the additional energy on the NPC needs to be assessed.

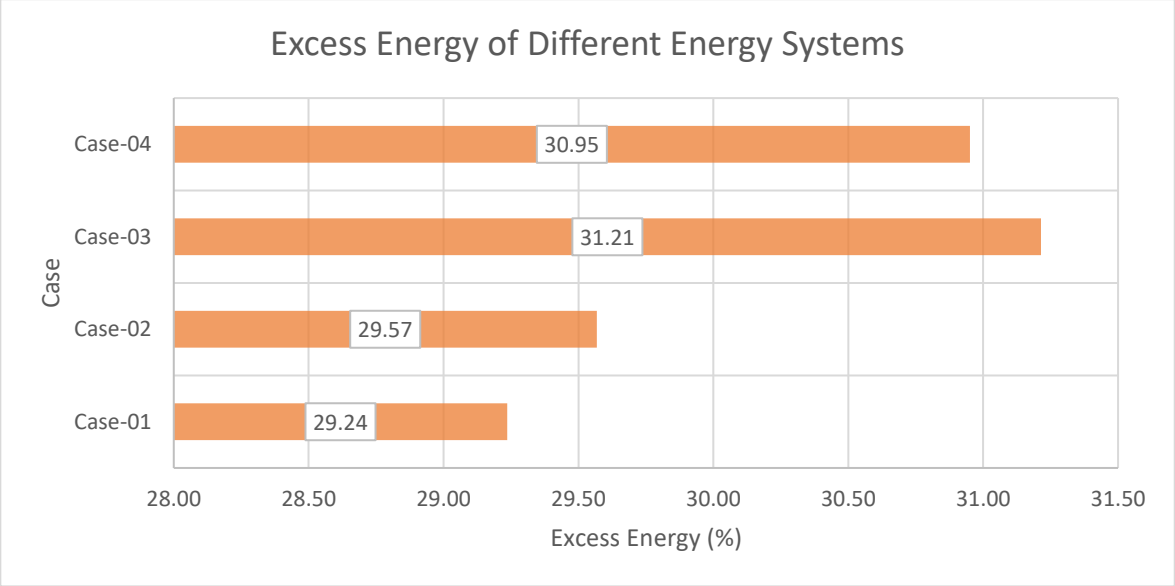

Figure 6-17: Excess Energy of Different Energy Systems

Figure 6-18 shows the convergence plot for Case-01. Till the 8th iteration, the static penalty is added to the NPC. From the 9th iteration, the NPC is calculated without any penalty, and the optimization moves towards the minimum NPC. Figure 6-19 illustrates the cost breakdown of Case-01. More than two-thirds of the total cost of Case-01 is associated with the fuel cost (72.67%), and the O&M cost has the smallest portion (1.87%). The replacement cost has the second-largest share (14.93%) of the total cost. The capital cost is accounted for 2.97% of the cost while the carbon penalty made up 7.56%.

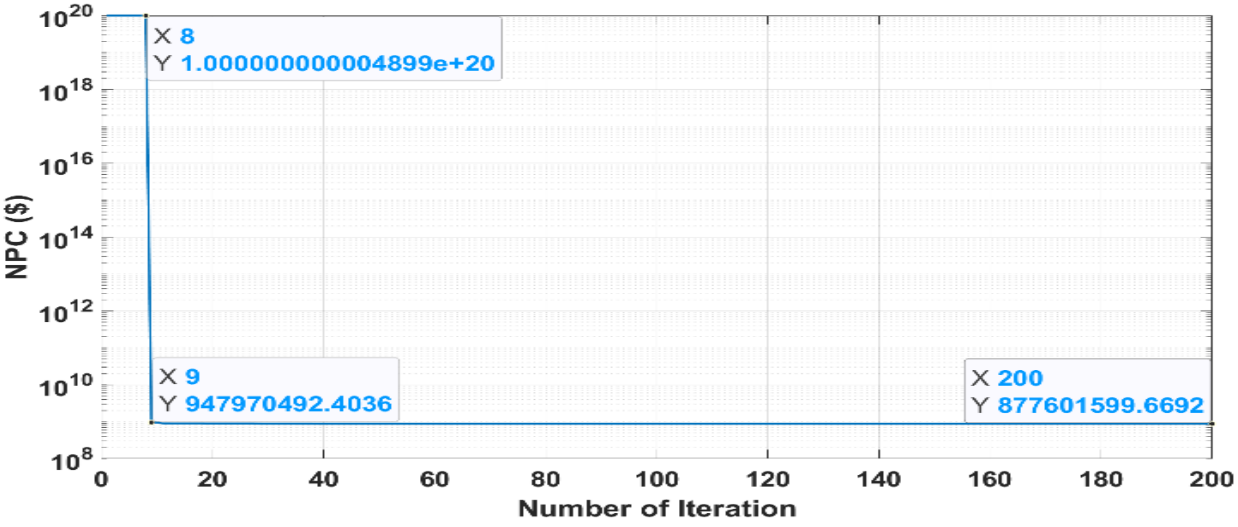

Figure 6-18: Convergence Plot (Case-01)

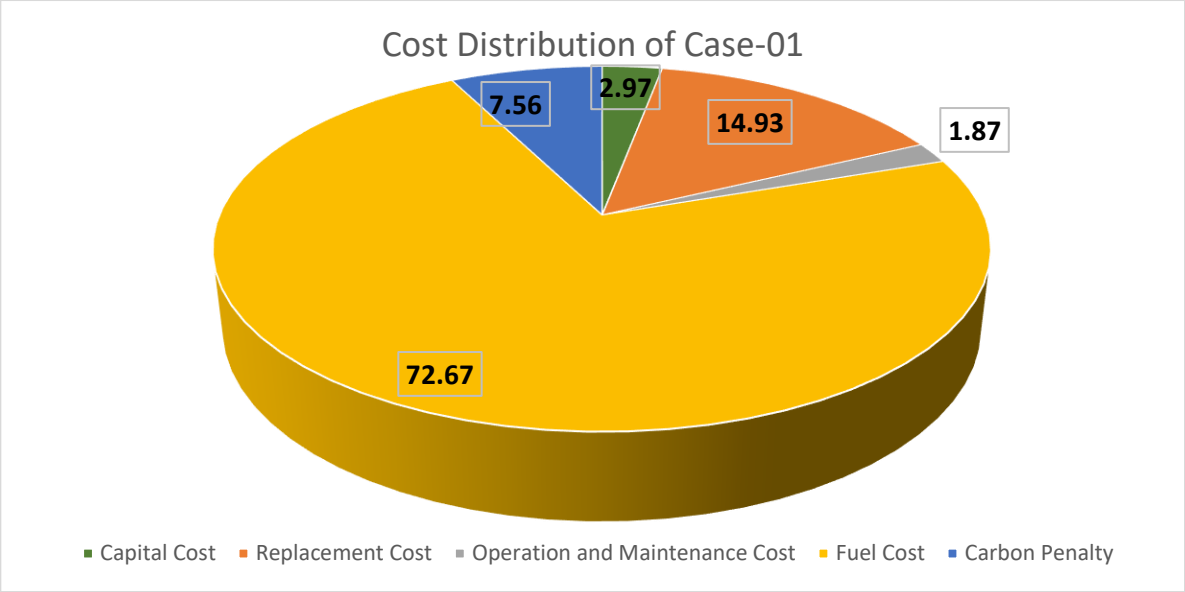

Figure 6-19: Cost Distribution (Case-01)

The convergence plot of Case-02 is presented in Figure 6-20. The static penalty is added up to the 8th iteration and after the 200th iteration, the algorithm reaches the final NPC. The cost distribution of Case-02 is illustrated in Figure 6-21. The cost distribution is similar to Case-01. The fuel cost makes up the largest portion (72.78%) of the total cost. The share of the replacement cost of Case-02 (14.83%) is a little bit lower compared to Case-01 (14.93%). The capital cost and the O&M cost comprised only 2.95% and 1.86% of the total cost respectively. The CO_2 emissions penalty contributes 7.57% of the total cost of Case-02.

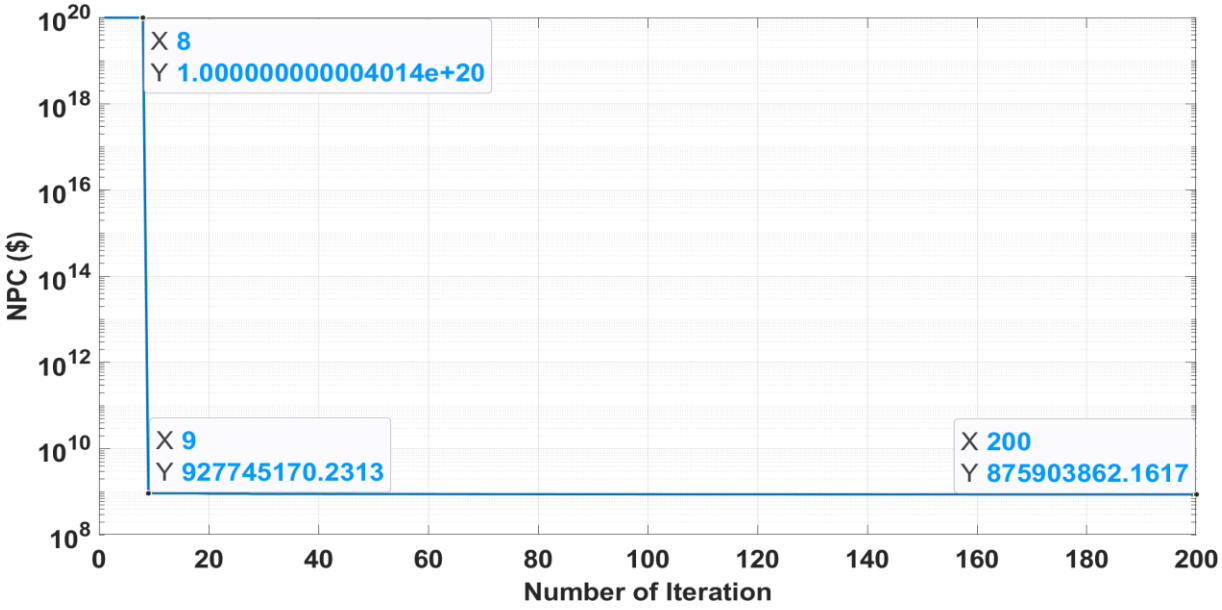

Figure 6-20: Convergence Plot (Case-02)

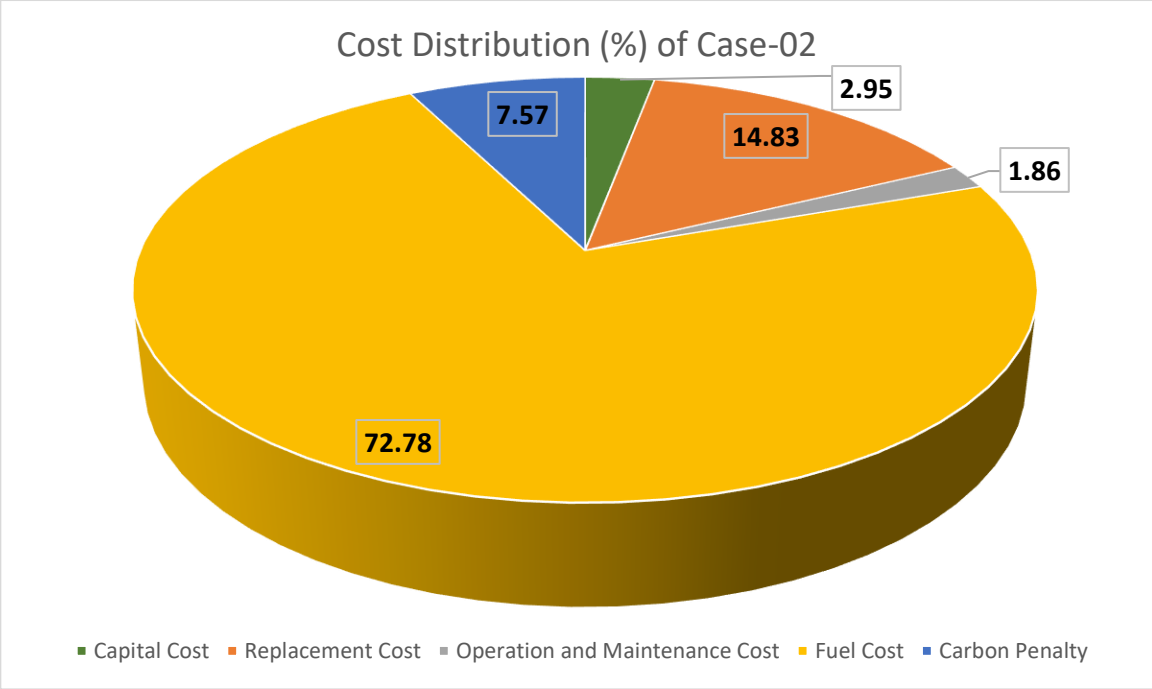

Figure 6-21: Cost Distribution (Case-2)

Figure 6-22 represents the convergence plot of Case-03. From the 1st iteration, the algorithm finds the NPC without any static penalty. The algorithm moves to the optimal NPC range very quickly. The cost breakdown of Case-03 is shown in Figure 6-23. Unlike, Case-01, and Case-02, the capital cost contributes more than half of the total cost (58.22%). The O&M cost makes up the second-largest (28.79%) portion of the total cost. The fuel cost, refueling cost, and decommissioning cost comprise 6.04%, 3.73%, and 3.02% cost respectively. The share of the replacement cost and the CO_2 emissions penalty cost is very low (less than 1%) for Case-03.

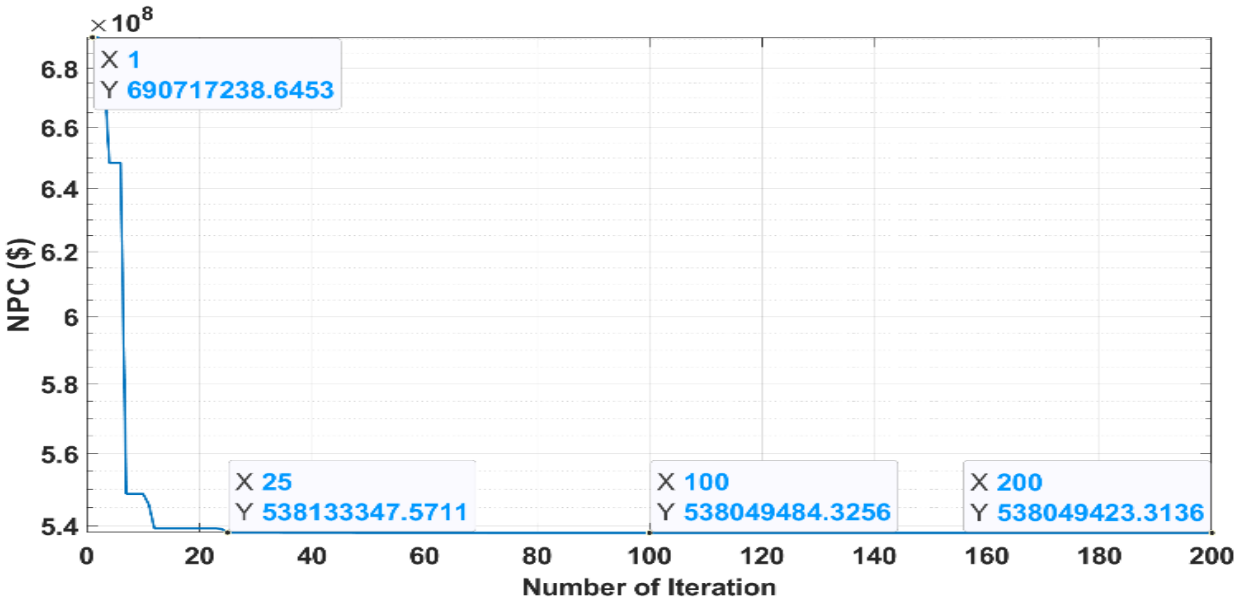

Figure 6-22: Convergence Plot (Case-03)

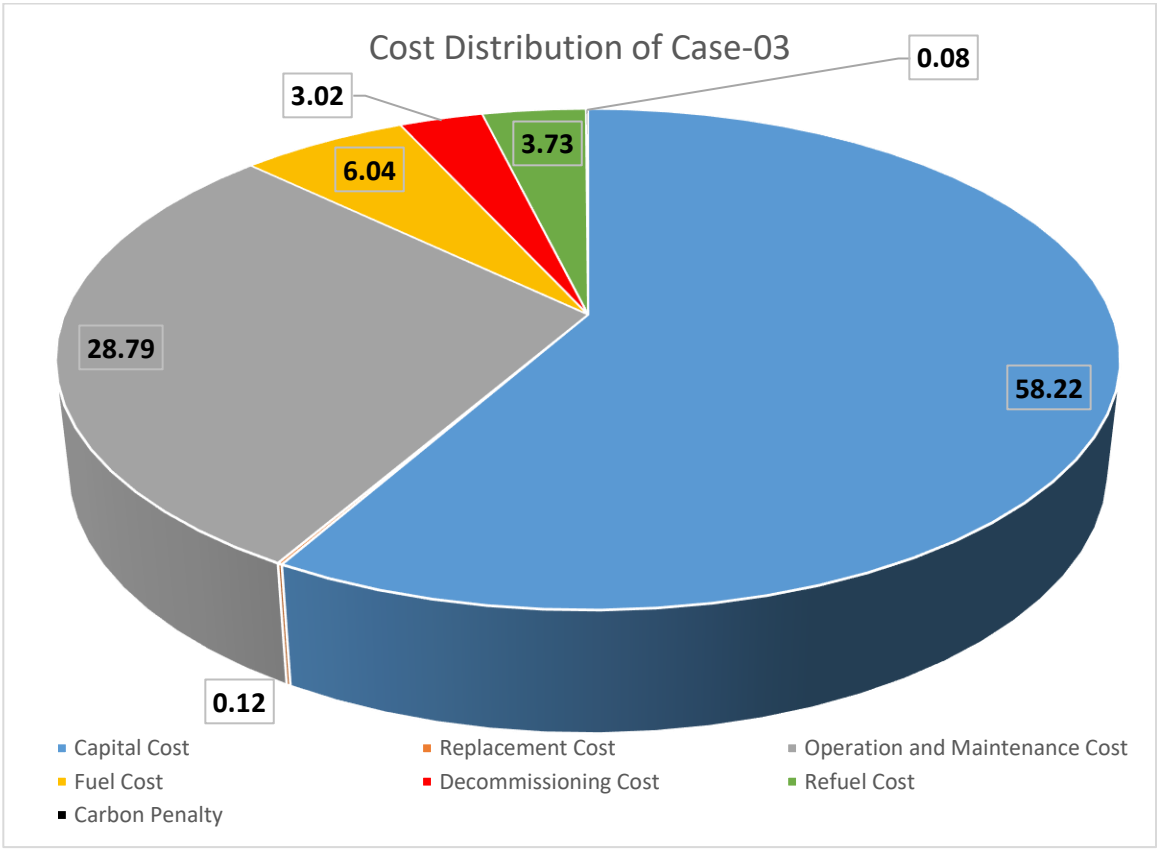

Figure 6-23: Cost Distribution (Case-03)

The convergence plot of Case-04 is presented in Figure 6-24. By the 100th iteration, the algorithm is within the optimal range of NPC ($532,280,244), and the 150th iteration shows the NPC as $532,117,560 which is very close to the value of the 200th iteration

($532,112,182). The cost distribution of Case-04 is illustrated in Figure 6-25. Like Case-03, the capital cost is accounted for more than half of the total cost (57.97%). The O&M cost comprises 28.63% of the cost. The fuel cost, decommissioning cost, and refueling cost make up 5.90%, 2.95%, and 3.77% of the total cost respectively. The replacement cost and the cost associated with CO_2 emissions comprise only 0.70% and 0.08% cost sequentially. The total supply and total demand of energy of Case-04 are presented in Figure 6-26. The figure shows that the supply always fulfills the demand in each time step within the acceptable margin of LPSP. However, due to 8% LPSP, energy supply is less than the energy demand in five time steps (t=989, 990, 4894, 6823,6824)). The deficit energy at t=6824 is shown in Figure 6-27 where the total demand is 29,644 kW and the total supply is 27,999 kW. Figure 6-28 shows the total demand and consumption after dumping the excess energy.

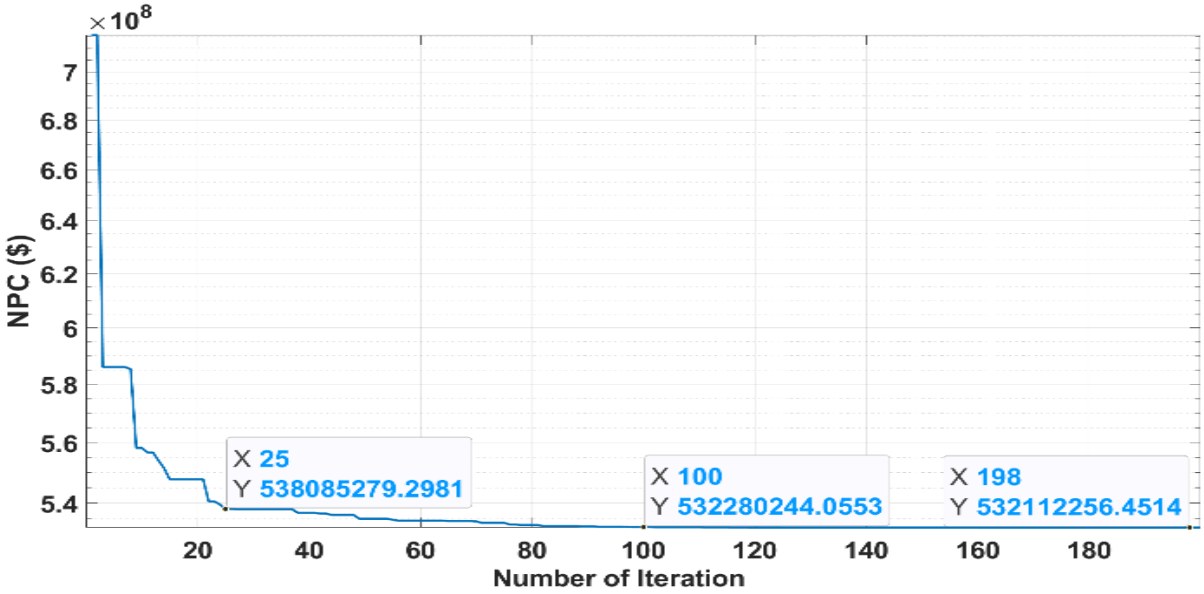

Figure 6-24: Convergence Plot (Case-04)

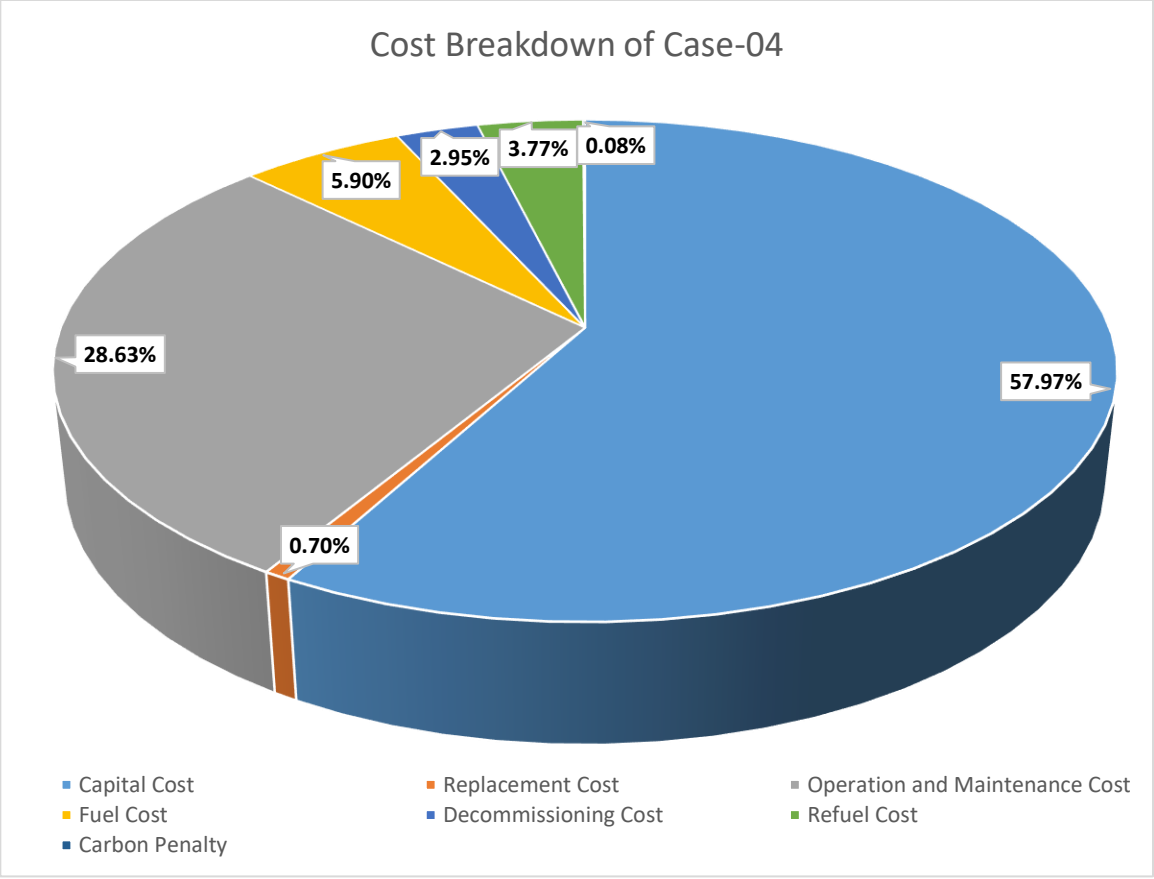

Figure 6-25: Cost Distribution (Case-04)

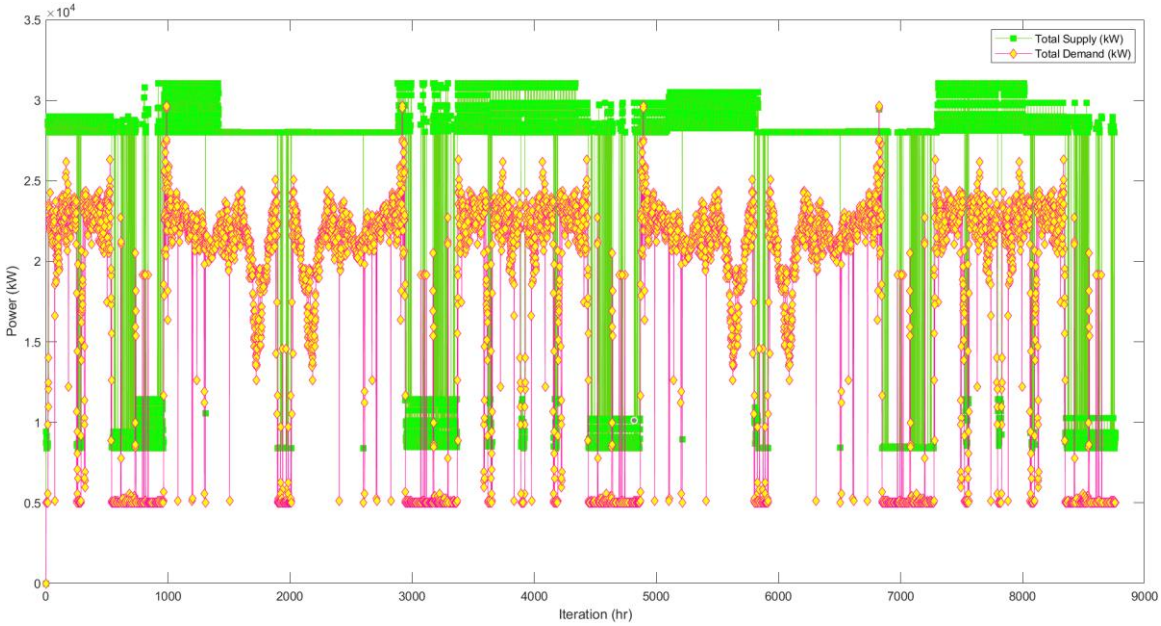

Figure 6-26: Total Energy Supply and Demand (Case-04)

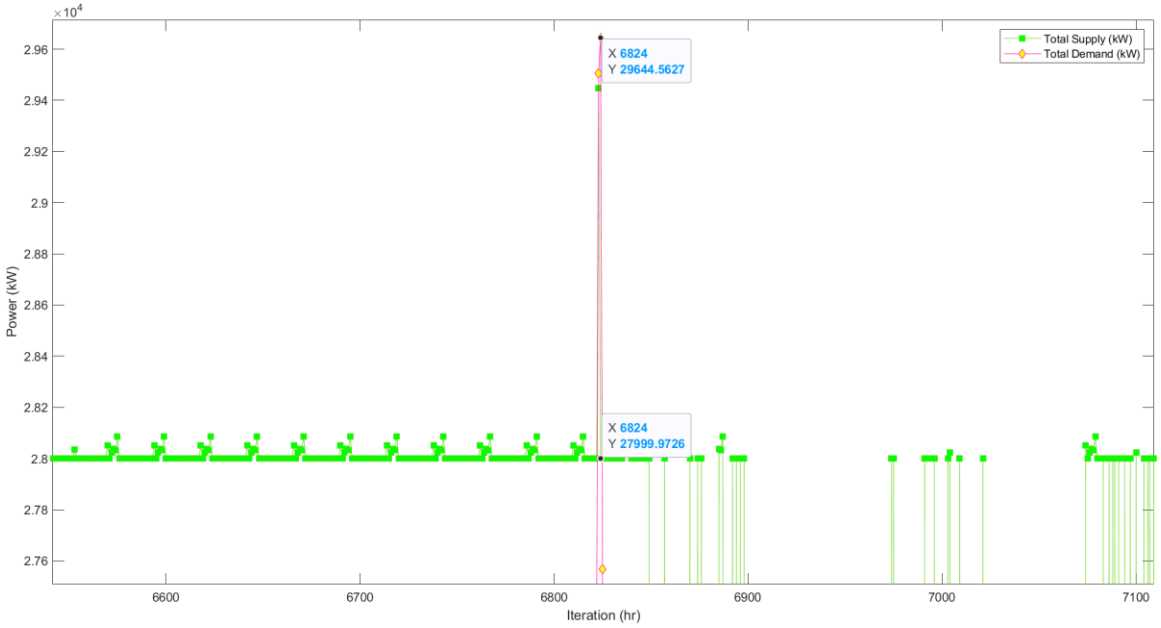

Figure 6-27: Total Energy Supply and Demand at t=6824 (Case-04)

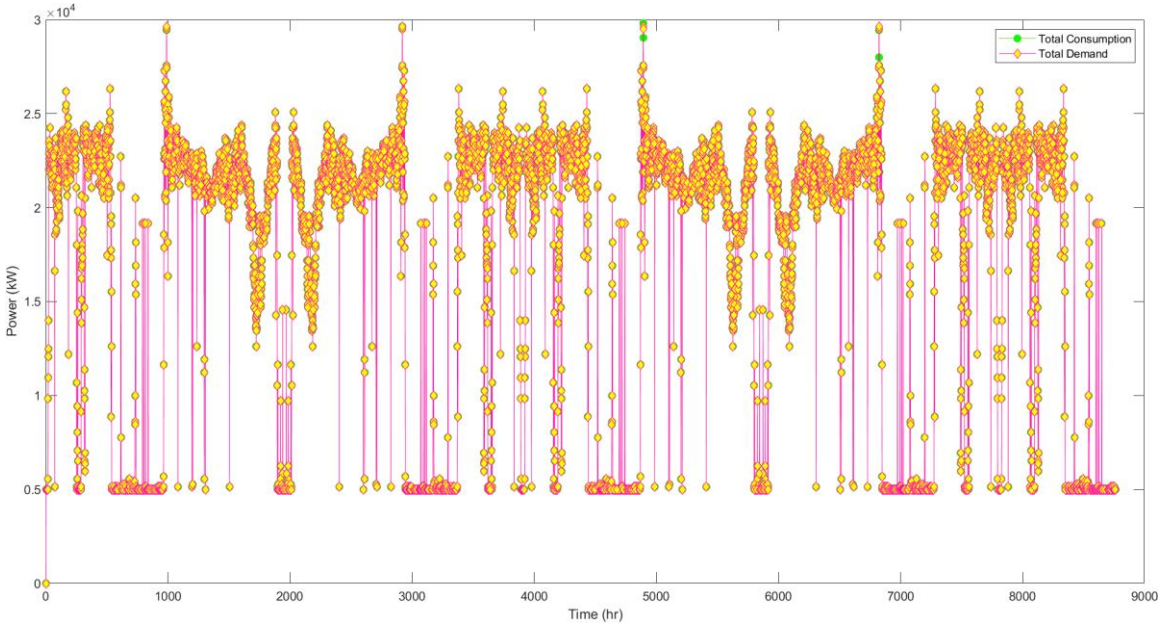

Figure 6-28: Total Energy Consumption and Demand (Case-04)

6.3. Comparison among Different Optimization Techniques

6.3.1. Comparison among Different Optimization Techniques Based on NPC

From the findings of section 6.2, it is evident that Case-04 is best among all the four energy systems for marine transportation. The Differential Evolution (DE) optimization technique is used to optimize the system. Hence, it is important to compare the findings of DE optimization with other widely used optimization techniques to validate and reinforce the results. Also, to evaluates the impact of the control parameters (scaling factor and crossover probability), the findings of DE are compared with ADE. Figure 6-29 shows the NPC of Case-04 for DE, ADE, and PSO optimization techniques. The lowest NPC ($532,112,182.13) is obtained by using the DE optimization technique although the NPC (532,114,720.56) determined by the ADE is very close to DE. The difference between DE and ADE is only 0.0005%. This suggests that the impact of the control parameter of DE optimization is very minimal on finding the lowest value of the objective function. Although the NPC (532118322.71) determined by the PSO optimization is the highest among all the optimization techniques, the difference is very low (0.0012%) compared to the DE optimization technique. This finding validates and reinforces the findings of the DE algorithm compared to other optimization techniques.

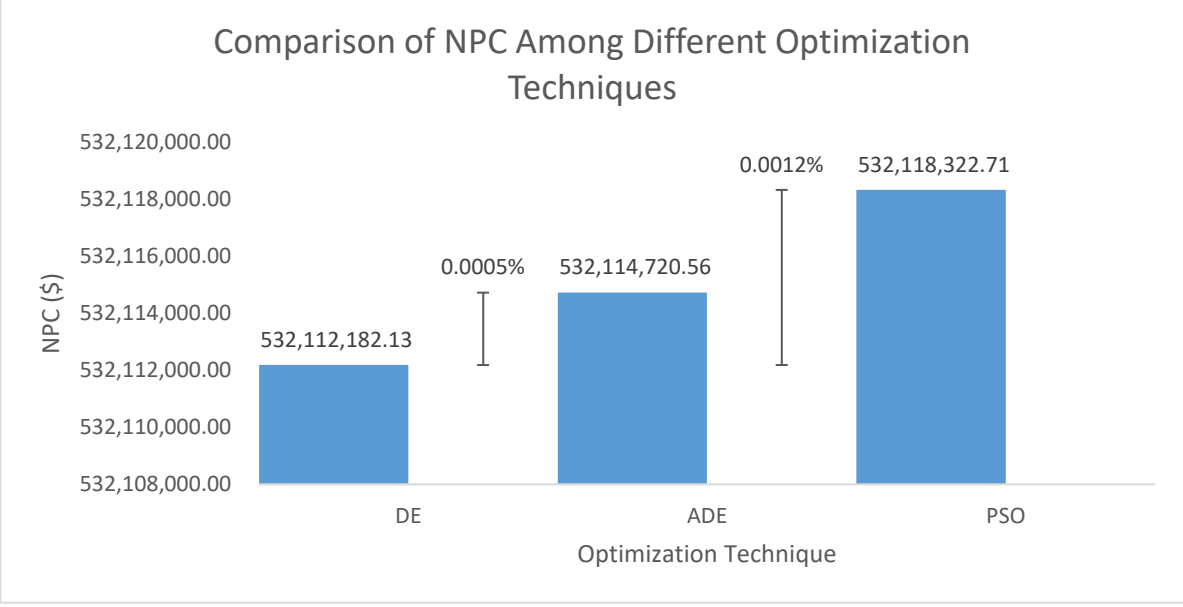

Figure 6-29: Comparison of NPC Among Different Optimization Techniques

The convergence plot of DE for Case-04 is shown in Figure 6-30. The algorithm is within the optimal range of NPC ($532,280,244.0553) by the 100th iteration. By moving forward, the NPC is getting close to the lowest value. By the 150th iteration, the NPC is $532,117,560.2854 which is very close to the value of the 200th iteration ($532,112,182.1253). Figure 6-31 shows the convergence plot of ADE for Case-04. For ADE, the algorithm reaches the optimal range of NPC ($532,388,216.3234) within the 95th iteration which is quite similar to DE. The algorithm moves forward by lowering the NPC further. Within the 150th iteration, the NPC (532,159,664.4846) is very close to the final NPC (532,114,720.5605). The convergence plot of PSO for Case-04 is presented in Figure 6-32. Within the 100th iteration, the algorithm is within the optimal range ($532,195,069.80) of NPC. By the 150th iteration, the NPC ($532,120,333.79) of the PSO algorithm is very close to the optimal value ($532118322.71) of the 200th iteration.

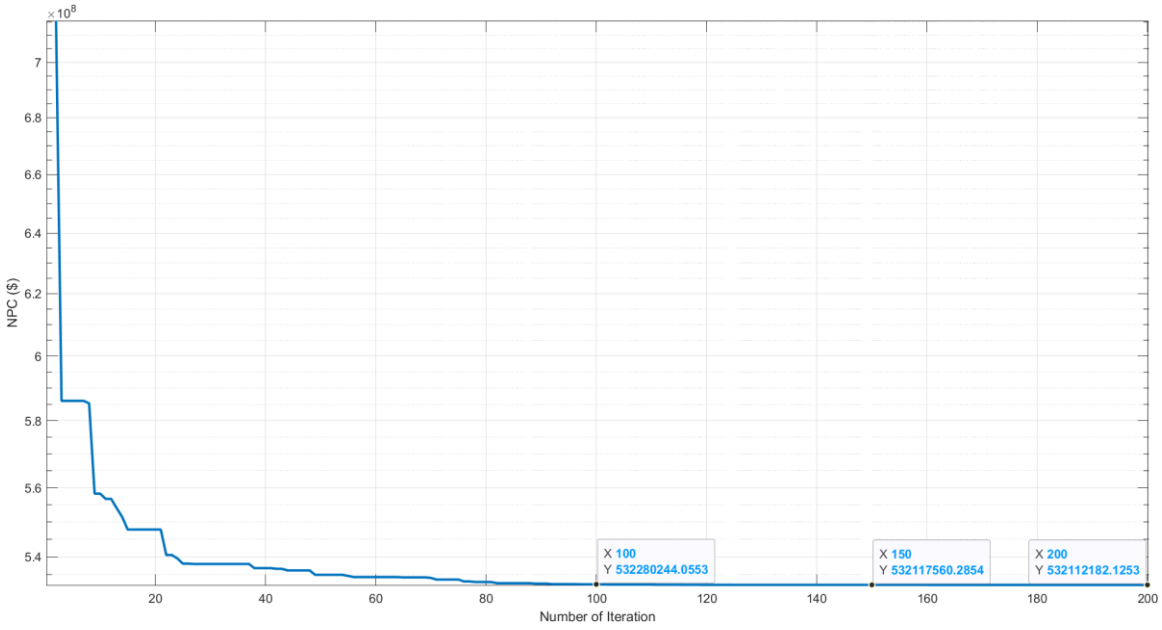

Figure 6-30: Convergence Plot of DE (Case-04)

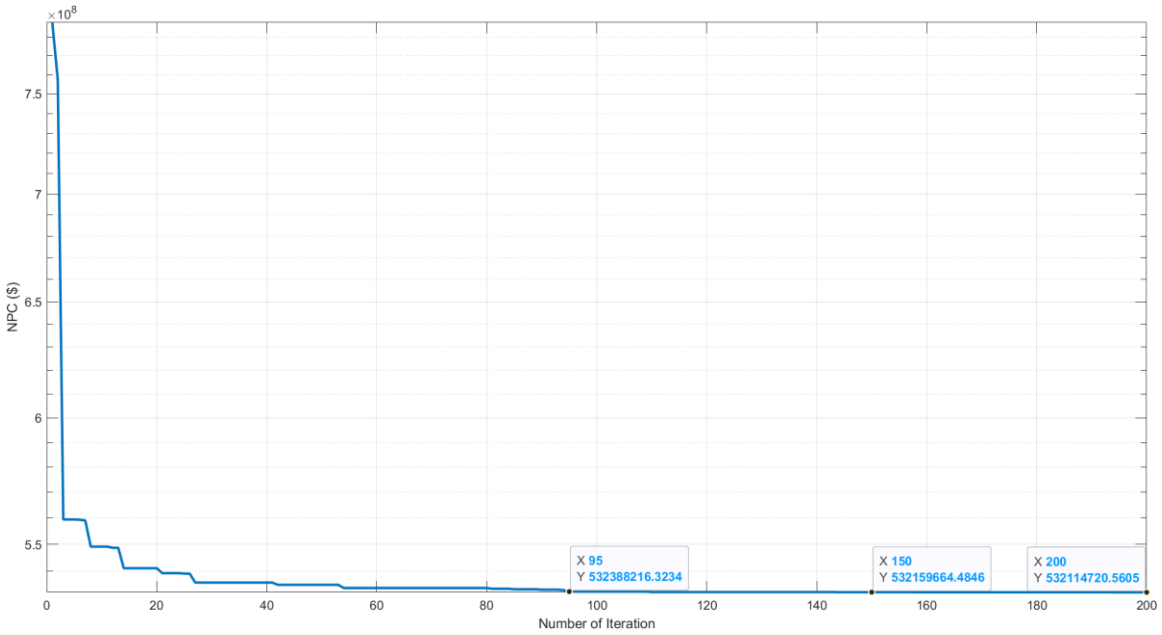

Figure 6-31: Convergence Plot of ADE (Case-04)

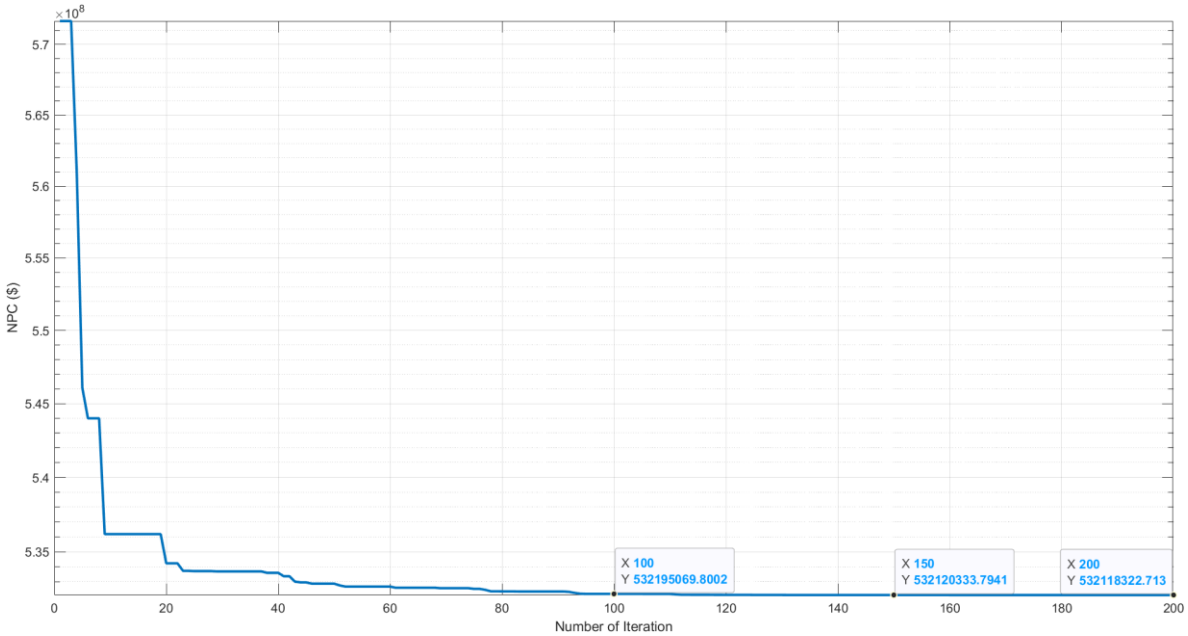

Figure 6-32: Convergence Plot of PSO (Case-04)

6.3.2. Comparison among Different Optimization Techniques Based on Different Costs

In this section, the major costs (Capital Cost, Replacement Cost, Operation and Maintenance Cost, and Fuel Cost) of Case-04 determined by different optimization techniques are evaluated and compared. The focus of this section is to identify the variation in major costs for different optimization techniques. Figure 6-33 shows the comparison of the capital cost of Case-04 for three different optimization techniques. Although the capital cost obtained by DE optimization is the highest ($308,562,984.45) among all the optimization techniques, the difference with the other two optimization techniques is very low. The capital cost of the ADE optimization technique is $ 308,551,402.80 that is 0.0038% less than the DE optimization. The PSO algorithm shows the lowest capital cost ($308,502,326.38) which is 0.0197% less than the DE optimization. The comparison of O&M cost among different optimization techniques is presented in Figure 6-34. The DE optimization illustrates the highest O&M cost ($152,358,576.04). The O&M cost of ADE optimization is 0.0082% less than the DE optimization technique. The PSO optimization shows the minimum O&M cost (152,302,873.82) among all the three optimization techniques, and it is 0.0366% lower than the DE optimization. Figure 6-35 represents the fuel cost of different optimization algorithms. The ADE optimization gives the lowest fuel cost ($31,402,362.62) among all the optimization techniques. The fuel cost of ADE is 0.0010% lower than the fuel cost of DE ($31,402,690.09). The fuel cost of the PSO algorithm is $31,402,519.71 which is 0.0005% less than the DE optimization. The replacement cost comparison among the three optimization algorithms is depicted in Figure 6-36. Unlike other costs, replacement cost is minimal ($3,710,762.34) for the DE algorithm. The replacement cost ($3,736,831.04) of ADE is 0.7025% higher than the DE. The PSO shows the highest replacement cost ($3,828,668.66) and it is 3.1552% higher than the DE optimization algorithm.

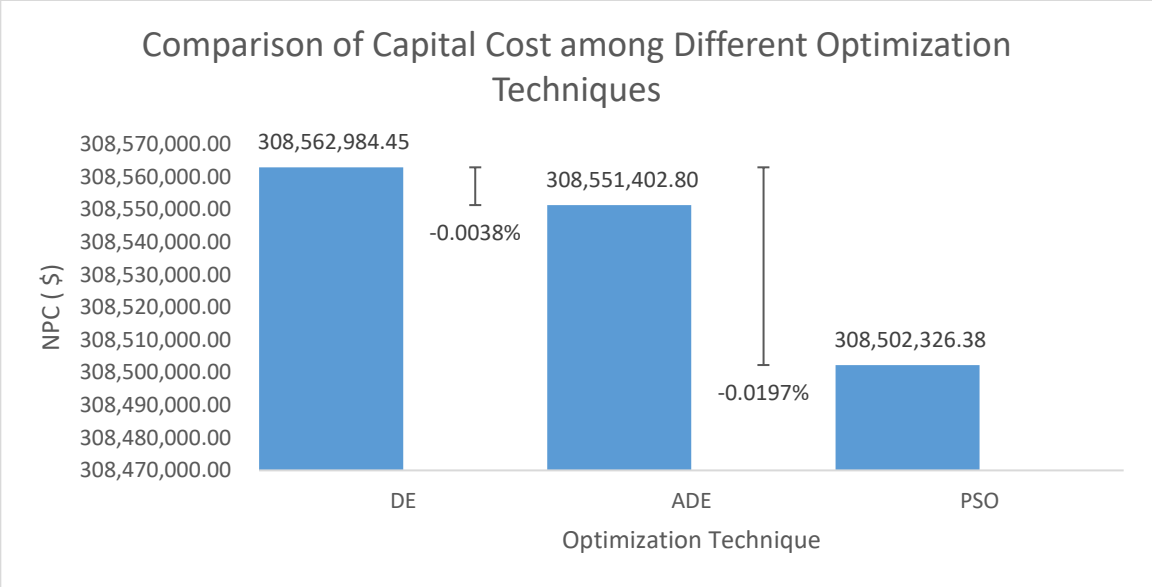

Figure 6-33: Comparison of Capital Cost among Different Optimization Techniques

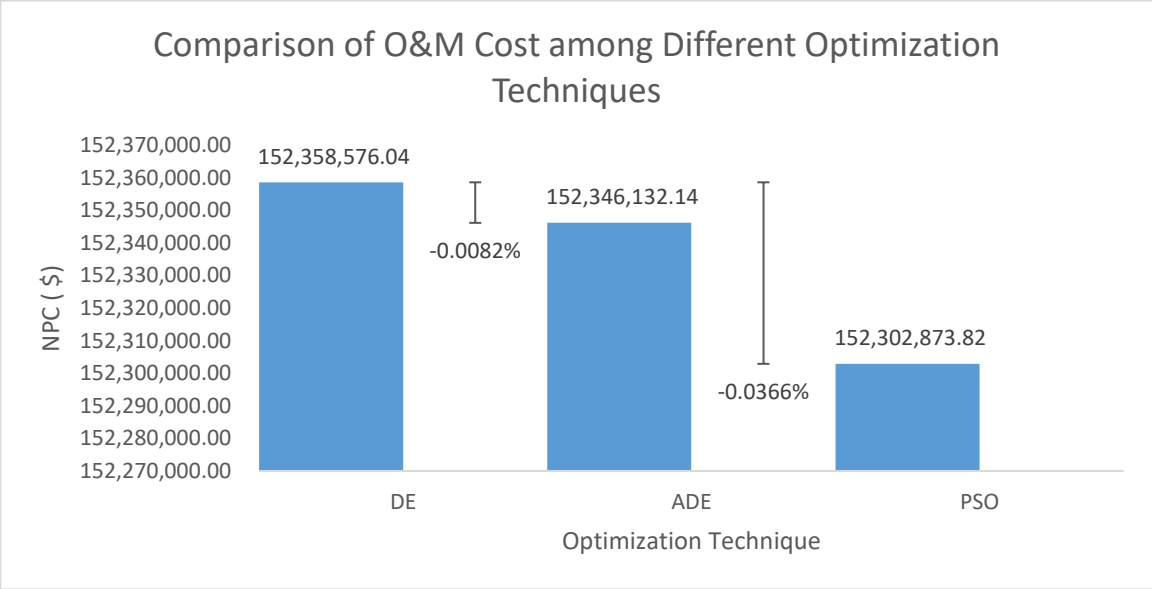

Figure 6-34: Comparison of O&M Cost among Different Optimization Techniques

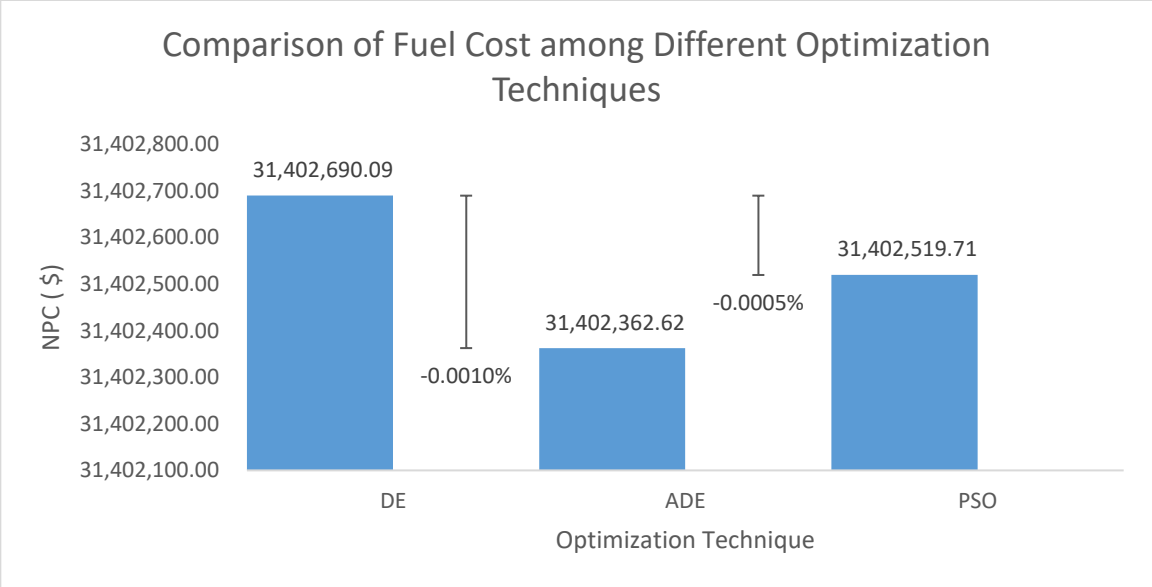

Figure 6-35: Comparison of Fuel Cost among Different Optimization Techniques

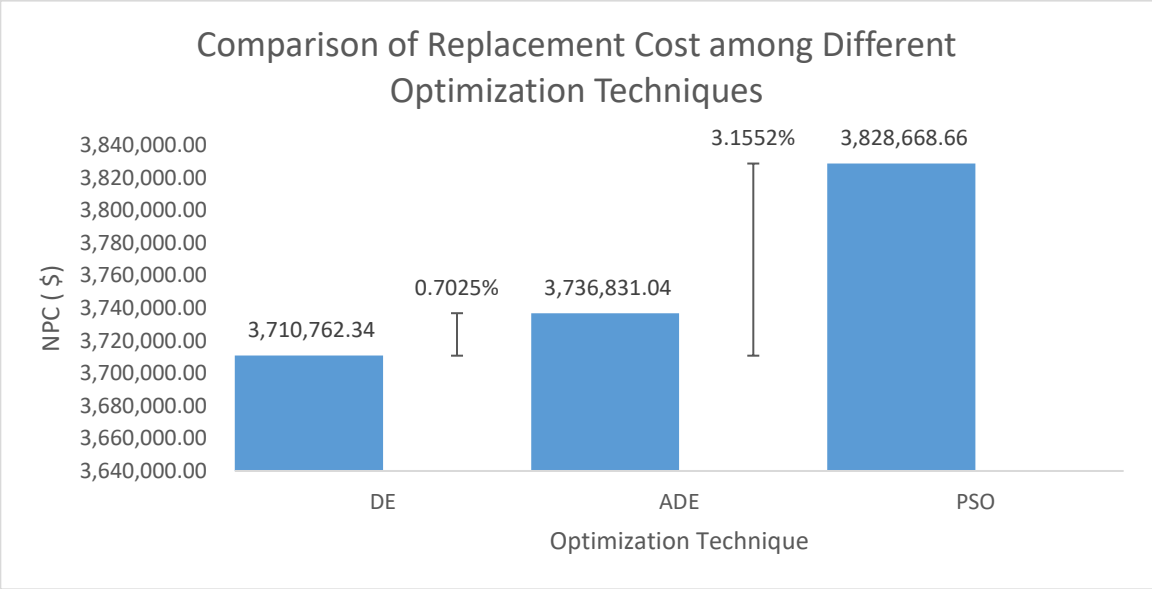

Figure 6-36: Comparison of Replacement Cost among Different Optimization Techniques

6.4. **Sensitivity Analysis**

The N-R HES for marine transportation employs several economic, technical, and environmental variables like water temperature, water density, solar irradiance, wind speed, air temperature, discount rate, inflation rate, project lifetime, fuel cost, replacement cost, capital cost, operation and maintenance cost, CO_2 penalty, W_{ratio}, and LPSP. Hence, a sensitivity analysis is crucial to assess the impact of these variables on the findings of the base model. The sensitivity analysis reinforces the result and validates the findings for a range of different parameters The sensitivity analysis is also important to determine how sensitive the system to different parameters. The following subsections will assess the impact of different economic, technical, and environmental variables on the NPC of the four energy systems. For each parameter change in the sensitivity analysis, the energy systems are optimized separately to get the optimized value of NPC.

6.4.1. Sensitivity Assessment of Discount Rate on NPC

In the base case, the discount rate is considered as 8%. In the sensitivity analysis, the discount rate is varied from 5% to 10% to determine the impact on NPC. Figure 6-37 shows the NPC of the four energy systems for different discount rates varied from 5% to 10%. From the figure, it can be seen that irrespective of the discount rate, Case-04 always demonstrates the lowest NPC for the marine vessels. Also, with the increment of the discount rate, the NPC of all the energy systems decreases. To determine the rate of change in NPC with the discount rate, each energy system is assessed individually. Figure 6-38 shows the rate of change in NPC in Case-01 with different discount rates. Case-01 shows the maximum change is about 14% between 5% and 6% discount rate while the lowest change (10.31%) is observed between 9% and 10% discount rate. The rate of change in NPC with discount rate decreases with the increase of discount rate. The rate of change in NPC with the discount rate is shown in Figure 6-39 for Case-02. The maximum and minimum rate of change for Case-02 is 14.04% and 10.19% respectively. Unlike Case-01, the minimum rate of change is observed between the 8% and 9% discount rates. Figure 6-40 illustrates the change of NPC of Case-03 with the discount rate. The rate of change is very low compared with the Case-01 and Case-02. The maximum rate of change is 7.56% and the minimum rate of change is 4.19%. Like Case-01, the rate of change in NPC reduces with the increase of discount rate. The change in NPC with the discount rate for Case-04 is represented in Figure 6-41. The figure shows that Case-04 is less sensitive to the discount rate among all the energy systems. The maximum and minimum rate of change in NPC with the discount rate is 7.54% and 4.23% respectively.

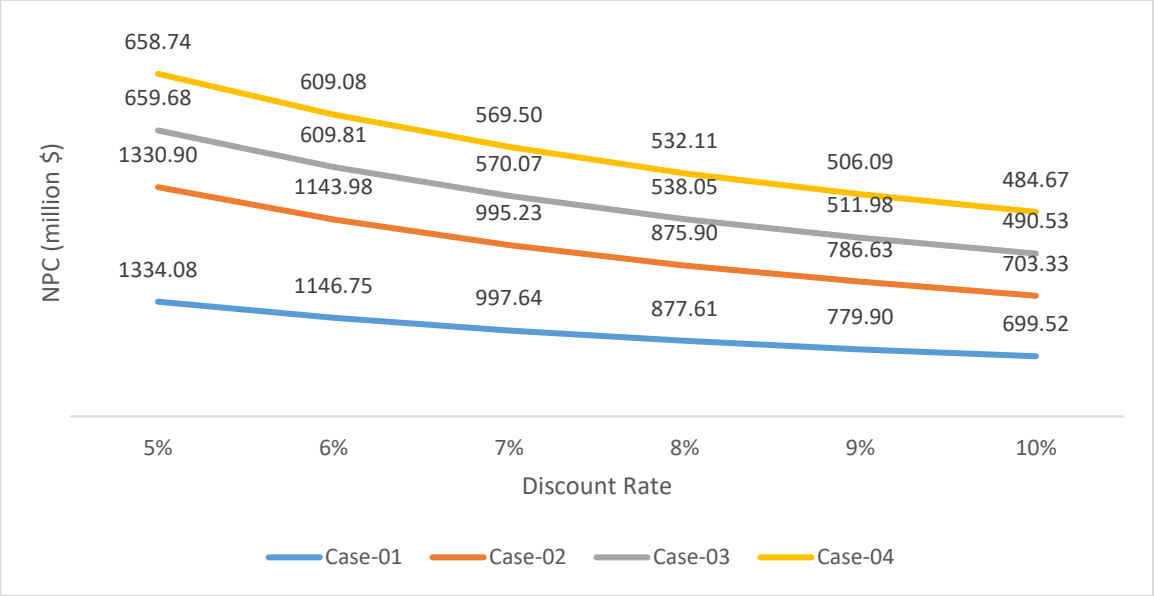

Figure 6-37: Sensitivity Assessment of Discount Rate on NPC

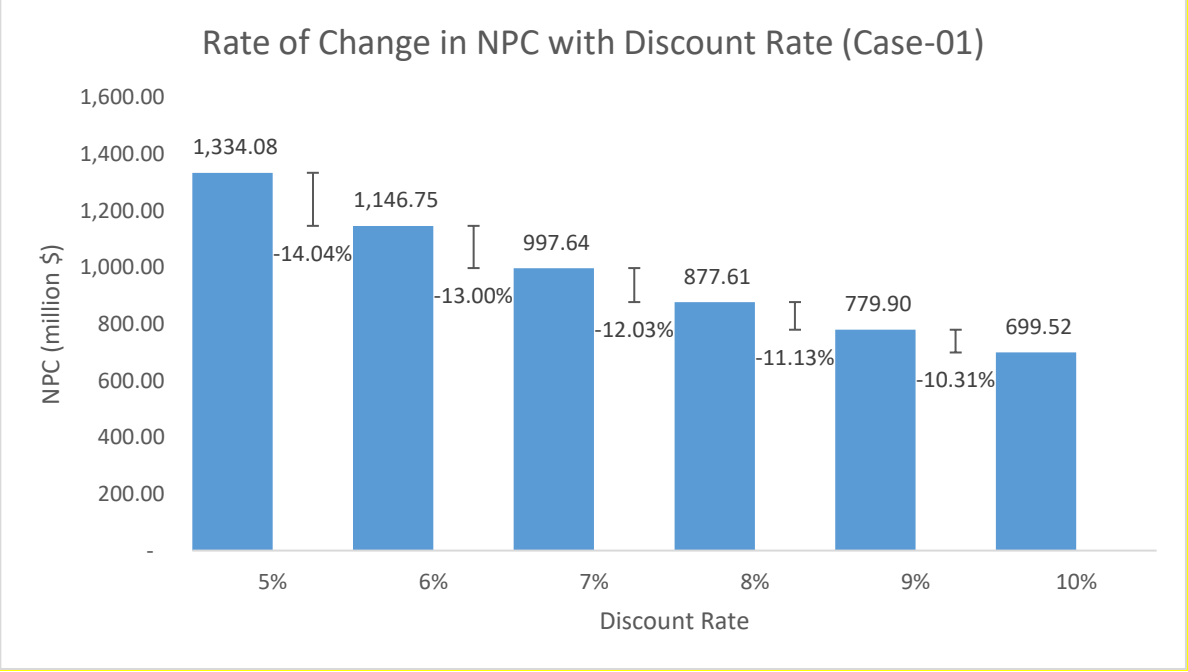

Figure 6-38: Rate of Change in NPC with Different Discount Rates (Case-01)

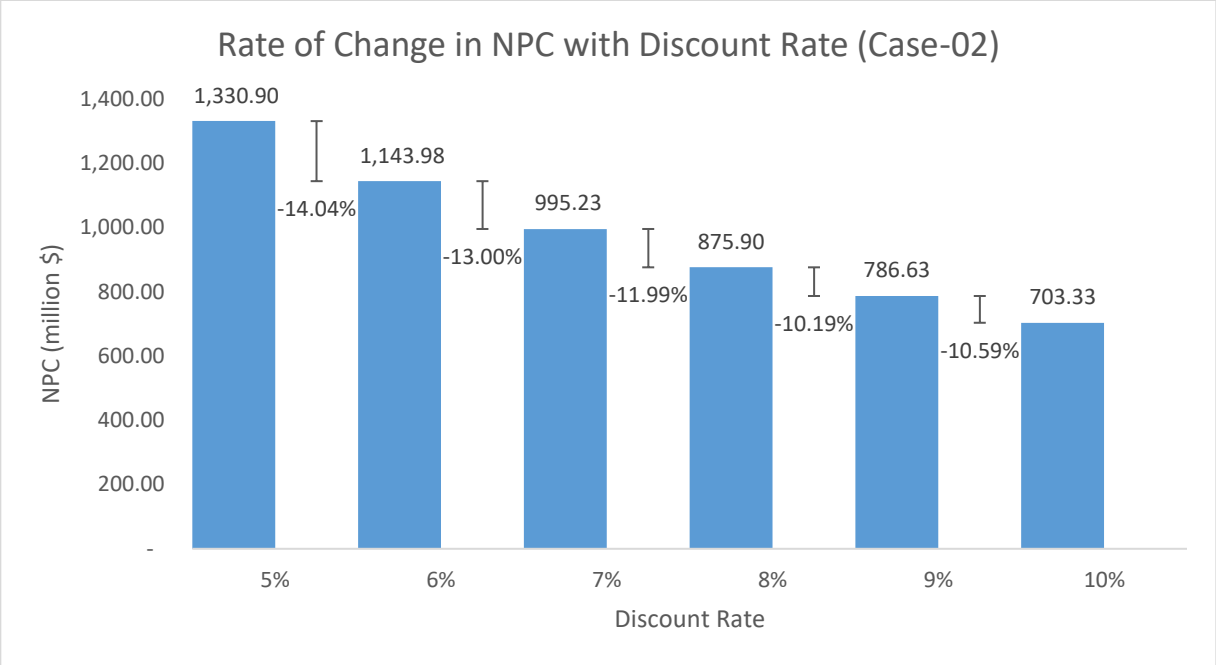

Figure 6-39: Rate of Change in NPC with Different Discount Rates (Case-02)

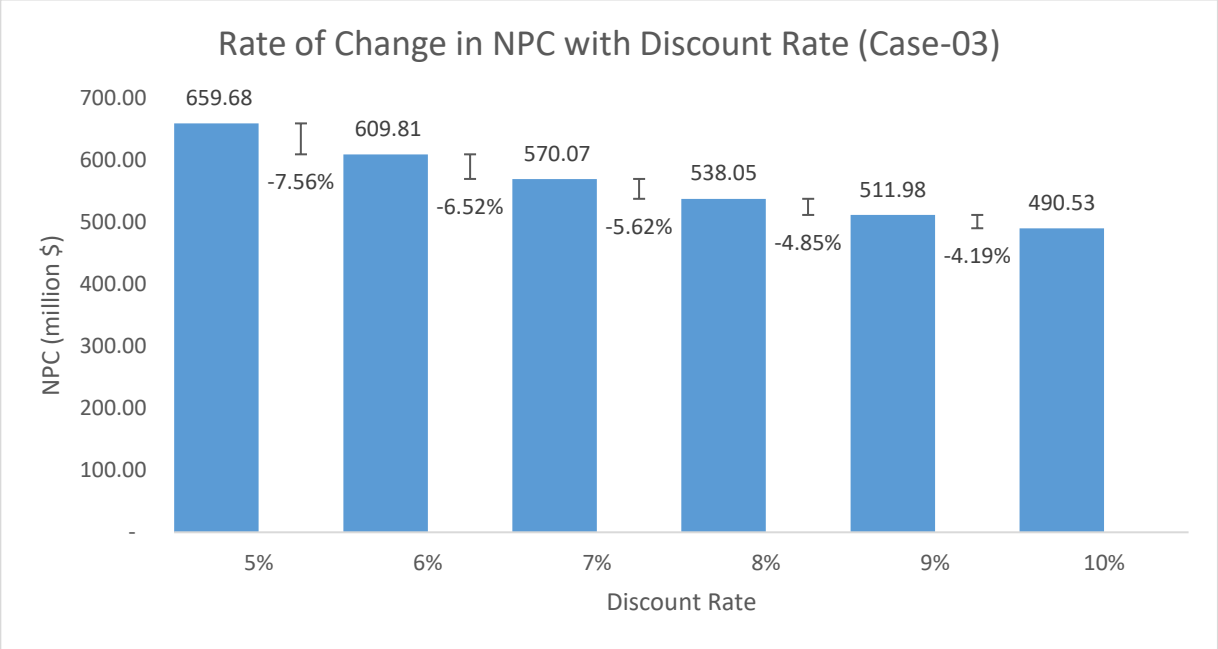

Figure 6-40: Rate of Change in NPC with Different Discount Rates (Case-03)

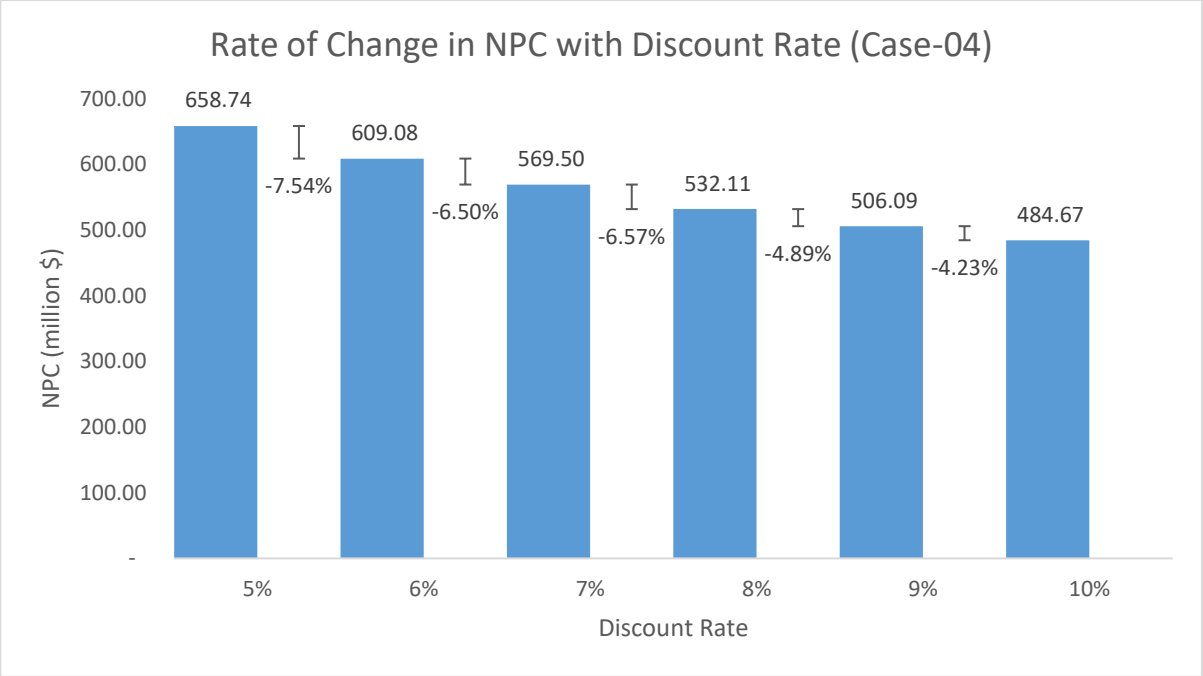

Figure 6-41: Rate of Change in NPC with Different Discount Rates (Case-04)

6.4.2. Sensitivity Assessment of Inflation Rate on NPC

The inflation rate was considered 2% in the base case of the analysis. In the sensitivity analysis, the inflation rate is varied from 1% to 5% to identify the impact of the inflation rate on NPC of different energy systems. Figure 6-42 shows the NPC of different energy systems for different inflation rates. The NPC increases with the increase of the inflation rate with a varying range. However, Case-04 shows the lowest NPC among all the energy systems irrespective of the inflation rate. To identify the rate of change in NPC for different energy systems, each case is assessed separately. The rate of change in NPC with different inflation rates for Case-01 is presented in Figure 6-43. The maximum rate of change is 16.61% between 4% and 5% inflation rate, and the minimum rate of change is 13.41% between 1% and 2% inflation rate. Figure 6-44 shows the rate of change in NPC with different inflation rates for Case-02. The rate of change in NPC for Case-02 is the same as Case-01 in 4% and 5% inflation rate. The maximum and minimum rate of change for Case-02 is 16.61% and 12.67% respectively. The NPC for Case-02 is a little bit higher than Case-01 for 1% inflation rate due to the high initial investment for renewable energy sources with low inflation rate. The rate of change is reduced for Case-03 that is shown Figure 6-45. The maximum rate (8.36%) of change occurs between 4% and 5% inflation rate where the minimum rate (5.43%) of change observes between 1% and 2% inflation rate. Figure 6-46 shows the change for Case-04. The lowest rate of change is observed for Case-04 with minimum and maximum rate of change is 5.48% and 8.26% sequentially. Unlike Case-03, the maximum rate of change happens between 3% and 4% of the inflation rate.

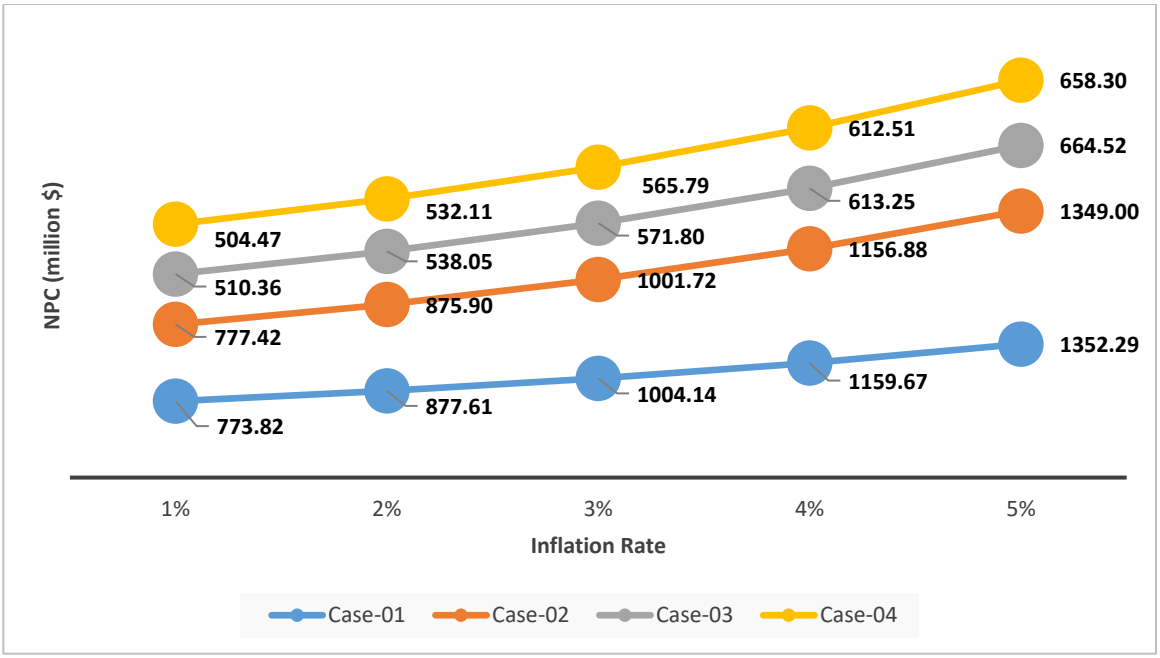

Figure 6-42: Sensitivity Assessment of Inflation Rate on NPC

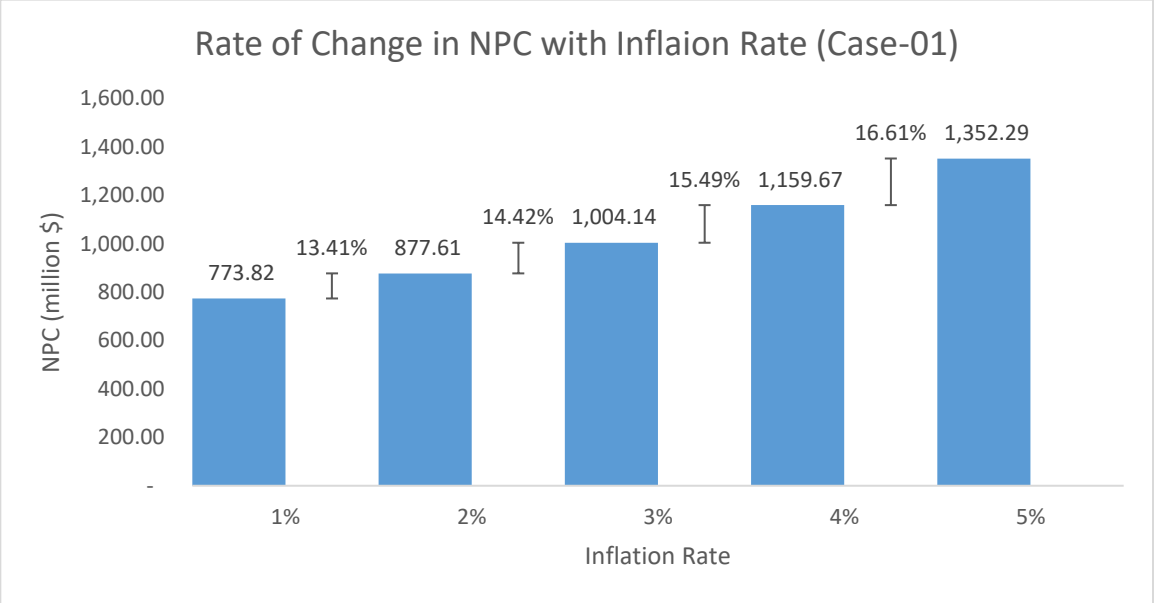

Figure 6-43: Rate of Change in NPC with Different Inflation Rates (Case-01)

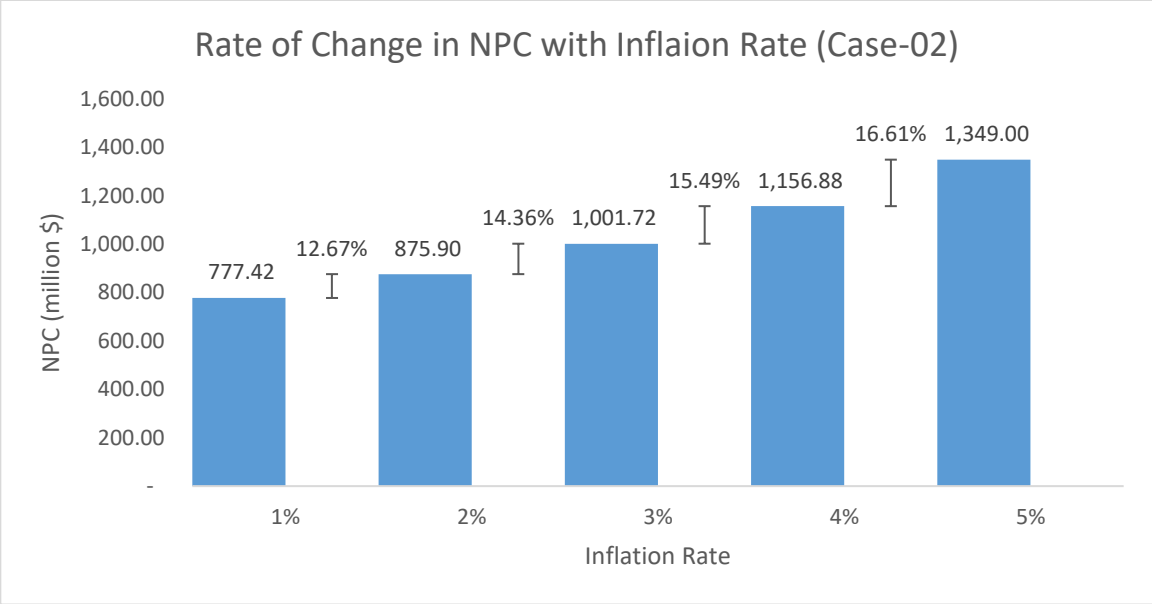

Figure 6-44: Rate of Change in NPC with Different Inflation Rates (Case-02)

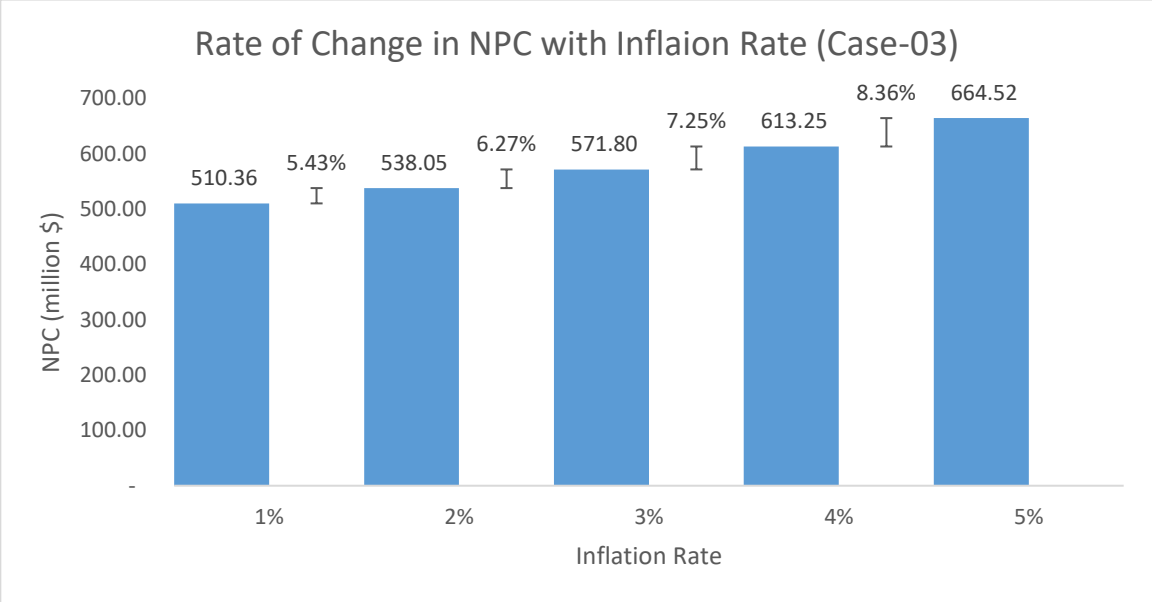

Figure 6-45: Rate of Change in NPC with Different Inflation Rates (Case-03)

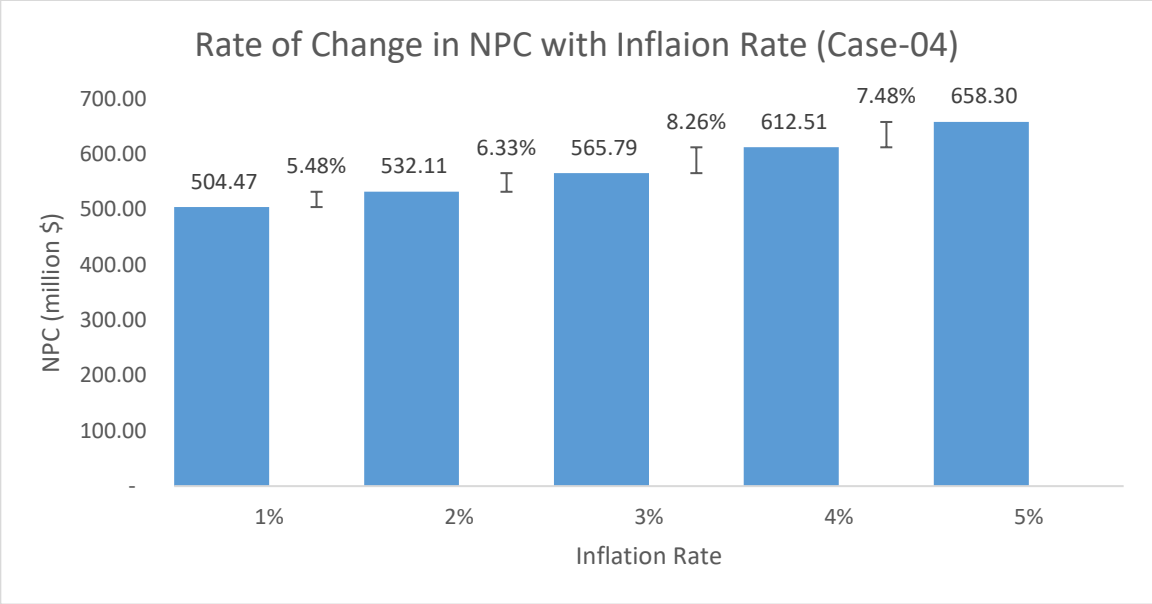

Figure 6-46: Rate of Change in NPC with Different Inflation Rates (Case-04)

6.4.3. Sensitivity Assessment of Project Life on NPC

The project life is considered as 40 years in the base case analysis. The project lifetime can be different based on the requirement of the ship operator, and lifetime of the ship. Hence, a sensitivity analysis is carried out for different project lifetimes. The project lifetime is varied from 20 years to 60 years with 10 years interval. The NPC of different energy systems for different project lifetimes is presented in Figure 6-47. The figure illustrates that with the increase of project lifetime NPC increases for all the cases. However, Case-04 shows the lowest NPC among all the energy systems irrespective of the project lifetime. The rate of change in NPC with different project lifetimes varies differently in each case. To determine the rate of change in NPC for different energy systems, each case has been evaluated separately. The rate of change in NPC for Case-01 is presented in Figure 6-48. The maximum (20.33%) rate of change is observed between 20 years and 30 years project lifetime while the minimum (2.65%) rate of change occurs between 50 years and 60 years project lifetime. Figure 6-49 depicts the rate of change in NPC for Case-02 for different project lifetimes. The rate of change in Case-02 is similar to Case-01, and the maximum and minimum rate of change is 20.89% and 2.17%, respectively. The rate of change for Case-03 is illustrated in Figure 6-50. The rate of change is less compared to Case-01 and Case-02. The maximum and minimum rate of change is 17.12% and 2.68% sequentially. Figure 6-51 represents the rate of change in NPC for Case-04. The rate of change in Case-04 is similar to Case-03. The maximum rate of change is 17.17% and the minimum rate of change is 2.68%. By assessing all the energy systems, it can be concluded that the rate of change in NPC with the variation of project lifetime decreases with the increase of project lifetime.

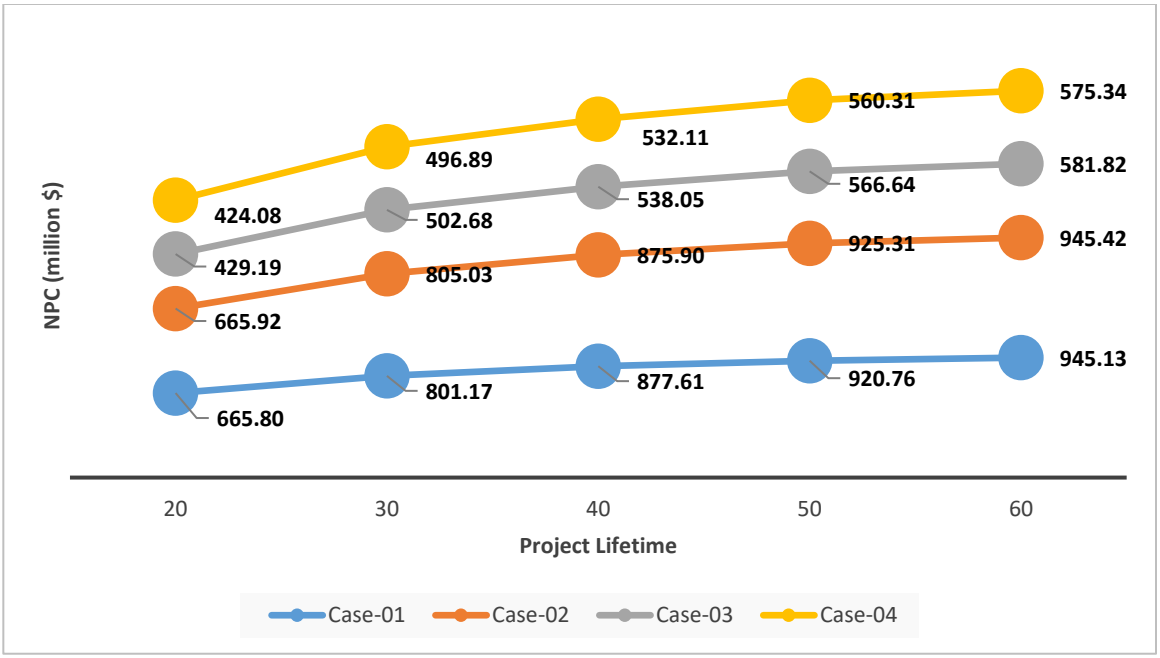

Figure 6-47: Sensitivity Assessment of Project Lifetime on NPC

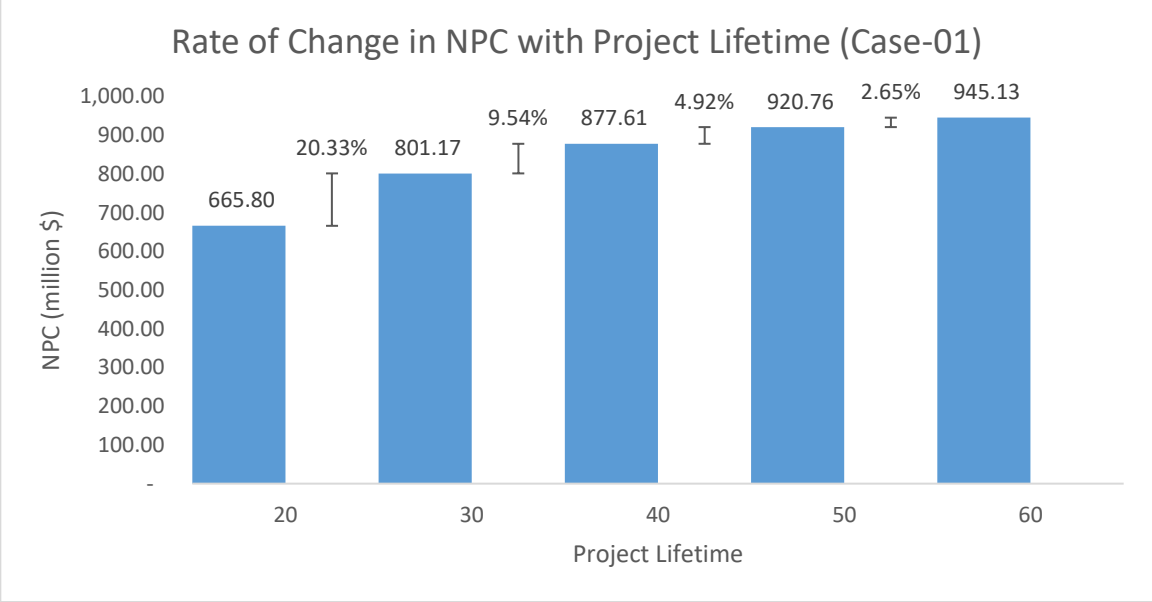

Figure 6-48: Rate of Change in NPC with Different Project Lifetimes (Case-01)

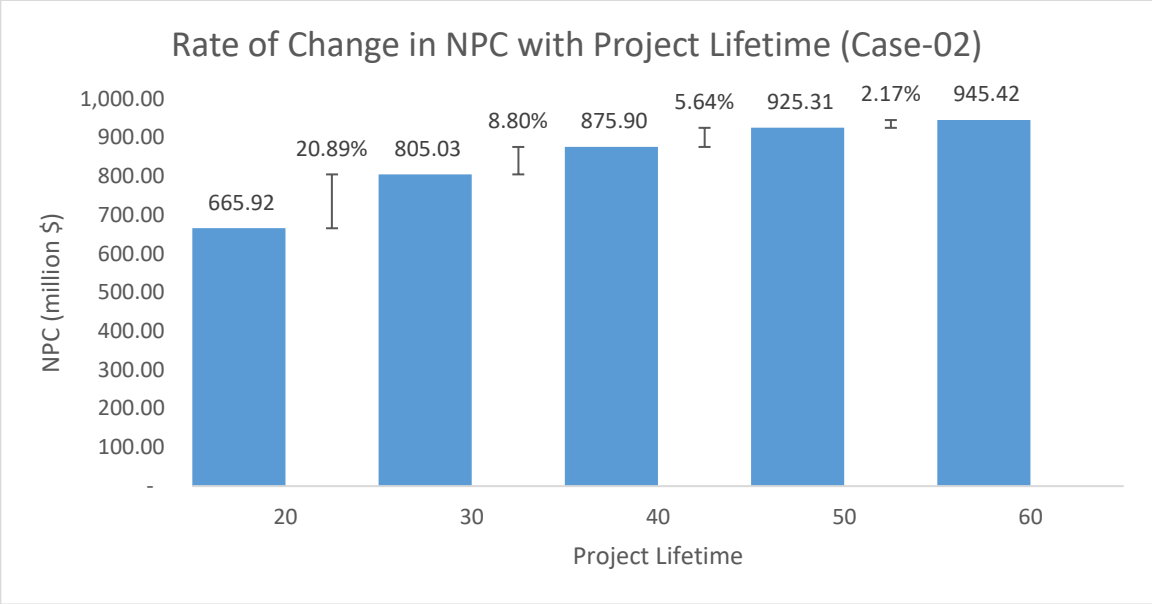

Figure 6-49: Rate of Change in NPC with Different Project Lifetimes (Case-02)

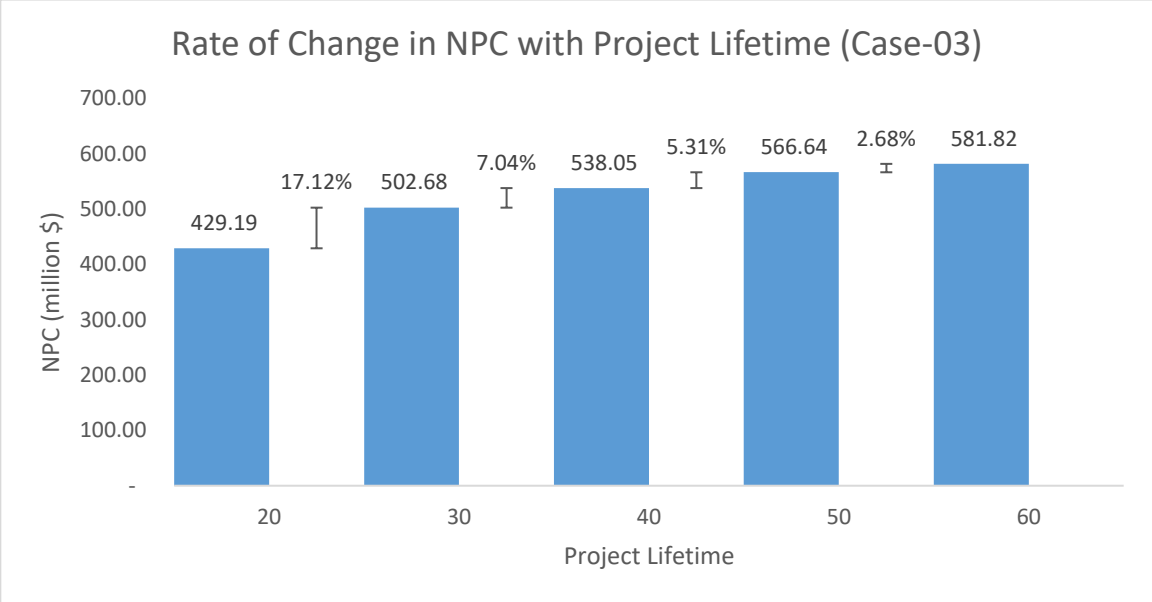

Figure 6-50: Rate of Change in NPC with Different Project Lifetimes (Case-03)

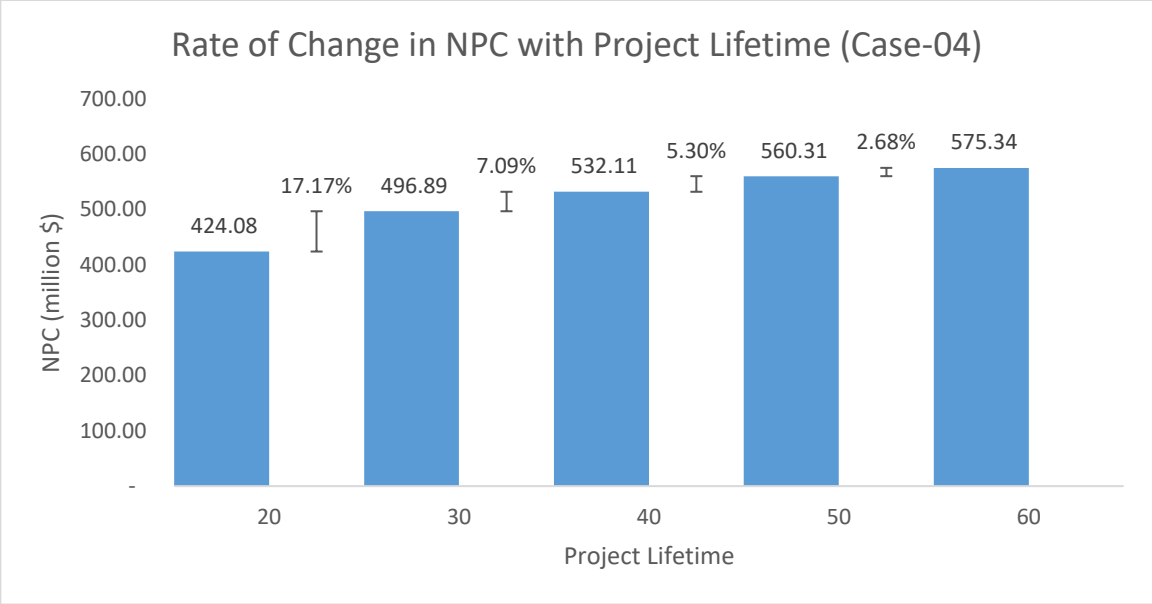

Figure 6-51: Rate of Change in NPC with Different Project Lifetimes (Case-04)

6.4.4. Sensitivity Assessment of Electrical Load on NPC

This study employs several parameters, like seawater temperature, seawater density, length and width of the ship, average speed of the ship, and draught of the ship to estimate the ship power. These parameters change with the position of the ship, weather, and type of the ship. Any change in these parameters will result in different electrical power requirements. Hence, it is important to assess the performance of the energy systems for different electrical power requirements. In this section, the electrical power of the ship is varied from -20% to +20% with a 10% increment. Figure 6-52 shows the NPC of different energy systems with different electrical power. The figure tells that with the increase of electrical power, the NPC increases accordingly. However, Case-04 illustrates the lowest NPC irrespective of the electrical power. This implies that N-R HES is the most feasible energy system among all other energy systems for different electrical power. As the larger ships need higher electrical power, the W_{ratio} has changed accordingly for increased power requirements. The rate of change for different energy systems is assessed separately. Figure 6-53 shows the rate of change in NPC for different electrical power requirements in Case-01. The maximum rate of change (26.94%) is observed between 0% and +10% while the lowest rate of change (9.34%0 is between +10% and +20%. The rate of change for Case-02 is presented in Figure 6-54. The rate of change of Case-02 is similar to Case-01 with a maximum and minimum rate of change is 25.20% and 9.24% respectively. Figure 6-55 shows the rate of change for Case-03. The maximum rate of change is 10.93% between -20% and -10%, and the minimum rate of change is 8.06% between +10% and +20%. The rate of change is low in Case-03 compared to Case-01 and Case-02. The rate of change of Case-04 is shown in Figure 6-56. The maximum rate of change in Case-04 is 11.92% which

is observed between -20% and -10%. The minimum rate of change is observed between -10% and 0% which is 9.09%.

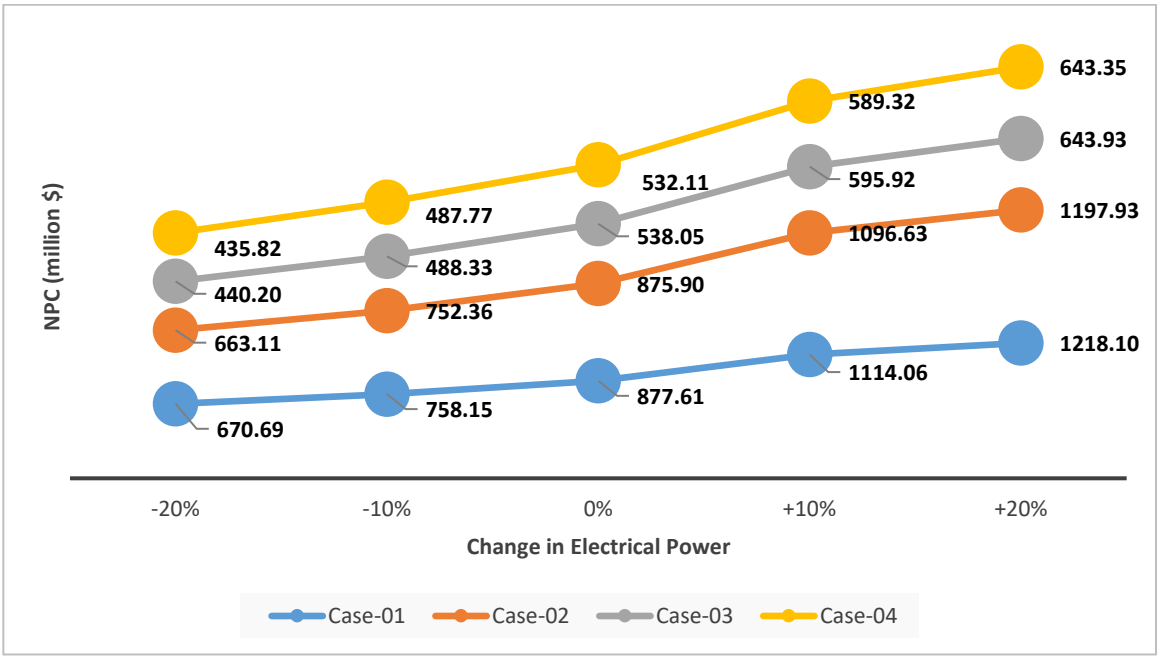

Figure 6-52: Sensitivity Assessment of Electrical Load on NPC

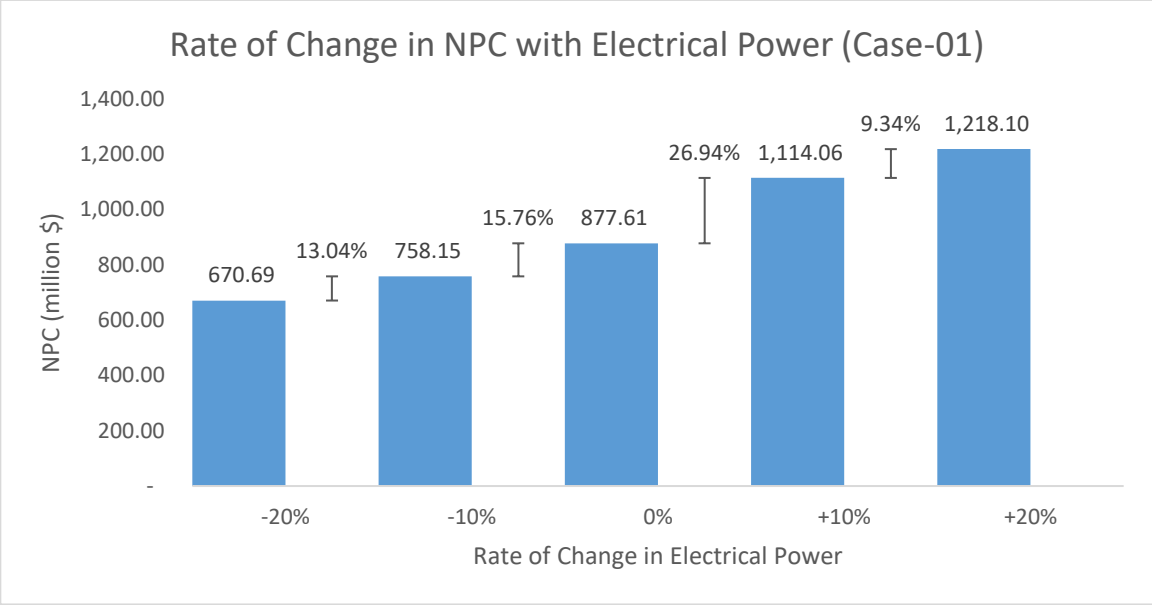

Figure 6-53: Rate of Change in NPC with Different Electrical Loads (Case-01)

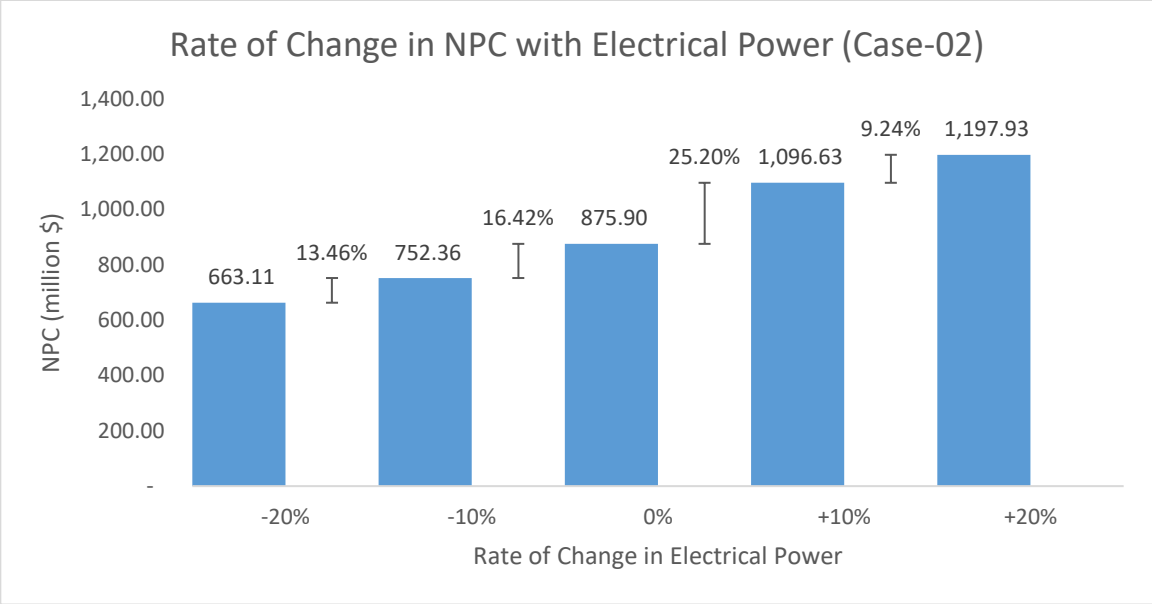

Figure 6-54: Rate of Change in NPC with Different Electrical Loads (Case-02)

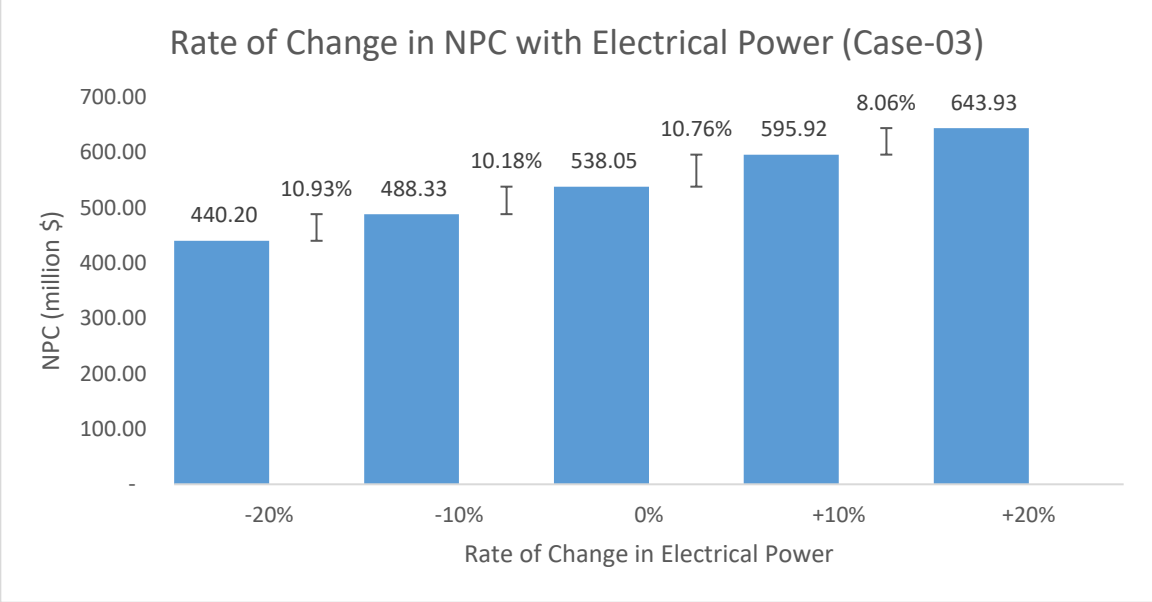

Figure 6-55: Rate of Change in NPC with Different Electrical Loads (Case-03)

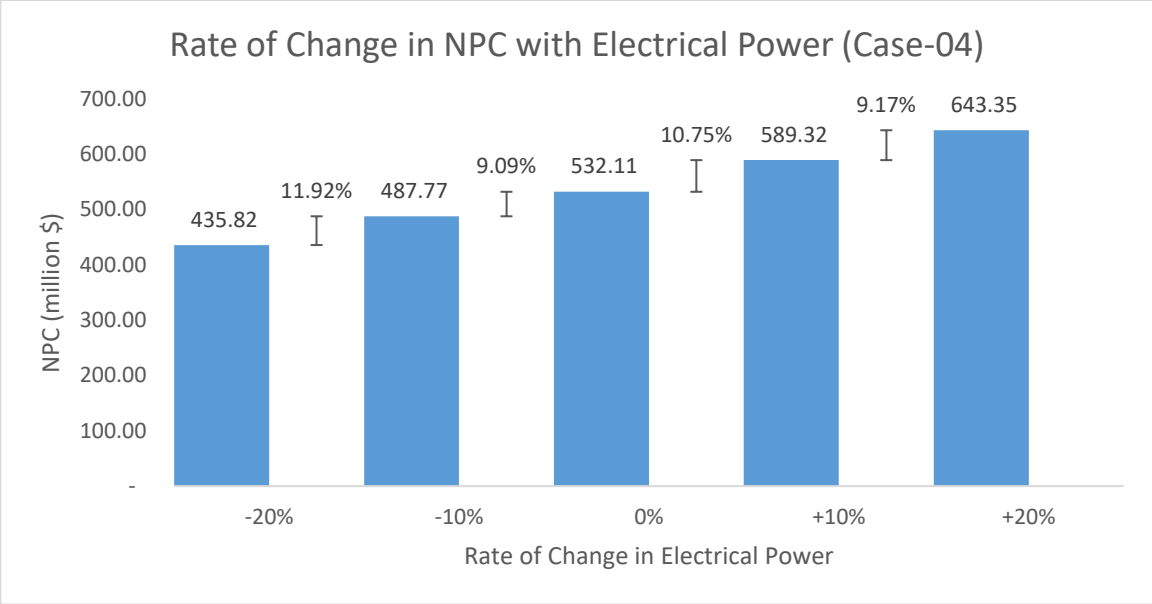

Figure 6-56: Rate of Change in NPC with Different Electrical Loads (Case-04)

6.4.5. Sensitivity Assessment of Solar Irradiance on NPC

In this study, the voyage route of the 'Baltic Sunrise' is considered from Iraq to Singapore. Renewable energy resources like solar energy depend on the position of the ship. The solar irradiance will not be the same all the time, and the ship will not use the same route each time. Hence, a sensitivity assessment of solar irradiance is necessary to determine the impact on NPC. Since Case-01 and Case-03 don't have any solar PV, any change in the solar irradiance will not affect the NPC of these 2 cases. Therefore, only Case-02 and Case-04 are considered for the assessment of solar irradiance on NPC. In this study, solar irradiance is varied from -20% to +20% with a 10% increment. Figure 6-57 shows the NPC of Case-02 and Case-04 for different solar irradiance. The NPC of Case-02 decreases slightly with the increase of solar irradiance while no impact on the NPC of Case-04 is observed with the change of solar irradiance as the penetration of solar PV is very minimal in Case-04. However, irrespective of the change in solar irradiance, Case-04 shows the lowest NPC among all the energy systems. The rate of change in NPC of Case-02 with the change in solar irradiance is depicted in Figure 6-58. The maximum and minimum rate of change is 0.11% and 0.02%, respectively. The maximum rate of change is observed between -20% and -10% change of solar irradiance while the minimum rate of change occurs between +10% and +20%

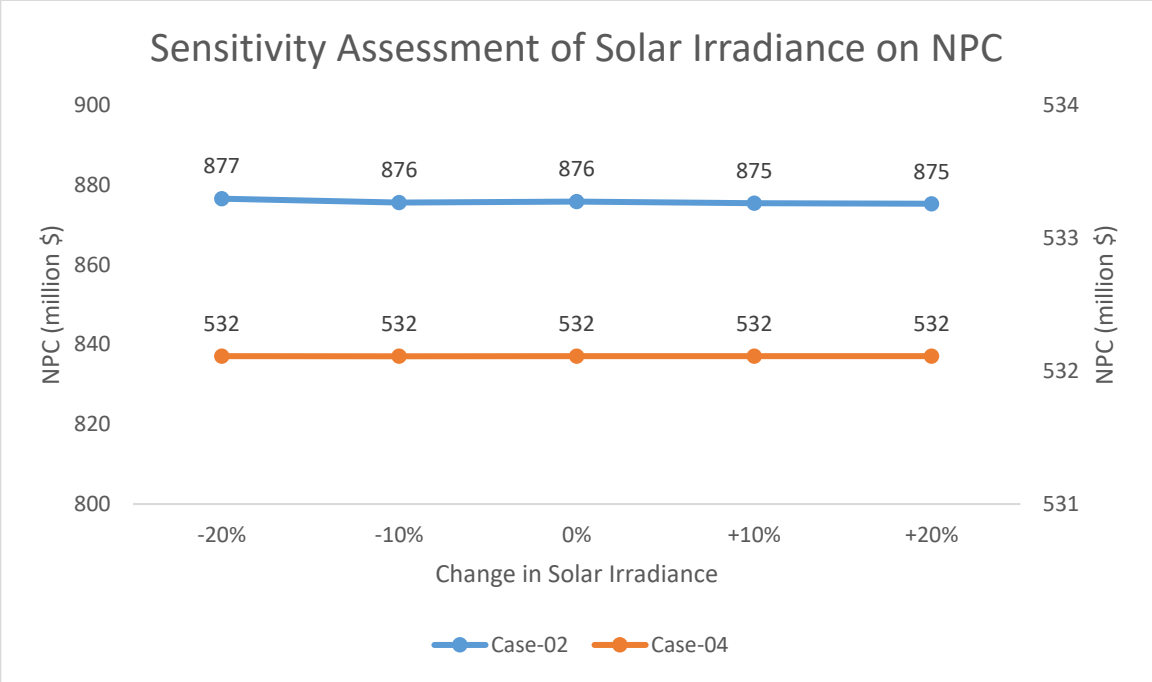

Figure 6-57: Sensitivity Assessment of Solar Irradiance on NPC

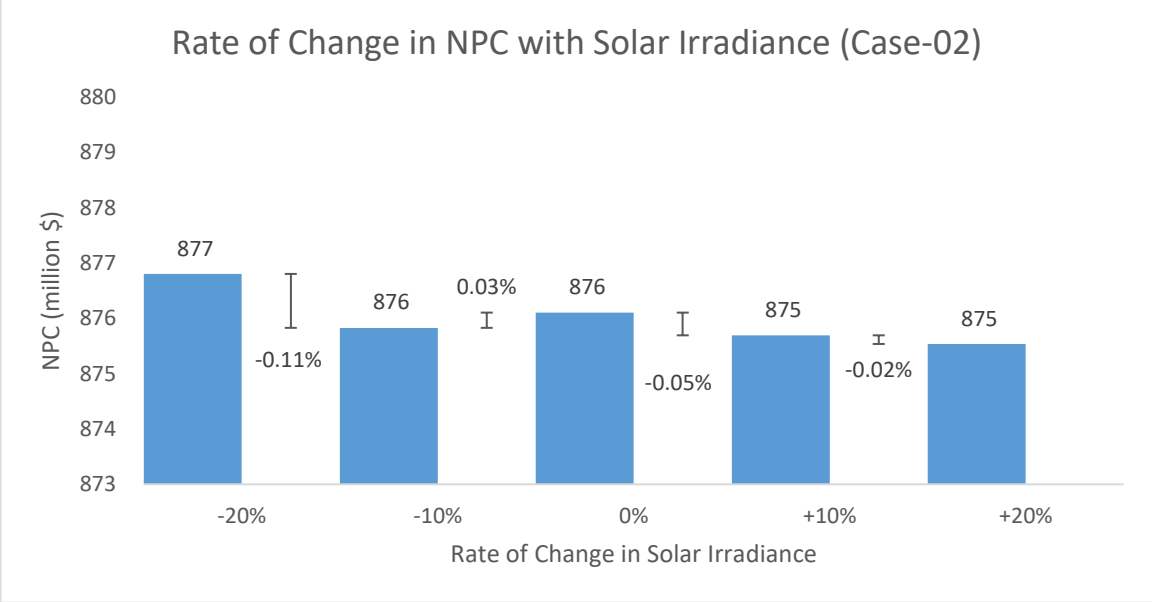

Figure 6-58: Rate of Change in NPC with Different Solar Irradiances (Case-02)

6.4.6. Sensitivity Assessment of Wind Speed on NPC

Similar to solar irradiance, wind speed also varies with the time and the route of the ship. Hence, a sensitivity assessment is carried out to identify the impact of wind speed on NPC on different energy systems. As there is no wind turbine for Casse-01 and Case-03, there is no impact with the change of wind speed on these cases. In this assessment, wind speed is varied from -20% to +20% with a 10% increment. Figure 6-59 shows the NPC of Case-02 and Case-04 for different wind speeds. The NPC of Case-04 decreases with the increase of wind speed while no impact on the NPC of Case-02 is observed with the change of wind speed. However, irrespective of the change in solar irradiance, Case-04 shows the lowest NPC among all the energy systems. The rate of change in NPC of Case-04 with the change in solar irradiance is depicted in Figure 6-60. The maximum and minimum rate of change is 0.66% and 0.22% respectively. The maximum rate of change is observed between -10% and 0% chance of wind speed while the minimum rate of change occurs between +10% and +20%

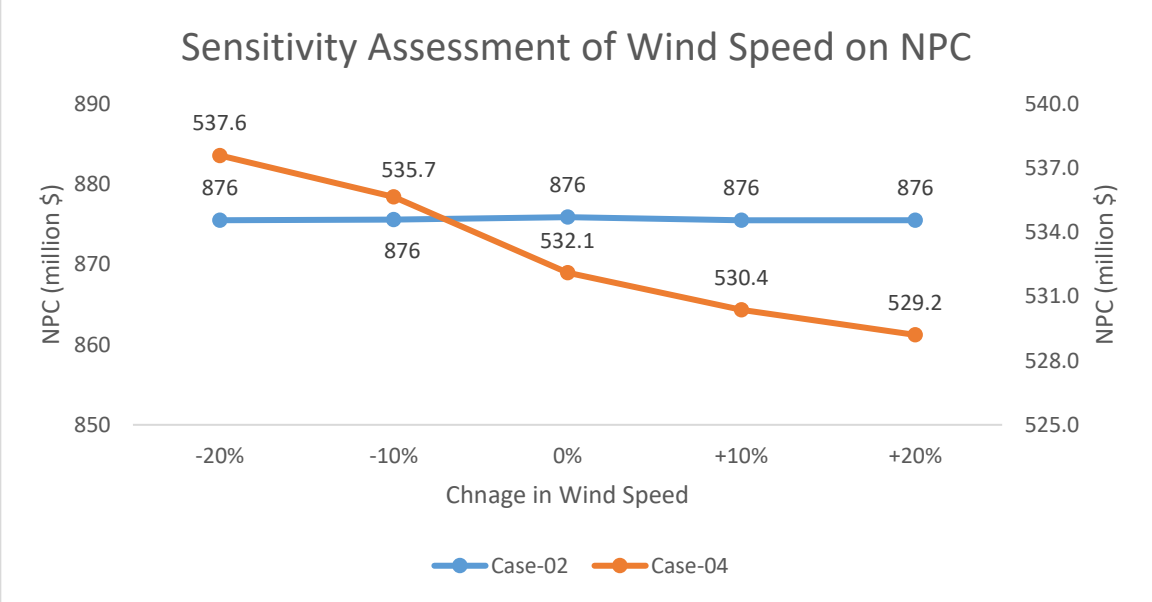

Figure 6-59: Sensitivity Assessment of Wind Speed on NPC

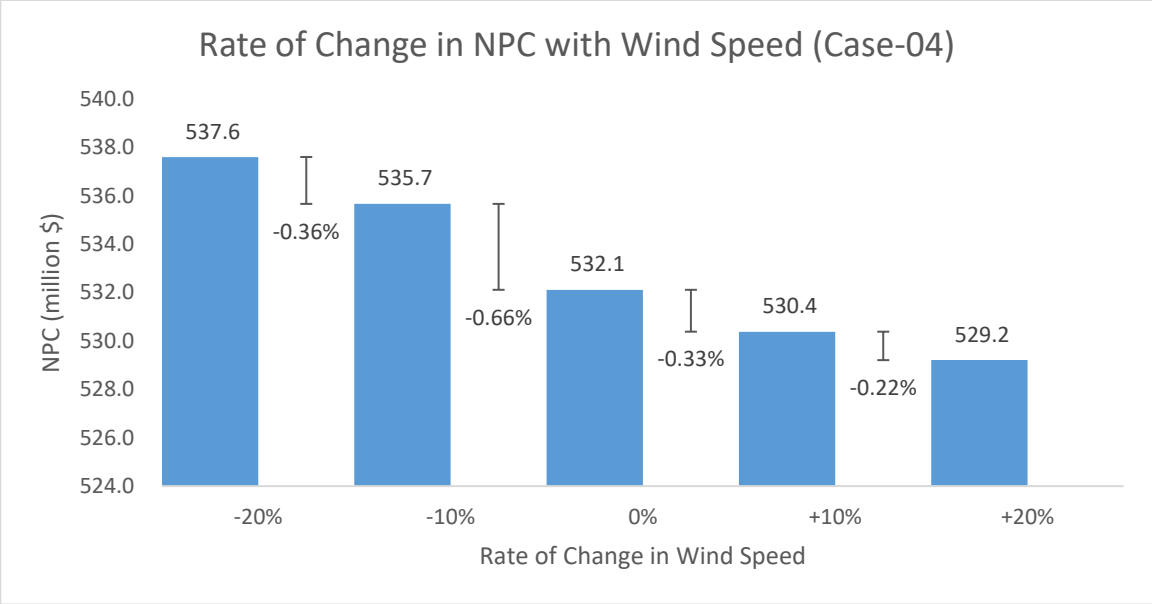

Figure 6-60: Rate of Change in NPC with Different Wind Speeds (Case-04)

6.5. Stress Test of N-R HES (Case-04)

The stress test is a popular method to check the system's performance in extreme conditions. Popular online sales company run stress test to check the system performance before any major event like 'Black Friday' or 'Chrismas Sale'. The results from HOMER software, MATLAB optimization, and sensitivity analyses indicate that N-R HES (Case-04) is the best energy system for marine ships compared to other energy systems. In this section a stress test is conducted on Case-04 to see in which condition it is no more a best case. To run a stress test, the fuel price is considered a variable and reduced 60% with 20% interval. It can be seen from Figure 6-16 that fuel price is the main contributor for Case-01 and Case-02. So, theoretically, these cases can perform better compared to Case-03 and Case-04 if the fuel price is reduced. Table 6-2 represents the change in NPC with the change of fuel price. Figure 6-61 shows the result of the stress test on Case-04. It can be seen that with the reduction of fuel price the NPC of Case-01 and Case-02 is reduced to a higher rate than Case-03 and Case-04. Till 40% reduction in fuel price, Case-04 has the lowest NPC compared to other energy systems. However, between 40% and 60% reduction of fuel price, Case-02 has the lowest NPC compared to other energy systems and Case-04 is no longer the best case. However, around 60% reduction in fuel price is impractical as industry experts are expecting a rise in fossil fuel in the future [152]

Table 6-2: Change in NPC with fuel price change

Case	Change in NPC (million $) with Fuel Price Change			
	0%	-20%	-40%	-60%
Case-01	877.61	750.05	622.38	493.84
Case-02	875.90	748.28	620.61	492.27
Case-03	538.05	531.55	525.06	518.56
Case-04	532.11	525.83	519.55	513.27

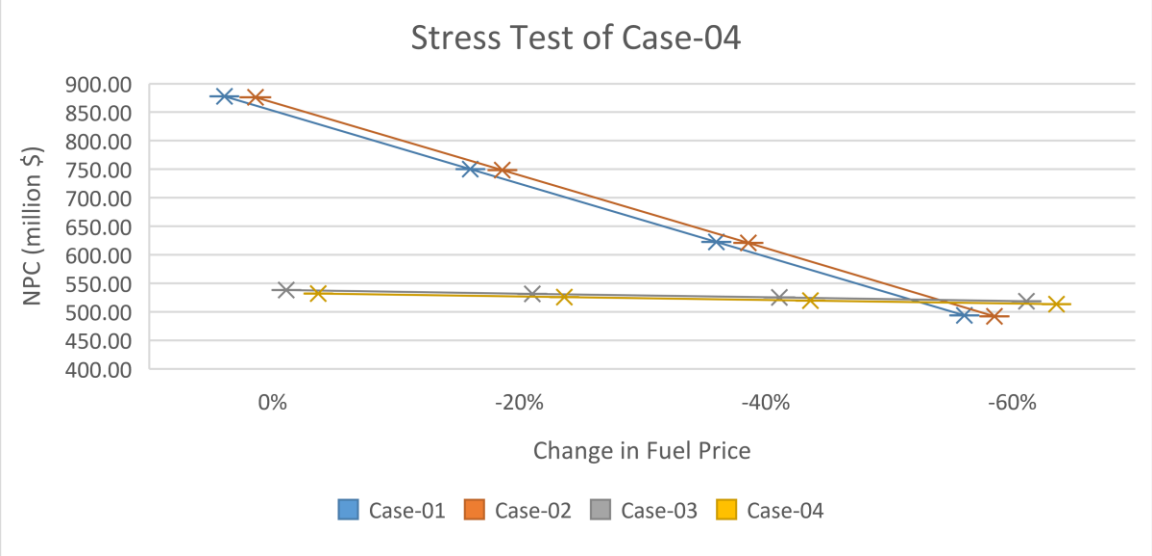

Figure 6-61: Stress Test on Case-04

Chapter 7: Conclusions and Recommendations

This chapter summarizes the findings of the research, the contribution of this thesis, and the future scope of work.

7.1. Summary and Conclusions

Several studies have been carried out on stand-alone nuclear energy systems and renewable and fossil fuel-based hybrid energy systems for ocean-going marine ships to reduce GHG emissions. However, both systems have some limitations in terms of economic, regulatory, and technical points of view. Therefore, a nuclear-renewable hybrid energy system on marine ships has been proposed in this paper to overcome these limitations. The energy demand of a ship is estimated by using actual data to simulate the real-world scenario. The base model is developed by using HOMER software which is extended to mathematical modeling and simulation in MATLAB environment by implementing Differential Evolution (DE) algorithm. The findings of this paper suggest that an integrated nuclear-renewable hybrid energy system could be the best solution to make ocean-going ships free from all kinds of emissions, and it is technically and economically feasible. Among the four energy systems, N-R HES shows the lowest NPC ($532.11 million) compared to Stand-alone Fossil Fuel-based Energy System ($877.61 million), Renewable Energy and Fossil Fuel-based Hybrid Energy System ($875.90 million), and Stand-alone Nuclear Energy System ($538.05 million). The proposed N-R HES emits the lowest CO_2 gas compared to other energy systems in whole project life. This study identifies the 'Capital Cost' and 'O&M Cost' as the major contributors of NPC for Case-03 and Case-04 whereas for Case-01 and Case-02, 'Fuel Cost' and 'Replacement Cost' have the major contribution towards NPC. This study also ensures the reliability of the proposed energy systems with adequate margins during the optimization of the systems. This study determines the MR as a competent candidate to replace the diesel generator from maritime transportation.

The optimized result of Case-04 obtained by the Differential Evolution (DE) algorithm is compared with PSO and ADE to assess the performance and validate the findings of the DE technique. Among all the optimization techniques, DE performs better than other algorithms. The NPC gained by DE algorithm ($532,112,182) is the lowest compared to ADE ($532,114,720), and PSO ($532,118,322). In the latter section, sensitivity analysis is carried out to reinforce the findings. The sensitivity assessment is conducted by varying the discount rate, inflation rate, project lifetime, electrical power requirement, solar

irradiance, and wind speed. The sensitivity analysis shows NPC increases with the increase of inflation rate, project lifetime, and electrical power demand for energy systems. The NPC decreases with the increase of discount rate. The sensitivity analysis concludes that irrespective of any change in the parameter, Case-04 always shows the lowest NPC among all the energy systems.

7.2. Contributions of the Thesis

The main objective of this study to provide a sustainable and innovative solution to the emissions-free energy crisis for maritime transportation. To achieve this goal, the feasibility of N-R HES is evaluated in this study. To address a real-world problem, practical data of an oil tanker is considered in this study. The energy requirement is estimated by using real data. Four energy systems are evaluated and compared to identify the best energy system for maritime vessels in terms of technical, economical, and environmental KPIs. Computer software (HOMER) is used to build a base model and get the primary idea. Later, mathematical modeling is developed in MATLAB software and optimized by a meta-heuristic optimization algorithm to address more constraints and parameters which are out of the scope of HOMER. The performance of the proposed optimization technique is measured by comparing it with other widely used optimization algorithms. Finally, the findings are verified by conducting a sensitivity analysis. The main contribution of this thesis is summarized below.

- ✓ A comprehensive literature review on the impact of maritime transportation on the environment, renewable and fossil fuel-based hybrid energy systems, nuclear propulsion, development of N-R HES in land-based applications, development of SMR and MR to identify the problem and gaps.
- ✓ Proposing a reasonable solution to the problem and mitigate the gap of previously proposed solutions.
- ✓ Estimate the energy requirement of an oil tanker with the collaboration of industry (FleetMon) to address a real-world problem in this study.
- ✓ Four energy systems are introduced to determine the most feasible energy system for maritime transportations. The feasibility is assessed based on technical, economical, and environmental KPIs. To ensure the reliability of the energy system, certain constraints are added.
- ✓ Initially, HOMER software is used to build the base model of the four energy systems to identify the feasible option for maritime vessels. Later, the limitation of HOMER software to optimize the energy systems and shortcomings to address some real-world problems are identified.
- ✓ To overcome the limitations and shortcomings of HOMER software, an economical model of all the system components is developed mathematically. This mathematical model is then optimized in the most

popular and versatile simulator MATLAB. The Differential Evolution (DE) algorithm is used to optimize the energy systems.

- ✓ The performance of the DE algorithm is compared to another widely used optimization technique, PSO. This comparison confirms the superior performance of the DE algorithm over PSO. Also, the impact of the control parameters of the DE algorithm is measured by the Adaptive Differential Algorithm (ADE).
- ✓ To address the variability of the parameters like discount rate, inflation rate, project lifetime, electrical power requirements, solar irradiance, and wind speed, a sensitivity analysis is conducted to reinforce the findings.

7.3. Future Work and Recommendations

This research evaluates the feasibility of N-R HES in maritime transportation in terms of technical, economical, and environmental KPIs. Several works need to be done in the future to check the feasibility more comprehensively. The future works and recommendations are as follows

- ➢ In this study, average solar irradiance, temperature, and wind speed are used while optimizing the systems. In the future, the actual solar irradiance, temperature, and wind speed can be used to make the study more realistic
- ➢ In this study, a specific ship route is considered. However, analysis can be extended to different major international shipping routes to assess the most feasible route for N-R HES.
- ➢ The safety of the N-R HES can be assessed in the future to check the feasibility in maritime transportation
- ➢ The licensing procedure and port approval of nuclear-powered merchant ships need to be addressed.
- ➢ In this study, no secondary commodities are considered to utilize the excess heat of the nuclear reactor. In the future, the excess energy can be utilized to produce secondary commodities like seawater desalination or utilize it by using in heating and cooling system.
- ➢ A sensitivity analysis can be carried out by varying the cost of different systems components and assess the impact on NPC.
- ➢ The findings of this study can be used as an initial point to make assessment N-R HES in shipping industry to reduce GHG emissions
- ➢ A multi-objective optimization can be conducted to add more flexibility to the users to trade-off among technical, economical, and environmental KPIs.
- ➢ Policy maker should focus on the uniform carbon penalty irrespective of the position of the ship in different countries to make the uniform distribution of the carbon penalty.

7.4. **Limitations**

There are some limitations of this study as listed below:

- The SMR or MR are not in practice till now. They are under the development phase. The data relating to MR have been collected from literature, email communication, and associated reports. Further tuning need to be required to align this study with more data once MR is in operation
- This study uses three months' data of 'Baltic Sunrise' to replicate the twelve month's data. Entire data set from the industry could make the assessment more realistic.
- Using weather data based on the position of the ship to the nearest port is another limitation of this study. Using accurate data based on the position of the ship will be more useful and will reflect the real-world scenario. However, measuring the weather data based on the position of the ship is quite challenging.
- This study assumes that the refueling of the nuclear reactor will be done when the ship will be in the port for loading and unloading the cargo or oil. In another word, the impact of refueling on energy management has not been considered in this study.
- This study only considers the electrical requirement of the ship. Other applications like CHP or the production of secondary commodities (e.g. seawater desalination, and hydrogen production) are out of the scope of this study.
- This study considers a single CO_2 penalty. However, in practice single amount of penalty for all the international ships is quite challenging and any significant change in the CO_2 may result in different values of NPC. However, the feasibility of N-R HES is expected to be unchanged as per sensitivity analyses.
- The study considers that the manufacturers can provide MR/vSMR, solar PV, and wind turbine as per the required rating from the customer (ship operators/ shipbuilders)

REFERENCES

[1] "Shipping Pollution," *OCEANA Protecting the World's Ocean*. https://europe.oceana.org/en/shipping-pollution-1 (accessed Oct. 17, 2020).

[2] NAYA OLMER, BRYAN COMER, BISWAJOY ROY, XIAOLI MAO, and DAN RUTHERFORD, "GREENHOUSE GAS EMISSIONS FROM GLOBAL SHIPPING, 2013–2015," Oct. 2017. Accessed: Jan. 05, 2021. [Online]. Available: https://theicct.org/sites/default/files/publications/Global-shipping-GHG-emissions-2013-2015_ICCT-Report_17102017_vF.pdf

[3] "Emissions Scenarios — IPCC." https://www.ipcc.ch/report/emissions-scenarios/ (accessed Apr. 01, 2021).

[4] J. Yuan, S. H. Ng, and W. S. Sou, "Uncertainty quantification of CO2 emission reduction for maritime shipping," *Energy Policy*, vol. 88, pp. 113–130, Jan. 2016, doi: 10.1016/j.enpol.2015.10.020.

[5] A. G. Koumentakos, "Developments in Electric and Green Marine Ships," *Appl. Syst. Innov.*, vol. 2, no. 4, Art. no. 4, Dec. 2019, doi: 10.3390/asi2040034.

[6] "Gravina, J., Blake, J.I.R., Shenoi, A., Turnock, S.R., Hirdaris, S.E., 2012. Concepts for a modular nuclear powered containership. In: 17th International Conference on Ships and Shipping Research (NAV 2012), Napoli, Italy.".

[7] Jeremy Helms, "World's 15 Biggest Ships Create More Pollution Than All The Cars In The World." Accessed: Oct. 17, 2020. [Online]. Available: https://www.industrytap.com/worlds-15-biggest-ships-create-more-pollution-than-all-the-cars-in-the-world/8182

[8] "IMO ACTION TO REDUCE GREENHOUSE GAS EMISSIONS FROM INTERNATIONAL SHIPPING," *A wide variety of design, operational and economic solutions*. https://wwwcdn.imo.org/localresources/en/MediaCentre/HotTopics/Documents/IMOACTIONTOREDUCEGHGEMISSIONSFROMINTERNATIONALSHIPPING.pdf (accessed Jan. 05, 2021).

[9] Lokukaluge P. Perera, Brage Mo, and Leifur A. Kristjánsson, "Identification of Optimal Trim Configurations to improve Energy Efficiency in Ships," *IFAC*, vol. 48, no. 16, pp. 267–272, 2015, doi: https://doi.org/10.1016/j.ifacol.2015.10.291.

[10] Joo Hock Ang, Cindy Goh, Alfredo Alan Flores Saldivar, and Yun Li, "Energy-Efficient Through-Life Smart Design, Manufacturing and Operation of Ships in an Industry 4.0 Environment," *MDPI*, doi: 10.3390/en10050610.

[11] "Global merchant fleet - number of ships by type 2019," *Statista*. https://www.statista.com/statistics/264024/number-of-merchant-ships-worldwide-by-type/ (accessed Feb. 24, 2021).

[12] T. R. Walker *et al.*, "Chapter 27 - Environmental Effects of Marine Transportation," in *World Seas: an Environmental Evaluation (Second Edition)*, C. Sheppard, Ed. Academic Press, 2019, pp. 505–530. doi: 10.1016/B978-0-12-805052-1.00030-9.

[13] G. Villalba and E. D. Gemechu, "Estimating GHG emissions of marine ports—the case of Barcelona," *Energy Policy*, vol. 39, no. 3, pp. 1363–1368, Mar. 2011, doi: 10.1016/j.enpol.2010.12.008.

[14] L. Styhre, H. Winnes, J. Black, J. Lee, and H. Le-Griffin, “Greenhouse gas emissions from ships in ports – Case studies in four continents,” *Transp. Res. Part Transp. Environ.*, vol. 54, pp. 212–224, Jul. 2017, doi: 10.1016/j.trd.2017.04.033.
[15] C.-C. Chang, “Marine energy consumption, national economic activity, and greenhouse gas emissions from international shipping,” *Energy Policy*, vol. 41, pp. 843–848, Feb. 2012, doi: 10.1016/j.enpol.2011.11.066.
[16] “FUTURE SHIP POWERING OPTIONS Exploring alternative methods of ship propulsion,” Jul. 2013. Accessed: Apr. 12, 2021. [Online]. Available: https://www.raeng.org.uk/publications/reports/future-ship-powering-options
[17] Luciano Ondir Freire and Delvonei Alves de Andrade, “Historic survey on nuclear merchant ships,” *Nucl. Eng. Des.*, vol. 293, pp. 176–186, 2015, doi: https://doi.org/10.1016/j.nucengdes.2015.07.031.
[18] “S.E. Hirdaris, Y.F. Cheng, P. Shallcross, J. Bonafoux, D. Carlson, B. Prince, and G.A. Sarris, ‘Considerations on the potential use of Nuclear Small Modular Reactor (SMR) technology for merchant marine propulsion’. Ocean Engineering 79 (2014) 101–130.”.
[19] “J S Carlton, R Smart, and V Jenkins (2011) The nuclear propulsion of merchant ships: Aspects of engineering, science, and technology, Journal of Marine Engineering & Technology, 10:2, 47-59.”.
[20] J. Vergara and C. B. McKesson, “NUCLEAR PROPULSION IN HIGH-PERFORMANCE CARGO VESSELS.,” *Mar. Technol. Soc. J.*, vol. 39, pp. 1–11, 2002.
[21] “JACOBS, J. G. C. C. 2007. Nuclear Short Sea Shipping. M.Sc., Delft University of Technology.”
[22] “Nuclear-Powered Ships,” *World Nuclear Association*. https://www.world-nuclear.org/information-library/non-power-nuclear-applications/transport/nuclear-powered-ships.aspx#:~:text=Nuclear%20power%20is%20particularly%20suitable,from%20icebreakers%20to%20aircraft%20carriers. (accessed Jan. 28, 2021).
[23] John Konrad, “Bill Gates Launches A Nuclear Ship Battery Partnership,” Nov. 2020. [Online]. Available: https://gcaptain.com/bill-gates-nuclear-ship-battery/
[24] C. Filippone and K.A. Jordan, “The Holos Reactor: A Distributable Power Generator with Transportable Subcritical Power Modules.”
[25] “Shuli Wen, Hai Lan, Jinfeng Dai, Ying-Yi Hong, David C. Yu & Lijun Yu (2017) Economic Analysis of Hybrid Wind/PV/Diesel/ESS System on a Large Oil Tanker, Electric Power Components and Systems, 45:7, 705-714, DOI: 10.1080/15325008.2017.1292569”.
[26] “Yuanchao Qiu, Chengqing Yuan, Jinrui Tang, Xujing Tang, ‘Techno-economic analysis of PV systems integrated into ship power grid: A case study’, https://doi.org/10.1016/j.enconman.2019.111925.”.
[27] “Fahd Diab, Hai Lan, and Salwa Ali. ‘Novel comparison study between the hybrid renewable energy systems on land and on ship’. Renewable and Sustainable Energy Reviews Volume 63, September 2016, Pages 452-463.”.
[28] Hai Lan, Shuli Wen, Ying-Yi Hong, David C. Yu, and Lijun Zhang, “Optimal sizing of hybrid PV/diesel/battery in ship power system,” *Appl. Energy*, vol. 158, pp. 26–34, 2015, doi: https://doi.org/10.1016/j.apenergy.2015.08.031.

[29] “Batteries on board ocean-going vessels.” https://www.man-es.com/docs/default-source/marine/tools/batteries-on-board-ocean-going-vessels.pdf?sfvrsn=deaa76b8_12
[30] Chaouki Ghenai, Maamar Bettayeb, Boris Brdjanin, and Abdul Kadir Hamid, “Hybrid solar PV/PEM fuel Cell/Diesel Generator power system for cruise ship: A case study in Stockholm, Sweden,” *Case Stud. Therm. Eng.*, doi: https://doi.org/10.1016/j.csite.2019.100497.
[31] M. F. Ruth, O. R. Zinaman, M. Antkowiak, R. D. Boardman, R. S. Cherry, and M. D. Bazilian, “Nuclear-renewable hybrid energy systems: Opportunities, interconnections, and needs,” *Energy Convers. Manag.*, vol. 78, pp. 684–694, Feb. 2014, doi: 10.1016/j.enconman.2013.11.030.
[32] L. Boldon, P. Sabharwall, S. Bragg-Sitton, N. Abreu, and L. Liu, “Nuclear Renewable Energy Integration: An Economic Case Study,” *Int. J. Energy Environ. Econ.*.
[33] S. Suman, “Hybrid nuclear-renewable energy systems: A review,” *J. Clean. Prod.*, vol. 181, pp. 166–177, Apr. 2018, doi: 10.1016/j.jclepro.2018.01.262.
[34] M. Ruth, D. Cutler, F. Flores-Espino, G. Stark, and T. Jenkin, “The Economic Potential of Three Nuclear-Renewable Hybrid Energy Systems Providing Thermal Energy to Industry,” NREL/TP-6A50-66745, 1335586, Dec. 2016. doi: 10.2172/1335586.
[35] T. E. Baker, A. S. Epiney, C. Rabiti, and E. Shittu, “Optimal sizing of flexible nuclear hybrid energy system components considering wind volatility,” *Appl. Energy*, vol. 212, pp. 498–508, Feb. 2018, doi: 10.1016/j.apenergy.2017.12.061.
[36] A. Borisova and D. Popov, “An option for the integration of solar photovoltaics into small nuclear power plant with thermal energy storage,” *Sustain. Energy Technol. Assess.*, vol. 18, pp. 119–126, Dec. 2016, doi: 10.1016/j.seta.2016.10.002.
[37] H. A. Gabbar, M. R. Abdussami, and Md. I. Adham, “Techno-Economic Evaluation of Interconnected Nuclear-Renewable Micro Hybrid Energy Systems with Combined Heat and Power,” *Energies*, vol. 13, no. 7, p. 1642, Apr. 2020, doi: 10.3390/en13071642.
[38] H. A. Gabbar, M. R. Abdussami, and M. I. Adham, “Micro Nuclear Reactors: Potential Replacements for Diesel Gensets within Micro Energy Grids,” *Energies*, vol. 13, no. 19, Art. no. 19, Jan. 2020, doi: 10.3390/en13195172.
[39] J. Chen, H. E. Garcia, J. S. Kim, and S. M. Bragg-Sitton, “Operations Optimization of Nuclear Hybrid Energy Systems,” *Nucl. Technol.*, vol. 195, no. 2, pp. 143–156, Aug. 2016, doi: 10.13182/NT15-130.
[40] H. A. Gabbar, M. R. Abdussami, and M. I. Adham, “Optimal Planning of Nuclear-Renewable Micro-Hybrid Energy System by Particle Swarm Optimization,” *IEEE Access*, vol. 8, pp. 181049–181073, 2020, doi: 10.1109/ACCESS.2020.3027524.
[41] Morales Pedraza, J., *Small Modular Reactors for Electricity Generation*, 2017th ed. Cham, Switzerland: Springer.
[42] “World Nuclear Association. Small Nuclear Power Reactors.” https://www.world-nuclear. org/information-library/nuclear-fuel-cycle/nuclear-power-reactors/small-nuclear-power-reactors.aspx
[43] “MICROREACTORS FREQUENTLY ASKED QUESTIONS | MICROREACTORS.” https://inl.gov/trending-topic/microreactors/frequently-asked-questions-microreactors/ (accessed Dec. 25, 2020).

[44] “Advances in Small Modular Reactor Technology Developments A Supplement to: IAEA Advanced Reactors Information System (ARIS) 2018 Edition.” https://aris.iaea.org/Publications/SMR-Book_2018.pdf
[45] Francesco Venneri, “Micro Modular Reactor (MMR) Energy Systems,” Ultra Safe Nuclear (USNC), Warsaw, Poland. Accessed: Dec. 26, 2020. [Online]. Available: https://www.ifnec.org/ifnec/upload/docs/application/pdf/2019-09/3-4._usnc_mmr.pdf
[46] “Project Description - Micro Modular Reactor Project at Chalk River,” Jul. 15, 2019. https://iaac-aeic.gc.ca/050/evaluations/document/132175 (accessed Apr. 03, 2021).
[47] M. Moore, “THE ECONOMICS OF VERY SMALL MODULAR REACTORS IN THE NORTH,” Canadian Nuclear Laboratories, Delta Ottawa City Centre Hotel CW-120200-CONF-012 Ottawa, Ontario, Canada, Nov. 2016. Accessed: Dec. 25, 2020. [Online]. Available: https://www.cnl.ca/site/media/Parent/Moore_ITMSR4.pdf
[48] Kara Michelle Godsey, “Life Cycle Assessment of Small Modular Reactors Using U.S. Nuclear Fuel Cycle,” Clemson University. Accessed: Dec. 26, 2020. [Online]. Available: https://core.ac.uk/download/pdf/287319878.pdf
[49] N. A. C., R. Jyoti, and A. B. Raju, “Economic analysis and comparison of proposed HRES for stand-alone applications at various places in Karnataka state,” in *ISGT2011-India*, Kollam, Kerala, India, Dec. 2011, pp. 380–385. doi: 10.1109/ISET-India.2011.6145346.
[50] H. Ren, Q. Wu, W. Gao, and W. Zhou, “Optimal operation of a grid-connected hybrid PV/fuel cell/battery energy system for residential applications,” *Energy*, vol. 113, pp. 702–712, Oct. 2016, doi: 10.1016/j.energy.2016.07.091.
[51] D. Emad, M. A. El-Hameed, M. T. Yousef, and A. A. El-Fergany, “Computational Methods for Optimal Planning of Hybrid Renewable Microgrids: A Comprehensive Review and Challenges,” *Arch. Comput. Methods Eng.*, vol. 27, no. 4, pp. 1297–1319, Sep. 2020, doi: 10.1007/s11831-019-09353-9.
[52] B. Zhao, X. Zhang, J. Chen, C. Wang, and L. Guo, “Operation Optimization of Standalone Microgrids Considering Lifetime Characteristics of Battery Energy Storage System,” *IEEE Trans. Sustain. Energy*, vol. 4, no. 4, pp. 934–943, Oct. 2013, doi: 10.1109/TSTE.2013.2248400.
[53] V. Sánchez, J. M. Ramirez, and G. Arriaga, “Optimal sizing of a hybrid renewable system,” in *2010 IEEE International Conference on Industrial Technology*, Mar. 2010, pp. 949–954. doi: 10.1109/ICIT.2010.5472544.
[54] M. Iwan, R. Akmeliawati, T. Faisal, and H. M. A. A. Al-Assadi, “Performance Comparison of Differential Evolution and Particle Swarm Optimization in Constrained Optimization,” *Procedia Eng.*, vol. 41, pp. 1323–1328, Jan. 2012, doi: 10.1016/j.proeng.2012.07.317.
[55] J. L. Bernal-Agustín and R. Dufo-López, “Simulation and optimization of stand-alone hybrid renewable energy systems,” *Renew. Sustain. Energy Rev.*, vol. 13, no. 8, pp. 2111–2118, Oct. 2009, doi: 10.1016/j.rser.2009.01.010.
[56] “HOMER Optimizer™, a Faster Path to Finding Least-Cost Microgrid Options.” https://microgridnews.com/homer-optimizer-a-faster-path-to-finding-least-cost-microgrid-options/ (accessed Oct. 16, 2020).

[57] E. S. Hrayshat, “Techno-economic analysis of autonomous hybrid photovoltaic-diesel-battery system,” *Energy Sustain. Dev.*, vol. 13, no. 3, pp. 143–150, Sep. 2009, doi: 10.1016/j.esd.2009.07.003.
[58] S. M. Shaahid, L. M. Al-Hadhrami, and M. K. Rahman, “Review of economic assessment of hybrid photovoltaic-diesel-battery power systems for residential loads for different provinces of Saudi Arabia,” *Renew. Sustain. Energy Rev.*, vol. 31, pp. 174–181, Mar. 2014, doi: 10.1016/j.rser.2013.11.055.
[59] “Modeling and Simulation of Smart Grid Integrated with Hybrid Renewable Energy Systems.” https://www.researchgate.net/publication/318456560_Modeling_and_Simulation_of_Smart_Grid_Integrated_with_Hybrid_Renewable_Energy_Systems (accessed Feb. 03, 2021).
[60] D. Kaur and P. S. Cheema, “Software Tools for Analyzing the Hybrid Renewable Energy Sources:-A Review,” p. 4.
[61] H. Borhanazad, S. Mekhilef, V. Gounder Ganapathy, M. Modiri-Delshad, and A. Mirtaheri, “Optimization of micro-grid system using MOPSO,” *Renew. Energy*, vol. 71, pp. 295–306, Nov. 2014, doi: 10.1016/j.renene.2014.05.006.
[62] A. Askarzadeh and L. dos Santos Coelho, “A novel framework for optimization of a grid independent hybrid renewable energy system: A case study of Iran,” *Sol. Energy*, vol. 112, pp. 383–396, Feb. 2015, doi: 10.1016/j.solener.2014.12.013.
[63] M. B. Shadmand and R. S. Balog, “Multi-Objective Optimization and Design of Photovoltaic-Wind Hybrid System for Community Smart DC Microgrid,” *IEEE Trans. Smart Grid*, vol. 5, no. 5, pp. 2635–2643, Sep. 2014, doi: 10.1109/TSG.2014.2315043.
[64] J.-H. Cho, M.-G. Chun, and W.-P. Hong, “Structure Optimization of Stand-Alone Renewable Power Systems Based on Multi Object Function,” *Energies*, vol. 9, no. 8, p. 649, Aug. 2016, doi: 10.3390/en9080649.
[65] T. Khatib, A. Mohamed, and K. Sopian, “Optimization of a PV/wind micro-grid for rural housing electrification using a hybrid iterative/genetic algorithm: Case study of Kuala Terengganu, Malaysia,” *Energy Build.*, vol. 47, pp. 321–331, Apr. 2012, doi: 10.1016/j.enbuild.2011.12.006.
[66] A. Haghighat Mamaghani, S. A. Avella Escandon, B. Najafi, A. Shirazi, and F. Rinaldi, “Techno-economic feasibility of photovoltaic, wind, diesel and hybrid electrification systems for off-grid rural electrification in Colombia,” *Renew. Energy*, vol. 97, pp. 293–305, Nov. 2016, doi: 10.1016/j.renene.2016.05.086.
[67] A. Ajlan, C. W. Tan, and A. M. Abdilahi, “Assessment of environmental and economic perspectives for renewable-based hybrid power system in Yemen,” *Renew. Sustain. Energy Rev.*, vol. 75, pp. 559–570, Aug. 2017, doi: 10.1016/j.rser.2016.11.024.
[68] R. Islam, “Feasibility Study of Small Nuclear Power Plant within Modern Microgrids,” p. 146.
[69] R. Luna-Rubio, M. Trejo-Perea, D. Vargas-Vázquez, and G. J. Ríos-Moreno, “Optimal sizing of renewable hybrids energy systems: A review of methodologies,” *Sol. Energy*, vol. 86, no. 4, pp. 1077–1088, Apr. 2012, doi: 10.1016/j.solener.2011.10.016.

[70] R. K. Rajkumar, V. K. Ramachandaramurthy, B. L. Yong, and D. B. Chia, "Techno-economical optimization of hybrid pv/wind/battery system using Neuro-Fuzzy," *Energy*, vol. 36, no. 8, pp. 5148–5153, Aug. 2011, doi: 10.1016/j.energy.2011.06.017.
[71] H. A. Gabbar, M. R. Abdussami, and Md. I. Adham, "Techno-Economic Evaluation of Interconnected Nuclear-Renewable Micro Hybrid Energy Systems with Combined Heat and Power," *Energies*, vol. 13, no. 7, p. 1642, Apr. 2020, doi: 10.3390/en13071642.
[72] Mai Farid, Michael Keen, Michael Papaioannou, Ian Parry, Catherine Pattillo, Anna Ter-Martirosyan, and other IMF Staff, "After Paris: Fiscal, Macroeconomic, and Financial Implications of Climate Change." [Online]. Available: https://www.imf.org/en/Publications/Staff-Discussion-Notes/Issues/2016/12/31/After-Paris-Fiscal-Macroeconomic-and-Financial-Implications-of-Global-Climate-Change-43484
[73] Ian Parry, "Countries Are Signing Up for Sizeable Carbon Prices." https://blogs.imf.org/2016/04/21/countries-are-signing-up-for-sizeable-carbon-prices/#more-12399 (accessed Jan. 06, 2021).
[74] "IMF calls for carbon tax on ships and planes." Accessed: Oct. 17, 2020. [Online]. Available: https://www.theguardian.com/environment/2016/jan/13/imf-calls-for-carbon-tax-on-ships-and-planes
[75] "14 Terminologies Used for Power of the Ship's Marine Propulsion Engine," *Marine Insights*. https://www.marineinsight.com/main-engine/12-terminologies-used-for-power-of-the-ships-marine-propulsion-engine/ (accessed Jan. 07, 2021).
[76] "Power-to-weight ratio," *FANDOM*. https://automobile.fandom.com/wiki/Power-to-weight_ratio (accessed Jan. 07, 2021).
[77] Jay Maisler, "Small Modular Reactors." Accessed: Jan. 07, 2021. [Online]. Available: http://hpschapters.org/florida/6spring.pdf
[78] "RTA84T." https://pdf.nauticexpo.com/pdf/waertsilae-corporation/rta84t/24872-12529.html#https://img.nauticexpo.com/pdf/repository_ne/24872/rta84t-12529_1b.jpg (accessed Oct. 16, 2020).
[79] "Canadian Solar CS6U-335P Silver Poly Solar Panel." https://www.wholesalesolar.com/1930010/canadian-solar/solar-panels/canadian-solar-cs6u-335p-silver-poly-solar-panel (accessed Oct. 16, 2020).
[80] "Norwin > 47-ASR-500 kW," *The WIND POWER*. https://www.thewindpower.net/turbine_en_832_norwin_47-asr-500-kw.php (accessed Jan. 25, 2021).
[81] "What is Net Present Value (NPV)?," *Net Present Value (NPV)*. https://corporatefinanceinstitute.com/resources/knowledge/valuation/net-present-value-npv/ (accessed Jan. 03, 2021).
[82] "Converting Nominal Interest Rates to Real Interest Rates | TVMCalcs.com." http://www.tvmcalcs.com/index.php/calculators/apps/converting_nominal_interest_rates_to_real_interest_rates (accessed May 11, 2021).
[83] "About FleetMon." https://www.fleetmon.com/company/our-story/ (accessed Oct. 17, 2020).
[84] H. E. Garcia *et al.*, "Nuclear Hybrid Energy Systems Regional Studies: West Texas & Northeastern Arizona," Idaho National Lab. (INL), Idaho Falls, ID (United States), INL/EXT-15-34503, Apr. 2015. doi: 10.2172/1236837.

[85] M. S. Ismail, M. Moghavvemi, T. M. I. Mahlia, K. M. Muttaqi, and S. Moghavvemi, "Effective utilization of excess energy in standalone hybrid renewable energy systems for improving comfort ability and reducing cost of energy: A review and analysis," *Renew. Sustain. Energy Rev.*, vol. 42, pp. 726–734, Feb. 2015, doi: 10.1016/j.rser.2014.10.051.
[86] "MarineTraffic: Global Ship Tracking Intelligence | AIS Marine Traffic." https://www.marinetraffic.com/en/ais/home/centerx:-12.0/centery:25.0/zoom:4 (accessed Feb. 27, 2021).
[87] "Live AIS Vessel Tracker with Ship and Port Database," *FleetMon.com*. https://www.fleetmon.com/ (accessed Feb. 27, 2021).
[88] "Ship Finder | Live Marine Traffic | AIS Ship Tracker and Tracking," *Shipfinder*. https://shipfinder.co (accessed Feb. 27, 2021).
[89] "Free AIS Ship Tracking of Marine Traffic - VesselFinder." https://www.vesselfinder.com/ (accessed Feb. 27, 2021).
[90] "Terrestrial & Satellite AIS Tracking Service in Realtime - vesseltracker.com." https://www.vesseltracker.com/ (accessed Feb. 27, 2021).
[91] "Vessel Tracking, Real Time and Historical AIS data by VT Explorer," *VT Explorer*. http://www.vtexplorer.com/ (accessed Feb. 27, 2021).
[92] "My Ship Tracking Free Realtime AIS Vessel Tracking Vessels Finder Map - ship tracker," *myShipTracking*. //www.myshiptracking.com (accessed Feb. 27, 2021).
[93] "Cruise Ship Tracker, Itineraries, Schedules, Deck Plans," *CruiseMapper*. https://www.cruisemapper.com/ (accessed Feb. 27, 2021).
[94] "Auke Visser's International Super Tankers." http://www.aukevisser.nl/supertankers/VLCC%20T-V/id1147.htm (accessed Oct. 17, 2020).
[95] "Voyage Analyser DEMO." https://voyage.vesselfinder.com/3a9abdd131b21a2a4f7d6acf52f0d2d2 (accessed Oct. 17, 2020).
[96] "Chuku, Azubuike John; Ukeh, Michael Edwin; and Mkpa, Ante; 'ESTIMATION OF BARE HULL RESISTANCE OF A ROPAX VESSEL USING THE ITTC-57 METHOD AND GERTLER SERIES DATA CHART', wjert, 2017, Vol. 3, Issue 6, 406-422".
[97] "ENGR 4011 Resistance & Propulsion of Ships." Accessed: Mar. 06, 2021. [Online]. Available: https://www.engr.mun.ca/~bveitch/courses/r-p/Assignments/ITTC-calculation-procedures-Lab1.pdf
[98] "Anthony F. Molland; Stephen R. Turnock; Dominic A. Hudson; 'Ship Resistance and Propulsion, PRACTICAL ESTIMATION OF SHIP PROPULSIVE POWER', Chapter 10, Page: 207.".
[99] Grzegorz NICEWICZ and Dariusz Tarnapowicz, "Assessment of marine auxiliary engines load factor in ports", Accessed: Dec. 22, 2020. [Online]. Available: https://www.researchgate.net/publication/298026922_Assessment_of_marine_auxiliary_engines_load_factor_in_ports
[100] Z. Huang and Y. Chen, "An Improved Differential Evolution Algorithm Based on Adaptive Parameter," *Journal of Control Science and Engineering*, Sep. 19, 2013. https://www.hindawi.com/journals/jcse/2013/462706/ (accessed Mar. 01, 2021).

[101] "Computer Aided Applied Single Objective Optimization - Course." https://onlinecourses.nptel.ac.in/noc20_ch19/preview (accessed Mar. 02, 2021).
[102] C. G. S. T.-A.-C. Ltd, "World Water Temperature | Sea Temperatures." http://www.seatemperature.org/ (accessed Mar. 02, 2021).
[103] Lewis, C, MacSweeney, R, Kirschel, M, Josten, W, Roulstone, T, and Locatelli, G, "Small modular reactors Can building nuclear power become more costeffective," National Nuclear Laboratory: Cumbria, UK, 2016.
[104] Alan McDonald and Leo Schrattenholzer, "Learning rates for energy technologies," *Energy Policy*, vol. 29, pp. 255–261, 2001.
[105] Hossam A. Gabbar, Muhammad R. Abdussami, and Md. Ibrahim Adham, "Micro Nuclear Reactors: Potential Replacements for Diesel Gensets within Micro Energy Grids", doi: https://doi.org/10.3390/en13195172.
[106] "Cost Competitiveness of Micro-Reactors for Remote Markets." https://www.nei.org/resources/reports-briefs/cost-competitiveness-micro-reactors-remote-markets
[107] "Small Modular Reactors (SMRs) for Mining: Frequently Asked Questions." https://www.nrcan.gc.ca/our-natural-resources/energy-sources-distribution/nuclear-energy-uranium/canadas-small-modular-reactor-ro/small-modular-reactors-smrs-mining-frequently-asked-questions/22698 (accessed Jan. 01, 2021).
[108] Author, "How CSP Works: Tower, Trough, Fresnel or Dish," *SolarPACES*, Jun. 11, 2018. https://www.solarpaces.org/how-csp-works/ (accessed Mar. 04, 2021).
[109] "Solar Cells: Everything to Know About Photovoltaics | EnergySage," *Solar News*, Feb. 02, 2021. https://news.energysage.com/how-solar-photovoltaic-cells-work/ (accessed Mar. 04, 2021).
[110] "Solar Panel Size Guide: How Big Is A Solar Panel?" https://www.wholesalesolar.com/blog/solar-panel-size-guide
[111] A. Heydari and A. Askarzadeh, "Optimization of a biomass-based photovoltaic power plant for an off-grid application subject to loss of power supply probability concept," *Appl. Energy*, vol. 165, pp. 601–611, Mar. 2016, doi: 10.1016/j.apenergy.2015.12.095.
[112] T. Markvart, *Solar Electricity*. John Wiley & Sons, 2000.
[113] "Solar Panel Maintenance Costs | Solar Power Maintenance Estimates," *Fixr.com*. https://www.fixr.com/costs/solar-panel-maintenance (accessed Apr. 16, 2020).
[114] "What Is the Lifespan of a Solar Panel?" https://www.engineering.com/DesignerEdge/DesignerEdgeArticles/ArticleID/7475/What-Is-the-Lifespan-of-a-Solar-Panel.aspx (accessed Apr. 16, 2020).
[115] "Solar panel efficiency: most efficient solar panels in 2021," *Solar Reviews*. https://www.solarreviews.com/blog/what-are-the-most-efficient-solar-panels (accessed Mar. 05, 2021).
[116] "SUN2000-(25KTL, 30KTL)-US, User Manual." HUAWEI TECHNOLOGIES CO., LTD., Apr. 01, 2017. [Online]. Available: https://www.huawei.com/minisite/solar/en-na/service/SUN2000-25KTL-30KTL-US/User_Manual.pdf
[117] L. Lu, H. Yang, and J. Burnett, "Investigation on wind power potential on Hong Kong islands—an analysis of wind power and wind turbine characteristics," *Renew. Energy*, vol. 27, no. 1, pp. 1–12, 2002.

[118] B. S. Borowy and Z. M. Salameh, "Methodology for optimally sizing the combination of a battery bank and PV array in a Wind/PV hybrid system," *IEEE Trans. Energy Convers.*, vol. 11, no. 2, Art. no. CONF-950727-, Jun. 1996, doi: https://doi.org/10.1109/60.507648.
[119] H. Yang, L. Lu, and W. Zhou, "A novel optimization sizing model for hybrid solar-wind power generation system," *Sol. Energy*, vol. 81, no. 1, pp. 76–84, Jan. 2007, doi: 10.1016/j.solener.2006.06.010.
[120] H. X. Yang, L. Lu, and J. Burnett, "Weather data and probability analysis of hybrid photovoltaic–wind power generation systems in Hong Kong," *Renew. Energy*, vol. 28, no. 11, pp. 1813–1824, Sep. 2003, doi: 10.1016/S0960-1481(03)00015-6.
[121] S. Diaf, G. Notton, M. Belhamel, M. Haddadi, and A. Louche, "Design and techno-economical optimization for hybrid PV/wind system under various meteorological conditions," *Appl. Energy*, vol. 85, no. 10, pp. 968–987, Oct. 2008, doi: 10.1016/j.apenergy.2008.02.012.
[122] R. N. S. R. Mukhtaruddin, H. A. Rahman, M. Y. Hassan, and J. J. Jamian, "Optimal hybrid renewable energy design in autonomous system using Iterative-Pareto-Fuzzy technique," *Int. J. Electr. Power Energy Syst.*, vol. 64, pp. 242–249, Jan. 2015, doi: 10.1016/j.ijepes.2014.07.030.
[123] L. Bauer, "Endurance E-3120 - 50,00 kW - Wind turbine." https://en.wind-turbine-models.com/turbines/372-endurance-e-3120 (accessed Mar. 06, 2021).
[124] N. E. B. Government of Canada, "NEB – Market Snapshot: The cost to install wind and solar power in Canada is projected to significantly fall over the long term," Feb. 13, 2020. https://www.cer-rec.gc.ca/nrg/ntgrtd/mrkt/snpsht/2018/11-03cstnstllwnd-eng.html (accessed Jul. 24, 2020).
[125] "US wind O&M costs estimated at $48,000/MW; Falling costs create new industrial uses: IEA | New Energy Update." https://analysis.newenergyupdate.com/wind-energy-update/us-wind-om-costs-estimated-48000mw-falling-costs-create-new-industrial-uses-iea (accessed Apr. 17, 2020).
[126] T. Stehly, P. Beiter, D. Heimiller, and G. Scott, "2017 Cost of Wind Energy Review," *Renew. Energy*, p. 61, 2018.
[127] P. W. Stackhouse, "Surface Meteorology and Solar Energy (SSE) Data Release 5.1." Accessed: Jul. 24, 2020. [Online]. Available: https://ntrs.nasa.gov/search.jsp?R=20080012141
[128] "Aeolos Wind Turbine Company – 50kw Wind Turbine – Wind Power Generation - Aeolos 50kw Turbine Wind Energy." https://www.windturbinestar.com/50kwh-aeolos-wind-turbine.html (accessed Mar. 06, 2021).
[129] "Marine Electrical Technology." https://www.goodreads.com/work/best_book/10132141-marine-electrical-technology (accessed Mar. 06, 2021).
[130] "SHIP'S EMERGENCY POWER," *DieselShipDieselShip, Connecting Mariners Worldwide*. https://dieselship.com/marine-technical-articles/marine-electro-technology/ships-emergency-power/ (accessed Jan. 01, 2021).
[131] "CEC Inverter Test Protocol," *PV. Performance Modeling Collaborative*. https://pvpmc.sandia.gov/modeling-steps/dc-to-ac-conversion/cec-inverter-test-protocol/ (accessed Jan. 01, 2021).

[132] Luo, X, Wang, J, Dooner, M, and Clarke, J, "Overview of current development in electrical energy storage technologies and the application potential in power system operation," *Appl Energy*, pp. 511–536, 2015, doi: 10.1016/j.apenergy.2014.09.081.
[133] S. Kharel and B. Shabani, "Hydrogen as a Long-Term Large-Scale Energy Storage Solution to Support Renewables," *Energies*, vol. 11, no. 10, p. 2825, Oct. 2018, doi: 10.3390/en11102825.
[134] S. C. Johnson *et al.*, "Selecting Favorable Energy Storage Technologies for Nuclear Power," in *Storage and Hybridization of Nuclear Energy*, Elsevier, 2019, pp. 119–175. doi: 10.1016/B978-0-12-813975-2.00005-3.
[135] X. Luo, J. Wang, M. Dooner, and J. Clarke, "Overview of current development in electrical energy storage technologies and the application potential in power system operation," *Appl. Energy*, vol. 137, pp. 511–536, Jan. 2015, doi: 10.1016/j.apenergy.2014.09.081.
[136] "PV Performance Modeling Collaborative | CEC Inverter Test Protocol." https://pvpmc.sandia.gov/modeling-steps/dc-to-ac-conversion/cec-inverter-test-protocol/ (accessed Jul. 24, 2020).
[137] H. A. Gabbar, M. R. Abdussami and M. I. Adham, "Optimal Planning of Nuclear-Renewable Micro-Hybrid Energy System by Particle Swarm Optimization," *IEEE Access*, vol. 8, pp. 181049–181073, 2020, doi: 10.1109/ACCESS.2020.3027524.
[138] "Qulliq Energy Corporation, '14th Annual Report,'" Nunavut, Canada, 2015. [Online]. Available: https://assembly.nu.ca/sites/default/files/TD%20127-4(3)%20EN%20QEC%20Annual%20Report%202014-2015.pdf
[139] "Salvage Value." https://www.homerenergy.com/products/pro/docs/latest/salvage_value.html (accessed Jul. 13, 2020).
[140] E. S. Rubin, I. M. L. Azevedo, P. Jaramillo, and S. Yeh, "A review of learning rates for electricity supply technologies," *Energy Policy*, vol. 86, pp. 198–218, Nov. 2015, doi: 10.1016/j.enpol.2015.06.011.
[141] A. M. Abdelshafy, H. Hassan, A. M. Mohamed, G. El-Saady, and S. Ookawara, "Optimal grid connected hybrid energy system for Egyptian residential area," in *2017 International Conference on Sustainable Energy Engineering and Application (ICSEEA)*, Jakarta, Indonesia, Oct. 2017, pp. 52–60. doi: 10.1109/ICSEEA.2017.8267687.
[142] A. M. Abdelshafy, H. Hassan, A. M. Mohamed, G. El-Saady, and S. Ookawara, "Optimal grid connected hybrid energy system for Egyptian residential area," *Int. Conf. Sustain. Energy Eng. Appl. ICSEEA*, pp. 52–60, Oct. 2017, doi: 10.1109/ICSEEA.2017.8267687.
[143] "Cost Competitiveness of Micro-Reactors for Remote Markets." Nuclear Energy Institute, Apr. 15, 2019.
[144] "Land Needs for Wind, Solar Dwarf Nuclear Plant's Footprint," *NEI*. https://www.nei.org/news/2015/land-needs-for-wind-solar-dwarf-nuclear-plants#:~:text=A%20nuclear%20energy%20facility%20has,1%2C000%20megawatts%20of%20installed%20capacity.&text=A%20solar%20PV%20facility%20must,45%20and%2075%20square%20miles. (accessed Jan. 13, 2021).

[145] Rita Greco and Ivo Vanzi, “New few parameters differential evolution algorithm with application to structural identification,” *J. Traffic Transp. Eng.*, vol. 6, no. 1, pp. 1–14.
[146] G. Pranava and P. V. Prasad, “Constriction Coefficient Particle Swarm Optimization for Economic Load Dispatch with valve point loading effects,” in *2013 International Conference on Power, Energy and Control (ICPEC)*, Feb. 2013, pp. 350–354. doi: 10.1109/ICPEC.2013.6527680.
[147] “Fuel comparison,” *ENS*, May 22, 2019. https://www.euronuclear.org/glossary/fuel-comparison/ (accessed Mar. 21, 2021).
[148] “Nuclear energy: how does it work, and how renewable is it? | OVO Energy.” https://www.ovoenergy.com/guides/energy-sources/nuclear-energy.html, https://www.ovoenergy.com/guides/energy-sources/nuclear-energy.html (accessed Mar. 21, 2021).
[149] “Freight Transport Revenue per Ton-Mile | The Geography of Transport Systems.” https://transportgeography.org/contents/chapter5/transportation-modes-modal-competition-modal-shift/modaltransportcosttonmile/ (accessed Feb. 17, 2021).
[150] “Distance from Iraq to Singapore.” https://www.distancefromto.net/distance-from-iraq-to-singapore (accessed Feb. 17, 2021).
[151] A. Demiroren and U. Yilmaz, “Analysis of change in electric energy cost with using renewable energy sources in Gökceada, Turkey: An island example,” 2010, doi: 10.1016/J.RSER.2009.06.030.
[152] “How the COVID-19 Pandemic Will Affect Oil Prices in 2021,” *The Balance*. https://www.thebalance.com/oil-price-forecast-3306219 (accessed Jun. 16, 2021).